AFRPL-TR-71-84

ADVANCED ACS VALVE SEALING SURFACE COMPATIBILITY INVESTIGATION

G. R. Pfeifer
H. Wichmann
Dr. R. Kratzer

Approved for public release; distribution unlimited

FOREWORD

This is the final report on the Advanced ACS Valve Sealing Surface Compatibility Investigation performed by The Marquardt Company, CCI Aerospace Corporation, Van Nuys, California, for the Air Force Rocket Propulsion Laboratory under contract FO-4611-70-C-0052 dated 20 April 1970. This task was conducted under the USAF Project 3058. The objective of the program was to determine the causes leading to leakage of the Marquardt Advanced ACS Valve when operated using chlorine pentafluoride or gaseous fluorine as propellants. Objectives of the program were accomplished with design data developed which can lead to a completely successful seat and poppet closure. The period of performance covered by this report is from 15 May 1970 through 15 July 1971. Edwin L. Lantzer, 1st Lt., USAF was the AFRPL Project Engineer for the program.

Marquardt principal investigators were H. Wichmann, Program Manager, and G. R. Pfeifer, Project Engineer. Marquardt personnel who contributed to the program effort included: A. Malek, Design Manager; R. Loustau, design of test fixtures; I. C. Dickens, Structural Analysis and R. Dickenson, Test Operations. The program literature survey was performed by Dr. R. H. Kratzer, Dynamic Sciences Company under subcontract to The Marquardt Company. Consultation was also provided by Dr. Kay Paciorek of Dynamic Sciences. This technical report has been given Marquardt Report No. S-1017.

This technical report has been reviewed and is approved.

Edwin L. Lantzer, 1st Lt., USAF
Project Engineer

ABSTRACT

An integrated program of theoretical chemical analysis and testing was conducted to determine the cause of failure of the Marquardt Advanced ACS valve to meet defined leakage goals when operated in chlorine pentafluoride or gaseous fluorine. A total of 23 poppets and 8 valve seats of five materials were tested in either static propellant exposure or dynamic propellant exposure in test bed valves during the test program. Prime objective, that of determining the mechanism of sealing surface deterioration, was accomplished during the program. In addition, design parameters were evolved which can lead to a completely successful design meeting all of the design objectives for valve operational performance in chlorine pentafluoride and gaseous fluorine.

Failure mechanism of the valve was found to be progressive degradation of the poppet and seat sealing surfaces through structural failure of the passive fluoride film formed on the parts under impact of the poppet with the seat during valve closing. The use of materials which form only gaseous fluorides as a seat and poppet material was investigated and found to be a viable means of eliminating surface deterioration leading to leakage of the valve. Program test results indicated only fluorides were formed during exposure of the test materials to chlorine pentafluoride in contrast to some previously reported data that indicated the presence of both chlorides and fluorides. Since all materials react to some degree with these extremely active oxidizers, materials which form only gaseous fluorides provided a sacrificial surface which was evenly eroded with total erosion during the test cycle being an amount acceptable within the operating mechanical performance requirements for the valve such as valve stroke and pressure drop characteristics.

Chemical wear was determined to be the primary means of seat and poppet erosion. Wear rate was determined to be a function of the impact force with which the poppet impacted the seat during valve closing. The rate of wear with impact force was documented for two of the candidate valve materials tested. Chemical wear was, in some cases, accelerated by friction generated by lateral movement of the poppet relative to the seat after closing which led to grooving of the poppet and seat surfaces and consequent unacceptable leakage rates for some materials which were otherwise acceptable.

TABLE OF CONTENTS

Section			Page
I.	INTRODUCTION		1
II.	SUMMARY		3
III.	LITERATURE SURVEY AND MATERIAL ANALYSIS		7
	1.	Objectives	7
	2.	Scope of Review	8
	3.	Results	9
	4.	Reactions of Fluorinated Oxidizers with Metals and Refractories	10
	5.	Mechanism of Surface Reaction	13
	6.	Film Properties and Protective Mechanisms	15
	7.	Discussion of the Problem	19
	8.	Possible Solutions and Materials Recommended for Testing	28
IV.	VALVE SEAT TO POPPET IMPACT TESTS		30
	1.	Summary of Test Results	30
	2.	Test Hardware Configuration	30
	3.	Impact Force Prediction Technique	32
	4.	Test Setup	35
	5.	Test Results	39
	6.	Discussion of Test Results	46
	7.	Impact Test Conclusions	50
V.	SURFACE EVALUATION TERMINOLOGY, METHODS AND TEST DEVICES		53
	1.	Parameters of Interest	53
	1.1	Surface Texture	53
	1.2	Flaws	53
	1.4	Roughness Height	54
	1.5	Roughness Width and Cutoff	54

TABLE OF CONTENTS (CONTINUED)

Section			Page
	1.6	Waviness	54
	1.7	Linear Measurements	54
	2.	Surface Measurement Instrumentation	54
	2.1	Interference Microscope	55
	2.2	Bendix Proficorder	55
	2.3	Electron Microprobe X-Ray Analyzer-Scanning Microscope (EMX-SM)	59
VI.	PROPELLANT TEST PROGRAM		63
	1.	Pre-Test Sample Identification and Test Matrix	63
	2.	Static Exposure Tests	63
	2.1	General Test Procedures	66
	2.1.1	Cleaning	66
	2.1.2	Pre-Test Documentation	66
	2.1.3	Interference Microscope Examination	66
	2.1.4	Final Preparation for Static Exposure Testing	66
	2.1.5	Moisture Protection of Static Exposure Poppets	68
	2.1.6	Facility Installation and Static Exposure Testing	68
	2.1.7	Post Test Handling and Examination	68
	2.1.8	Electron Microscope Examination	70
	2.1.9	Final Interference Microscope Examination and Proficording	70
	3.	Static Exposure Test Results Summary	71
	3.1	K-96 (Tungsten Carbide) Static Exposure Test Results	72

TABLE OF CONTENTS (CONTINUED)

Section			Page
	3.2	Nickel-301 Static Exposure Test Results	78
	3.3	Boron Carbide (B_4C) Static Exposure Test Results	85
	3.4	Tungsten Carbide (WC) Static Exposure Test Results	92
	3.5	Aluminum Oxide (Al_2O_3) Static Exposure Test Results	98
	4.	Dynamic Exposure Tests	98
	4.1	Valve Configurations	103
	4.2	Valve Preparation and Poppet to Seat Alignment	103
	4.3	Final Preparations and Assembly into the Test Facility	107
	4.4	Test Procedure	107
	4.5	Post Test Handling and Examination	107
	4.6	Leakage Test Results	109
	4.7	Poppet and Seat Inspections and Data Evaluation	118
	4.7.1	Ni-301 Material Evaluation	119
	4.7.2	Tungsten Carbide (K-96) Material Evaluation	129
	4.7.3	Boron Carbide Material Evaluation	138
	4.7.4	Pure Tungsten Carbide Material Evaluation	152
	4.7.5	Aluminum Oxide Material Evaluation	155
	5.	Data Evaluation Summary	175
VII.	CONCLUSIONS		181
VIII.	RECOMMENDATIONS		183

LIST OF ILLUSTRATIONS

Figure	Title	Page
1	Marquardt Advanced ACS Valve Assembly	31
2	Impact Force as a Function of Strain Energy	36
3	Valve Seat Impact Load Test Set-up	37
4	Valve Poppet to Seat Closing Impact Test Set-up Photo	38
5	Oxidizer Valve Mounted on Impact Test Fixture	40
6	Closing Force as a Function of Time	41
7	Valve Seat Closing Impact Force and Poppet Travel Time as a Function of Inlet Pressure for Configuration No. 1	42
8	Valve Seat Closing Impact Force and Poppet Travel Time as a Function of Inlet Pressure for Configuration No. 2	43
9	Valve Seat Closing Impact Force and Poppet Travel Time as a Function of Inlet Pressure for Configuration No. 3	44
10	Valve Seat Closing Impact Force and Poppet Travel Time as a function of Inlet Pressure for Configuration No. 4	45
11	Comparison of Impact Forces in GN_2	47
12	Comparison of Impact Forces in Water	48
13	Closing Force as a Function of Time	51
14	Wild Interference Microscope	56
15	Principle of Interference Microscope	57
16	Proficorder Type RLC, Model 6 and Type RLJ, Model 4	58
17	Profile Measurement Error	60
18	Electron Microprobe X-Ray Analyzer Scanning Microscope	61
19	Test Matrix	65
20	Proficorder Inspection	67

LIST OF ILLUSTRATIONS (CONTINUED)

Figure	Title	Page
21	Static Propellant Exposure Test Set-up, MJL-Cell 4	69
22	Surface Photos and Interferograms of K-96 Poppet Before and After Static GF_2 Exposure Test	73
23	Surface Photos and Interferograms of K-96 Poppet Before and After Static ClF_5 Propellant Exposure Test	74
24	K-96 "As Lapped" Poppet, S.E.M. Photo at 5000X	75
25	K-96 Static GF_2 Exposed Poppet, S.E.M. Photos	76
26	K-96 Static ClF_5 Exposed Poppet, S.E.M. Photos	77
27	K-96 Static Exposure Poppet, Surface Profile Before and After ClF_5 Static Exposure	79
28	Ni-301 Poppet, Surface Photos and Interferograms Before and After Static GF_2 Exposure Test	80
29	Ni-301 Poppet, Surface Photos and Interferograms Before and After Static ClF_5 Exposure Test	81
30	Ni-301, S.E.M. Photos of "As Lapped" Surface	82
31	Ni-301, S.E.M. Photos after Static GF_2 Exposure	83
32	Ni-301, S.E.M. Photos after Static ClF_5 Exposure	84
33	Ni-301 Static Exposure Poppet, Surface Profile before and after ClF_5 Static Exposure	86
34	B_4C Poppet, Surface Photos and Interferograms before and after ClF_5 Static Exposure	87
35	B_4C Static Exposure Poppet, Surface Profile before and after ClF_5 Static Exposure	88
36	B_4C Poppet, S.E.M. Photo of "As Lapped" Surface	89
37	B_4C Poppet, S.E.M. Photos after Static GF_2 Exposure	90
38	B_4C Poppet, S.E.M. Photos after Static ClF_5 Exposure	91
39	WC Poppet, Surface Photos and Interferograms before and after ClF_5 Static Exposure	93
40	WC Poppet, S.E.M. Photo of "As Lapped" Surface	94

LIST OF ILLUSTRATIONS

Figure	Title	Page
1	Marquardt Advanced ACS Valve Assembly	31
2	Impact Force as a Function of Strain Energy	36
3	Valve Seat Impact Load Test Set-up	37
4	Valve Poppet to Seat Closing Impact Test Set-up Photo	38
5	Oxidizer Valve Mounted on Impact Test Fixture	40
6	Closing Force as a Function of Time	41
7	Valve Seat Closing Impact Force and Poppet Travel Time as a Function of Inlet Pressure for Configuration No. 1	42
8	Valve Seat Closing Impact Force and Poppet Travel Time as a Function of Inlet Pressure for Configuration No. 2	43
9	Valve Seat Closing Impact Force and Poppet Travel Time as a Function of Inlet Pressure for Configuration No. 3	44
10	Valve Seat Closing Impact Force and Poppet Travel Time as a function of Inlet Pressure for Configuration No. 4	45
11	Comparison of Impact Forces in GN_2	47
12	Comparison of Impact Forces in Water	48
13	Closing Force as a Function of Time	51
14	Wild Interference Microscope	56
15	Principle of Interference Microscope	57
16	Proficorder Type RLC, Model 6 and Type RLJ, Model 4	58
17	Profile Measurement Error	60
18	Electron Microprobe X-Ray Analyzer Scanning Microscope	61
19	Test Matrix	65
20	Proficorder Inspection	67

LIST OF ILLUSTRATIONS (CONTINUED)

Figure	Title	Page
21	Static Propellant Exposure Test Set-up, MJL-Cell 4	69
22	Surface Photos and Interferograms of K-96 Poppet Before and After Static GF_2 Exposure Test	73
23	Surface Photos and Interferograms of K-96 Poppet Before and After Static ClF_5 Propellant Exposure Test	74
24	K-96 "As Lapped" Poppet, S.E.M. Photo at 5000X	75
25	K-96 Static GF_2 Exposed Poppet, S.E.M. Photos	76
26	K-96 Static ClF_5 Exposed Poppet, S.E.M. Photos	77
27	K-96 Static Exposure Poppet, Surface Profile Before and After ClF_5 Static Exposure	79
28	Ni-301 Poppet, Surface Photos and Interferograms Before and After Static GF_2 Exposure Test	80
29	Ni-301 Poppet, Surface Photos and Interferograms Before and After Static ClF_5 Exposure Test	81
30	Ni-301, S.E.M. Photos of "As Lapped" Surface	82
31	Ni-301, S.E.M. Photos after Static GF_2 Exposure	83
32	Ni-301, S.E.M. Photos after Static ClF_5 Exposure	84
33	Ni-301 Static Exposure Poppet, Surface Profile before and after ClF_5 Static Exposure	86
34	B_4C Poppet, Surface Photos and Interferograms before and after ClF_5 Static Exposure	87
35	B_4C Static Exposure Poppet, Surface Profile before and after ClF_5 Static Exposure	88
36	B_4C Poppet, S.E.M. Photo of "As Lapped" Surface	89
37	B_4C Poppet, S.E.M. Photos after Static GF_2 Exposure	90
38	B_4C Poppet, S.E.M. Photos after Static ClF_5 Exposure	91
39	WC Poppet, Surface Photos and Interferograms before and after ClF_5 Static Exposure	93
40	WC Poppet, S.E.M. Photo of "As Lapped" Surface	94

LIST OF ILLUSTRATIONS (CONTINUED)

Figure	Title	Page
41	WC Poppet, S.E.M. Photos after Static GF_2 Exposure	95
42	WC Poppet, S.E.M. Photos after Static ClF_5 Exposure	96
43	WC Poppet, Surface Profile before and after ClF_5 Static Exposure	97
44	Al_2O_3 Poppet, Surface Photos and Interferograms before and after ClF_5 Static Exposure	99
45	Al_2O_3 Poppet, Surface Profile before and after ClF_5 Static Exposure	100
46	Al_2O_3 Poppet, S.E.M. Photos after Static GF_2 Exposure	101
47	Al_2O_3 Poppet, S.E.M. Photos after Static ClF_5 Exposure	102
48	Poppet Alignment Fixture	106
49	Dynamic Impact Exposure Test, MJL - Cell 4	108
50	Valve Leakage vs Cum Cycles, K-96, Normal Impact, ClF_5	110
51	Valve Leakage vs Cum Cycles, Ni-301, Low Impact, ClF_5	111
52	Valve Leakage vs Cum Cycles, B_4C, Normal Impact, ClF_5	112
53	Valve Leakage vs Cum Cycles, B_4C, Low Impact, ClF_5	113
54	Valve Leakage vs Cum Cycles, WC, Normal Impact, ClF_5	114
55	Valve Leakage vs Cum Cycles, Al_2O_3, Low Impact, ClF_5	115
56	Valve Leakage vs Cum Cycles, Al_2O_3, Normal Impact, GF_2	116
57	Valve Leakage vs Cum Cycles, Al_2O_3, Low Impact, GF_2	117
58	Ni-301 Seat, Surface Photos and Interferograms before and after Valve Test, Low Impact, ClF_5	120
59	Ni-301 Seat, Surface Profile before and after Valve Test, Low Impact, ClF_5	121

LIST OF ILLUSTRATIONS (CONTINUED)

Figure	Title	Page
60	Ni-301 Seat, Surface Photos of Impact and Non-Impact Areas after Low Impact Valve Test, ClF_5	122
61	Ni-301 Poppet, 200X S. E. M. Photos after Low Impact Valve Test in ClF_5	124
62	Ni-301 Poppet, 1000X S. E. M. Photos after Low Impact Valve Test in ClF_5	125
63	Ni-301 Poppet, 5000X S. E. M. Photos after Low Impact Valve Test in ClF_5	126
64	Component Valve Seat Seals	128
65	K-96 Seat, Surface Photos and Interferograms before and after Normal Impact Valve Test, ClF_5	131
66	K-96 Seat, Surface Profile before and after Normal Impact Valve Test in ClF_5	132
67	Non-Uniform Bumper Impact	133
68	K-96 Poppet, 200X S. E. M. Photos after Normal Impact Valve Test in ClF_5	134
69	K-96 Poppet, 1000X S. E. M. Photos after Normal Impact Valve Test in ClF_5	136
70	K-96 Poppet, 5000X S. E. M. Photos after Normal Impact Valve Test in ClF_5	137
71	B_4C Seat, Surface Photos and Interferograms before and after Low Impact Valve Test in ClF_5	140
72	B_4C Seat, Surface Photos and Interferograms before and after Normal Impact Valve Test in ClF_5	141
73	B_4C Poppet, 200X S. E. M. Photos after Low Impact Valve Test in ClF_5	142
74	B_4C Poppet, 1000X S. E. M. Photos after Low Impact Valve Test in ClF_5	143
75	B_4C Poppet, 5000X S. E. M. Photos after Low Impact Valve Test in ClF_5	145
76	B_4C Seat, Surface Profile before and after Low Impact Valve Test in ClF_5	146

LIST OF ILLUSTRATIONS (CONTINUED)

Figure	Title	Page
77	B_4C Seat, Surface Profile before and after Normal Impact Valve Test in ClF_5	147
78	B_4C Poppet, 200X S.E.M. Photos after Normal Impact Valve Test in ClF_5	148
79	B_4C Poppet, 1000X S.E.M. Photos after Normal Impact Valve Test in ClF_5	149
80	B_4C Poppet, 5000X S.E.M. Photos after Normal Impact Valve Test in ClF_5	150
81	WC Seat, Surface Photos and Interferograms before and after Normal Impact Valve Test in ClF_5	153
82	WC Seat, Surface Photos and Interferograms of Non-Impact and Bumper Zones after Normal Impact Valve Test in ClF_5	154
83	WC Seat, Surface Profile before and after Normal Impact Valve Test in ClF_5	156
84	WC Poppet, 200X S.E.M. Photos after Normal Impact Valve Test in ClF_5	157
85	WC Poppet, 1000X S.E.M. Photos after Normal Impact Valve Test in ClF_5	158
86	WC Poppet, 5000X S.E.M. Photos after Normal Impact Valve Test in ClF_5	159
87	Al_2O_3 Seat, Surface Photos and Interferograms before and after Low Impact Valve Test in ClF_5	161
88	Al_2O_3 Seat, Surface Profile before and after Low Impact Valve Test in ClF_5	162
89	Al_2O_3 Poppet, 200X S.E.M. Photos after Low Impact Valve Test in ClF_5	163
90	Al_2O_3 Poppet, 1000X S.E.M. Photos after Low Impact Valve Test in ClF_5	164
91	Al_2O_3 Poppet, 5000X S.E.M. Photos after Low Impact Valve Test in ClF_5	165
92	Al_2O_3 Seat, Surface Photos and Interferograms before and after Low Impact Valve Test in GF_2	167

LIST OF ILLUSTRATIONS (CONTINUED)

Figure	Title	Page
93	Al_2O_3 Seat, Surface Profile before and after Low Impact Valve Test in GF_2	168
94	Al_2O_3 Seat, Surface Photos and Interferograms before and after Normal Impact Valve Test in GF_2	169
95	Al_2O_3 Seat, Surface Profile before and after Normal Impact Valve Test in GF_2	170
96	Al_2O_3 Poppet, 200X S.E.M. Photo after Normal Impact Valve Test in GF_2	172
97	Al_2O_3 Poppet, 1000X S.E.M. Photos after Normal Impact Valve Test in GF_2	173
98	Al_2O_3 Poppet, 5000X S.E.M. Photos after Normal Impact Valve Test in GF_2	174

LIST OF TABLES

Table	Title	Page
I	Some Gaseous and Liquid Fluorides	21
II	Volume Expansion During Fluoride Formation	24
III	Impact Test Valve Critical Dimensions	33
IV	Calculated Impact Forces for Materials Tested	49
V	Test Sample Usage Allocation	64
VI	Calculated Impact Forces for Materials Tested	104
VII	Seat Surface Erosion Data	177

SECTION I

INTRODUCTION

This program was necessitated by the finding that the Marquardt developed magnetically linked bipropellant valve showed extensive finish deterioration of both the poppet and seat mating surfaces after being operated in chlorine pentafluoride (CPF). The same valve design, using the same materials of construction, performed properly when operated using liquid monomethyl hydrazine. Surface roughness measurements on CPF exposed poppets furthermore revealed that the surface finish deterioration was far more severe in sealing and impact areas than on nonsealing surfaces.

Prime objective of this program was to determine the mechanism leading to failure of the Marquardt Advanced ACS valve to seal when operated in a liquid chlorine pentafluoride environment. Adjunctive objectives included:

- Development of data regarding the nature of the chemical reactions taking place between the test materials and the test fluid
- Hypothesis of the most probable failure mode
- Recommendation of candidate materials which might allow meeting the design operational goal of helium leakage rates of less than 30 SCCH after 100,000 operational cycles
- Testing of the candidate materials to confirm the hypothesized failure mode and determine if the recommended materials would in fact meet the design leakage goal.

Scope of the program provided for performing a thorough chemical analysis and literature survey to determine available information pertinent to the nature of the thin passive films formed by exposure of materials to CPF and to predict types of film properties which could be most beneficial in a valve seal environment. Tests were performed to determine the impact force levels typical of valve closing so that energy of closing impact might be related to the chemical and/or mechanical degradation of the seat surfaces. Material samples were statically exposed to both gaseous fluorine and to CPF to determine effects of the propellants on the materials in a static environment. Valve sealing closures were fabricated and operational sealing closure performance documented as a function of total accumulated valve cycles.

This report presents the results of that program and the significant findings which were obtained. The report is subdivided into several sections, corresponding to major program work tasks. Each subsection is complete in itself describing the specific objectives, actions taken, and results of the specific portion of the program. All results are integrated into a section describing specific details leading to the program conclusions.

Additional test techniques were discovered during the course of the program which might shed some insight on the nature of the failure mechanism, however, further pursuit was beyond scope of the original program.

SECTION II

SUMMARY

The program reported herein was a basic technology program intended to further develop a high response valve suitable for use in handling chlorine pentafluoride and gaseous fluorine. The basic valve design was developed under a previous program, Reference (1), during which operating mechanisms and response characteristics proved satisfactory to meet all operational goals. The valve failed, however, to meet leakage requirement goals when operated using chlorine pentafluoride as the test fluid even though it met all leakage goals when operated using monomethylhydrazine and N_2O_4 as the test fluids. It was hypothesized that the sealing surface degradation seen on the test valve seats and poppets resulted from breakdown of the passive film formed on the surfaces under the impact loads of valve closing. This program was designed to determine the failure mechanism of the valve and to recommend and test materials which might be successfully used to meet all leakage goals for the otherwise satisfactory valve.

The program, as conducted, was a three phase program. The first portion was a literature survey to determine the known information on the formation and properties of films formed on materials under exposure to fluorinated oxidizers and based on study of the available information, to recommend material systems which might satisfy all requirements. The second phase of the program was intended to document loads generated between seat and poppet during valve closing for correlation with material/film properties. The third phase consisted of static and dynamic propellant exposure of the candidate materials to fluorinated oxidizer environments to evaluate surface degradation of the candidate materials under both static and impact environments.

Results of the literature survey indicated that there was relatively little information about the properties of films formed on metals as a result of exposure to chlorine pentafluoride and fluorine. However, sufficient information was found to formulate an analytical and theoretical model of the failure mechanism, and to predict with the aid of the model the effects that CPF and gaseous fluorine have on surface finish and surface properties and to recommend promising materials for the construction of the oxidizer valve sealing components. Results of the test program indicated that only fluorides were formed during contact of the propellants with the materials tested.

All materials theoretically react to some degree with the oxidizers of interest in this program. Therefore, considering the degradation of seats and poppets tested during the previous program, a failure mechanism was postulated which provided that the surface degradation seen on the poppets and seats was a function of breakdown of the passive surface films under the impact loads of valve closing. That conclusion was based on the difference in crystal lattice properties of the films as related to the base structures which indicated that all solid films would be weaker than the base

material and probably have tendencies not to adhere under the influence of the impact forces. It was hypothesized that the surface degradation could be eliminated by selection of materials for the poppet and seat which could form only gaseous fluorides under the use temperature conditions. Thus, although the seat/poppet surfaces might be slowly eroded away under the added energy of poppet to seat impact, the surfaces would remain smooth because attack would not be preferential and no solid fluorides would be present to provide a buildup and consequent surface roughness leading to valve leakage.

Five materials were selected for testing to determine the failure mechanism of previously used materials and the relative success of using materials which would provide sacrificial surfaces (gaseous fluorides). These materials were:

Nickel 301 - A high nickel alloy previously tested at normal impact levels with little success. This alloy was selected for testing at low impact force levels to determine if film structural properties were sufficient to maintain a good surface if the energy level of closing impact was sufficiently lowered.

Tungsten Carbide K-96 - An alloy of tungsten carbide with 6% cobalt binder which had previously shown some promise in other tests. This alloy was selected as a reference for testing at normal impact levels for the valve to hopefully obtain another successful operating data point.

Pure tungsten carbide - This material was selected because it forms only gaseous fluorides at room temperature. Since solid fluoride formation was suspected to be a strong contributor to leakage failure of previous materials, the good performance of the K-96 was expected to be extended without the presence of cobalt, a material which forms solid fluorides.

Boron Carbide - This material was selected because it forms only gaseous fluorides over a wide range of temperature and if structurally adequate would demonstrate that the sacrificial surface approach to sealing was correct.

Aluminum oxide - Selected for testing because of apparent low reactivity with the oxidizers. It does form a solid fluoride, however, since the fluoride is formed by replacement of the oxygen by fluorine, the volume of the reaction product is very small relative to other solid fluoride forming materials.

An in-propellant test program was performed to evaluate the selected materials under both static and impact environments in chlorine pentafluoride and gaseous fluorine after completion of bench tests to document the normal design valve impact force levels as well as the impact force levels to be expected from a modified valve designed to provide extremely low closing impact forces.

Each of the candidate materials was tested under static exposure conditions providing more than one week of propellant exposure. Results of these tests were somewhat surprising and inconclusive. Least apparently affected was the Ni-301, a "bad" valve performer while the tungsten carbide base materials showed significant etching of the original highly finished surfaces. The aluminum oxide, also a material forming a solid fluoride showed no effects of the static exposure. Pure boron carbide showed only minor etching or surface flaking as a result of the exposure.

The in-propellant valve cycling portion of the program was initially designed to test only four of the five candidate materials. One material was to have been eliminated from valve cycling tests through evaluation of static exposure test results. Because of the surprising static exposure test results, the program was reoriented to allow valve tests to be conducted on each of the candidate materials. A total of eight valve-seat pairs were tested to 100,000 cycles in either CPF or gaseous fluorine. Three of the five materials tested, pure boron carbide, tungsten carbide K-96, and aluminum oxide, demonstrated considerable promise as poppet and seat materials. Pure boron carbide appears to be the best material tested considering ultimate requirements for cryogenic applications. The K-96 has demonstrated consistently good performance in this valve application, both in these tests and in tests conducted at AFRPL. Pure aluminum oxide, while presenting some design problems because of its brittle nature, also appears to be a material which could be successfully used as a seat and poppet material for this application.

All the poppets used in the tests were examined using a scanning electron microscope and microprobe analyzer to aid in determining the nature of surface degradation of the seats and poppets. Examination of the data obtained directly from test part inspections combined with re-evaluation of the valve operating mechanism and assembly structure led to the conclusion that the leakage test results obtained on some of the valve tests were strongly influenced by outside factors not associated with true poppet to seat seal material performance. Thus some of the valves which demonstrated leakage should probably leak considerably less with correction of minor design deficiencies.

The accumulation of data indicates that the original program hypothesis of failure of the valves to seal through progressive deterioration of the poppet and seat under impact loads was correct. The degree of chemical wear of the seat was bracketed as a function of impact level for two of the test materials, boron carbide and aluminum oxide. Design criteria were developed for the unique failure mechanism of each of the materials tested as well as determination of minor design deficiencies of the valves tested which require correction to provide completely successful operation in chlorine pentafluoride or fluorine.

In conclusion, it is entirely possible to construct a valve which will meet and exceed the leakage goal requirements. Boron carbide was selected as the primary candidate seat and poppet material for further study and testing with K-96 and aluminum oxide demonstrating sufficiently promising results to warrant more tests.

SECTION III

LITERATURE SURVEY AND MATERIAL ANALYSES

1. Objectives

The objectives of this portion of the program was a search and analysis of the literature as it pertains to the behavior of materials of construction in contact with fluorinated oxidizers, especially how surface properties are changed upon exposure to these oxidizers and how the exposed surfaces are affected by impact. The materials of construction to be considered were those employed under a previous program (Reference 1): Duranickel 301 (Ni, Al), Pyromet X-15 (Fe, Co, Cr), Berylco Nickel 440 (Ni, Be), KT Silicon Carbide (SiC), Kennametal K602 (WC, TaC, Co), K96 (WC, Co), K801 (WC, Ni), and chromium deposited on K801, in addition to aluminum, aluminum oxide, zirconium boride and its alloys, and any other material or material combination, which could be reasonably expected to be a candidate for poppet and seat construction.

Most metals on exposure to oxidizers such as fluorine, chlorine trifluoride, chlorine pentafluoride, oxygen difluoride, and even atmospheric oxygen become covered with a coating which is called a passivating film and which in many cases protects the underlying element from further attack. It is obvious that the presence of a film on the sealing surfaces of the valve (and actually all surfaces exposed to the oxidizer) changes the mechanics of sealing in a very important way, since sealing is not accomplished anymore by metal contacting metal but by contact between the passivating films present on both poppet and seat. One major objective of the literature survey was therefore to gather and evaluate data on film properties such as thickness, hardness, impact strength, stress versus strain characteristics, capability to adhere to the substrate, and friction coefficient. In the course of the literature review it became apparent that other properties may play an even greater role in respect to maintaining surface integrity and sealing capability. These were crystal structure, thermal expansion and thermal conductivity coefficients, density, and molar volume. For the purposes of this program it was, however, not only important to determine what these film properties were, but to deduce how these properties affect surface finish and consequently influence the capability of the valve to produce a tight seal after impact.

Inasmuch as Task 2 of this program was concerned with an experimental attempt to prove and analyze the valve failure mechanism one further objective of this literature survey was to evaluate methods for measuring properties of films as present on poppets and seats after exposure to fluorine containing oxidizers. These films are very thin, as will be described later, and measurement techniques had to be primarily capable of detecting surface finish deterioration. A secondary requirement, not

necessarily less important, was that the measurement and analysis of the films, while on the substrate, should provide some insight into the chemical and physical processes which produced the surface finish deterioration and therefore caused leakage.

The final objective of the literature survey was to use the compiled data for development of an analytical and theoretical model of the failure mechanism, to predict, with the aid of this model, the effects that CPF and gaseous fluorine have on surface finish and surface properties, and to recommend those materials most promising for the construction of oxidizer valve sealing components.

2. Scope of Review

To cover the technical subject in the most efficient and comprehensive way, machine searches were requested from DDC and NASA at the start of the program. The DDC search (Search Control No. 042171), covering the period 1950-1969, produced a total of 272 references, 96 of which were possibly useful and 22 of which were reviewed as original reports. The NASA machine search listed 108 references out of which 36 were possibly applicable. Of these 36 references, 7 were duplicates of the DDC compilation. Four references were inspected in the form of original reports. It should be mentioned here that many of the above described reports are reviews by themselves which reference and abstract the disappointingly few experimental investigations that were conducted in this area. Accordingly, the number of reports containing experimentally generated data is considerably smaller than the above numbers would indicate.

The manual literature search consisted of reviewing the following handbooks and publications: Hologen Chemistry (Reference 2), Advances in Fluorine Chemistry (Reference 3), Thin Solid Films (Reference 4), and Gmelins Handbook of Inorganic Chemistry (Reference 5). The first three of these publications were search completely; in Gmelin's handbook all those System Numbers were searched which were considered important to this literature review. These were:

System No.	Element	System No.	Element
5	fluorine	50	tantalum
13	boron	52	chromium
14	carbon	53	molybdenum
15	silicon	54	tungsten
26	beryllium	57	nickel
27	magnesium	58	cobalt
35	aluminum	59	iron
41	titanium	60	copper
42	zirconium	68	platinum

All issued volumes of above system numbers were studied in regard to interaction of halogens with the metals, properties of halides, and rates of reaction. In addition to pure metal reactions the following binary systems were evaluated: the carbides of boron, silicon, tantalum, and tungsten, the borides of zironium and tungsten, also boron nitride and aluminum oxide.

At random the following publications were searched: Chemical Abstracts, U. S. Government R&D Reports, International Aerospace Abstracts, and NASA Scientific and Technical Aerospace Reports. In this manner the manual literature search produced 35 references in addition to those uncovered in the machine searches. All of these 35 references were evaluated, at least in the form of abstracts.

3. Results

In this section the data and information gathered in the literature search are compiled in a fashion suitable for analysis. The analysis is shown in a later section. The summary in this section will serve for introducing the necessary background information on which the analysis of the oxidizer valve problem is based.

In 1967 a literature survey of problems with seats and poppets was reported as particularly unrewarding (Reference 6). The present literature search was in no way more productive as far as specific and quantitative data are concerned. The scattered qualitative information, which may have some bearing on the problems encountered with metal to metal seals for fluorine containing oxidizers, is not very extensive and in addition quite often contradictory. As will be seen below, these contradictions do not arise so much from poorly specified reaction conditions, e.g., presence of unknown impurities or not sufficiently prepared or cleaned metal specimens. The main reason for many of the apparent contradictions is that the metal/oxidizer systems were evaluated with differing applications in mind. For the purposes of storing a fluorinated oxidizer the passivating film is justly called strongly adhering, because the storage vessel, after all, retains its structural integrity, although the presence of the passivating film is recognized. On the other hand, when filters are found to remove much particulate matter from an oxidizer stream, or are found to become clogged, the passivating film is called poorly adhering, again with some degree of justification.

An effort has been made to cite here only those references which were felt to contain information on the problem of hard metal to metal seals for fluorinated oxidizer valves. For more general and more extensive data the bibliographies and literature reviews by Cabaniss (Reference 7), Cabaniss and Williamson (Reference 8), and by Muraca, et al (Reference 9) can be inspected.

For clarity of presentation the results of the literature search will be described in the following sections on reactions of fluorinated oxidizers with metals and refractories, film properties, and film measurement techniques. It is realized that this breakdown into subjects cannot avoid some overlap and duplication, yet most of the information to be reported can be clearly identified as belonging to one of the above enumerated subjects.

4. Reactions of Fluorinated Oxidizers with Metals and Refractories

Theoretically all metals, their carbides, borides, nitrides, and oxides will react with fluorine and the fluorinated oxidizers under the proper conditions. Why one material will remain "unaffected" at room temperature depends to some degree on the oxidizer used, on impurities present in the oxidizer or present on the metal surface, or the form in which the metal is present (bulk or powder, available surface area), and finally on the rate of reaction, that is how fast the reaction proceeds at a given temperature. In connection with a hard metal to metal seal, there are more factors that have to be considered. Static Systems, as opposed to dynamic environments in general, show a lower reactivity of the metal (or carbide, boride, nitride, oxide). The presence of foreign particles can cause reaction where the metal would not be affected in the absence of the particle. Also the past history of the metal has an influence on its reactivity. Surface treatments, heat treatments, and stresses produced in the metal (Reference 10), especially in the surface, will influence the chemical stability of the specimen in an oxidizing atmosphere.

The oxygen fluorides, OF_2 and O_3F_2, and perchlorylfluoride, $FClO_3$, have been found to react slower than fluorine (Reference 10), and chlorine trifluoride, ClF_3, was shown to be more reactive than chlorine pentafluoride, ClF_5, (Reference 11) and was said to be the most corrosive of all the interhalogens (Reference 12). Based on chemical considerations, especially the presence of positive halogen, Cl^+, it would appear that ClF_3 and ClF_5 should be as reactive as fluorine if not more as discussed in the following section.

In general, however, it is not so much the different types of oxidizers that influence the reaction with the metal but the presence of impurities. In fluorine, the following foreign substances were found to be present (Reference 13): HF, OF_2, SiF_4, SF_6, CO_2, SO_2F_2, and CF_4. The same authors (Reference 13) report that the deliberate addition of oxygen difluoride (OF_2) to liquid fluorine caused somewhat larger (metal) weight changes as compared to pure fluorine, and that these weight changes for 15 and 75 min immersions were mostly negative, pointing to solution of metal or of passivating film in the liquid oxidizer. Tiner and English (Reference 10) also stress the importance of the oxidizer condition such as composition, presence of impurities, and relative movement of oxidizer and test material. Cabaniss, et al (Reference 8) find

that the presence of O_2, OF_2, O_3, HF, H_2O_2, and H_2O in fluorine increase the rate of corrosion, whereas Sterner and Singleton (Reference 14) report that highly polished samples of titanium, aluminum, and copper remain bright and lustrous when submerged in liquid fluorine, but become covered with visible, hazy patches of film when the fluorine is evaporated. This behavior indicates that at very low temperatures film formation does not take place due to either the fact that the rate of reaction is slow, or, more likely, that most of the above listed impurities are solids at LF_2 temperatures and do not react in that state.

Aside from thermodynamic and kinetic reasons, a major cause for differing reactivity of even the same metal is the degree of distribution. For example, copper sheet in fluorine showed no signs of corrosion up to 900°F, whereas copper wool burned at 100-200°F (Reference 15). Boron is said to react with fluorine at 20°C (Reference 16), but it also was found that no weight change (equal to no reaction) was produced when boron particles coarser than 325 mesh were exposed to fluorine for four hours at 20°C (Reference 17). The same variation of reactivity with pretreatment and distribution is observed for aluminum oxide. Vacuum baked and fused Al_2O_3 (Lucalux) do not react with fluorine at 150°C, whereas activated alumina reacts at ambient temperature to produce perchlorylfluoride, chlorine, and aluminum fluoride. Mixed oxides behave in the same manner. Dry fluorine can be safely handled in quarts (SiO_2) or Pyrex (mixture of Si, Al, B, Na, Ca oxides) vessels, whereas asbestos, a high surface area material composed of Si, Ca, Mg, Fe oxides ignites at room temperature in 1 atm of fluorine (in 20% fluorine no ignition occurs) (Reference 18). However, Fink and White (Reference 19) report that asbestos may be used in fluorine (no details given). The number of examples which show the influence of the degree of distribution on reactivity can be expanded. For example, tungsten was selected as the chemically most stable nozzle material for a F_2/H_2 engine, which was designed for a 3 minute operating time (Reference 20). Tungsten also was reported to react with fluorine at 1600°F (Reference 15), whereas another reference states that tungsten powder reacted with fluorine at room temperature. The same report lists stainless steels among the resistant materials. Steels contain a large percentage of iron, which in the form of a steel slab does not react. Yet, powdered iron reacts with fluorine even at -253°C (Reference 21).

This enumeration of variations of reactivity with degree of distribution serves, in the present literature search, as an illustration of the important effect which the surface area has on the chemical stability of a specimen in an oxidizer environment. After all, powders differ (from the standpoint of a chemist) from bulk materials only in the surface to volume ratio and, more importantly, in surface energy. This was amply demonstrated by Tiner, et al (Reference 22). They found that in OF_2 individual scratches (small increase in surface area) on a metal surface do not noticeably change

the appearance of the film as compared to unscratched specimens. However, wire brushed coupons (large increase in surface area) had greater corrosion rates than unbrushed specimens. Implications of these findings are discussed in a following section.

Impurities in the metal or, in general, the materials of construction also play an important role in the compatibility of a specimen with fluorinated oxidizers. For example, nickel alloys were found to be less resistant to fluorine at high temperatures than pure nickel (Reference 23) and the addition of 0.2% Si to Fe alloys resulted in a greatly increased corrosion rate (Reference 8). In general, however, copper, nickel, aluminum and their alloys, as well as stainless steels, are considered to be compatible with these oxidizers (Reference 9). In addition to these materials, magnesium alloys, monel, gold, and platinum are said to be compatible with ClF_3 and $FClO_3$ (Reference 24). Monel and nickel alloys are often preferred because of the resistance of their passivating film to HF and/or HCl (Reference 12). Platinum was found to be stable to 700°F (Reference 15) and was used as cladding on Ni-base alloys for high temperature halogenations (Reference 25).

Among metal oxides alumina is reported to be stable to fluorine up to 750°C (1382°F) (Reference 8) and ZnO, HgO, SiO_2, ZrO_2, ThO_2, and Fe_2O_3 are said not to react with ClF_3, though the author states correctly that this nonreactivity is probably just a matter of reaction conditions (Reference 26). It is of general interest, that many metal oxides have been found to react with ClF_5, whereas the respective metals were found by the same investigators to be inert. This is in direct contradiction to what would be expected thermodynamically and can be again (probably) explained by the degree of subdivision of the substrates, e.g., the available surface area. Regarding the metal carbides, for which data could be found, TiC cermets are reported to be stable towards fluorine (Reference 27). ZrC burns in fluorine at 250-300°C (Reference 28) and HfC (Reference 29) reacts more readily. The carbides of boron, tungsten, and silicon do not react at ambient temperature and they seem to react only slightly at 150°C, although another paper (Reference 30) describes SiC as reacting with fluorine without difficulty. The boride of zirconium does not burn in fluorine at room temperature but breaks up into bits (Reference 28) as hafnium boride does, which on the other hand shows no measurable reaction with fluorine up to 500°C (Reference 29). A similar room temperature disintegration upon exposure to fluorine was observed for silicon and boron specimens (Reference 31). Titanium boride was found to react with fluorine at 264°C, no mention being made of disintegration without reaction (Reference 32). Also, boron nitride is said to react at room temperature.

In regard to compatibility of materials of construction with fluorinated oxidizers in a dynamic system, such as a valve, three more findings are worth reporting. Toy, et al (Reference 33) describe all initiated reactions as confined to small areas. This may be explained by the statement of Tellier, et al (Reference 6) that a normally inert particle may react when impacted between poppet and seat. Since increased reaction

is most often caused by elevated temperature, which in this case is generated locally by impact energy, it is of interest that materials with high thermal conductivity are reported to resist ignition in fluorine better than those with low thermal conductivity (Reference 23), which would imply that materials are more resistant to fluorine if any locally created heat is carried away efficiently.

The initial rates of reactions between materials of construction and all the fluorinated oxidizers are high. The formation of the passivating film occurs rapidly (Reference 34) and passivation times of 30 minutes (Reference 22) up to a few hours (Reference 9) are considered sufficient. After this time film growth becomes negligible (Reference 9), although Myers, et al (Reference 35) found on nickel, monel, inconel, copper, aluminum, and steels no significant decrease of the corrosion rate with time (up to 15 hrs) and they concluded that the films of corrosion products formed on the samples were not protective. In view of the vast majority of references mentioning the essential cessation of film growth after a certain thickness is reached, the results of Myers et al, must be questioned, however. The fact that initial rates are high makes rates appear to decrease with time (Reference 14). For the reaction of copper with fluorine, some investigators report the rate to be pressure dependent (Reference 36), others find it up to 300°C independent of pressure (Reference 37) and explain it by random cracking of the fluoride film on the substrate. The overall rates for this reaction with fluorine are, however, consistently reported to be low and to be not much higher for chlorine trifluoride (Reference 38). Where reaction rates were found to be independent of temperature (ZrC, ZrB_2 + F_2), it was considered possible that the actual surface temperature of the specimen was much higher than the temperature measured, or that the reaction was diffusion limited (Reference 28). With ClF_3 and $FClO_3$, all materials tested were found to have low corrosion rates (0.0002 - 0.0004 inches per year) at 30°C (Reference 39) and tabulations of rates with fluorine (References 8, 15) and chlorine pentafluoride (Reference 11) have been published.

5. Mechanism of Surface Reaction

In all the cases where a solid surface is exposed to a (gaseous) fluorinated oxidizer, this surface is originally covered with an adsorption layer, which may consist of nitrogen or, more likely, oxygen. The first step in the surface reaction therefore has to be diffusion of the oxidizer to the metal surface, displacement of the adsorbed (oxygen) layer, and adsorption of the oxidizer molecules on the metal surface. In the adsorbed state, an activated complex is formed which entails dissociation of bonds in the oxidizer molecule (e.g., F - F) and breaking or weakening of the metal bonds (e.g., Ni - Ni). This process is followed by decomposition of the activated complex with concurrent formation of the primary products. If there are gaseous materials amongst these primary products, these will desorb from the surface (displaced by new oxidizer molecules) and diffuse away (Reference 29). The absorption of fluorine has been found by the same investigators (Reference 29) to be the controlling step up to

150°C with Si and up to 352°C with B. Above these temperatures, the diffusion of fluorine to the surface and of products away from the surface (both Si and B form gaseous products) become rate determining and thus the activation energy approaches zero. This diffusion of fluorine through the product layer has been shown to occur up to a critical thickness of the fluoride film when nickel oxide was fluorinated (Reference 40). When this thickness was reached, the film recrystallized opening grain boundaries for further attack. Jarry, et al (Reference 41) also concluded that fluorine migration to a nickel surface must be the governing process, since up to 700°C they could exclude diffusion of nickel through the film. Above this temperature, nickel migration also takes place. In the fluorination of iron, O'Donnel (Reference 42) concludes that up to a film thickness of 350 Å growth occurs by electron tunneling, whereas thicker films grow by fluorine diffusion.

It must be stressed here, that the above description of the film formation is largely simplified and that many other processes can and most likely do take place. For example, some of the variations in results from corrosion rate measurements (liquid fluorine) were suggested to be due to galvanic coupling, which may accelerate the corrosion on one member of the couple (Reference 19). On the other hand, no galvanic corrosion of metals in contact with aluminum strips could be detected at 66°C in CPF (Reference 11). It was also found that the rate of CuF_2 formation was increased when fluorine-chlorine mixtures, instead of pure fluorine, were reacted with copper, although only CuF_2 was produced, and the best method for CuF_2 production was shown to be the reaction between Cu and ClF_3 (Reference 43). This indicates that chlorine or the chlorine in CPF plays a role similar to that of a catalyst. This finding also supports the above statement that CTF and CPF may be more corrosive than fluorine.

In regard to the mechanism of the reaction of binary systems, Margrave, et al (Reference 28) were unable to say whether zirconium or carbon reacted preferentially when zirconium carbide was exposed to fluorine. Since after removal of the produced ZrF_4 the inner core of the specimen was rough and black, they believed it possible that Zr reacted first. However, it has to be realized that any carbon fluoride (CF_4) formed would have left as gas, and that finely divided powders or highly etched and roughened surfaces, in many cases, absorb all light to give the appearance of a black color.

During the above described surface reaction, the products formed are the fluorides of the elements forming the solid surface. With CPF and other fluorinated oxidizers, chlorine is also a product, yet it is of minor interest in connection with this literature review since the preferential reactions lead to primarily fluoride production. The fluorides formed are at ambient temperatures, depending on the element, solids, liquids, or gases. Since this fact is of major importance for an analysis of the metal to metal seal problems with fluorinated oxidizers, a detailed discussion will be reserved for later.

6. Film Properties and Protective Mechanisms

The films formed from fluorinated oxidizers and metals or binary compounds, where the products are solids at room temperature, can be safely considered to be composed of fluoride only, and also to contain the metal in its highest valence state; copper, for example, forms only the difluoride (Reference 38). Apparently, solid monofluoride is unstable (Reference 44). This also occurs with ClF_3 (References 38, 43) and the absence of CuCl in the film was proven. There is a report (Reference 36) that upon reaction of copper with fluorine a mixture of the mono- and difluoride is formed; however, this result is probably due to an improper analytical technique. That only fluorides are formed and no chlorides is supported by the fact that CuF_2 is formed from many copper salts, including $CuCl_2$ (Reference 45). The same behavior of chlorides towards fluorine can be found with sodium chloride (Reference 13) and iron trichloride (Reference 5). The film formed on iron has been shown by X-ray diffraction to consist exclusively of FeF_3 (Reference 42) although another paper mentions also the presence of FeF_2 (Reference 8). The statement, that exposure of iron to wet $FClO_3$ produced a film of magnetite (Fe_3O_4) (Reference 39) does not contradict the above results since it was proven that dry OF_2 forms only the fluoride and that the oxide can only form in the presence of water (Reference 46). The formation of only the highest valence state fluoride must be expected on a thermodynamic basis. Even zirconia was shown to produce only the fluoride (ZrF_4) and the absence of zirconyl-fluoride ($ZrOF_2$) was established by X-ray powder diffraction (Reference 47). In general, it is reported that chlorine and oxygen are replaced in the presence of fluorine (References 15, 48) and it is stated that for a given metal the film composition is the same whether it was formed from fluorine or a fluorinated oxidizer (References 9, 46). The finding (Reference 13) that on highly polished Al samples after exposure to GF_2 and LF_2 only hydrated aluminum oxide was detectable by electron diffraction is probably due to subsequent reaction of the fluoride film with atmospheric moisture, since AlF_3 is particularly hydrolytically unstable.

Fluoride film thicknesses have been measured on various materials including the following:

Material	Exposure Time	Film Thickness	Remarks
Aluminum	115 Min.	4.5 Å	(Ref. 23)
Aluminum	90 Hr.	13.5 Å	(Ref. 23)
Copper	105 Min.	5.3 Å	(Ref. 23)
Copper	90 Hr.	20.0 Å	(Ref. 23)
Iron	-	> 300 Å	(Ref. 42)
Nickel	1 Yr.	50-150 Å	Ref. 9 Extrapolated Data
Aluminum	1 Yr.	50-150 Å	Ref. 9 " "
Copper	1 Yr.	50-150 Å	Ref. 9 " "
Monel	1 Yr.	50-150 Å	Ref. 9 " "
316 Stainless Steel	1 Yr.	~ 1000 A	Ref. 9 " "

investigations (Reference 34) have reported that reaction practically ceases after film thicknesses have grown to 5 to 50 Å (on copper 50 Å are equivalent to 10-15 molecular layers (Reference 37). When the reported one year corrosion rates for Al, Ni, and Cu alloys and those for stainless steels are taken as a measure for film thicknesses produced in gaseous and liquid OF_2 (below 0.002 mils/year) (Reference 22), the thicknesses assuming the absence of sloughing-off and peeling, correspond to less than 500 Å. These film thicknesses are those produced during a single exposure to fluorine or fluorinated oxidizers. When these films are exposed to the atmosphere and then again brought into contact with e.g., fluorine, a reaction re-starts which can increase the film thickness considerably. For copper, for example, it is reported (Reference 9) that the original film is not thicker than 100 Å, however, the "regenerated" film is much thicker and tends to slough off. In many other cases it is believed (Reference 9) that repassivation of damaged films may lead to a nearly imperceptible production of particulate substances. In connection with the present problem that would mean that all surfaces, after contact with fluorine containing oxidizers and subsequent exposure to the atmosphere, have to be thoroughly cleaned of all films before the specimen can be re-exposed to an oxidizer.

The fluoride films are generally reported to be strongly adhering (Reference 8), especially while exposed to the oxidizer (Reference 9). Wire brushing in LF_2 (Reference 13) and flexing of the specimen (Reference 34) do not diminish adherence or create flaking or cracking of the film. Copper and high copper-nickel alloys in fluorine (Reference 49) and 410 stainless steel in CPF supposedly form particularly strongly adhering coatings. However, fluoride films formed on copper at 450°C have been found to exfoliate upon cooling (Reference 36), probably due to the different thermal expansion coefficients of the metal and the salt. An inexplainable behavior of the fluoride film on hafnium carbide is that it does not adhere up to 400°C, whereas it is more adhesive at 500°C (Reference 29). Despite the large number of references cited, which call the films adhering, the adhesion of the films is most likely not enough for a valve application. Work on contamination of propellant systems by particulates calls the fluoride films poorly adhering (Reference 6) and one paper (Reference 48) points out that adherent films are formed only on those metals into the atomic distribution of which the fluoride fits with a minimum distortion of the lattice structure. Since there will hardly exist a metal, the fluoride of which has the same crystal structure and lattice parameters as the metal, it can be concluded that passivating films cannot be sufficiently tightly bonded to the metal to withstand the continuous impacting of a valve. Other considerations responsible for reaching this conclusion are that in any case the corrosion products occupy a larger volume than the metal destroyed (Reference 50), in the case of iron, for example, the volume of FeF_3 is 4.9 times that of the iron consumed to form the fluoride (Reference 42).

The data found on impact sensitivy and impact strength are mainly concerned with proving that impact on the metal in the presence of an oxidizer does not initiate a catastrophic failure. Thus these impact tests do not reveal what effect impact has on the passivating film, it only can be deduced that the film was not damaged or, more likely, immediately reformed in a controlled reaction if the system is found not to be sensitive to impact. Thus, Al, Cu, Mg, or Ti showed no impact sensitivity in ClF_3 (Reference 12), Al, Ni, and Mg in CPF at 30°C did not ignite upon impact (Reference 11), and Al, Ni, Cu alloys and stainless steels did not exhibit impact sensitivity with liquid OF_2, whereas in that medium Ta was slightly, Ti moderately, and Mg extremely reactive (Reference 22). In liquid fluorine, titanium was found to be impact sensitive, also monel occassionally. The usual effect on Ti was pitting and discoloration. No reaction occurred when a LF_2 filled Ti-tube was impacted from the outside (Reference 51). Other investigators (Reference 19) observed that burning and explosion of Ti can be initiated by impact or other mechanical shocks only under special conditions, that this behavior is not reproducible and not limited only to Ti (monel also reacted). They conclude that such ignition is most often caused by a primer of some sort, which may be supported by another author (Reference 6) stating that a normally inert particle may cause reaction due to impact. Impact tests with metals contaminated with tungsten powder in LF_2 revealed that passivation reduced, but did not eliminate shock sensitivity. One out of 18 samples containing up to 10% by weight of tungsten reacted (Reference 34). These tests were performed because the fact that tungsten forms a gaseous fluoride was feared to possibly lead to complete disintegration of the specimens. The same group of authors (Reference 52) however, mention that impact sensitivity in LF_2 can also be caused by residues left after passivation. These residues were shown still to contain organic components and to be shock sensitive in LF_2.

The passivating films are described as hard by some authors, e.g., harder than the base metal (when formed from OF_2) (Reference 53), harder than the metal, like thin ice on water (Reference 54), hard and elastic, since flexing does not cause detectable cracking or flaking (References 13, 34); others describe the films as inelastic and brittle, since cyclic stressing and vibration may be sufficient to cause the film to break or spall (Reference 19), and finally the films are called relatively soft (Reference 6). Throughout this literature survey there could not be found any quantitative data on hardness, which may be not surprising since it is difficult in this case to separate the properties of the thin film from the properties of the base metal.

Data on friction coefficients of films were absent from the literature reviewed with one exception (Reference 27); however, these data were surprisingly quantitative. The friction coefficients of films produced on a 55 Ni/45 Cr alloy upon exposure to fluorine were measured to be $< 0.10 - 0.12$. Friction coefficients of synthetic films (76 CaF_2 + 23 LiF + 1 NiF_2 and 62 BaF_2 + 38 CaF_2) were found to be in the order of 0.17 - 0.24. Both types of films were beneficial in reducing friction and wear.

Although bromine trifluoride, BrF_3, is known to be a good solvent for metal fluorides (Reference 3), the solubility of films in the liquid oxidizers considered here is apparently low. Only TiF_4 on titanium is reported to be soluble in ClF_3 (Reference 9). That the films are at all soluble was shown by Kleinberg (Reference 13), who obtained on immersion in LF_2 negative weight changes for the specimens upon short exposures, whereas weight gains were recorded on long exposures. The explanation was that on short exposure the films are dissolved, whereas on long exposure no dissolution can occur because of saturation of the solvent (LF_2).

One film property to be kept in mind in a practical application is the tremendous affinity of the metal fluorides for water, which can even lead to hydrolysis (formation of oxides or oxyfluorides upon contact with water) (References 3, 38, 47). Even tungsten hexafluoride (WF_6), a gas, is hydrolytically unstable, although it is otherwise quite inert (Reference 55). This may be due, in part, to the observation that fluorides are the more hygroscopic, the higher the oxidation state of the metal is (Reference 3). Such surfaces, which were exposed to moisture, can be repassivated with the exception of copper (Reference 34), which forms under these conditions very thick films of corrosion products. In general, however, it is advantageous to clean such surfaces before re-exposure to oxidizer, since the water in the films can form in the presence of oxidizers products such as HF, which by itself increases corrosion. Interestingly, however, exposure to the atmosphere of copper (and stainless steel) surfaces, which were treated with fluorine, was reported not to produce etching or deposits (Reference 56).

Some miscellaneous properties of fluoride films are that they lose their protective capability when subjected to heat and vacuum (CuF_2) (Reference 36) and that they can form complexes and compounds with CPF under certain conditions (Reference 57). The film on copper or on $>60\%$ Cu-Ni-alloys is reported to be impervious to fluorine (Reference 49), whereas the NiF_2 film formed on nickel oxide is said to be porous (Reference 40). One property apparently common to all films is that they strongly absorb fluorine, fluorinated oxidizers, or hydrogen fluoride. NiF_2 thus absorbs strongly ClF_3 (Reference 40, 58), films on a variety of metals and alloys absorb appreciable amounts of fluorine, halogen fluorides, and hydrogen fluoride (Reference 34). In all cases these absorbed species are very difficult to remove which may explain that metal chlorides are reported to be formed together with fluorides where e.g., ClF_3 was used. The chlorine found in the film was most likely derived from absorbed ClF_3, which was notdesorbed from the film under the conditions employed. The recrystallization (Reference 40) of NiF_2 films on NiO, after reaching a critical thickness, has already been mentioned above. Through this recrystallization, the previously more or less homogeneous film becomes a mosaic network of crystallites, the grain boundaries between them providing paths for further reaction.

The mechanism, by which the metals are protected from continuous oxidizer attack, is generally agreed to be the formation of a passivating film. Exceptions are those metals and binary systems, which do not form solid fluorides. Thus it is recommended (Reference 51) that alloys containing C, Si, Nb, Mo, or W be avoided, because the volatility of the fluorides of these elements may cause pitting and accelerated corrosion. The formation of a solid fluoride film, however, is not the only mechanism providing protection from oxidizer attack. As a matter of fact, Sterner and Singleton (Reference 14) conclude that film protection is not the controlling mechanism since wire brushing of Cu and Mg specimens, submerged in LF_2, did not produce increased corrosion rates. Other factors contributing to passivation are the self-healing properties of the metal fluoride films and, very importantly, the "solution" of oxidizer in the films (References 36, 58). Whether this solution occurs by physical adsorption or by complex formation (reaction between oxidizer and metal fluoride) is unknown. Additional properties of the films influencing the protection of the metal are solubility of the fluorides in the oxidizer and the melting points of the fluorides. Both of these, of course, would be affected by the above mentioned possible complex formation between fluoride and oxidizer.

7. Discussion of the Problem

At the start of an analysis of the valve problem and a discussion of possible improvements or solutions, it is advantageous to focus on two established facts:

- The Marquardt designed ACS valve performs to specifications when operated with a fuel such as monomethyl hydrazine.

This satisfactory performance proves that valve failure in fluorine or chlorine pentafluoride is not due to the design, the impact load, the particles present in the propellant stream, or the material of construction as such. Friction, insufficient alignment, and adhesive wear by themselves or in combination, cannot be the reasons for leakage, at least not within the requirements for the 100,000 cycles operating period. The conclusions to be drawn from this experimental finding are that failure is due to the oxidizers, and since, under proper conditions, all materials of construction will react with CPF or GF_2 it can be said that excessive leakage is due to chemical reactions degrading surface finish, not due to surface finish deterioration brought about by physical or mechanical processes. This is not to say that mechanical or physical action may not be one of the original causes which initiate the chemical reaction in the presence of the oxidizer, where the same mechanical action in the absence of oxidizer would not lead to leakage, but instead, continuous impacting may reconstitute almost original surface finish if damage had occurred.

The second established fact to be kept in mind is:

- Many materials, after cleaning, resist CPF and GF_2 at ambient temperatures under static conditions. No special surface finish is required for this application.

This resistance of many materials to the very energetic oxidizers is generally agreed to be due to a process called passivation. Passivation consists mainly of the buildup of a layer of corrosion products (passivating film) on the material exposed to the oxidizer. This film hinders or prevents altogether further attack on the material, so that the coated material becomes compatible with the oxidizer. Previous experience has shown that nickel valves showed excessive leakage after relatively few cycles, although nickel is a favored material of construction for fluorinated oxidizers containers.

The conclusion, for the purpose of the valve failure analysis, is that the passivating film does not or cannot fulfill its function under impact conditions. Thus, for materials forming passivating films, impact forces on the film can be concluded to be reasons for leakage.

There are three more experimental observations on oxidizer valves which are of major importance for an analysis of the valve failure mechanism:

- Nickel poppets (Duranickel 301) after service in fluorinated oxidizers show general surface finish deterioration, but the most pronounced surface roughness is found in the sealing area.

- The surface roughness on nickel parts after operation in oxidizer can be substantially reduced by wiping or washing.

- A tungsten carbide (K-96) poppet, after being operated in CPF, showed no drastic surface finish deterioration, but a groove in the sealing area. The surface finish in the groove itself was comparable to that on the nonsealing surfaces.

These three observations point out that (a) the sealing area (the area where impact occurs) is a location of preferential reaction, (b) the excessive surface roughness on the nickel part in the sealing area is not caused by displaced metal, but by a water soluble compound, and, finally, (c) the tungsten carbide poppet has lost material (where the groove was formed), because tungsten carbide cannot form solid reaction products with CPF and GF_2. (The presence of 6% Co binder in K-96 is disregarded for the present time).

Without going into details, a preliminary analysis of the valve failure can be presented at this point. All valves perform to specifications when fuels are used, because fuels do not react with the materials of construction. At the same time, all materials of construction tested react with oxidizers such as CPF of GF_2, especially in the sealing areas. Materials, which form solid reaction products with the oxidizers, (e.g. nickel) react in such a way that excess amounts of solids are built up on the surfaces, especially in the sealing area, whereas materials, which form only liquid or gaseous reaction products, (e.g. tungsten carbide). lose weight, again preferentially in the sealing area.

As described above, under proper conditions all candidate materials of construction will react with CPF or GF_2. In the temperature range of interest to this valve program (-100 to 350°F, - 78.9 to 177°C), however, reaction of many materials with oxidizers is fortunately slight. Nevertheless, to select the proper material of construction, especially at the upper end of the above temperature range, it is not so m much a question of finding materials which do not react, but finding materials which react at a slow rate. The experimental findings substantiate this statement. If even slight reaction cannot be prevented, the nature and properties of the reaction products must be assessed as to whether sealing of the valve can be accomplished in the presence of these products. From all the literature data reviewed, it is apparent that these products are the fluorides of the elements present in the construction materials, no matter from which fluorinated oxidizer (e.g. GF_2 or CPF) they were formed. Of major importance for a valve application is the fact that some elements form gaseous or liquid fluorides (over the temperature range specified for the valve), whereas the vast majority of the elements form solid fluorides, which melt only at high temperatures. A compilation of some of the gaseous and liquid fluorides is presented in Table I.

TABLE I. SOME GASEOUS AND LIQUID FLUORIDES

	m. p.		b. p.	
	°C	°F	°C	°F
BF_3	-129.7	-202	-99.9	-148
CF_4	-184	-300	-128	-199
NF_3	-206.6	-340	-128.8	-200
SiF_4	- 90.2	-130	-86	-123
MoF_6	17.5	63	35	95
WF_6	2.5	36	17.5	63
PtF_6	57.6	136	Dec.	-
OsF_6	32.1	90	45.9	114
UF_6	64.5	148	56.2	133

As can be seen from the table, boron, carbon, and tungsten are among the elements forming gaseous (at room temperature) fluorides. At the same time tungsten carbide (K-96) was one valve construction material tested, which performed relatively well in both GF_2 and CPF. It is obvious that tungsten carbide (neglecting here the presence of 6% cobalt in K-96) cannot build up any solid corrosion products on exposed surfaces, since all products that possibly can be formed in contact with CPF or GF_2 (WF_6 and CF_4) are gases at room temperature. These are swept away with the oxidizer stream and therefore no product accumulation on either sealing or nonsealing surfaces can occur. This reasoning is substantiated by the experimental finding, that the K-96 poppet, operated in CPF and GF_2, showed a groove in the sealing area, but no materials buildup.

The majority of elements, however, form solid products which must be assumed to remain in the sealing area, at least to some extent. The excess material on the Ni-301 poppet, which could be removed by wiping or washing, tends to support this assumption. (Nickel fluoride is water soluble). A general review of fluoride films on metals and alloys revealed that these films can reach thicknesses from 10 to 2000 Å on static exposure, but normally are about or below 200 Å thick. These films are porous, and after reaching a certain thickness can recrystallize. In this process, islands of crystallized fluorides are formed, separated by grain boundaries which constitute cracks and channels in the fluoride surface. Due to porosity, the films can absorb oxidizer molecules, which apparently contribute to passivation, since the films lose their passivating capacity when exposed to heat and vacuum (the absorbed oxidizer molecules are removed). The films are also slightly soluble in the oxidizers and react readily with moisture.

These fluoride film properties are necessary, but not sufficient information for an analysis of the failure of e.g., the Ni-301 valve. To understand the reasons for leakage, when the valve is operated in fluorinated oxidizers, all the processes have to be considered which take place when the specimen is exposed to the oxidizer and subjected to impact.

Before exposure to oxidizer, the metal surface can be assumed to be covered with a thin oxide layer or at least with a layer of adsorbed oxygen. Upon exposure to oxidizer, the adsorbed oxygen is most likely very rapidly displaced by oxidizer molecules (due to higher heat of adsorption) and any oxide film present will be transformed into a fluoride film. The rate of this exchange will depend on the material of construction, but within sufficient time all oxide films will be replaced by fluoride films. Since these films are known to grow to appreciable thickness (e.g., 200 Å ~ 40-60 molecular layers), it becomes obvious that their presence cannot be neglected. Instead of a metal to metal seal, the valve shuts off through contact between the two fluoride films present on both poppet and seat. Thus, exposure to oxidizer has modified the most important part of the valve in regard to leak-tight closure, the sealing

surfaces. In this process the surface has lost, to a large extent, all properties which were inherent to the metal, and acquired many properties which are contributed by the metal fluoride. Among the surface properties which thus were changed in the process of metal fluoride formation are sensitivity to moisture, hardness, and coefficient of thermal expansion, but most importantly in regard to sealing, density, thermal conductivity, tensile and compressive strength, ductility, and crystalline structure.

Consider first the change in density occurring when the metal or alloy in the surface is transformed into the fluoride. (Only elements forming solid fluorides are evaluated now). It is clear from the literature that in most cases the density of the fluoride is considerably lower than that of the metal (one exception is, for example, beryllium). Such a density change must, by definition, be associated with a volume change. These volume changes have been compiled in Table II for some of the elements of interest to this literature search. It will be seen that this volume change is an expansion by a factor from 2.04 to 5.34, depending on the material. This means that the solid corrosion products (the metal fluorides) occupy from ~2 to ~5 times the volume of the material (the metal) from which these products were formed. From the standpoint of a leak-tight valve, this volume expansion by itself can be assumed to be not too severe a change, since the expansion of the film along the valve axis is very small compared to the stroke length. However, the important question arises whether during this volume expansion the original surface finish can be preserved. To arrive at an answer, it is necessary to investigate the crystal structures of the base metals and of the fluorides (it is assumed that the fluoride film has the same crystal structure as bulk fluoride) and to evaluate the interphase between metal and fluoride and its effect on sealing under impact. It is safe to say that there exists no metal fluoride which has the same crystal structure as the metal, from which it was formed. For example, metallic Co, Cr, Ni, Cu, and Fe all crystallize in the cubic system, whereas their fluorides are tetragonal (niF_2), hexagonal (CoF_3), rhombic (FeF_2, FeF_3), monoclinic (CoF_2, CrF_2), and even triclinic (CuF_2) (Reference 58).

Aside from these changes in volume and crystal structure, one more important change occurs when the metal surface is fluorinated, namely the change in the type of bonding between the particles in the surface. In the metal each atom is bonded to its neighbors by which is called a metallic bond, whereas each atom in the film is bonded to its nearest neighbors by an ionic bond, which in essence can be compared to electrostatic attraction of positive (metal ions) and negative (fluoride ions) particles. The major differences between metallic and ionic bond, which are of importance to this valve sealing problem, are the rather precise location of electrons in the ionic crystal as opposed to a relatively mobile "electron gas" in the metal (or alloy), and the resulting electron density between neighboring atoms. In the ionic crystal, this electron density reaches zero at some point between two neighboring ions (which are of

TABLE II

VOLUME EXPANSION DURING FLUORIDE FORMATION[a]

$$\Phi = \frac{d_m w_f}{d_f w_m} \cong \frac{V_{mol\ f}}{V_{atom}} \times \frac{w_f}{w_m}$$

Fluorides Formed	Material	d_m	d_f	w_m	w_f	Φ
Difluorides:	Be	1.85	1.97	9.01	47.01	4.90
	Cr	7.20	4.11	52.00	89.00	3.03
	Ni	8.90	4.8	58.71	96.71	3.05[b,c]
	Co	8.90	4.46	58.93	96.93	3.28
	Cu	8.92	4.23	63.54	101.54	3.37[d]
Trifluorides:	Al	2.70	2.88	26.98	83.98	2.92
	Al_2O_3	3.97	2.88	101.96	167.96	2.27[e]
	Fe	7.86	3.52	55.85	112.84	4.51
Tetrafluorides:	Zr	6.49	4.43	91.22	167.21	2.69
	ZrB_2	6.09	4.43	112.84	167.21	2.04[e,f]
Pentafluorides:	Ta	16.6	4.74	180.95	275.94	5.34
	TaC	13.9	4.74	192.96	275.94	4.19[e]

a) All densities from Handbook of Chemistry and Physics, (Ref. 59).

b) $\Phi = 3.11$ if $d_f = 4.72$ is used, (Ref. 60).

c) Compare volume change calculated from adjusted atomic and molecular volumes (Ref. 5)

$$\Phi = 3.03 \text{ from } \frac{V_{mol\ f}}{V_{atom}} \frac{w_f}{w_m} = \frac{20.1 \times 96.71}{10.9 \times 58.71}$$

d) $\Phi = 2.94$ if $d_f = 4.85$ is used, (Ref. 45).

e) Based on formation of solid fluoride only. Gaseous products such as O_2, BF_3, CF_4 neglected.

f) $\Phi = 2.06$ if $d_m = 6.17$ is used, (Ref. 61).

Terms Used Above

Φ	Volume expansion ratio from atom to fluoride molecule	w	= Weight
d	Density	w_{at}	= Weight of atom
		w_m	= Weight of molecule

opposite charge) and this is one reason that ionic crystals can be cleaved along crystal planes. In a metal or alloy, the electron density between neighboring atoms never reaches zero, which most likely is the reason for the high ductility of metals as compared to the brittleness of ionic crystals. Such electron density measurements have been carried out using Fourier analysis of X-ray interference lines. In a simplified form, the variation of electron density along the shortest distance between two neighboring atoms or ions can be represented for a metal, such as nickel, or a salt, such as nickel fluoride, by the following diagrams:

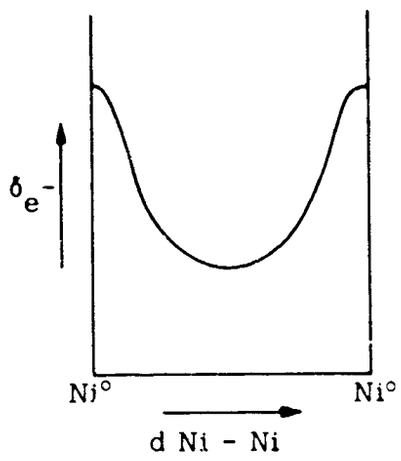

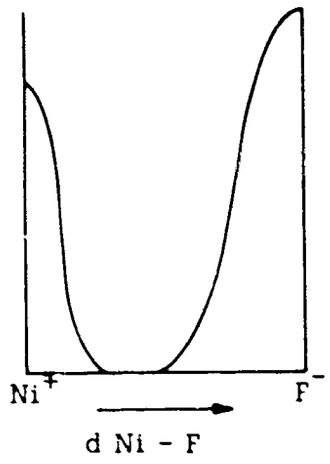

Having developed some knowledge about the fluoride film properties and about the changes produced on the surface during film formation it is now possible to analyze the reasons for the oxidizer valve failure. As stated above, one major difference between a valve performing to specifications in the fuel line while failing in the oxidizer line is the presence of a fluoride film on the surfaces of the latter valve. (This of course is true only for valves built from materials forming solid fluorides, such as e.g., nickel). Since sealing is now supposed to be accomplished by the fluoride films present on poppet and seat, the following questions arise: a) can the fluoride film be mechanically and structurally as good or better than the metal, b) can the fluoride film retain its integrity and protect the metal from the oxidizer under impact, and most importantly, c) can the fluoride film have the same or a better surface finish than the metal?

Based on the above described changes in density, volume, crystal structure, and the nature of bonding between the atoms forming the surface layers, all three questions must be answered with no. The fluoride film on a nickel surface must inherently be mechanically and structurally inferior to the base metal surface, because the film

is highly disordered compared to the metal. Under idealized conditions the metal surface is formed by regularly arranged metal atoms, the distances between them all being equal. Due to the metallic type of bonding, which holds these metal atoms together, the surface has a certain degree of ductility (displaced atoms are readily incorporated into the regular atom arrangement without major distortion) and is thermally quite conductant (any heat formed from any possible process is quickly transported away). On the other hand, the metal fluoride formed directly on the metal surface is in a state of disorder and strain. Since upon exposure to oxidizer, theoretically all metal atoms in the surface will form the fluoride, it is clear that these fluoride molecules cannot be accommodated in the surface based on the above calculated volume expansion. Consequently, buckling or similar processes must occur. In addition, these fluoride molecules are still under the influence of the metal lattice, thus not free to rearrange or organize themselves. Only when sufficient fluoride has been formed (the film has reached a certain thickness) can the fluorides crystallize in their own crystalline system, but only in places far enough away from the influence of the metal surface. Thus it becomes obvious that the interphase between metal and fluoride never can attain any degree of order, therefore the interphase must always remain mechanically weak. Even if there were the possibility that the fluoride can crystallize throughout to the metal surface the interphase would not become any stronger since, as pointed out above, the metals and their fluorides crystallize in different systems and are therefore not capable of intimate contact and bonding.

Based on the above described fluoride properties, it is also obvious that the fluoride film cannot retain its integrity (if it were perfectly crystallized and free of strain) and cannot protect the metal under impact. Since the fluoride film is an ionic lattice, it can readily be cleaved along crystal planes. It is of no importance that during the literature search no data on the hardness of fluorides could be found. Naturally, a particle harder than the fluoride can be assumed to cause cracking when pressed into the fluoride surface during impact. However, it is well known that, for example, a sodium chloride window can be split, when a sodium chloride chip is pressed into its surface. Thus, a particle of equal hardness is capable of cracking the film, and it is easy to imagine that many fluoride particles are available for cleaving any crystallized fluoride film while the valve is being operated. It becomes apparent that the fluoride film on, e.g., a nickel poppet during impacting never can reach a steady state. One loose fluoride particle can break the film, thus forming more fragments, which in turn can produce new cracks. This destruction of the film is counteracted by the self-healing capability of the film and by continuous recrystallization, so that (theoretically) at least a dynamic equilibrium is reached which prevents catastrophic failure of the nickel part.

With respect to a tightly sealing valve, however, it is not so much a question whether catastrophic failure is prevented but whether the valve will seal upon impact. One of the principles of the Marquardt designed ACS valve is to achieve sealing with two highly finished surfaces. From the above explanations, it would appear that original surface finish cannot be preserved during the formation of the film. Although with sufficient film thickness the metal fluoride can crystallize, the surface of the fluoride film will not be homogeneous, but will contain a large number of grain boundaries even if no impact occurs. The surfaces of the crystalline islands (separated by grain boundaries) must not necessarily lay in the same plane, resulting in a surface with many steps. The strongest argument against preservation of surface finish during film formation, however, is the above described volume expansion. Since it is clear that the fluoride film on e.g., the circular nickel poppet cannot grow to any large extent over the edge of the poppet (the circumference) this volume expansion must almost entirely occur in one direction only: perpendicular to the surface. Such a process is physically impossible without transport of metal fluoride both parallel and perpendicular to the surface. Considering all the factors influencing these migrating fluoride particles such as surface tension, crystal lattice forces of both metal and crystallized fluoride, and particularly continuous impacting between the two surfaces engaged in the same fluoride transport process (where migrating fluoride from the seat can even transfer to the poppet) it becomes very unlikely that the fluoride covered surface can retain the same high surface finish as the not exposed metal.

One more question demanding an answer is the greater extent of surface finish deterioration in the sealing area as compared to nonsealing areas. From the discussion so far, it is apparent that the chemical reaction (the fluoride formation) between oxidizer and material of construction is the reason for surface finish deterioration and finally leakage. Thus, the more severe corrosion in the sealing area can be assumed to be due to a larger degree of chemical reaction. One common method to make a reaction proceed faster is elevation of temperature. In regard to the larger extent of reaction in the sealing areas of the valve, it is quite apparent that elevated (higher than in nonsealing areas) temperatures can be generated by processes such as impact, friction, compression, and of course, the larger amounts of energy set free due to greater extent of reaction.

To summarize, oxidizer valve failure is primarily caused by chemical reaction between oxidizer and material of construction. This reaction produces metal fluorides which cannot provide highly finished surfaces for sealing. Under impact the metal fluorides cannot retain their integrity, but are continuously transported and rearranged, thus further complicating the problem. The more severe surface deterioration in the sealing area is caused by more extensive reaction, which is brought about by locally elevated temperatures. These elevated temperatures are the result of impact, friction, compression, and energy set free due to a larger extent of reaction.

8. Possible Solutions and Materials Recommended for Testing

Several approaches present themselves which, individually or in combination, should lead towards the production of a valve for CPF or GF_2 (or any other fluorinated oxidizer) service meeting the specification of less than 30 scc/hr of helium at 435 psig pressure after not less than 100,000 cycles.

Based on the discussion in the preceding section, it is evident that reaction between oxidizer and valve material cannot be prevented. It is also evident that this reaction on certain materials of construction forms solid fluoride films which are not capable of providing hard and smooth sealing surfaces. The first, most important, and probably only practical step to eliminate excessive leakage is therefore the elimination of the fluoride film. Since all materials under proper conditions will react with fluorinated oxidizers, the only possible way to eliminate a solid fluoride film is to employ a material of construction which, within the temperature range of valve operation (-100 to 350°F), cannot form a solid fluoride. Candidates for the lower end of this temperature range are boron, carbon, silicon, boron and silicon carbide, or boron nitride. At room temperature and above tungsten, tungsten carbide, or tungsten boride will also produce only liquid or gaseous fluorides. (Compare Table I). The relatively good performance of a K-96 valve (94% WC, 6% Co binder) is thus explained by the fact that only 6% of the K-96 material was able to form a solid fluoride, whereas 94% of all elements formed gaseous fluorides, which were swept away with the oxidizer stream. The appearance of a groove in the K-96 poppet is thus also explained. Extending this line of reasoning leads then to the conclusion, that a valve built from pure tungsten carbide or from tungsten carbide with e.g. tungsten binder should outperform the K-96 valve.

A second, yet less desirable step to produce a satisfactorily performing valve is to choose such a construction material, which will, during reaction with the oxidizer, produce the smallest amount of solid products or produce the smallest possible volume expansion on the corroding surface. Examples are the above mentioned K-96 and aluminum oxide (compare Table II). The reasoning behind this approach is that the less the amount of solid products formed on the sealing surfaces the better the chances of accommodating these products in the surface. According to this hypothesis aluminum oxide, Al_2O_3 was an attractive candidate. Firstly, during reaction with e.g. CPF the oxygen in Al_2O_3 will leave as a gas, which is the reason for the relatively small volume expansion of Al_2O_3 during reaction (2.27, compare Table II). Secondly, Al_2O_3 reacts with e.g. CPF at a considerably lower rate than K-96, thus producing less solid corrosion products within a given time.

The third approach was aimed solely at reducing or even preventing the preferential reaction in the sealing areas. It is postulated that this preferential reaction is due to locally elevated temperature. To prevent this temperature elevation the impact load should be reduced. In addition, and probably more important, a better alignment of poppet and seat will serve the same purpose. Through better alignment the impact load will, during initial impact, be distributed over the whole sealing area and not only over a small segment as is the case when poppet and seat meet under an angle. Complete alignment will also eliminate friction and sliding of the poppet relative to the seat.

For proper seal performance the common procedures used with fluorinated oxidizers have to be, of course, also observed. These are absence of foreign matter, absence of stress, strain, or porosity in the metal surface, and, most important and most difficult to achieve, absence of moisture in the system and the surrounding atmosphere.

Based on the approaches just described and based on the findings of the overall literature search, the most promising candidate materials in view of their physical and chemical properties were tungsten carbide, WC, and boron carbide, B_4C, both possibly with tungsten binder. Aluminum oxide, Al_2O_3, was a second choice candidate, yet believed worth an experimental evaluation.

SECTION IV

VALVE SEAT TO POPPET IMPACT TESTS

1. Summary of Test Results

One of the major tasks in determination of the passive film properties which were contributing to failure of the valve seal was determination of the impact force levels the film was being subjected to during valve closing. A series of tests were completed to determine the impact forces generated during valve closing by impact of the valve poppet with a force transducer simulating the valve seat.

Four armature configurations were tested to document impact characteristics of all hard seat advanced ACS valves. Measured valve configuration data was used to analytically predict the impacts for the test configurations. Analytical predictions were compared with test measurements made in the special test fixture simulating the valve seat. While data agreement with analytical predictions was not exact, test results were reasonably close to predictions for operation of the valve with GN_2 as the test fluid. Impact forces measured using water as the test fluid were consistently lower than the analytically predicted values.

Measured impact data was consistent enough to allow verification of the analytical technique developed for prediction of poppet to seat impact in gas and development of empirical correlation factors for operation of the value in water. The empirical relationships derived are:

1. For the integral poppet armature, $F_{water} = F_{gas}/1.5$
2. For the flexibly isolated poppet, $F_{water} = F_{gas}/3.0$ (Typical value for the current valve configuration is about 40 pounds force).

The difference between impact forces measured in GN_2 and water showed that fluid viscosity and density can significantly affect valve closing impact forces.

2. Test Hardware Configurations

Four basic valve configurations were tested during the program. Basic differences between configurations consisted primarily of changes in spring rates of either the poppet self alignment flexure or the armature guidance flexure or both. Figure 1 shows a typical valve assembly. The four configurations tested were as follows:

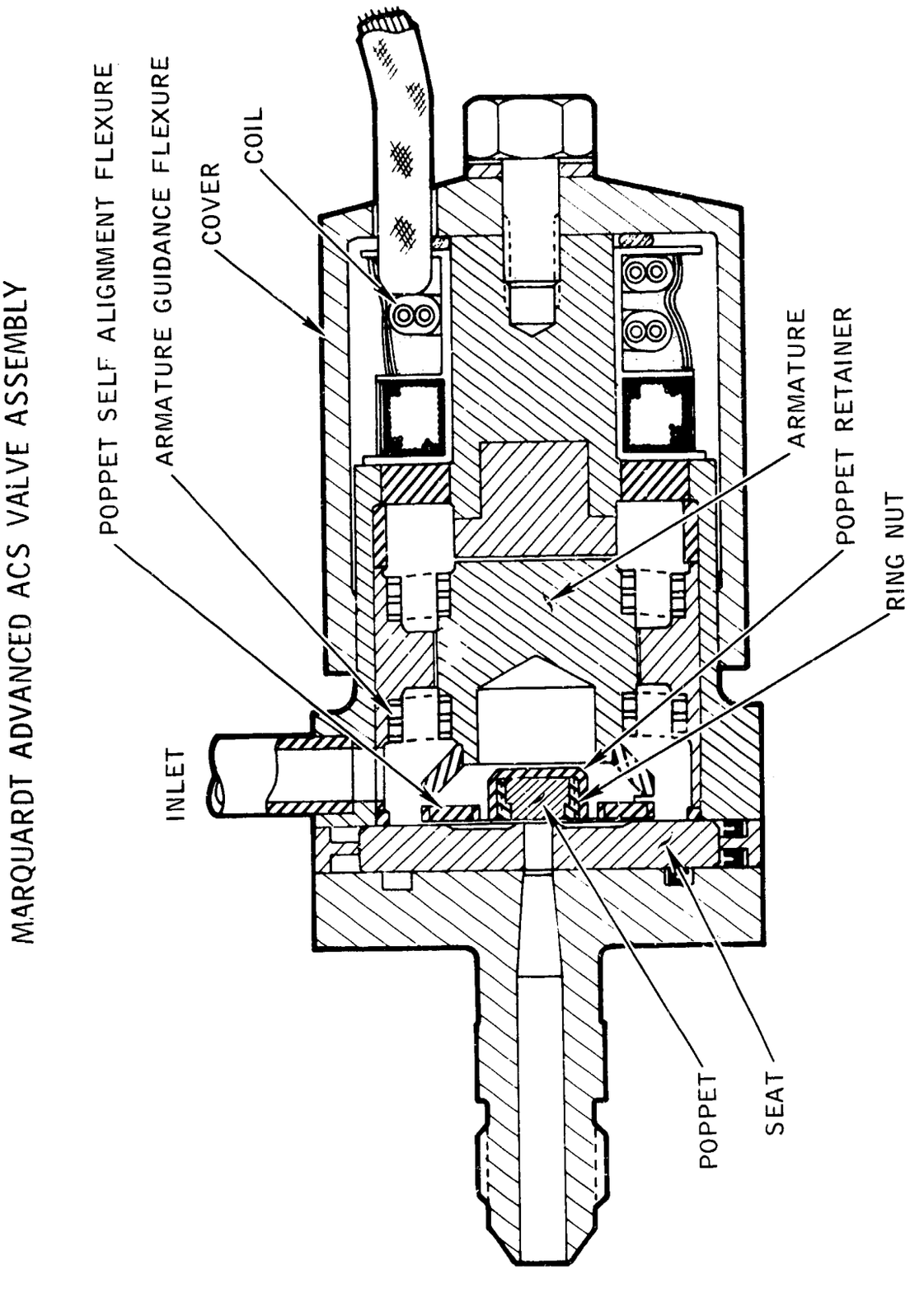
MARQUARDT ADVANCED ACS VALVE ASSEMBLY
POPPET SELF ALIGNMENT FLEXURE
ARMATURE GUIDANCE FLEXURE
COVER
COIL
INLET
ARMATURE
POPPET RETAINER
RING NUT
POPPET
SEAT

Figure 1

Configuration 1

The original ACS valve design. This configuration featured an integral poppet and high rate poppet self alignment flexure. The poppet self alignment flexure design spring rate was 13,000 lb/in. and the armature guidance flexure design spring rate was 680 lb/in. Nominal design valve stroke was 0.012 inch.

Configuration 2

The present valve armature design. This design incorporates a bumper into the poppet self alignment flexure. Poppet self alignment flexure design spring rate was 1300 lb/in. with armature flexure design spring rate of 280 lb/in. Nominal design valve stroke was 0.012 inch. This design was one of the two valve designs selected for propellant tests as the current version "normal impact" valve.

Configuration 3

The current configuration design with stroke increased from 0.012 inch to 0.024 inch to lower pressure drop for gaseous oxidizer usage.

Configuration 4

A modified version of the present valve design with the armature guidance flexure spring rate reduced from 280 lb/in. to a nominal design value of 60 lb/in. This design was fabricated to allow evaluation of impact forces and subsequent cyclic wear in propellant of a valve designed to have very low impact forces and was the second valve configuration used for propellant tests.

In order to accurately set up the closed seat preload, each test armature was checked to determine the actual combined spring rate of the flexures. The actual spring rates were used to determine the dimensions required to obtain seat preloads. Table III lists the actual valve strokes, preloads and combined spring rates measured prior to and during the tests with the baseline design values originally intended to be used during the tests. In general, all measured values were close to the desired values except for preload in the high rate armature valve. In that case, the preload was 1.5 pounds less than the value desired.

3. Impact Force Prediction Technique

Valve seat impact loads to be expected were analytically predicted prior to the tests. A straight forward analytical approach to predicting impact force was used based on the following assumptions. Figure 1 may be referred to for location of valve critical parts.

TABLE III

IMPACT TEST VALVE CRITICAL DIMENSIONS

		CONFIGURATION			
		1	2	3	4
Stroke (Inches)	Design Goal	.012	.012	.024	.012
	Actual	.012	.012	.024	.012
Seat Preload (lb)	Design Goal	3.0	1.5	1.5	0.4
	Actual	1.5	1.5	1.5	0.3
Poppet Flexure Combined Spring Rate (lb/inch)	Design	646	231	231	57.3
	Actual	583	187	187	38.7
Poppet Weight (X-15) (lb)	Design	.0013	.001429	.001429	.001429
	Actual	-	-	-	.001401
Ring Nut Weight (lb)	Design	None (Integral Poppet)	.00630	.00630	.000630
	Actual	-	-	-	.000603

1. The effective mass striking the seat was only considered to be that of the poppet, ring nut and center body. These masses were assumed to be effectively decoupled from the main armature mass by the poppet support flexure.

2. Typical values of valve armature closing travel time were used to calculate impact velocity of the poppet as follows:

   Assuming a linear velocity increase from the open to closed armature position with initial velocity equal to zero:

   $$\bar{V}avg = \frac{Stroke}{Time}$$

   $$Vavg = \frac{Vopen + Vimpact}{2}$$

   $$Vimpact = \frac{2(Stroke)}{Time}$$

   $\bar{V}avg$ = Average Velocity

   V = Instantaneous Velocity

3. Complete conservation of energy with no losses in energy to either viscous damping or internal spring resistance losses.

   From the assumed effective mass striking the seat and the calculated impact velocity, kinetic energy of the mass can be calculated:

   $$KE = 1/2\ MV^2$$

The kinetic energy of the system at impact can be equated to the potential energy stored in the seat after impact providing effective spring rate of the seat and local support is known. For a fixed edge plate similar to the valve seat support, deflection under load is defined as:

$$Y = \frac{\alpha W a^2}{Et^3}$$ (Ref. Roark, Formulas for Stress and Strain)

Spring rate of the seat support,

$$= \frac{W}{Y} = \frac{Et}{\alpha a^2} = R_{seat\ support}$$

Y = Deflection
W = Load applied
E = Modulus of Elasticity
t = Thickness
α = Deflection coefficient
a = Radial dimension

In addition to spring rate of the basic seat support, deflection of the raised annular portion of the valve seat was considered in calculation of total effective seat spring rate by:

$$Y = \frac{W\ell}{AE}$$

Total seat spring resistance, R, then becomes

$$R = \frac{W}{\Sigma Y}$$

Assuming conservation of energy and no energy losses in the system, Kinetic energy at impact can be fully converted to elastic strain energy in deflection of the valve seat:

$$\delta_{seat} = \frac{P \quad lb}{R \quad lb/in.}$$

δ = Deflection
P = Impact load
R = Seat spring resistance

The kinetic energy at impact is converted to strain energy of the deflected spring (seat) as shown in Figure 2:

$$KE = 1/2\ P\delta_{tot}; \qquad R = \frac{P}{\delta} \qquad \delta = \frac{P}{R}$$

$$KE = 1/2\ P\ \delta = 1/2\ P\ \frac{P}{R} = \frac{1P^2}{2R}$$

and the force required to deflect the seat can be solved for

or

$$P^2 = 2R\ (KE)$$

Thus from calculated kinetic energy and seat deflection resistance, values of impact can be computed assuming conservation of energy with no frictional or other losses.

4. Test Setup

The complete test setup shown schematically in Figure 3 allowed testing with either gaseous nitrogen or water with valve inlet pressure variable between 0 and 500 psi. A photograph of the physical setup is shown in Figure 4.

IMPACT FORCE AS A FUNCTION OF STRAIN ENERGY

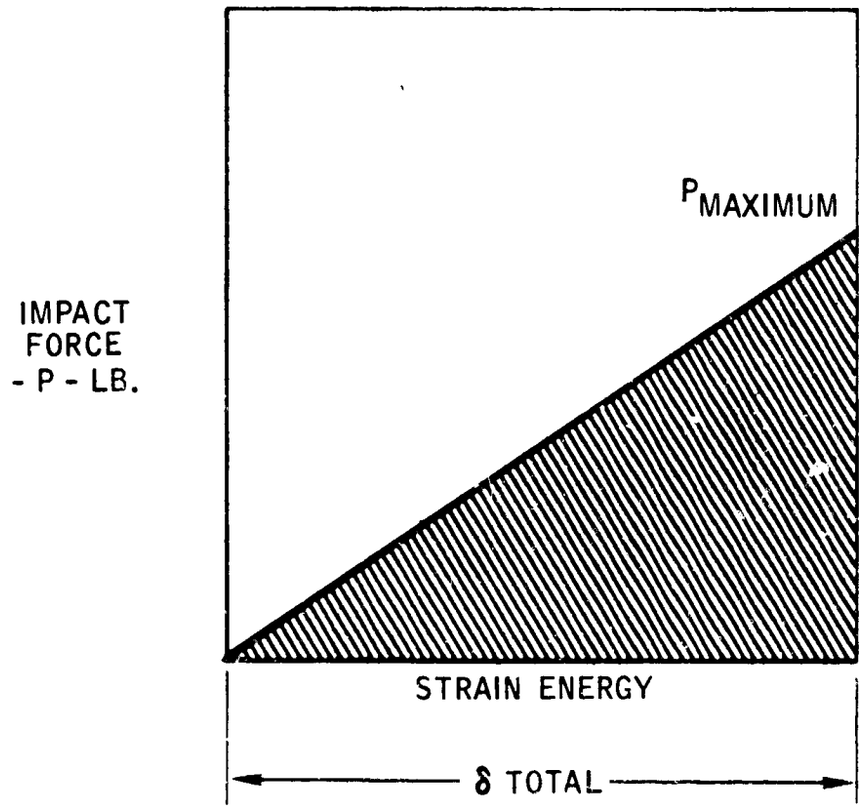

Figure 2

VALVE SEAT IMPACT LOAD TEST SETUP

TMC BUILDING 37

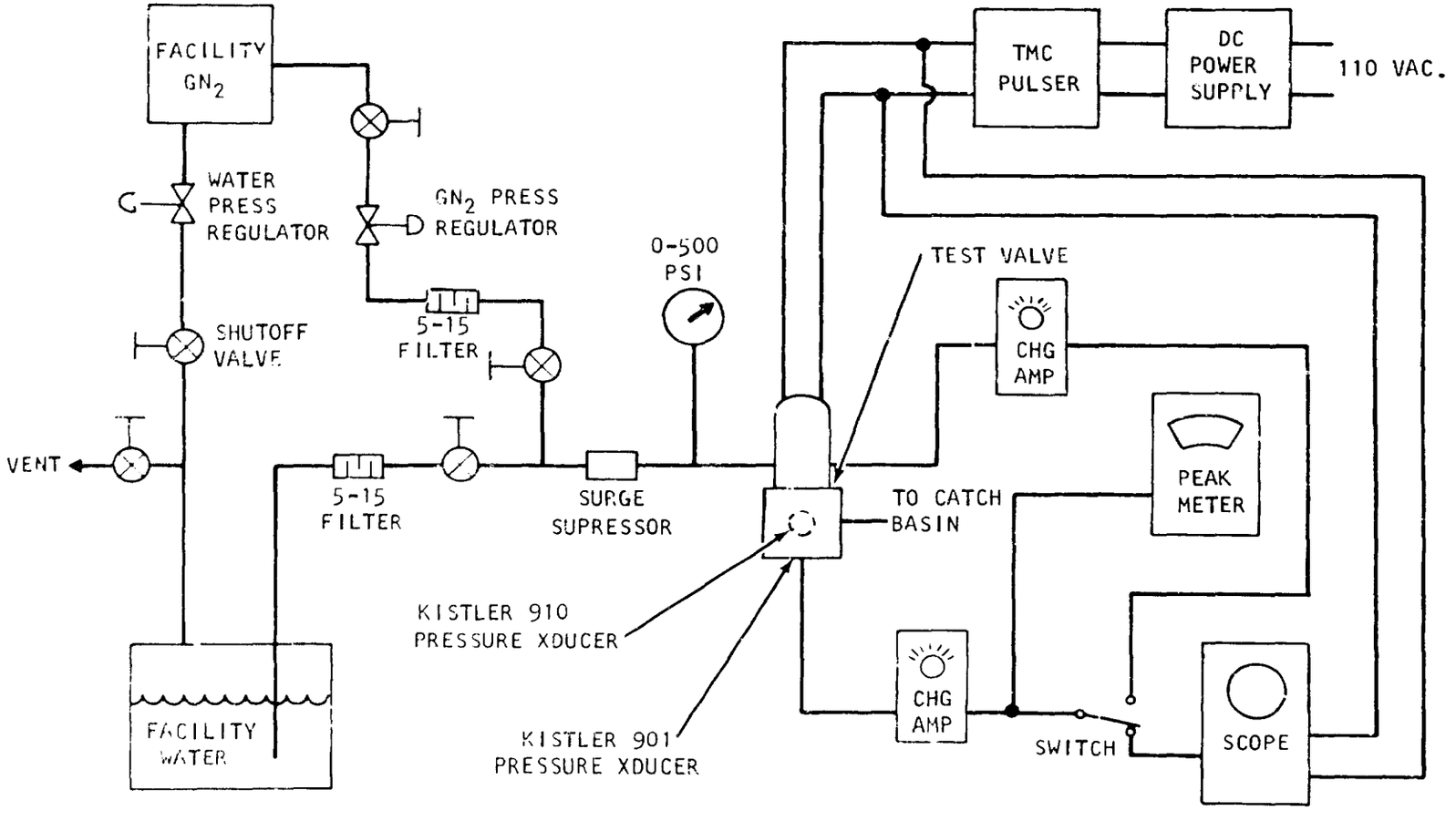

VALVE POPPET TO SEAT CLOSING IMPACT TEST SETUP

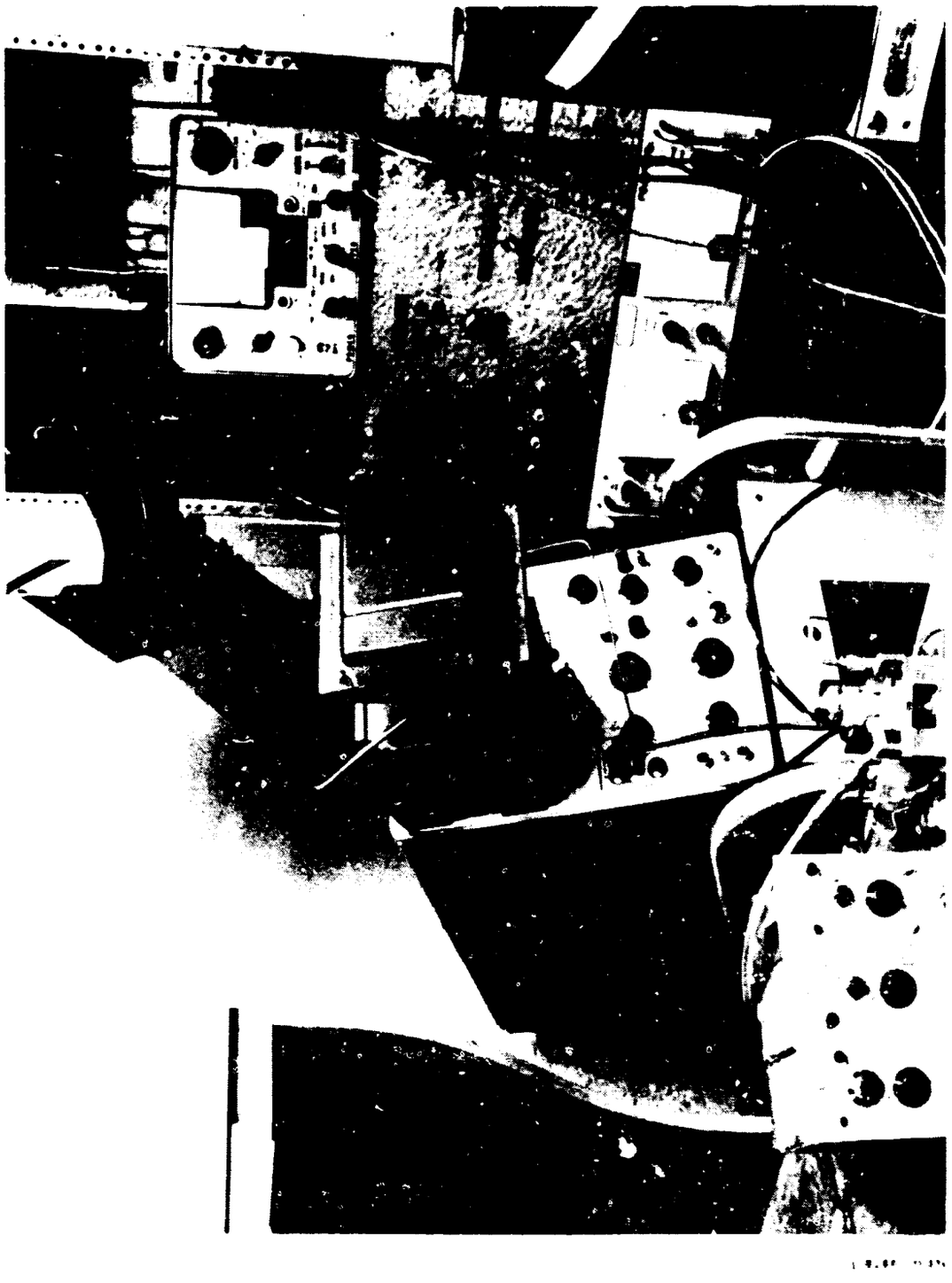

Figure 4

A special test fixture, P/N X26700, was designed and fabricated to allow measurement of the closing impact loads. The basic fixture, shown in Figure 5 with a valve installed, was designed to simulate and substitute for the normal seat of the valve. An 0.043 inch orifice was located downstream of the valve seat to provide a maximum delta P of 45 psi across the valve seat at 450 psi inlet pressure, the design point for valve operation on an engine. The actual seating location was direct-connected to a Kistler Model 910 high response piezoelectric force transducer to allow measurement of the valve closing impact loads.

Pressure variation in the valve seating area was measured with a Kistler Model 901 high response piezoelectric pressure transducer to assure that water hammer did not contribute significantly to closing loads. Response capabilities of both transducers are in excess of 100,000 Hertz. Output of the transducers was displayed on a Tektronics oscilloscope and recorded with a polaroid camera.

Response adequacy of the test setup for measuring the impact forces was checked by recording the waveform of the impact spike, determining the rise time of the pulse and comparing the frequency associated with the rise time with response capability of the measuring equipment. The impact force output, shown in Figure 6 as an expanded waveform, had a rise time of approximately 12 microseconds (or frequency of approximately 20,000 Hertz). These rise times were well within the capability of the measuring and recording instrumentation.

5. Test Results

Each of the four valve configurations was tested to determine impact forces resulting from valve closure. The tests were conducted using both water and gaseous nitrogen as test fluids. The impact forces resulting from valve closure were measured at 0, 100, 200, 300, 400 and 500 psi for all configurations except for Configuration No. 3, the long stroke valve. The coil in the valve used for the Configuration No. 3 test was sized for only a 0.012 inch stroke and had insufficient power to open the valve under high pressures with the 0.024 inch long stroke tested. As a result of the power problem, Configuration No. 3 was tested to only 350 psi inlet pressure. That was sufficient pressure to establish the trend and force levels to be expected in the test fixture at 500 psi.

Typical maximum measured impact force and poppet travel time in both GN_2 and water are shown in Figures 7, 8, 9 and 10 for test valve Configurations No. 1 through No. 4, respectively, as a function of inlet pressure. The figures allow direct comparison of impact forces measured in both GN_2 and water for each test configuration as well as with the analytically predicted forces. The data obtained in water are consistently lower than the data taken using GN_2 as the test fluid.

OXIDIZER VALVE MOUNTED ON IMPACT TEST FIXTURE

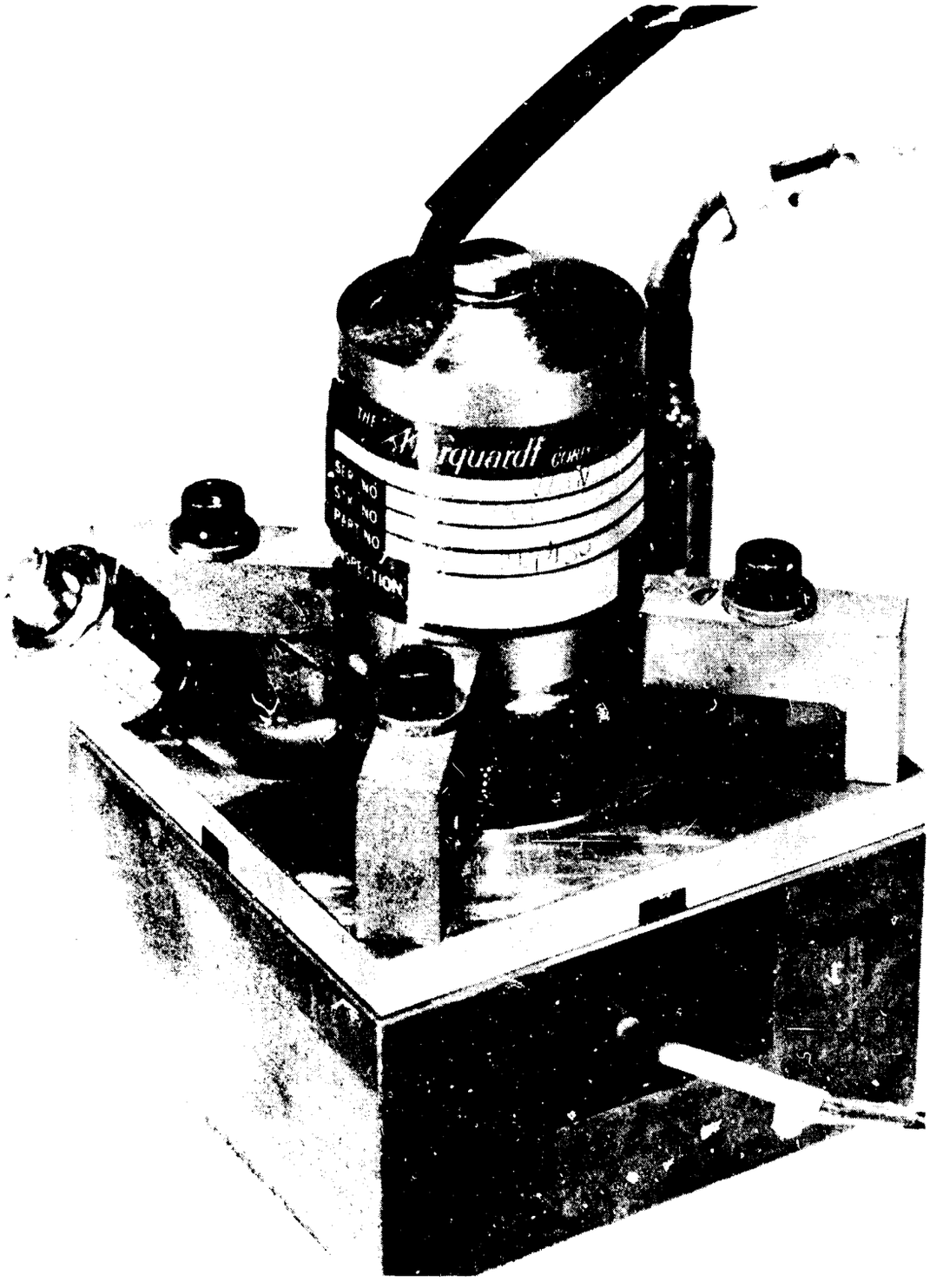

NEG. 9987-1

Figure 5

CLOSING FORCE AS A FUNCTION OF TIME

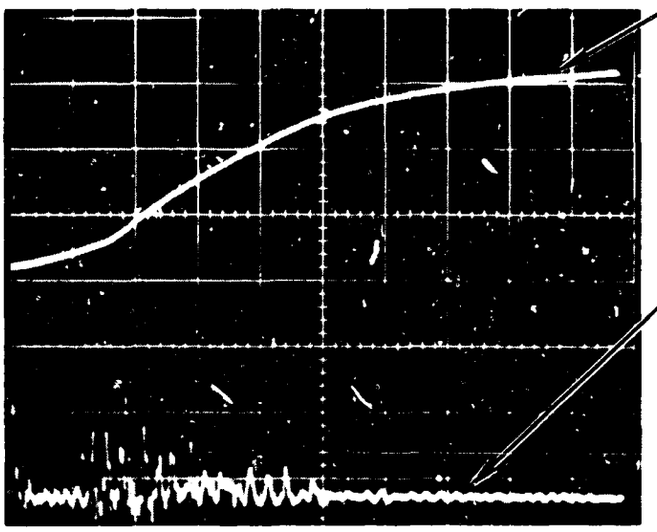

Figure 6

VALVE SEAT CLOSING IMPACT FORCE AND POPPET TRAVEL TIME AS A FUNCTION OF INLET PRESSURE FOR CONFIGURATION NO. 1

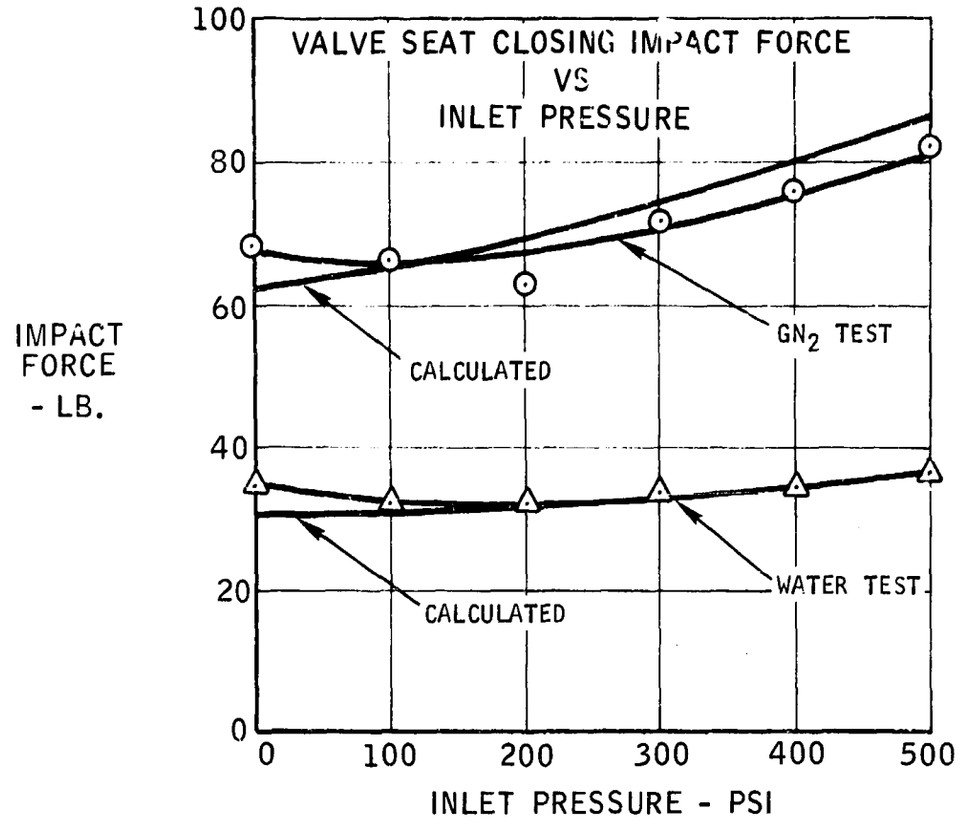

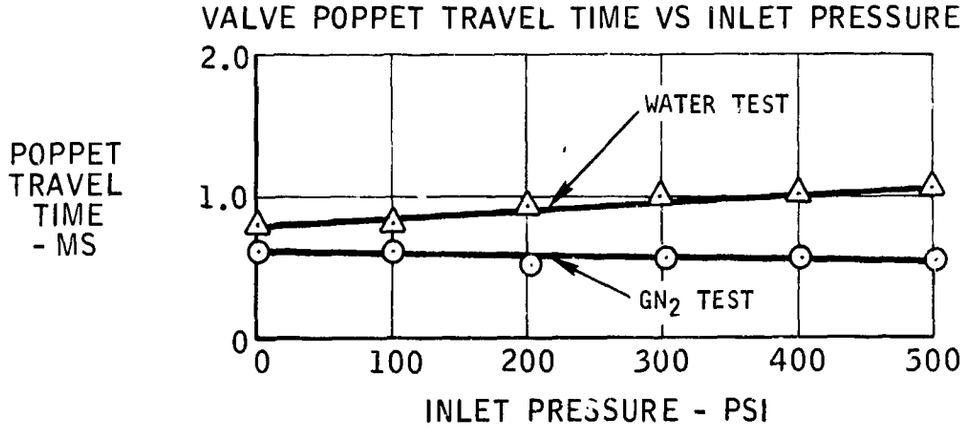

Figure 7

VALVE SEAT CLOSING IMPACT FORCE AND POPPET TRAVEL TIME AS A FUNCTION OF INLET PRESSURE FOR CONFIGURATION NO. 2

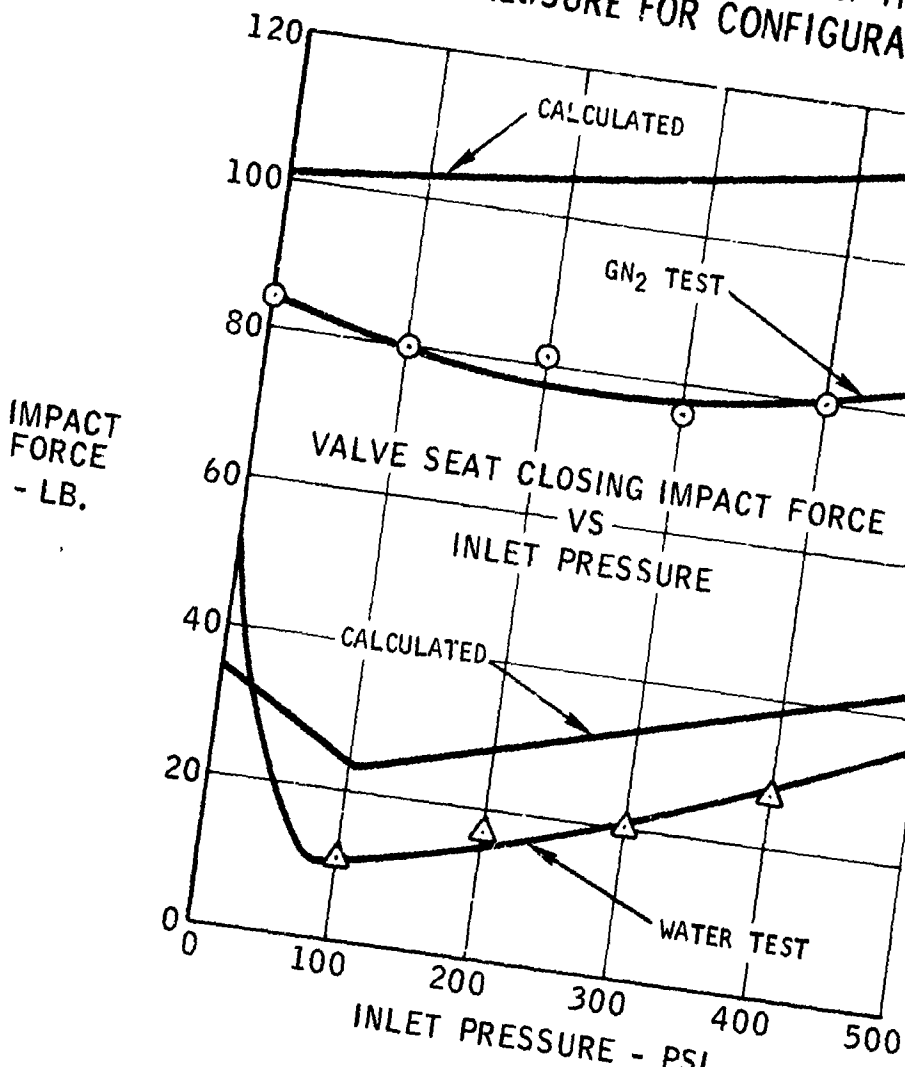

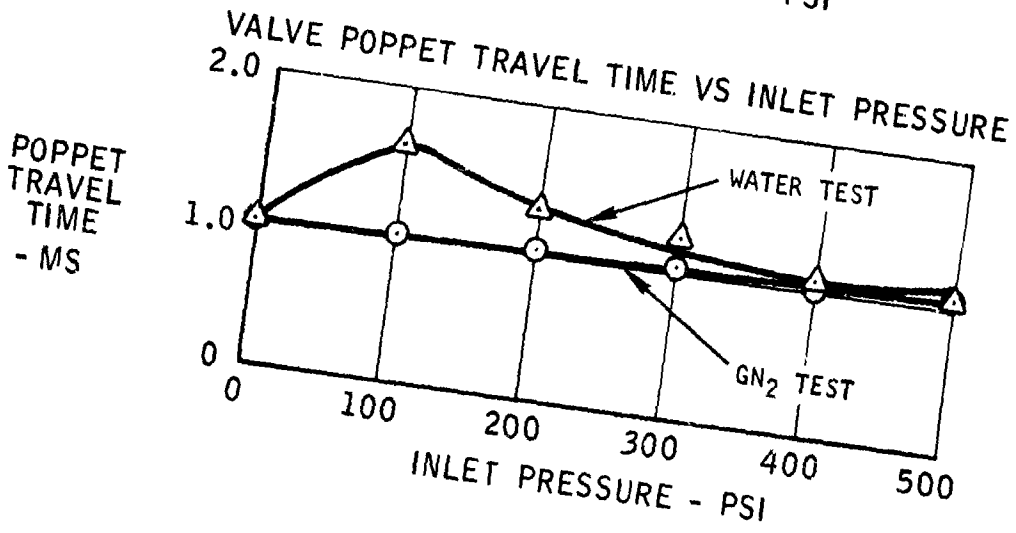

Figure 8

VALVE SEAT CLOSING IMPACT FORCE AND POPPET TRAVEL TIME AS A FUNCTION OF INLET PRESSURE FOR CONFIGURATION NO. 3

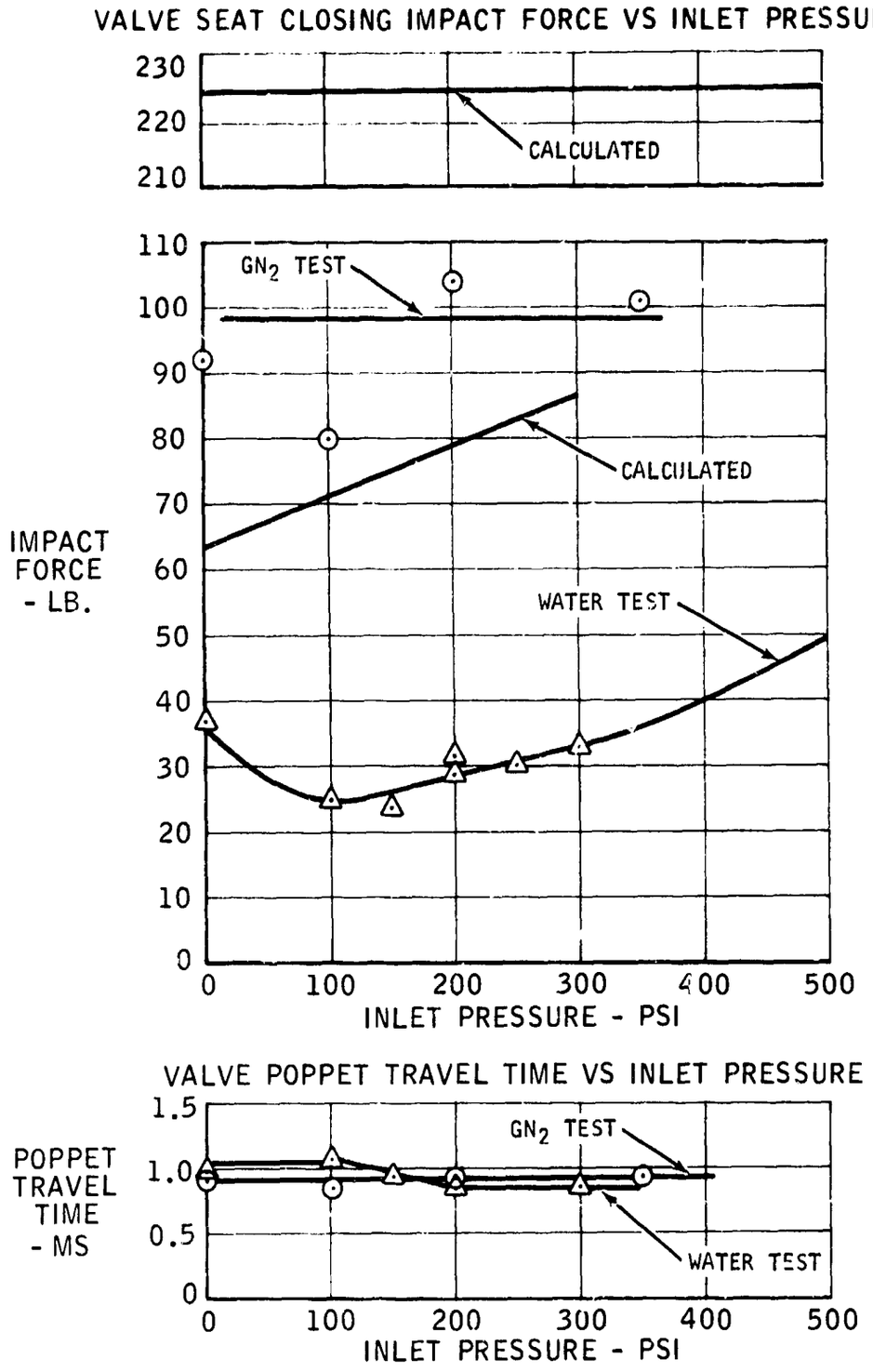

VALVE SEAT CLOSING IMPACT FORCE AND POPPET TRAVEL TIME AS A FUNCTION OF INLET PRESSURE FOR CONFIGURATION NO. 4

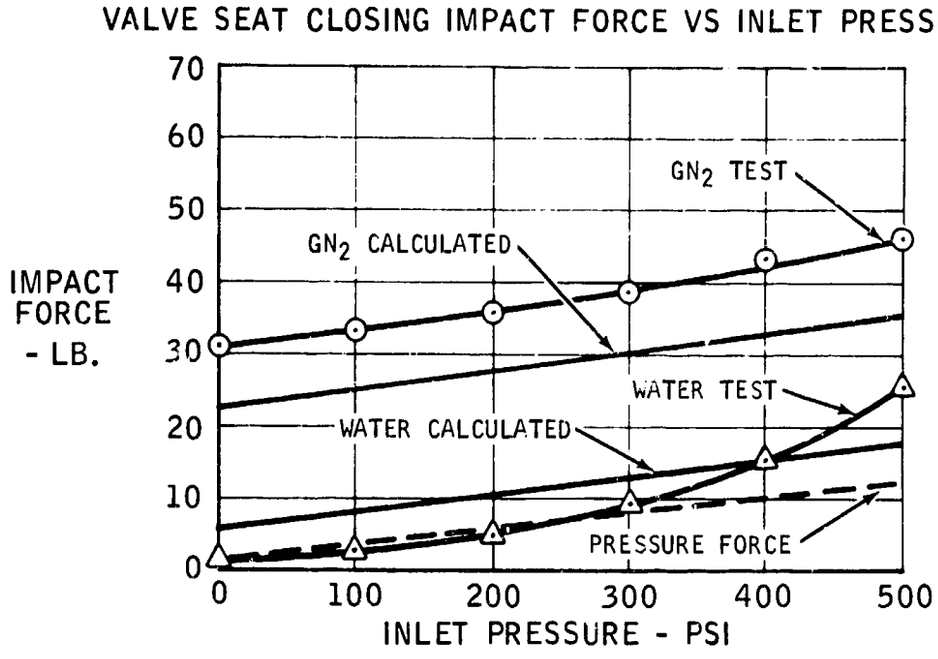

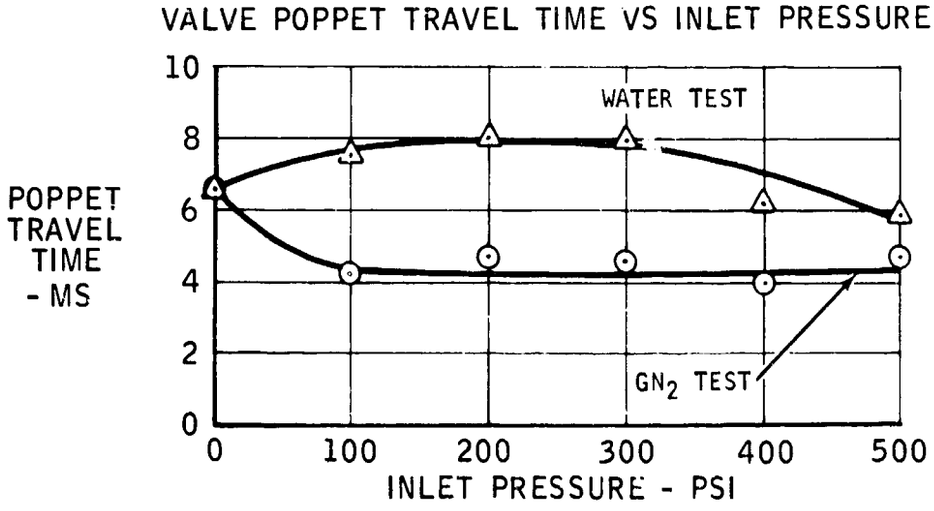

Fig. 16

Figure 11 shows a comparison of measured closing impact for four configurations in GN_2 and Figure 12 shows a comparison of the test results in water.

6. Discussion of Test Results

Analytically predicted and actual impact forces measured in GN_2 agree reasonably well considering the possibilities for variation, including internal spring friction, viscous drag effect, misalignment of the poppet with respect to the seat, accuracy of data acquisition and other factors which could influence the impact forces measured under actual test conditions. A comparison of the analytical predictions and measured test results in GN_2 is shown in Table IV.

The data was consistent enough to allow formulation of a correction factor for predicting impact forces to be measured in water from theoretical values. For the original integral poppet/armature type (Configuration No. 1) a factor of $F_{water} = F_{theoretical}/1.5$ should be used. For the current bumpered configuration (Nos. 2, 3 and 4), a factor of approximately 1/3 will provide a correction from theoretical to actual expected impact forces in water. These force values should be typical of forces to be expected in real valves since the real valves analytically yield only about 30% more impact force due to a stiffer seat.

The major portion of reduction from ideal impact force (as verified in GN_2) to impact forces measured with water is probably due to two factors:

1. Viscous drag of the poppet moving through a relatively stagnant flow field. This effect is partially compensated for by measured poppet closing travel time being slower in water than in gas operation.

2. During valve closure in water, a film of water is "squished" between the poppet and seating surfaces. Displacement shearing of the thin sheet of liquid probably has an almost constant energy absorption effect irrespective of valve stroke or travel time for the valves tested because of the geometrical symmetry between the test configurations, i.e., equal critical film thicknesses and identical seating geometry.

The data correlation between GN_2 operation and theory and between GN_2 and water are good enough to conclude that the analytical techniques used to predict the impact forces can adequately be used to predict impact forces in water.

Accurate prediction of impact forces to be expected during operation of the valves in Compound A may, however, be another matter. The amount of energy absorbed by the liquid sheet displaced during valve closing is undoubtedly affected by fluid density and viscosity.

COMPARISON OF IMPACT FORCES IN GAS

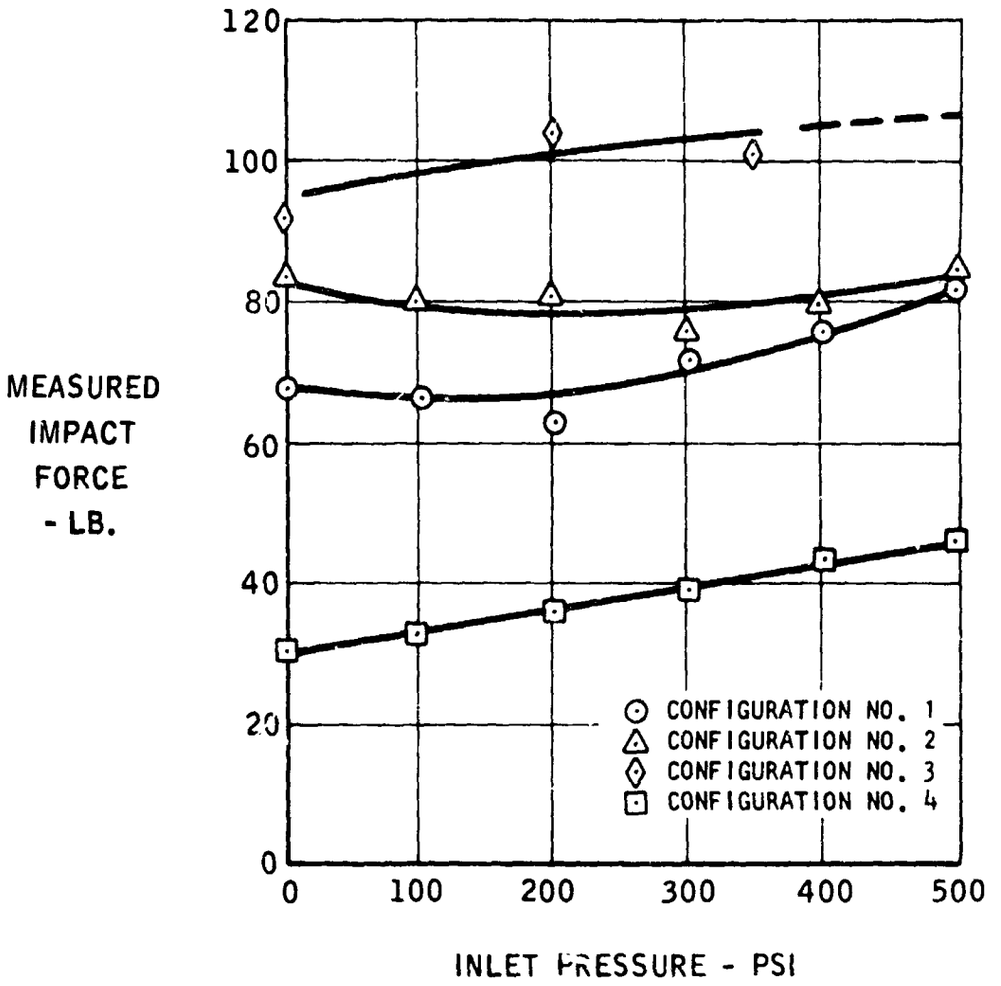

Figure 11

A71-9-036-98

COMPARISON OF IMPACT FORCES IN WATER

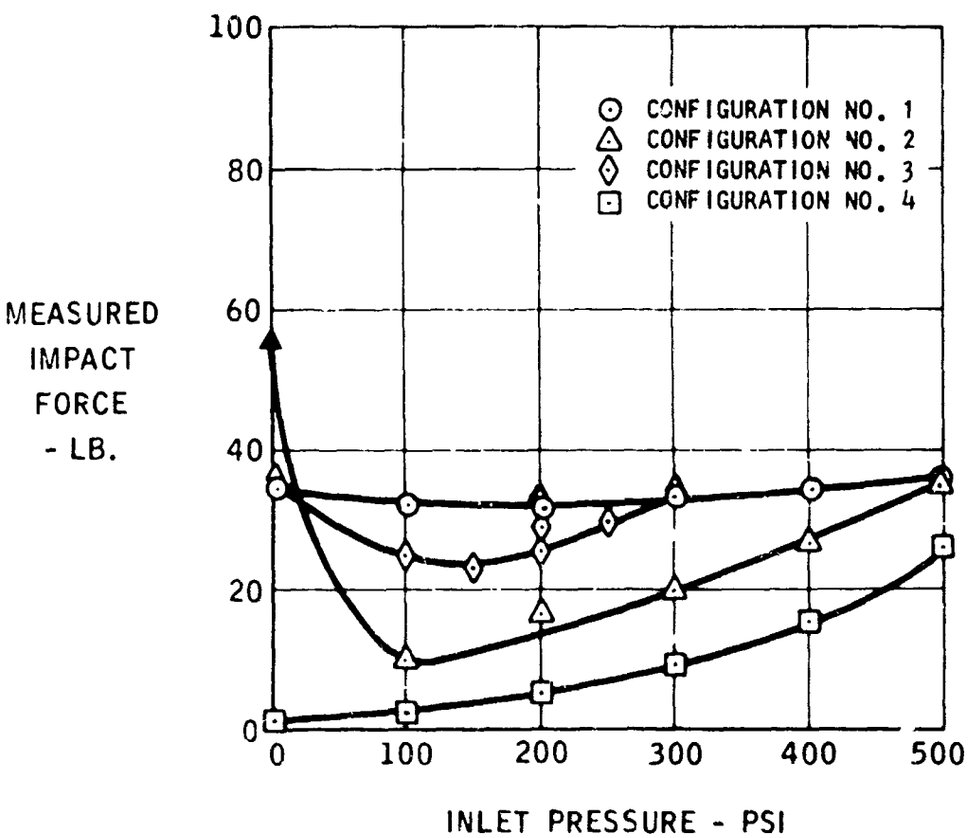

Figure 12

TABLE IV

PREDICTED AND MEASURED IMPACT LOADS IN GN_2 AT 500 PSI

Configuration	Calculated Impact Load (lb)	Measured Impact Load (lb)
1	86	82
2	113	85
3	224	98
4	35.3	46

Viscosity and density effect on absorption of the poppet impact energy is probably directly proportional to the differences in viscosity and density. Since the viscosity of Compound A is less than one half the viscosity of water and the density of Compound A is about 1.8 times the density of water it might be expected that the impact forces in propellant would be similar to the forces measured in water.

$$F_{propellant} = F_{water} \times \frac{\text{Density Liquid}}{\text{Density of Water}} \times \frac{\text{Viscosity of Liquid}}{\text{Viscosity of Water}}$$

A detailed analysis of the problem is beyond the scope of this program. Conclusive definition should be made of the effects of fluid viscosity and density on poppet seat impact forces by further analysis and testing in other fluid mediums which would provide a more compatible fluid interface. Probably one of the most important facts documented during this test program was demonstration that the change from the original armature configuration with no bumper to the present configuration with a bumper designed to absorb some of the armature energy was an effective change. Total energy absorbed by the seating area in valve closing is probably as significant a factor in valve wear as is the maximum impact force level. Figure 13 shows photographs of valve seat force-time relationship for the two basic geometric configurations as measured during this test program. It can be readily seen that the total energy required to be absorbed by the valve seat is much lower in the bumpered valve configuration even though the peak force impressed on the seat is similar.

Energy level required to be absorbed in the present configuration valve is much lower because the impact force level is impressed on the seat for a much shorter period of time.

It would be desirable to perform more analysis and limited test programs to quantitatively define the total energy absorbed by the seat and the effects on the valve seat protective film as a direct function of total energy absorbed by the seat.

7. Impact Test Conclusions

The following conclusions were reached at the completion of the impact tests:

1. The Marquardt developed analytical model for predicting closing impact of the advanced ACS valve poppet with the seat was verified for operation of the valve in gaseous nitrogen.

2. Empirical correlation factors can be developed for accurately predicting impact of the valve poppet/seat in water and other test fluids.

CLOSING FORCE AS A FUNCTION OF TIME

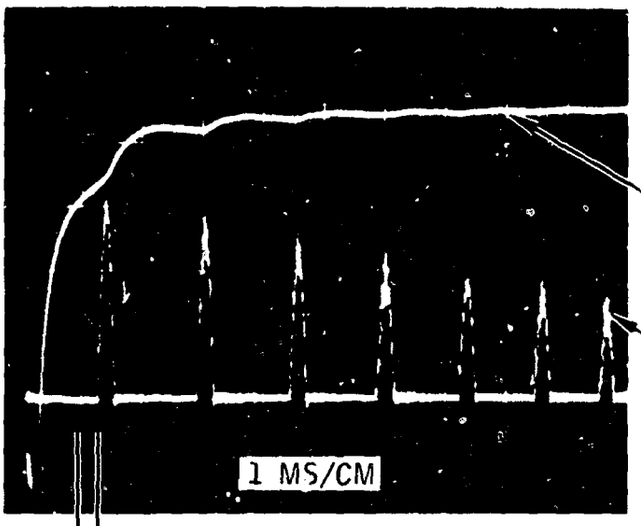

CONFIGURATION NO. 1
INTEGRAL POPPET

VALVE VOLTAGE

IMPACT FORCE
20 LB_F/CM

FULL CLOSED

START TO CLOSE

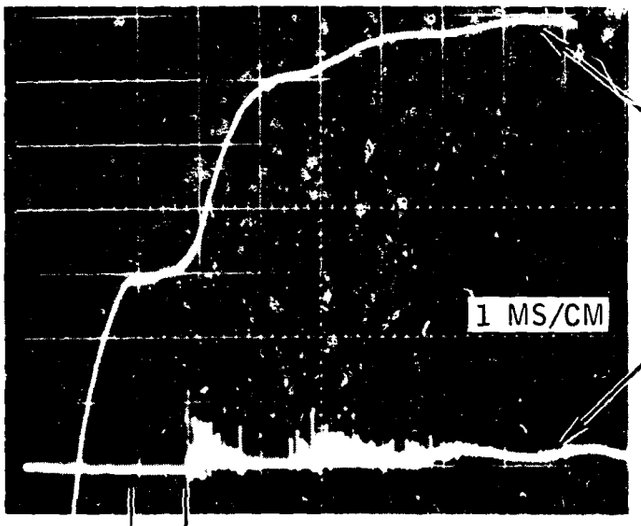

CONFIGURATION NO. 2
FLEXIBLY ISOLATED POPPET

VALVE VOLTAGE

IMPACT FORCE
20 LB_F/CM

FULL CLOSED

START TO CLOSE

Figure 13

3. The current, bumpered (flexibly isolated) version of the valve imparts less energy to the seat during valve closing. If impact force is a significant factor on seat wear in chlorine pentafluoride, the change to a flexibly isolated poppet should be reflected in increased valve cycle life.

SECTION V

SURFACE EVALUATION TERMINOLOGY, METHODS AND TEST DEVICES

The basic process of sealing in a metal to metal seat valve is primarily a function of the intimacy of contact between the seat and poppet contact areas. Evaluation of the metal to metal interface characteristic required detailed inspection of the surfaces of the parts tested in this program; both to determine initial surface conditions and the surface finish resulting from exposure of the parts to a fluorinated oxidizer environment under static exposure and dynamic impact exposure conditions. One of the most important aspects of the program was the requirement to determine and document surface condition of the test parts. The following sections describe the surface parameters considered to be most critical and the equipment and techniques used to document the surface conditions.

1. Parameters of Interest

1.1 Surface Texture

Surface texture in general is related to the deviations and asperities relative to the nominal surface of a test part. The general term surface texture is subjective but surface texture details including flaws, roughness, waviness and lay do provide specific information about the characteristics of a finished surface.

1.2 Flaws

Flaws are irregulatities which occur at one place or at relatively infrequent and varying intervals on a surface. Flaws include such defects as ridges, holes, checks, scratches, cracks, etc. In general, flaws are not included in a measurement of specific roughness height. However, flaws such as scratches are of particular interest in a hard seat valve when they cross metal to metal sealing areas.

1.3 Roughness

Roughness is defined as finer surface irregularities resulting from inherent action of the production process. These include machine feed marks and the asperities which result from final lapping producing a regular scratch pattern.

1.4 Roughness Height

Roughness height is rated as the arithmetical average deviation expressed in microinches measured normal to the center line of the part surface.

1.5 Roughness Width and Cutoff

Roughness width is the distance parallel to the nominal surface between successive peaks or ridges which form the predominant pattern of the surface. Roughness width is measured in inches and is the greatest spacing of repetitive irregulatities to be used in measuring the average roughness height. The roughness width cutoff must always be greater than the roughness width to obtain total roughness height accurately. During this program, all machine measurements were made using a roughness width cutoff of 0.03 inch. This value was significantly greater than the average surface asperity height measured.

1.6 Waviness

Waviness is the usually widely spaced component of surface condition and is of wider spacing than the roughness width cutoff. It approximates the general mean smoothed surface profile. Roughness can be considered to be superimposed on a wavy surface. Waviness can be a significant parameter in assessing potential causes of valve leakage. It is immediately obvious that even with superfinished parts, the required intimate contact between the sealing surfaces may be lost because of an excessively wavy surface which could allow creation of a large inherent leak path. Waviness height is measured as peak to valley height in microinches. All parts used during this program were flat to less than one helium light band.

1.7 Linear Measurements

The most commonly used units of measurement in surface finish assessment are the micron (one millionth of a meter) and the microinch (one millionth of an inch). There are 39.6 microinches per micron; however, the most convenient conversion considering the required accuracy of measurement in this program was to round and use 40 microinches per micron.

2. Surface Measurement Instrumentation

Three instruments were used during the program to aid in evaluating changes in the material critical surface characteristics. These instruments were the interference microscope, the Bendix Proficorder and the Applied Research Laboratory Electron Microprobe X-Ray Analyzer-Scanning Microscope. Capabilities and use of each of these instruments will be discussed in the following sections.

2.1 Interference Microscope

A Wild interference microscope was used for detailed assessment of seating poppet and land flatness, surface roughness and geometrical irregularities. Figure 14 shows the unit without the Polaroid camera attachment used for photographing test parts. This instrument allows surface roughness measurements to be made with interference fringes and interference contrast. In addition, comparisons can be made using standard bright field, dark field and polarization techniques. Three magnification powers were available for viewing the parts, 84X, 140X and 210X. The field of view for all magnifications was 1.3 mm. Most of the evaluations and surface photographs taken with this instrument were made at 210X. Use of this magnification allowed viewing of the whole width of the seating land with the maximum in magnification for evaluation of the surfaces.

The Wild interference microscope is designed on the Linnik principle and consists essentially of a beam splitter, two precisely matched objective lenses and a selection of reference mirrors.

As shown in Figure 15, light from the incident light attachment passes down the tube to a beam-splitting prism, where 50% of the light is reflected at 90 degrees through the internal reference objective on to a reference mirror and back to the prism. The remaining 50% of the light passes straight through the beam splitter and the viewing (external) objective and is subsequently reflected back along the same path from the surface of the specimen. In this way, the two components are reunited and interference is produced. The reference mirrors may be tilted and rotated, allowing the width and orientation of the interference fringes to be altered as required. The microscope is also equipped with an internal projecting scale with 10 micron divisions. This allows direct measurement of gross surface irregularities with estimating accuracy to about 2 micron.

2.2 Bendix Proficorder

Pretest and post test surface profiles of the poppets and seats tested were documented through use of the Bendix Proficorder. The Proficorder (Figure 16) is basically a stylus instrument. It consists of three principal working units, a tracing arm or stylus with diamond tip, a piloter for supporting the tracer and moving it exactly along the desired tracing path and associated electronic circuitry with a recorder to record the surface profile at various horizontal and vertical magnifications. The unit used for these tests had a 0.0005 inch radius stylus tip (supplied with a calibration plate). The output can be readily switched between AA (arithmetical average) roughness and waviness as well as to different magnifications depending on the surface finish of the part to be documented. As the stylus moves across the part, movement of the stylus in a vertical direction generates a voltage proportional to the change in stylus elevation.

WILD INTERFERENCE MICROSCOPE

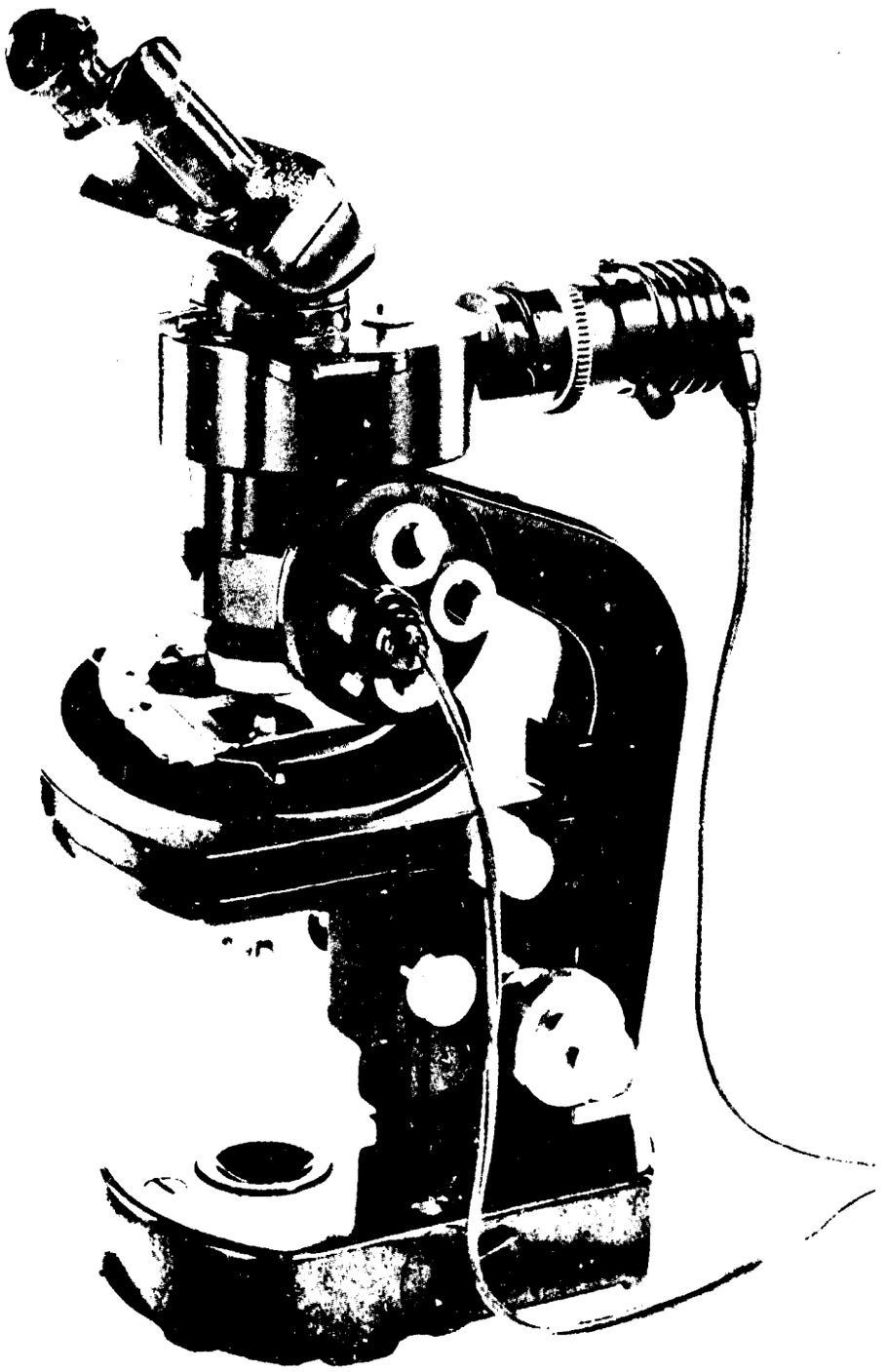

Figure 14

LIGHT PATH IN THE WILD INTERFERENCE ATTACHMENTS

The interference attachments have been designed on the Linnik principle and consist essentially of a beam splitter, two precisely matched objectives, (a Universal Epi-objective and a reference objective) and a selection of reference mirrors. Light from the incident light attachment passes down the tube to a beam-splitting prism, where 50% is reflected at 90° through the internal reference objective on to a reference mirror and then back to the prism. The remaining 50% of the light passes straight through the beam splitter and the viewing (external) objective and is subsequently reflected back along the same path from the surface of the specimen. In this way the two components of the beam are re-united and interference is produced. This method requires the lengths of the viewing and reference light paths to be matched very precisely during construction, so that when the specimen is focused in bright field the interference fringes are immediately visible. The reference mirrors may be tilted and rotated, allowing the width and orientation of the interference fringes to be altered as required. By setting the mirror in the vertical position, interference contrast is obtained.

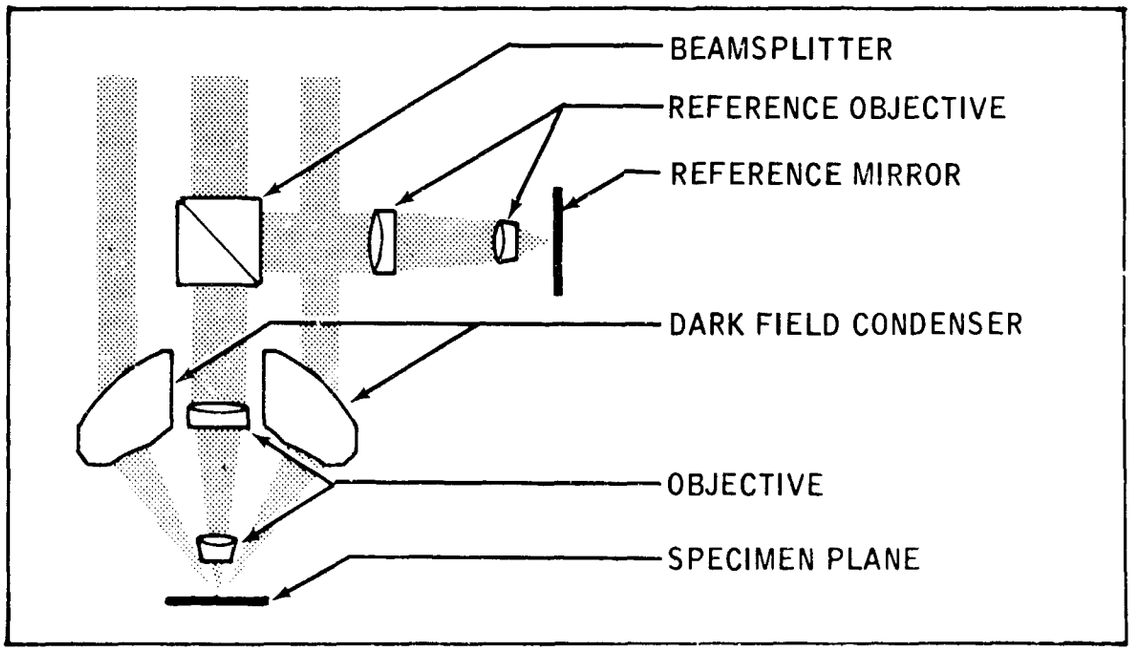

Figure 15

PROFICORDER TYPE RLC, MODEL 6 AND TYPE RLJ, MODEL 4

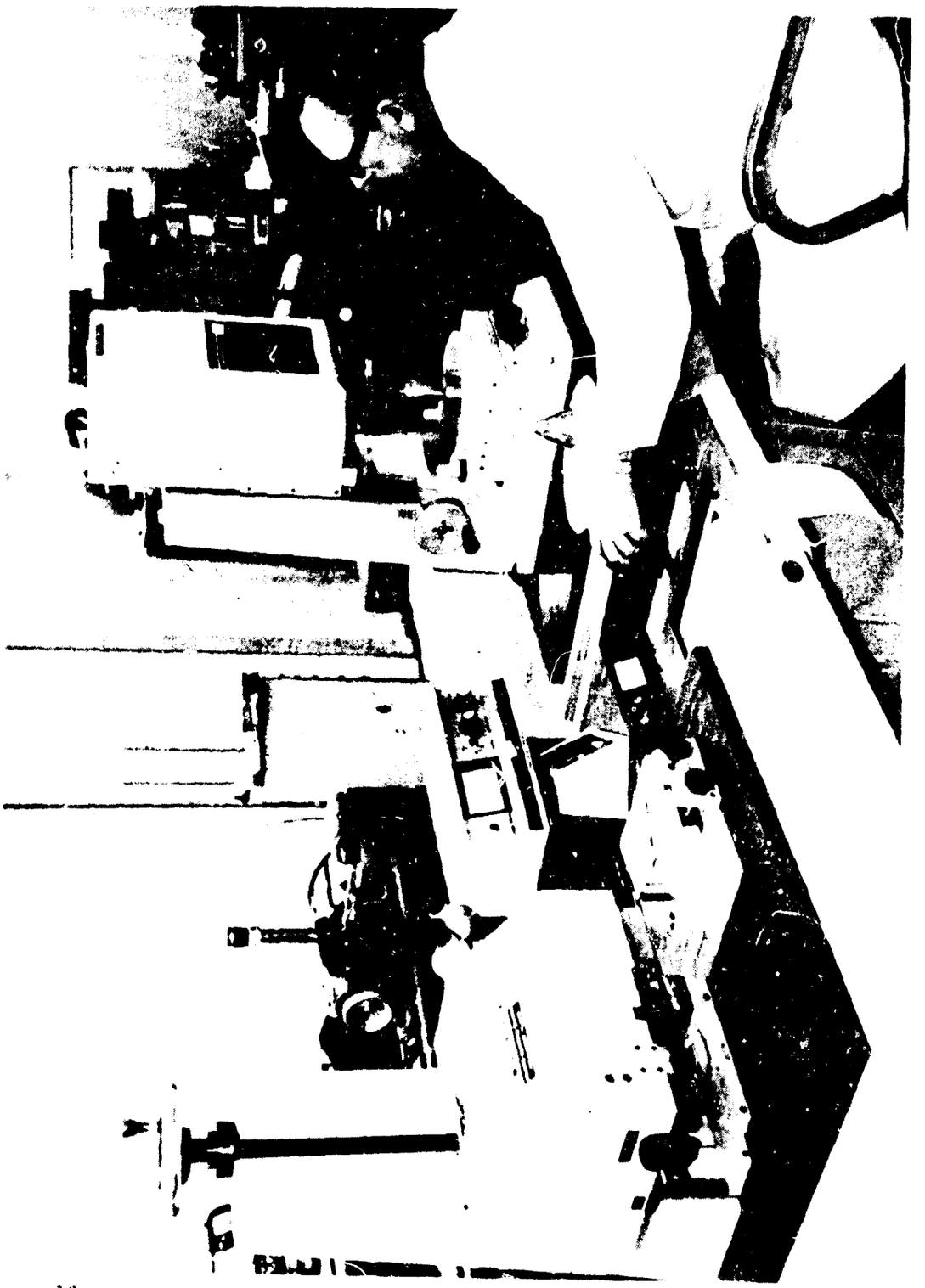

Figure 16

The output is presented as strip chart whose length is proportional to the horizontal distance traversed by the stylus tip. Use of the Proficorder allows discriminate evaluation of the surface detail of the part in a line across the test part. All of the test parts were documented by tracing two tracks across the part surface at 90 degrees to each other, giving a good feel as to the regularity of the part surface.

Several sources of error are possible when using the Proficorder to document a surface and its asperities. First, as shown in the sketch in Figure 17, the Arithmetic Average (AA) roughness indicated may be less than the real roughness as a result of the diameter of the tip being larger than the width of the surface scratch grooves preventing full excursion of the stylus tip. For these evaluations, the tip radius was not considered a serious problem since the prime objective was comparison of before and after conditions. Thus, even though the indicated AA finish may be in error by 20%, the relative variance of before to after test finish of 1 microinch would still be apparent. A second potential source of error is extraneous vibration. This is not a significant problem for these tests as the proficorder at Marquardt is well mounted on a relatively solid slab. No evidence of extraneous vibration effects was apparent. A third source of occasional problems results when the stylus crosses grooves at the natural frequency of the stylus arm. This condition can result in recording of a significantly rougher apparent surface than the real surface. Singing of the stylus arm was not an apparent problem during this program.

The proficorder served a useful function in evaluation of the test parts giving quantitative information regarding surface finish, waviness and overall profile of the test parts.

2.3 Electron Microprobe X-Ray Analyzer-Scanning Microscope (EMX-SM)

Scanning electron microscope and microprobe analysis of the test parts for surface finish was performed in the EMX-SM at Applied Research Laboratories, Sunland, California. The particular instrument used is the only instrument known to be available which can perform the electron microscope and microprobe analysis functions in the same instrument. Availability of the instrument provided the capability to examine both surface character and elemental composition of the test parts without requiring handling of the parts and potential additional exposure to atmospheric moisture.

The EMX-SM shown in Figure 18 is capable of providing qualitative measurement of elemental makeup of a material through microprobe studies. The instrument causes the surface of the part to be impacted by a high energy electron beam. This results in the generation of X-Rays characteristic of the particular material being examined. The emitted X-Rays are scanned using variable slit, high resolution spectrometer

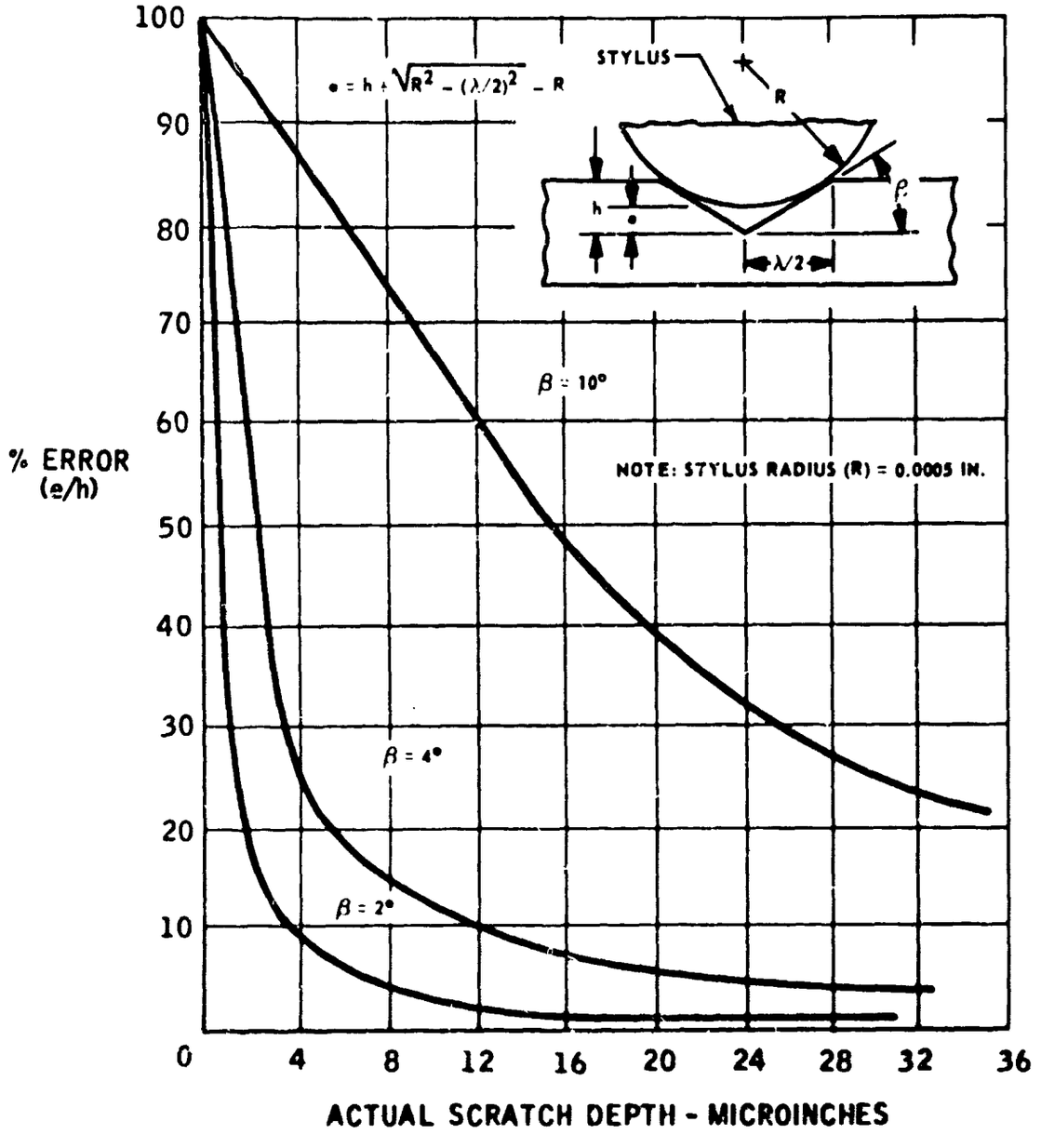

Figure 17 PROFILE MEASUREMENT ERROR

A71-6-036-1

ELECTRON MICROPROBE X-RAY ANALYZER SCANNING MICROSCOPE

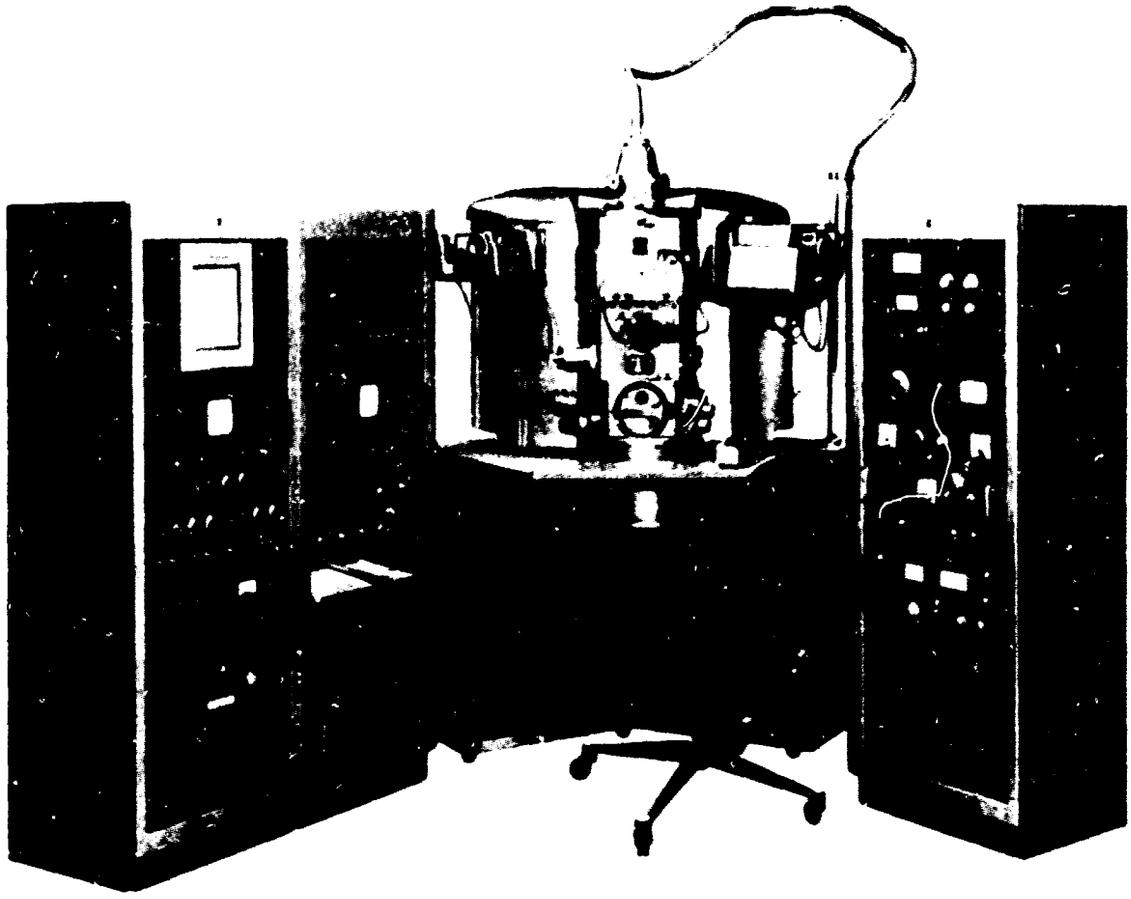

Figure 18

stages to determine the material causing the emission. One feature of the EMX-XM particularly valuable in normal material analysis is the capability to examine more than one line of X-Ray emission simultaneously. Thus it is possible to make a simultaneous dispersive analysis of up to five elements. The depth of penetration of the X-Ray beam and generation of data is typically from 0.2 to about 3 microns. That depth was too great to allow complete surface film chemical analysis during this program. The only microprobe studies conducted consisted of checks for the presence of fluorine or chlorine. All analysis is carried out in a 2×10^{-5} torr pressure.

The scanning microscope portion of the system was capable of operating simultaneously with the X-Ray microprobe system, providing sample current and backscattered electron displays. During this program, the instrument was primarily used as an electron scanning microscope.

Output of the EMX-SM is provided in several modes. Characteristic lines can be provided on a strip chart to show elemental peaking or photos can be taken showing the surface topography, X-Ray emission pattern, backscattered electron display or sample current. Selection of the display mode is dependent on maximizing the clarity of the characteristics of the object surface under study. The mode primarily used during this program was recording of secondary generated electrons using the device primarily as a scanning electron microscope to record surface topography changes on a polaroid photograph. Versatility of the system helped provide determination of qualitative evaluation of the wear patterns of poppets resulting from poppet to seat impact in the fluorinated oxidizer environment.

SECTION VI

PROPELLANT TEST PROGRAM

A two-phase propellants test program was undertaken to empirically document:

1. Reactions of the selected test materials to static exposure environments of gaseous fluorine and chlorine pentafluoride (CPF). The results of these tests were intended to allow elimination of one of the test materials from subsequent valve tests.

2. Actual performance of the final selected test materials in test valves representative of the use environment in both gaseous fluorine and CPF.

Objective of the program was to determine the valve failure mechanism and secondly to determine the most suitable valve seat and poppet material from those under consideration. A total of 23 poppets and 8 seats were examined during the course of the program. Five poppets were used as base material surface reference specimens. Ten poppets were used as static propellant exposure samples. Eight poppets and eight seats were used in the valve test program to document performance of the materials in the functional environment.

1. Pretest Sample Identification and Test Matrix

Each test poppet and seat was assigned a test sample number prior to start of the tests. Each sample was individually packaged and identified to preclude mixing of the test samples. Primary test usage of each sample and test flow of parts used in the program are shown in Table V. Sample holders used for containing the samples during the static exposure tests and for examining the poppets after completion of the tests were similarly identified so that sample identities could be maintained.

The test program was conducted per the test flow diagram shown in Figure 19 using the samples identified in the table.

2. Static Exposure Tests

Specific objective of the static propellant exposure tests was to determine the degree of surface degradation of each of the test materials after an extended period of static exposure to the test fluids, gaseous fluorine and chlorine pentafluoride (CPF). Based on the results of these tests, it was planned to eliminate one of the materials from further consideration and the subsequent valve tests.

TABLE V

TEST SAMPLE USAGE ALLOCATION

SAMPLE NUMBER	MATERIAL	USE
1	K-96	Reference EMX-SM
2	K-96	Static Test GF_2
3	K-96	Static Test CPF
4	K-96	Cyclic Test - Normal Impact CPF
5	Ni301	Reference EMX-SM
6	Ni301	Static Test GF_2
7	Ni301	Static Test CPF
8	Ni301	Cyclic Test - Low Impact CPF
9	Al_2O_3	Reference EMX-SM sample
10	l_2O_3	Static Test - GF_2
11	Al_2O_3	Static Test - CPF
12	Al_2O_3	Cyclic Test - Low Impact GF_2
13	Al_2O_3	Cyclic Test - Low Impact CPF
14	Al_2O_3	Cyclic Test - Normal Impact GF_2
15	WC	Reference EMX-SM Sample
16	WC	Static Test - GF_2
17	WC	Static Test - CPF
18	WC	Cyclic Test - Normal Impact - CPF
19	B_4C	Reference EMX-SM Sample
20	B_4C	Static Test - GF_2
21	B_4C	Static Test - CPF
22	B_4C	Cyclic Test - Low Impact - CPF
23	B_4C	Cyclic Test - Normal Impact - CPF

TEST MATRIX

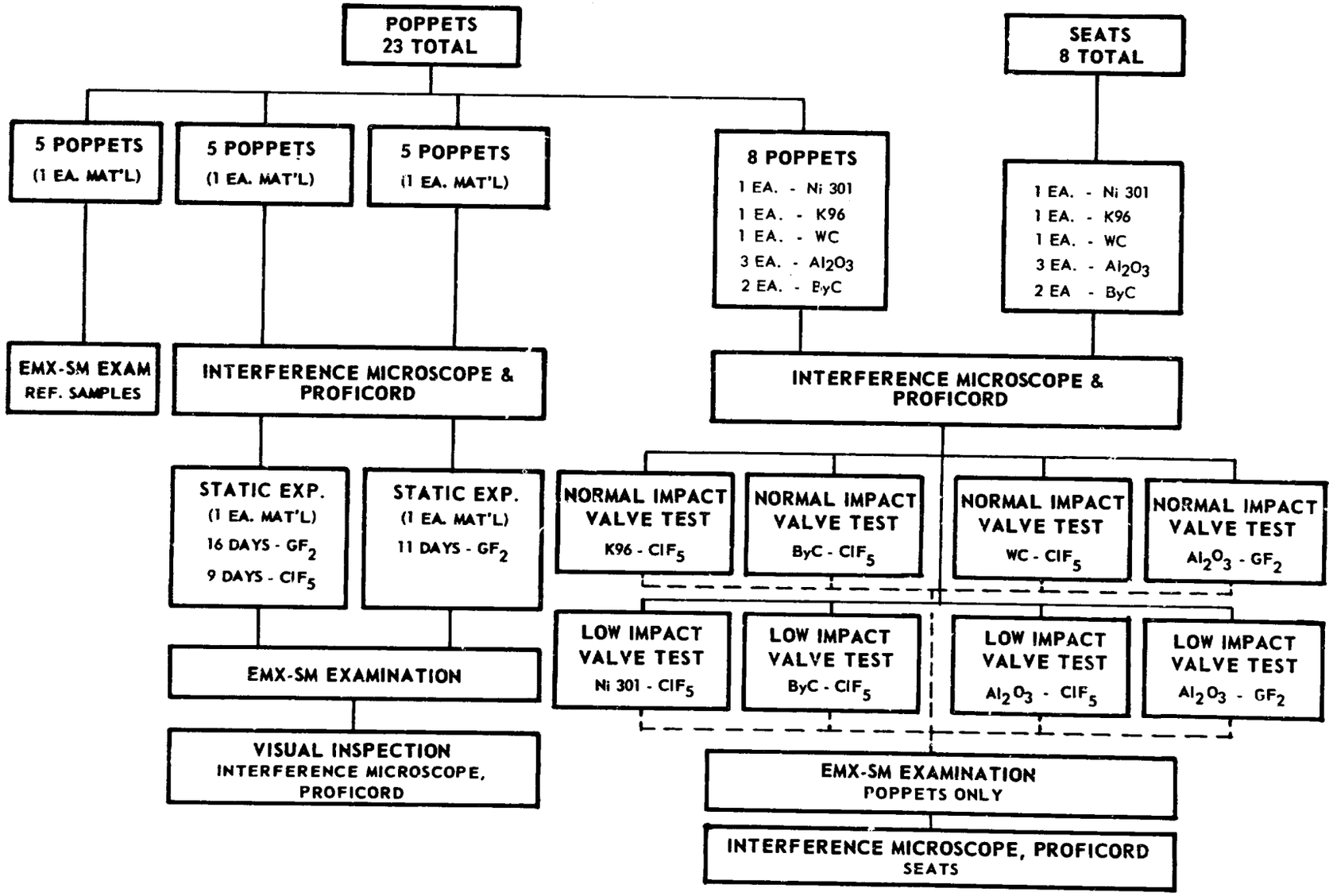

Figure 15

Timing of the valve tests and static exposure tests was such that the planned sequence was not possible. In addition, results of the static exposure tests were conflicting and not definitive enough to allow elimination of any of the materials from further testing in actual valves.

2.1 General Test Procedures

2.1.1 Cleaning

Prior to inspection and testing, each test sample was cleaned. This procedure consisted of an initial vapor degreasing by immersion in trichloroethylene. Vapor degreasing was followed by 3 minutes of exposure in an ultrasonic cleaner. Final preparation consisted of a water flush, a spray rinse with freon TF and drying with filtered, dry nitrogen.

2.1.2 Pretest Surface Documentation

Condition of the surfaces of each of the test poppets and seats was documented prior to the static exposure and valve tests. Two examinations of the parts were made. First, each poppet and seat was examined using the proficorder. Two traces were made at 90 degrees to each other across each poppet or surface as shown in Figure 20 to assure that the surface was uniform and that the measurements made were representative of the entire surface. All of the parts tested met the print requirements for surface flatness and waviness. The new Al_2O_3, WC and B_4C parts used in the static exposure tests had more scratches than could be allowed for a valve poppet. These surface blemishes were considered acceptable for the static exposure tests since the primary test purpose intent was to document changes in the poppet surfaces as a result of propellant exposure. Each of the poppets and seats designated for valve testing was relapped prior to testing since the surface scratches accepted for the static exposure tests would provide an excessively rough surface for effecting a good valve seat seal.

2.1.3 Interference Microscope Examination

Each of the test poppets and seats was examined using the interference microscope prior to subjecting the poppet or seat to propellant. An interferogram and an incident light photo were taken to typical surface areas for comparison with the post test propellant exposed surfaces.

2.1.4 Final Preparation for Static Exposure Testing

The poppets were subjected to a final cleaning operation as previously

A71-9-036-30

PROFICORDER INSPECTION

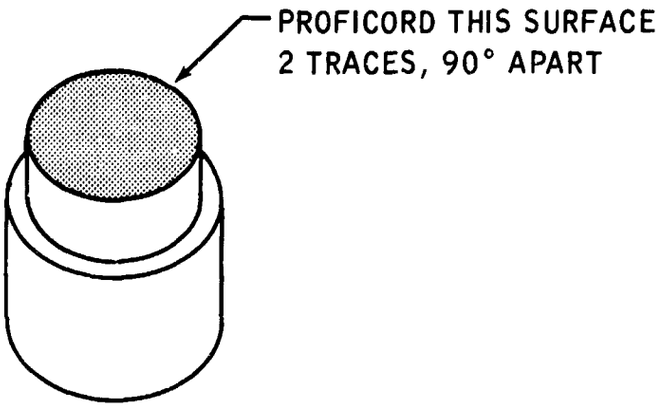

POPPET

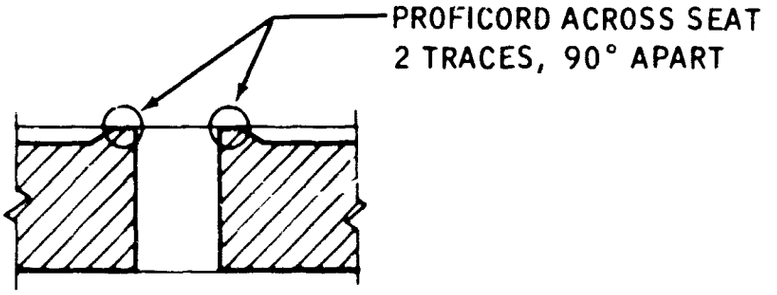

SEAT

Figure 20

described prior to the static exposure tests. They were then mounted in numbered sample holders as shown and installed into the exposure tube.

2.1.5 Moisture Protection of Static Exposure Poppets

Since both fluorine and CPF react readily with water, a procedure was developed to preclude the presence of water or absorbed surface moisture on the parts prior to subjecting them to the propellant environment. After installation into the sample test chamber in which the parts were to be statically exposed, the container and the parts were placed in a vacuum oven for a minimum period of 4 hours and baked at a temperature of 150°F. Both sets of static samples were actually allowed to remain in the oven under vacuum overnight for a period of more than 12 hours. Following completion of the bake cycle, the oven was pressurized with dry nitrogen to bring the pressure back to ambient. The inlet and outlet sample container valves were closed as soon as possible to prevent air entry. The container was then pressurized to 300 psi with dry nitrogen for transportation to the test facility and protection from moisture prior to exposure.

2.1.6 Facility Installation and Static Exposure Testing

Further precautions were taken during installation of the sample tube into the facility to preclude contamination of the test parts with atmospheric moisture. During installation, a helium purge was maintained through the upstream system while the sample tube connection was made to the facility. After upstream and downstream connections had been completed, the sample tube end closure valves were opened and the system further purged with gaseous helium. After completion of installation and facility passivation with gaseous fluorine in increasing concentrations up to 100 percent, the static exposure tests were started.

The first set of poppets tested were subjected to continuous exposure to gaseous fluorine for a period of eleven days. The second set was exposed to continuous fluorine exposure for a period of sixteen days followed by chlorine pentafluoride exposure for a period of nine days. All propellant exposure was carried out at a pressure of 450 psig. A photograph of the static propellant exposure facility setup is shown in Figure 21 with the exposure tube in place.

2.1.7 Post Test Handling and Examination

After completion of the propellant exposure period, each poppet set was removed from the test facility in the sample exposure tube with the tube pressurized to 300 psig with gaseous helium. The propellant exposure tube was then taken to a laboratory dry box which was maintained to a completely dry nitrogen atmosphere. The sample tube was opened in the dry box and the samples transferred to the sample

STATIC PROPELLANT EXPOSURE TEST SETUP

MJL - CELL 4

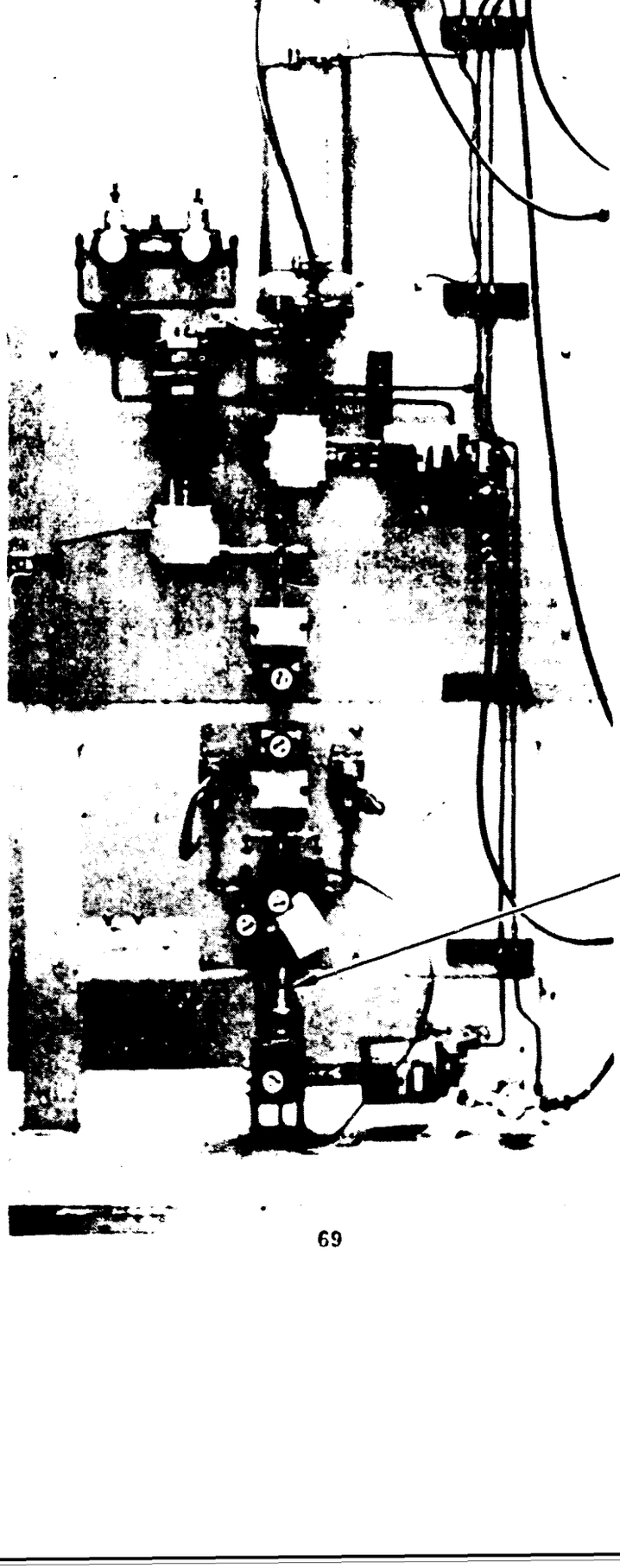

Figure 21

holders which would be used for subsequent electron microscope examination for surface deterioration.

Each part was subjected to a visual examination in the dry box at the time it was removed to see if there were any radical changes in character of the poppet surfaces. Only one part showed any significant apparent change. One tungsten carbide K-96 poppet which had been exposed to gaseous fluorine showed a significant loss in surface brightness after about an hour in the dry box. Since none of the other K-96 poppets examined showed a similar change, it was concluded that the poppet had been inadvertently contaminated by contact with something in the dry box during handling, probably a rubber glove.

After mounting in the proper sample holders, all poppets with the exception of the aluminum oxide poppets were ready for examination with the electron microscope.

2.1.8 Electron Microscope Examination

Each of the test poppets was examined using the electron microscope to determine if surface degradation had occurred as a result of the static propellant exposure. The parts were protected from moisture contamination both during installation and removal from the microscope. Since the sample holders and the sealed glass jars used to transport the poppets to the microscope were quite small, it was possible to perform all handling operations inside the sample chamber of the microscope which had been flooded with gaseous nitrogen. The parts were replaced into the sealed glass carrying jars after completion of the examination preserving their protected state.

2.1.9 Final Interference Microscope Examination and Proficording

An attempt was made to avoid surface changes due to water reactions with the fluorides on the part surfaces by removal of absorbed gaseous fluorides and/or propellant gases. This procedure consisted of a vacuum bake cycle. The part bottles were placed in an oven filled with gaseous nitrogen, the bottles opened and the oven door closed with vacuum being immediately applied. The parts were allowed to bake for a minimum period of 8 hours in the vacuum oven at a pressure of less than 0.1 psia and a temperature of 150°F. After completion of the bake period, the transport jar was again resealed in the vacuum oven which had been pressurized with dry nitrogen to bring the pressure back to ambient. The first test part subjected to this procedure was a Nickel 301 seat. Since the nickel forms a solid fluoride which should react with atmospheric moisture, it should have been an excellent part to determine effectiveness of the inerting procedure. The seat was observed for changes after exposure to air for a period of about two hours and again after about three

weeks using the interference microscope at a magnification of 210X. No visibly apparent changes occurred in the surface character during the observation period indicating that the procedure was relatively successful in preventing significant immediate further reaction of absorbed fluorine and/or chlorine pentafluoride with atmospheric moisture. The procedure was also performed using boron carbide, a material forming only gaseous fluorides. No changes were apparent in either surface indicating the procedure to have been accomplished, the intended purpose of inhibiting further gross reactions.

The surface of each test sample part was examined in detail after completion of the inerting procedure with both the interference microscope and the proficorder to document changes in sample surface characteristics resulting from the exposure period.

3. Static Exposure Test Results Summary

Taken by themselves, results of the static exposure tests performed on each of the test materials in gaseous fluorine and chlorine pentafluoride were not sufficiently definitive to allow rejection of any material sample from further consideration as a valve seat and poppet material.

Nickel 301, a "bad" material when previously tested as a valve poppet and seat in valves showed essentially no changes under the influence of either oxidizer. The K-96 samples, so called "good" materials, both demonstrated significant changes after exposure to the oxidizers. Both boron carbide and pure tungsten carbide showed detrimental effects of exposure. From examination of the static test poppets alone, reactivity of the parts to the propellant would probably result in ranking of the material probability of success as a valve seat material as follows:

1.	Ni-301	Nickel-301
2.	Al_2O_3	Aluminum Oxide
3.	B_4C	Boron Carbide
4.	K-96	Tungsten Carbide with 6% Cobalt Binder
5.	WC	Pure Tungsten Carbide

Relative rating of the K-96 and WC were made purely on the basis of micron size of the particles as hot pressed. It is possible that a smaller particle size could be obtained in either material. Based on the valve test results, however, the apparent reactivity of the part to static exposure is not sufficient to accurately rate the parts for gaseous fluorine or chlorine pentafluoride service as a valve seat or poppet. The passive surface film characteristics (strength, adherence, thickness, etc.)

play an important role in performance of the materials which cannot be evaluated by static exposure testing. Thus, while providing significant insight into the basic compatibility of the materials tested with the test oxidizers, the results alone were not sufficiently definitive to make material selections accurately.

3.1 K-96 (Tungsten Carbide) Static Exposure Test Results

The tungsten carbide K-96 static exposure sample poppets indicated a significant change in surface character as a result of exposure to both gaseous fluorine and chlorine pentafluoride.

No change in the surface brightness of either of the test poppets was apparent at the time they were removed from the test facility sample exposure tube in the dry box. Both still appeared to have the characteristic high surface brightness typical of a newly lapped part. After about an hour, the part which had been exposed to gaseous fluorine turned dull. Since none of the other parts in the holder changed color or surface brightness, it was concluded that the part had been contaminated during handling, probably by contacting a rubber glove. The comparable part, exposed to chlorine pentafluoride showed no changes in the dry box.

Figure 22 shows surface photographs and interferograms taken of the sample poppet surface before and after exposure to gaseous fluorine. Comparison of the surface photos shows that there was a definite change in character of the surface. In addition, the interferogram of the poppet after exposure was very difficult to even take because of surface textures. The entire surface, although relatively flat, has a surface finish which is dimpled with tiny chemical growths. Examination of the comparable set of photographs from the sample exposed to chlorine pentafluoride (Figure 23) also indicates significant surface character change quite different in nature. The surface appears to have developed a significant number of holes. Comparison of the interferograms indicates about the same finish on the raised portion of the surface, i.e., 1.4 AA for the unexposed part and 1.7 AA microinches for the exposed part.

The usefulness of the scanning electron microscope as an analysis tool in examining surfaces was proved in examination of these parts. Figure 24 shows a scanning electron microscope photograph taken at 5000X of the unexposed sample specimen. Electron microscope photographs of the ClF_5 exposed parts, taken at magnifications of 200X, 1000X and 5000X are shown in Figure 25 for the gaseous fluorine exposed part and in Figure 26 for the part exposed to chlorine pentafluoride. The fluorine exposed poppet is not shown because of the similarity between ClF_5 and GF_5 exposed poppets. Comparison of the unexposed surface and that of the poppet surface exposed to gaseous fluorine shows quite clearly why that part surface is rough in appearance.

K-96 STATIC GF_2 EXPOSURE POPPET NO. 2
210X SURFACE PHOTO BEFORE TEST

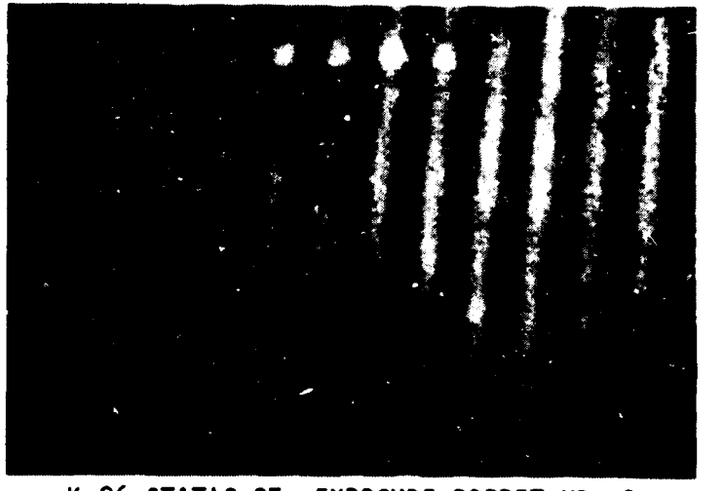

K-96 STATIC GF_2 EXPOSURE POPPET NO. 2
210X INTERFERENCE PHOTO BEFORE TEST

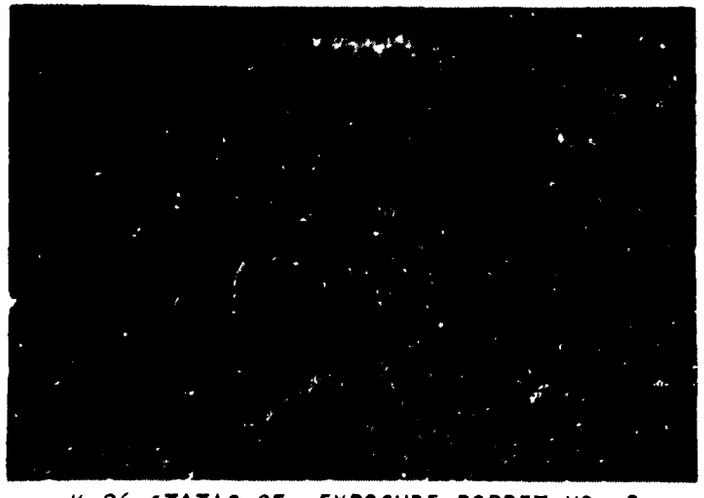

K-96 STATIC GF_2 EXPOSURE POPPET NO. 2
210X SURFACE PHOTO AFTER TEST

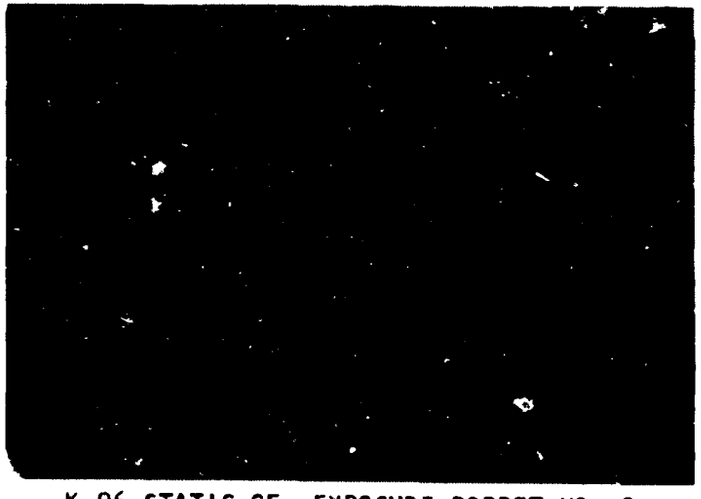

K-96 STATIC GF_2 EXPOSURE POPPET NO. 2
210X INTERFERENCE PHOTO AFTER TEST

A71-6-036-56

Figure 23

Figure 33

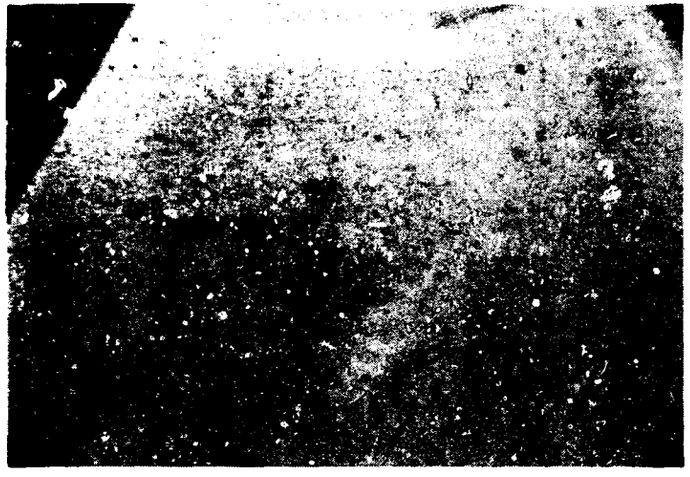

K-96 STATIC ClF_5 EXPOSURE POPPET NO. 3
210X SURFACE PHOTO BEFORE TEST

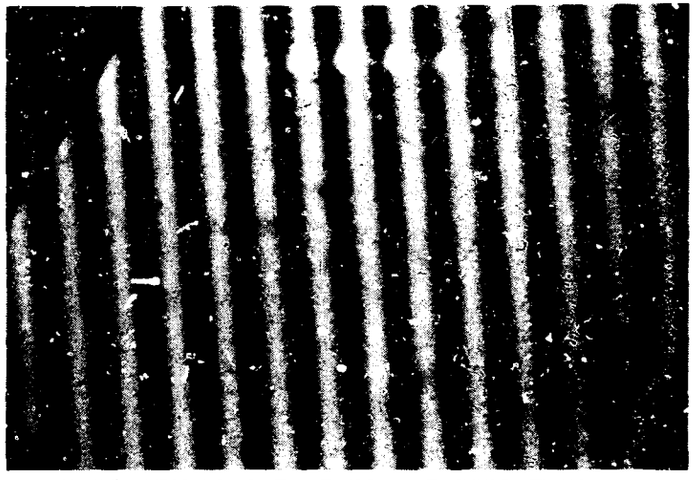

K-96 STATIC ClF_5 EXPOSURE POPPET NO. 3
210X INTERFERENCE PHOTO BEFORE TEST

K-96 STATIC ClF_5 EXPOSURE POPPET NO. 3
210X SURFACE PHOTO AFTER TEST

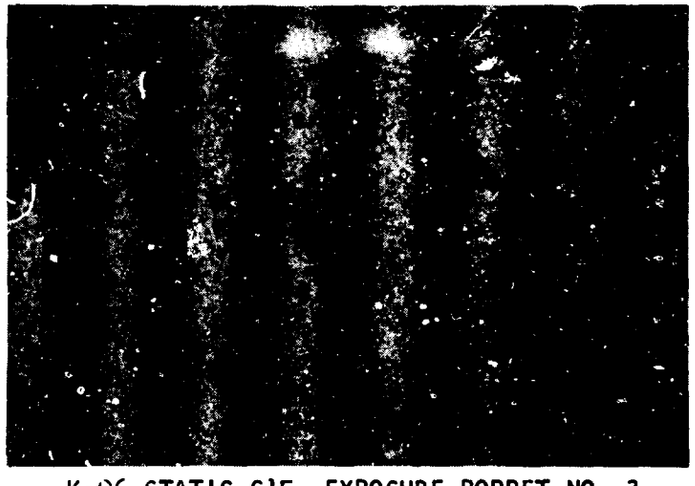

K-96 STATIC ClF_5 EXPOSURE POPPET NO. 3
210X INTERFERENCE PHOTO AFTER TEST

A71-6-036-50

K-96 "AS LAPPED" POPPET

S.E.M. PHOTO AT 5000X

Figure 21

TUNGSTEN CARBIDE K-96 - SAMPLE NO. 2
S.E.M. PHOTOS AFTER STATIC GF_2 EXPOSURE

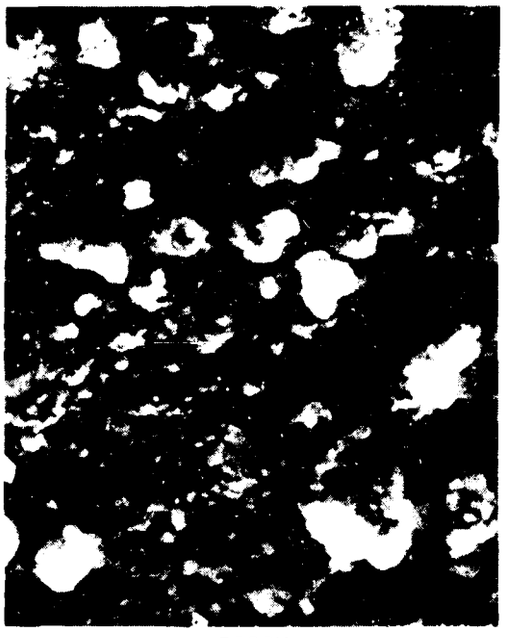

5000X

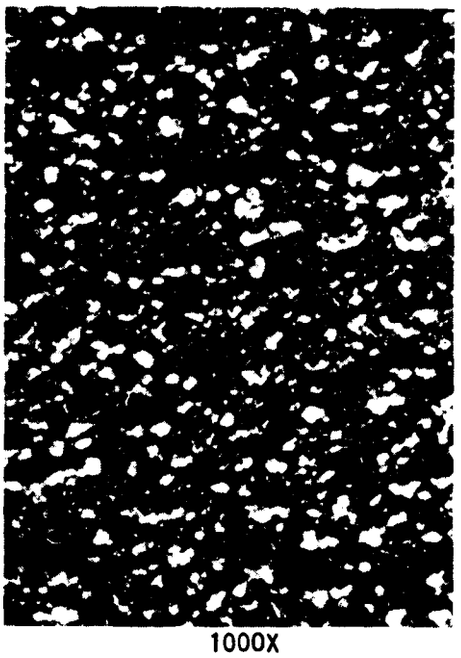

1000X

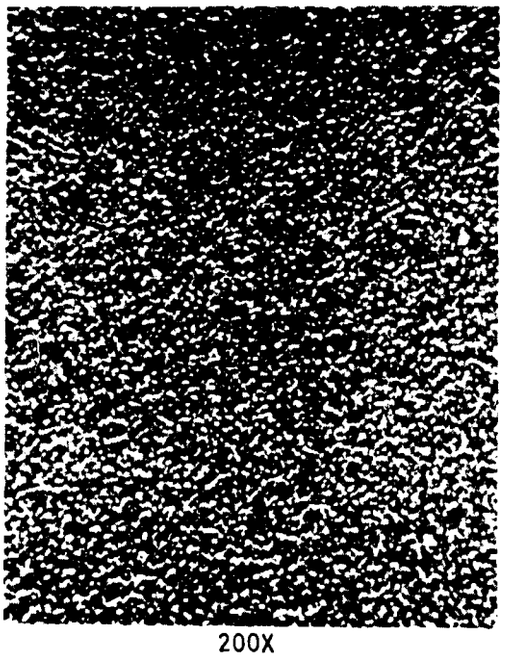

200X

Figure 25

TUNGSTEN CARBIDE K-96 - SAMPLE NO. 3
S.E.M. PHOTOS AFTER STATIC ClF_5 EXPOSURE

5000X

1000X

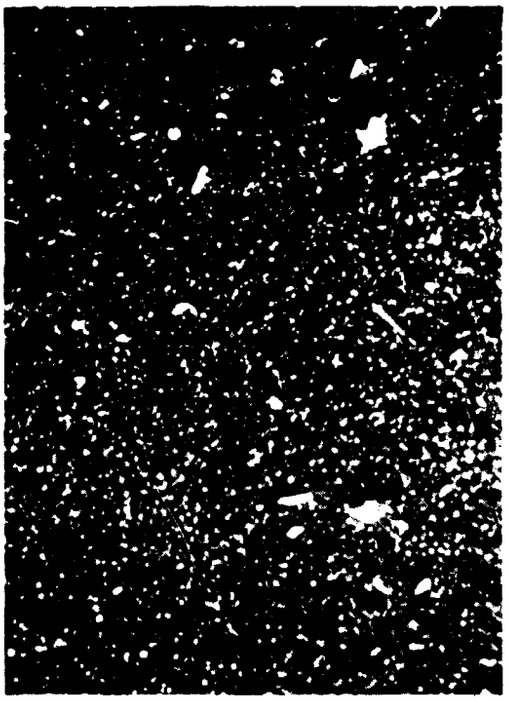

200X

Figure 26

The entire surface is covered with nodule like growths which are characteristic of a surface chemical reaction. These results support the hypothesis that the surface was contaminated in handling. The comparable set of photographs taken of the part exposed to chlorine pentafluoride show a surface which is highly etched and remarkably different than the unexposed surface. Apparently the lapping finishing process "smears" over or fills the tiny spaces between tungsten carbide particles with a very thin layer of tungsten carbide which reacts with the chlorine pentafluoride or gaseous fluorine leaving a surface which on a submicroscopic scale is covered with holes. It is also possible that the etched surface apparent after CPF exposure results from etching due to preferential attack at the grain boundaries. The radical change in surface character after exposure to chlorine pentafluoride was somewhat of a surprise since K-96 has been successfully used as a valve seat material in this application and is a so-called "good" material. It must be remembered, however, that the holes exposed are very small - on the order of 1/4 to 1/2 micron in maximum dimension and the remaining surface is still quite flat. Thus, the surface can still function as an intricate miniature labyrinth seal arrangement as long as the mean surface level is flat and the holes are not interconnected.

A final proficorder examination was made of the poppets after completion of all other testing. The pretest and post-test proficorder traces from the ClF_5 test poppet are shown in Figure 27. These figures confirm the change in surface character indicated by the proficorder, interference microscope and scanning electron microscope.

3.2 Nickel 301 Static Exposure Test Results

None of the Nickel 301 parts showed significant degradation as a result of static exposure to either chlorine pentafluoride or gaseous fluorine. The only changes in the parts which were exposed were the growth of random widely separated bumps on the surface which were about 10 microinches high.

Figure 28 shows surface photographs and interferograms taken of the surface of the poppet exposed to gaseous fluorine both before and after exposure. Surface finish in general was not apparently affected by the exposure. Both interferograms indicate about the same surface finish before and after exposure. The surface of the exposed part does indicate the presence of randomly oriented lumps on the surface which were not apparent before exposure or in the scanning electron microscope examination. Figure 29 shows comparable photos of the sample poppet exposed to chlorine pentafluoride. Again, the only surface difference apparent is indicated to be the presence of randomly oriented high spots. These high spots were not identified during examination with the scanning electron microscope. Figure 30 shows electron microscope photographs at 200X, 1000X and 5000X of the sample surfaces which were used as unexposed references. Comparable sets of photographs taken of the gaseous fluorine and chlorine pentafluoride exposed parts are shown in Figures 31 and 32. These photographs indicate essentially no difference between the exposed and nonexposed parts. About the same surface texture is apparent on all parts and the lapping scratches appear

K-96 STATIC EXPOSURE POPPET
SURFACE PROFILE BEFORE AND AFTER CIF_5 STATIC EXPOSURE

PRIOR TO CIF_5 STATIC EXPOSURE

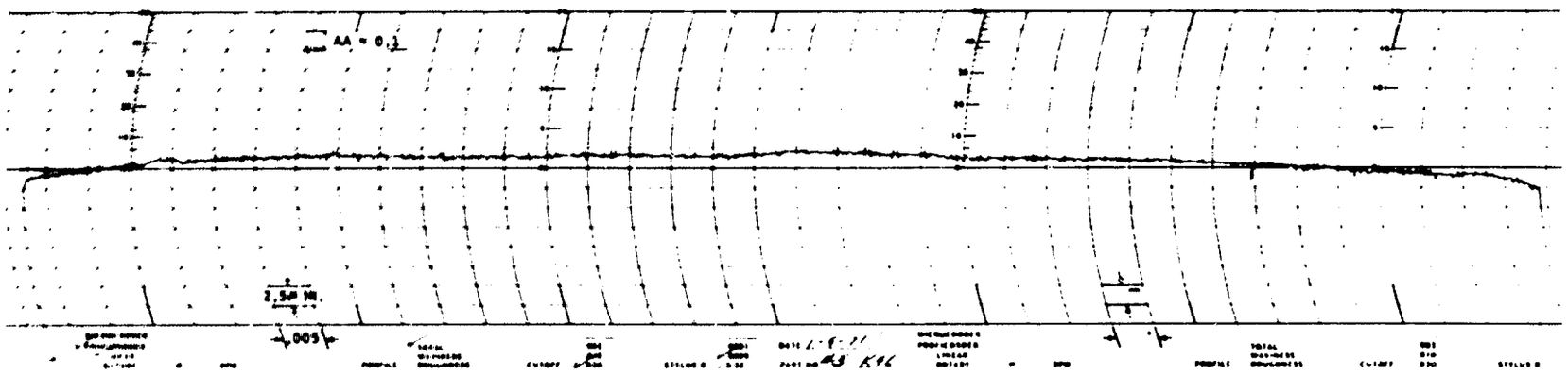

AFTER CIF_5 STATIC EXPOSURE

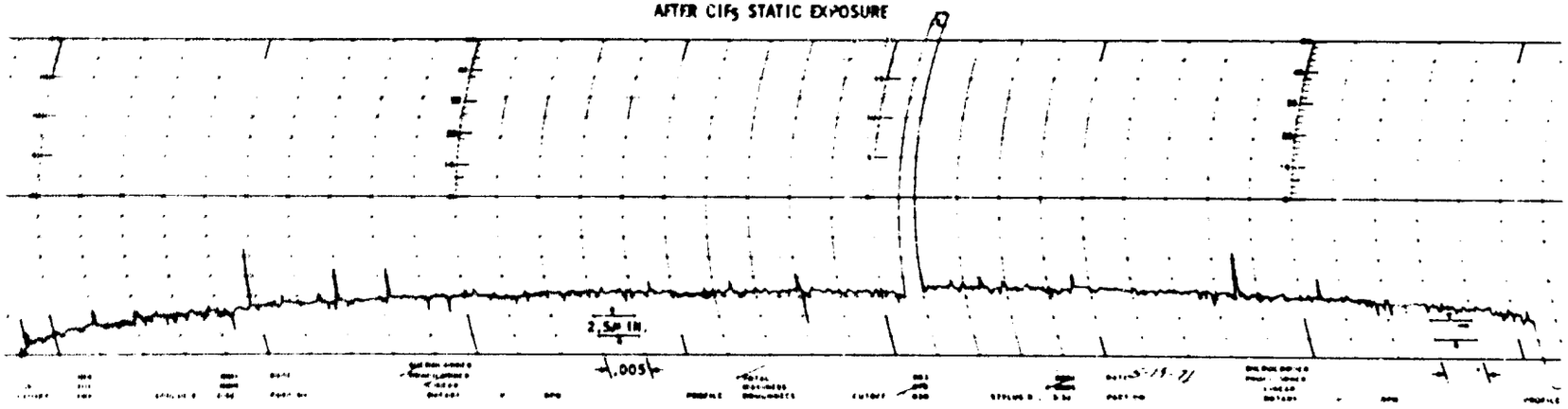

Figure 27

A71-6-035-40

Figure 2-

Ni-301 STATIC GF_2 EXPOSURE POPPET NO. 6
210X SURFACE PHOTO BEFORE TEST

Ni-301 STATIC GF_2 EXPOSURE POPPET NO. 6
210X INTERFERENCE PHOTO BEFORE TEST

Ni-301 STATIC GF_2 EXPOSURE POPPET NO. 6
210X SURFACE PHOTO AFTER TEST

Ni-301 STATIC GF_2 EXPOSURE POPPET NO. 6
210X INTERFERENCE PHOTO AFTER TEST

A71-6-035-51

Ni-301 STATIC ClF_5 EXPOSURE POPPET NO. 7
210X SURFACE PHOTO BEFORE TEST

Ni-301 STATIC ClF_5 EXPOSURE POPPET NO. 7
210X INTERFERENCE PHOTO BEFORE TEST

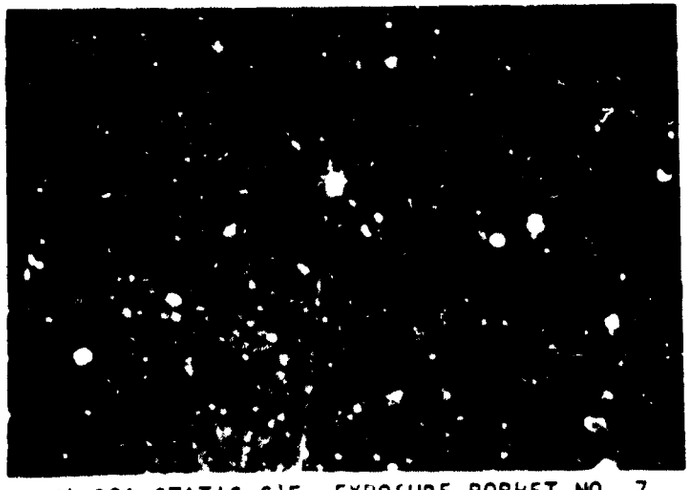

Ni-301 STATIC ClF_5 EXPOSURE POPPET NO. 7
210X SURFACE PHOTO AFTER TEST

Ni-301 STATIC ClF_5 EXPOSURE POPPET NO. 7
210X INTERFERENCE PHOTO AFTER TEST

A71-6-036-52

Figure 29

NICKEL-301 · SAMPLE NO. 5
S.E.M. PHOTOS OF "AS LAPPED" SURFACE

5000X

1000X

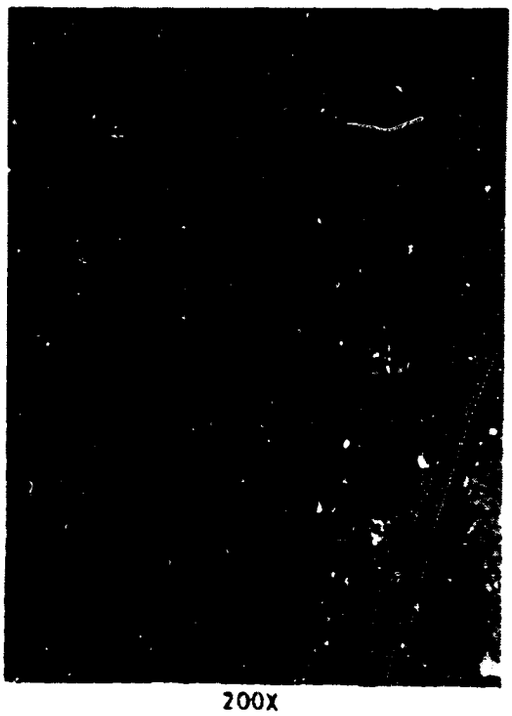

200X

Figure 30

NICKEL-301 - SAMPLE NO. 6
S.E.M. PHOTOS AFTER STATIC GF_2 EXPOSURE

5000X

1000X

200X

Figure 31

NICKEL-301 - SAMPLE NO. 7
S.E.M. PHOTOS AFTER CIF_5 STATIC EXPOSURE

5000X

1000X

200X

Figure 32

nearly identical on all parts. Both sets of scanning electron microscope photographs indicate the presence of a significant number or randomly oriented particles on the surfaces of the test poppets. An attempt was made to define the chemical nature of the particles using the microprobe analyzer; however, the particles had so little mass that an analysis was impossible. Because the particles had so little mass and the fact that they were seen on other parts also statically exposed probably indicates that they are particles which migrated from the mylar bag initially used to package the parts when they were removed from the test facility static exposure test tube. Since the base surface did not seem to be affected, it was concluded that the exposure did not significantly affect the surface character.

As with the other techniques of determining surface differences as a result of the propellant exposure, proficorder examinations of the exposed parts indicated essentially no change in the surface character of the Ni-301 sample poppets. Figure 33 shows comparative proficorder traces taken of the poppet exposed to ClF_5 prior to and after exposure. Traces of surface profiles from the part exposed to fluorine were virtually identical to those of the chlorine pentafluoride exposed part.

Results of all of the examinations of the Ni-301 parts indicate that there was essentially no difference between the pre-exposed and exposed surfaces.

3.3 Boron Carbide (B_4C) Static Exposure Test Results

The boron carbide sample poppets exposed to chlorine pentafluoride and gaseous fluorine apparently withstood the exposure quite well although there were some apparent changes in the surface characteristics. The boron carbide samples reacted to the propellant exposure somewhat similarly although not as severely as the K-96 poppets.

Figure 34 shows interference microscope photographs of the boron carbide poppet exposed to chlorine pentafluoride prior to and after exposure. The comparable set of photos taken of the sample exposed to fluorine has been eliminated because of the surface similarity. Study of these photographs indicate that minor changes occurred on the surface of the parts as a result of exposure. The surfaces do appear to be slightly rougher after exposure with general surface finish changing from about 2.8 to 3.0 AA as a result of exposure. Comparative proficorder traces of surface profile also indicate essentially no difference in character of the surface as shown in Figure 35. Somewhat conflicting data was obtained using the scanning electron microscope. Figure 36 shows a 5000X scanning electron microscope of an unexposed boron carbide surface in the "as lapped" condition. The surface appears to be quite dense with randomly scattered shallow holes on the surface. Figures 37 and 38 show photographs of the sample surfaces exposed to the oxidizers at 200X, 1000X and 5000X. Both sets of photos indicate the same type of activity may have occurred. The exposed

NI-301 STATIC EXPOSURE POPPET
SURFACE PROFILE BEFORE AND AFTER STATIC EXPOSURE TO CIF5

Figure 33

NI-301 POPPET BEFORE EXPOSURE

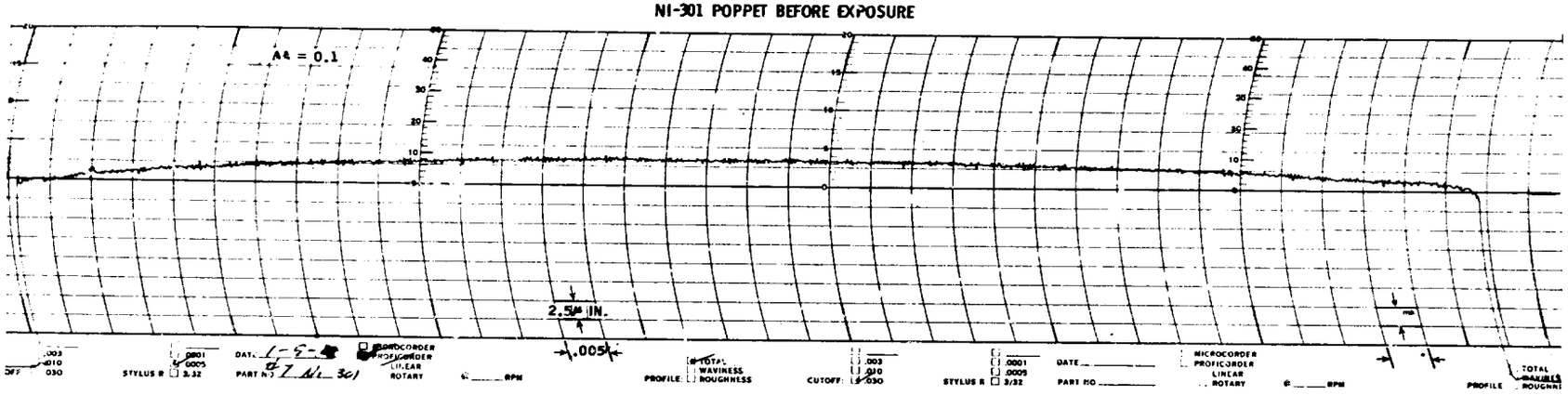

AFTER CIF5 STATIC EXPOSURE

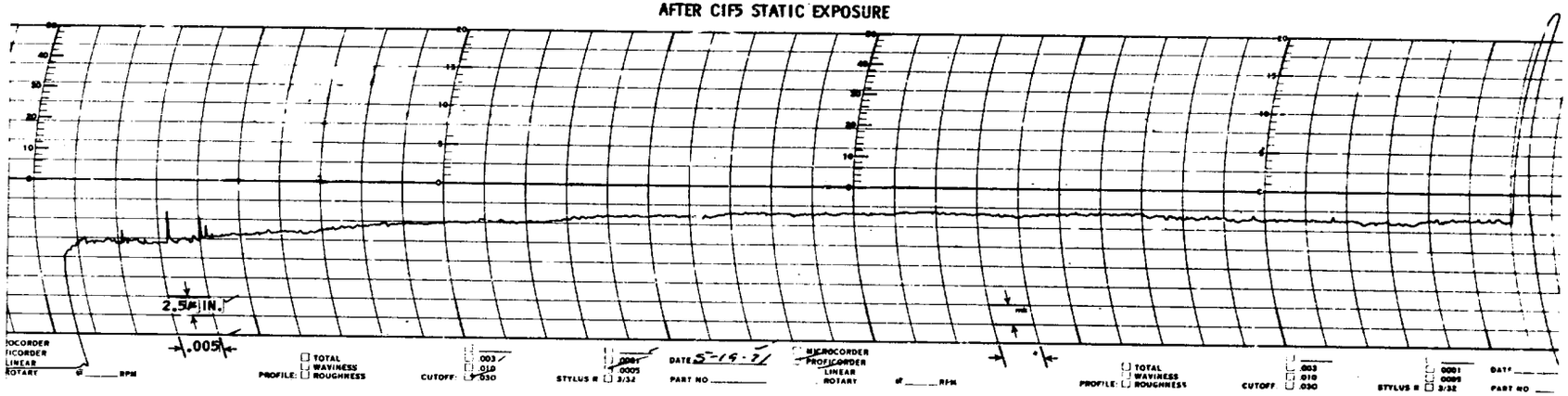

A71-6-10-37

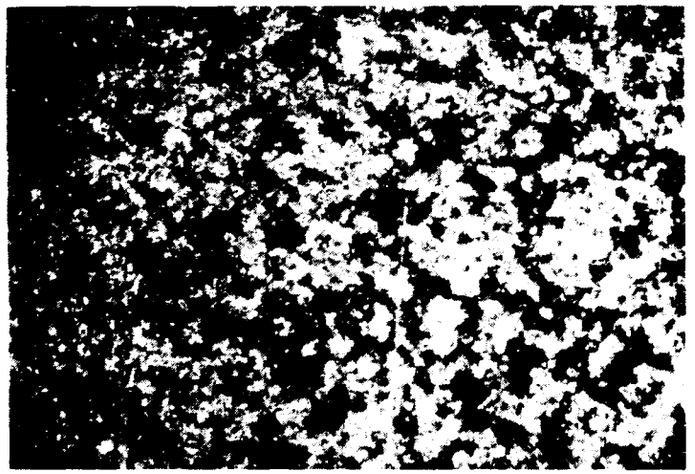

B_4C STATIC ClF_5 EXPOSURE POPPET NO. 23
210X SURFACE PHOTO BEFORE TEST

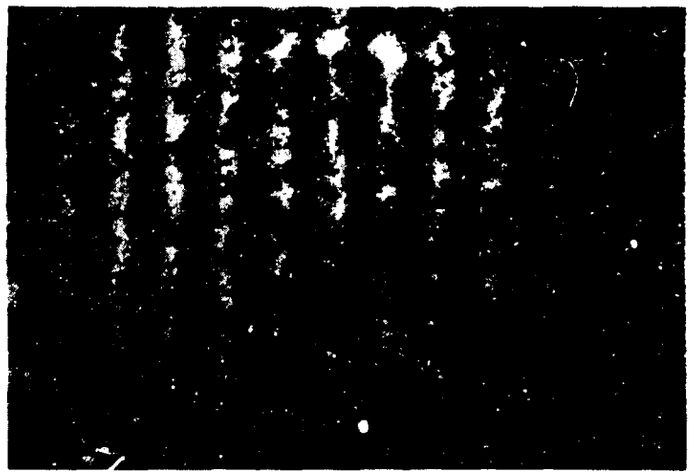

B_4C STATIC ClF_5 EXPOSURE POPPET NO. 23
210X INTERFERENCE PHOTO BEFORE TEST

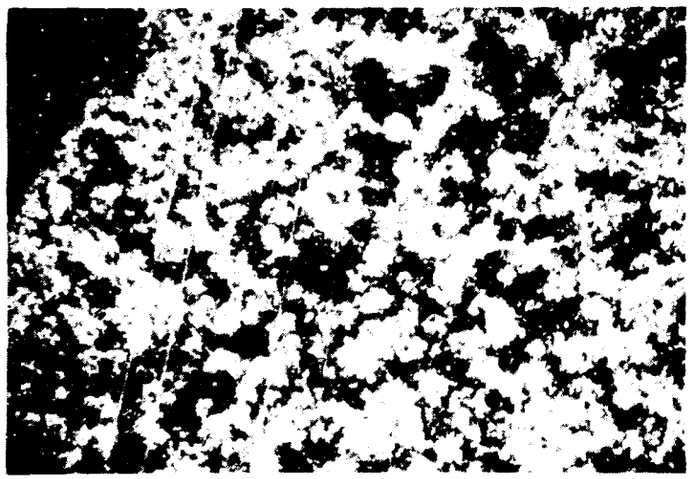

B_4C STATIC ClF_5 EXPOSURE POPPET NO. 23
210X SURFACE PHOTO AFTER TEST

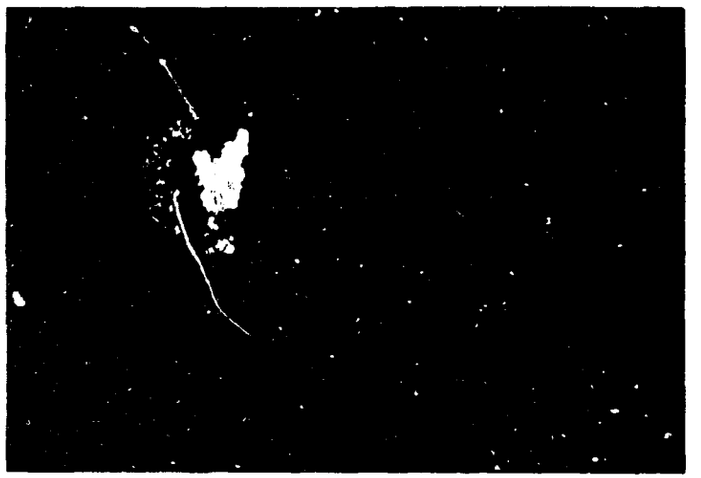

B_4C STATIC ClF_5 EXPOSURE POPPET NO. 23
210X INTERFERENCE PHOTO AFTER TEST

Figure 34

BORON CARBIDE

SURFACE PROFILE BEFORE AND AFTER CIF_5 STATIC EXPOSURE

PRIOR TO STATIC EXPOSURE

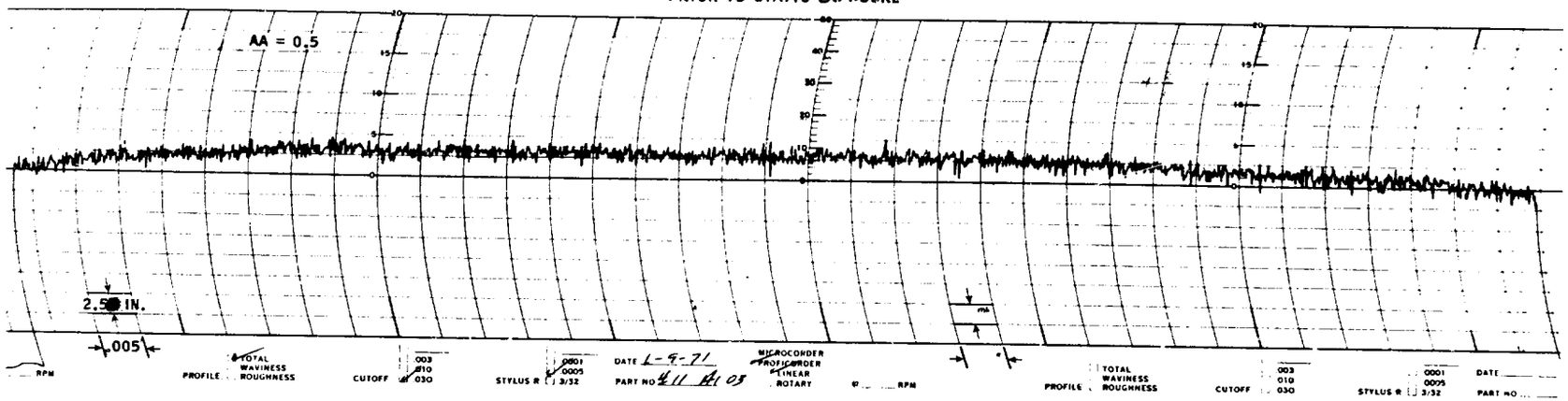

AFTER STATIC EXPOSURE

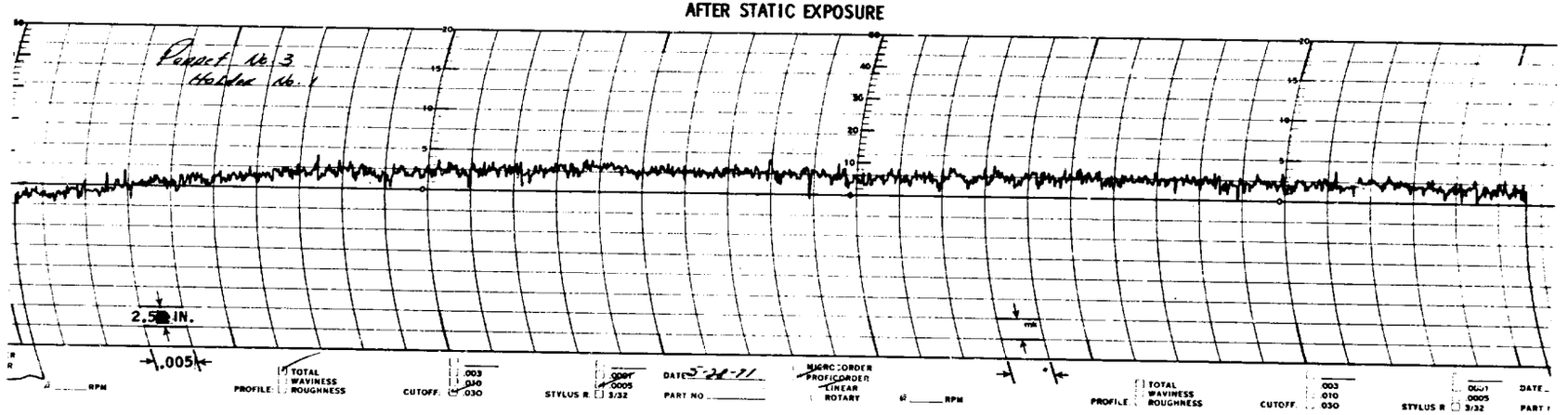

Figure 35

A71-6-036-75

BORON CARBIDE "AS LAPPED" SURFACE

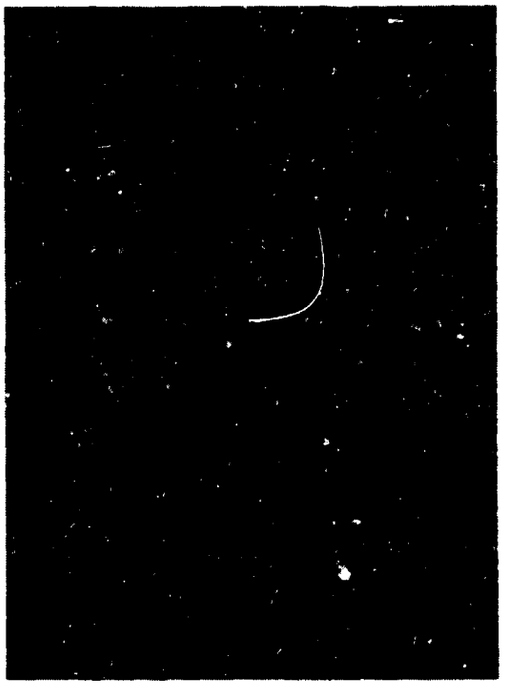

S.E.M. PHOTO AT 5000X

Figure 36

A71-6-036-21

BORON CARBIDE B_4C - SAMPLE NO. 22

S.E.M. PHOTOS AFTER STATIC GF_2 EXPOSURE

5000X

1000X

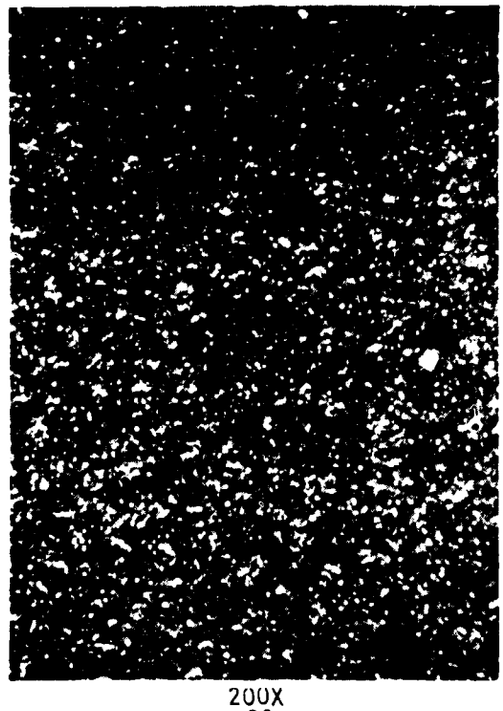

200X

Figure 37

BORON CARBIDE - SAMPLE NO. 23
S.E.M. PHOTOS AFTER STATIC ClF_5 EXPOSURE

5000X

1000X

200X

Figure 38

samples have the same type of random holes apparent on the surface as does the unexposed part. In addition, there are a significant number of what appear to be raised platelets loosened on the edges. As with the K-96, the reaction occurred on a very small scale but not to the degree apparent in the K-96 specimen. These apparent results must be reviewed with some caution since examination of the poppets tested in valves did not show the same degree of similar surface degradation after exposure. The apparent "reaction" may be associated with differences in the lapping process. The parts tested in static exposure were lapped by a different vendor than were the reference specimen or valve test parts with a significantly better finish apparent on the valve test and reference parts. Thus, the surface seen after exposure could be more typical of the lapping process used to finish the static exposure parts.

3.4 Tungsten Carbide (WC) Static Exposure Test Results

Results of exposure of the pure tungsten carbide sample to gaseous fluorine and to chlorine pentafluoride were virtually identical to those obtained with the K-96 tungsten carbide samples. Significant changes occurred on the part surfaces as a result of the exposure to the oxidizers.

Interferograms and surface photographs of the part exposed to chlorine pentafluoride are shown in Figure 39. The comparable set of photographs taken of the poppet exposed to gaseous fluorine is not shown because of similarity. Study of these photographs and interferograms alone would indicate that no significant changes took place on the part surface. The scanning microscope photographs, however, revealed that significant reaction took place. A comparison of the "as lapped" and as exposed surfaces shows that as with K-96 tungsten carbide parts, significant etching took place resulting in removal of the extremely fine finish obtained from lapping. An S.E.M. photograph of the unlapped reference poppet surface is shown in Figure 40. Figures 41 and 42 show the propellant exposed surfaces. The surfaces, similar to the K-96 parts, look like the type of microscopic surface which might be expected of an etched hot pressed or sintered part. Each grain particle is clearly defined and joined to the neighboring particle. The tops of the exposed particles are still flat however, leading to the conclusion that the part might still function quite adequately as a valve seat material even in the etched condition because the holes are very small relative to the width of the seating land of the valve. Thus, an effective microscopic layryinth seal still could be effected. The major difference noted between the K-96 and the pure tungsten carbide parts exposed to the oxidizers is that the grain size of the tungsten carbide parts is almost twice the size of the K-96 part grains. As a result, the holes between particles are larger. This difference in hole size was shown on the profi-corder recordings of surface profile before and after exposure as shown in Figure 43. The K-96 parts did not indicate a significant difference in surface finish; the pure tungsten carbide parts show a significantly degraded surface.

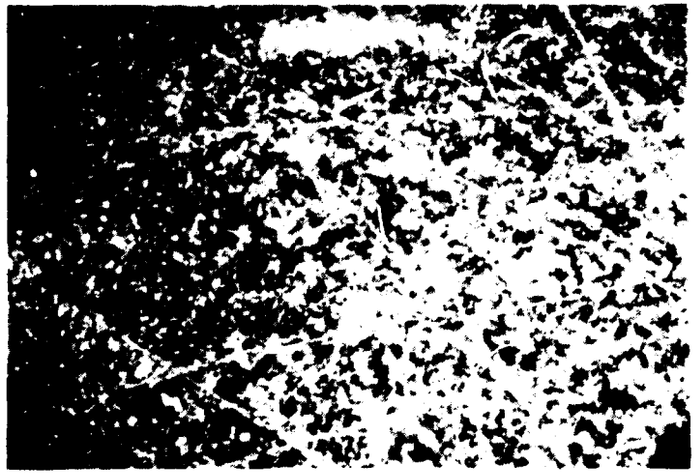

WC STATIC ClF_5 EXPOSURE POPPET NO. 17
210X SURFACE PHOTO BEFORE TEST

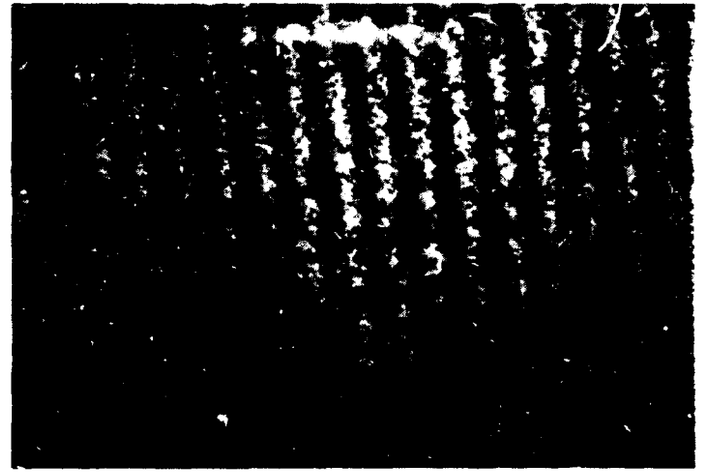

WC STATIC ClF_5 EXPOSURE POPPET NO. 17
210X INTERFERENCE PHOTO BEFORE TEST

WC STATIC ClF_5 EXPOSURE POPPET NO. 17
210X SURFACE PHOTO AFTER TEST

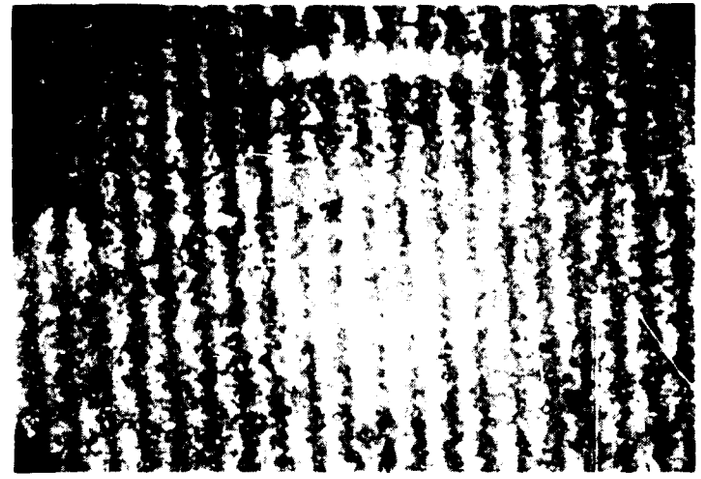

WC STATIC ClF_5 EXPOSURE POPPET NO. 17
210X INTERFERENCE PHOTO AFTER TEST

WC POPPET "AS LAPPED" SURFACE

S.E.M. PHOTO AT 5000X

Figure 40

TUNGSTEN CARBIDE (WC) - SAMPLE NO. 16
S.E.M. PHOTOS AFTER STATIC GF_2 EXPOSURE

5000X

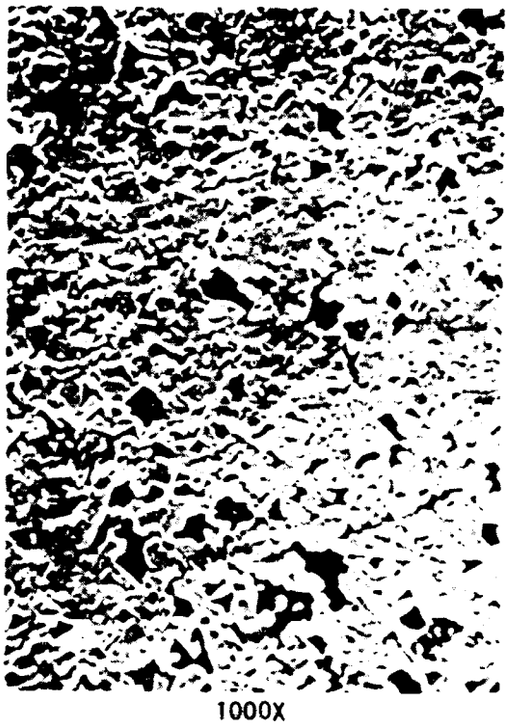

1000X

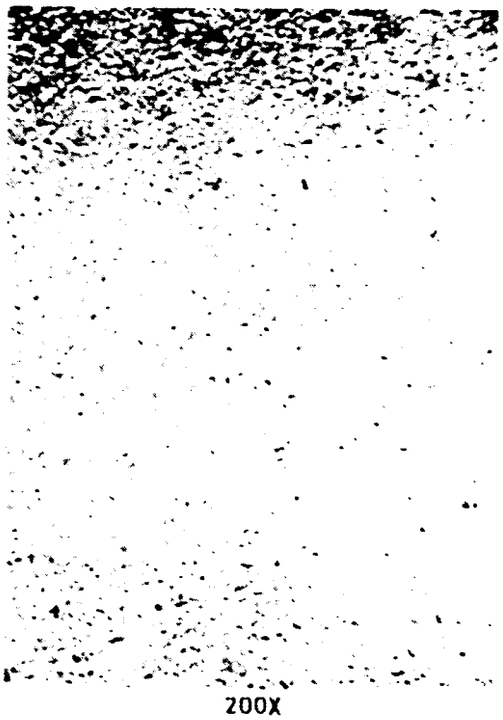

200X

Figure 11

TUNGSTEN CARBIDE - SAMPLE NO. 17
S.E.M. PHOTOS AFTER ClF_5 STATIC EXPOSURE

5000X

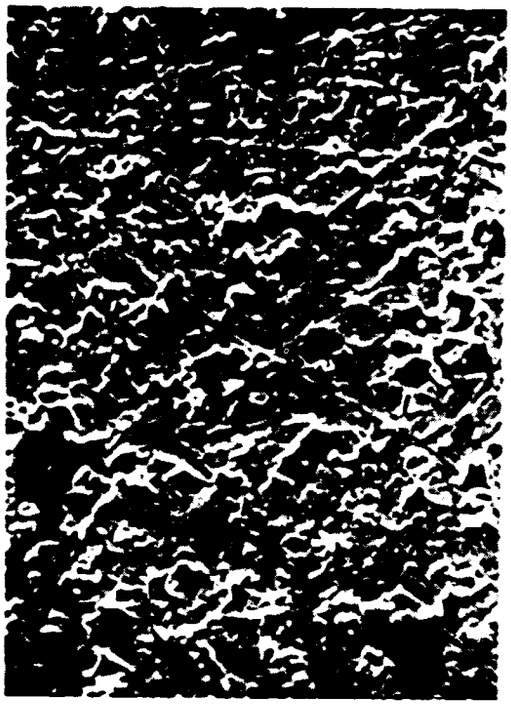

1000X

200X

Figure 42

WC - TUNGSTEN CARBIDE

SURFACE PROFILE BEFORE AND AFTER CIF_5 STATIC EXPOSURE

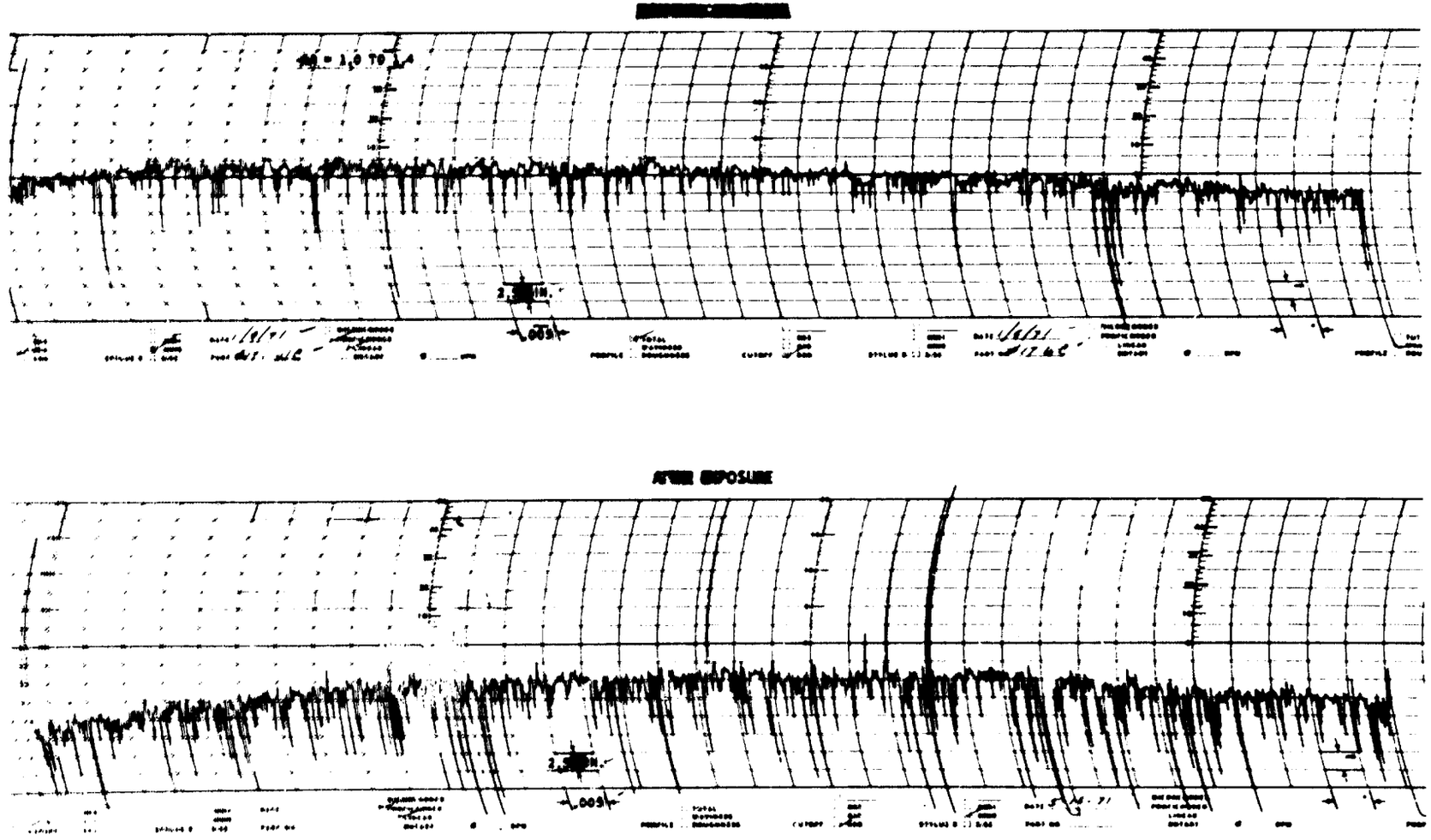

Figure 43

3.5 Aluminum Oxide (Al_2O_3) Static Exposure Test Results

The aluminum oxide sample poppets exposed to chlorine pentafluoride and gaseous fluorine were among the least affected by the period of propellant exposure. There was very little apparent affect on the surface of the propellant exposure.

Figure 44 shows interference microscope photographs of the poppet exposed to chlorine pentafluoride prior to and after exposure. The comparable set of photographs for the poppet exposed to gaseous fluorine is not shown because of similarity in the parts. No change in the poppet surface finish is apparent from either set of photographs. The lap marks are still as sharp and clear as on the pre-test condition. Proficorder traces of the poppet profile prior to and after exposure are shown in Figure 45 for the poppet exposed to chlorine pentafluoride. These traces would indicate that none of the minor sharp edged lap marks were removed by the exposure process.

Scanning electron microscope photographs were taken of each of the exposed poppets to further document the surfaces as exposed to chlorine pentafluoride. No S.E.M. photograph was taken on an "as lapped" poppet for comparison due to a shortage of time at the microscope; however, all data indicates that no significant degradation of the surface took place. Figure 46 shows S.E.M. photographs of the sample surface which had been exposed to gaseous fluorine at 200X, 1000X and 5000X. A comparable set of photos is shown in Figure 47 of the sample poppet exposed to chlorine pentafluoride. Both sets of photographs confirm that the reactivity of the aluminum oxide with the propellants was extremely low.

4. Dynamic Exposure Tests

The dynamic exposure (valve tests) were planned as proof tests to document capability of two of the three selected new materials as a valve seat and poppet material based on results of the static propellant exposure tests. Examination of the static exposure specimens was originally planned to occur significantly ahead of the valve tests so that the data could be examined and one material rejected based on static compatibility with the oxidizer. Timing of the program as actually performed, coupled with conflicting results obtained from static exposure testing, required a minor adjustment in the valve test program so that each of the materials could be tested in at least one of the two test valve configurations. A total of eight valves was tested during the valve test portion of the program. Six of the valves demonstrated acceptable leakage rates for a significant number of cycles during the program, indicating that the material selections which had been made were good candidate materials for incorporation into a finalized valve configuration.

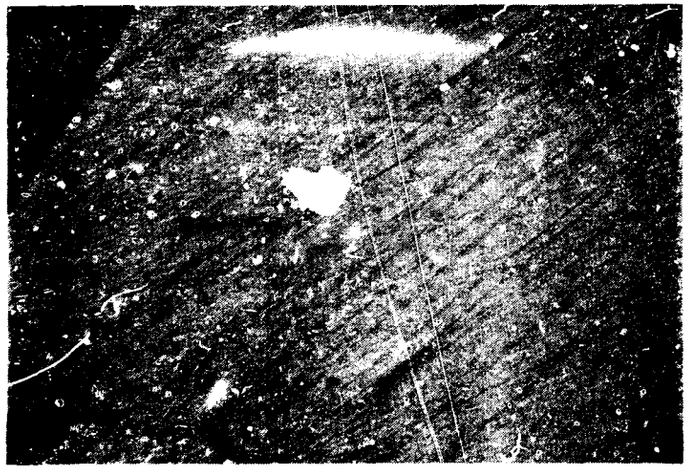

Al_2O_3 STATIC ClF_5 EXPOSURE POPPET NO. 11
210X SURFACE PHOTO BEFORE TEST

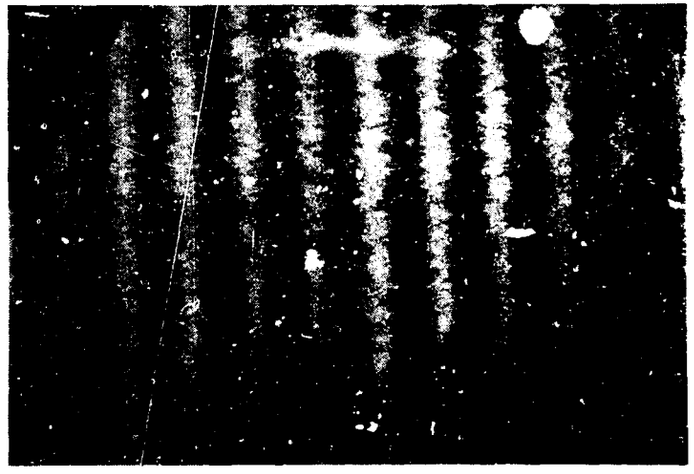

Al_2O_3 STATIC ClF_5 EXPOSURE POPPET NO. 11
210X INTERFERENCE PHOTO BEFORE TEST

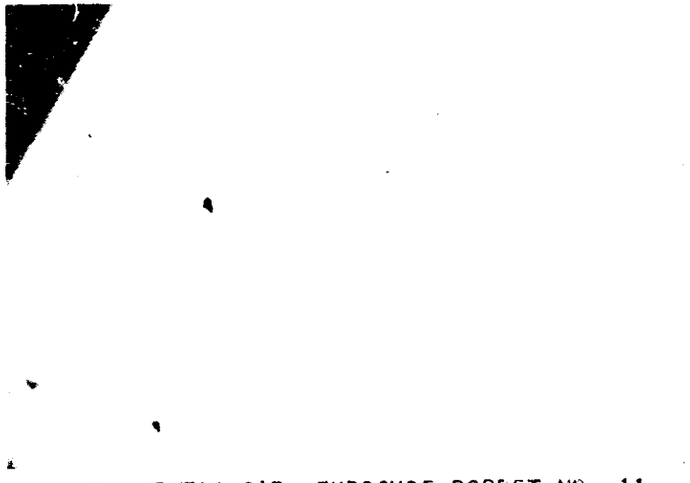

Al_2O_3 STATIC ClF_5 EXPOSURE POPPET NO. 11
210X SURFACE PHOTO AFTER TEST

Al_2O_3 STATIC ClF_5 EXPOSURE POPPET NO. 11
210X INTERFERENCE PHOTO AFTER TEST

Figure 45

AL_2O_3

SURFACE PROFILE BEFORE AND AFTER ClF_5 STATIC EXPOSURE

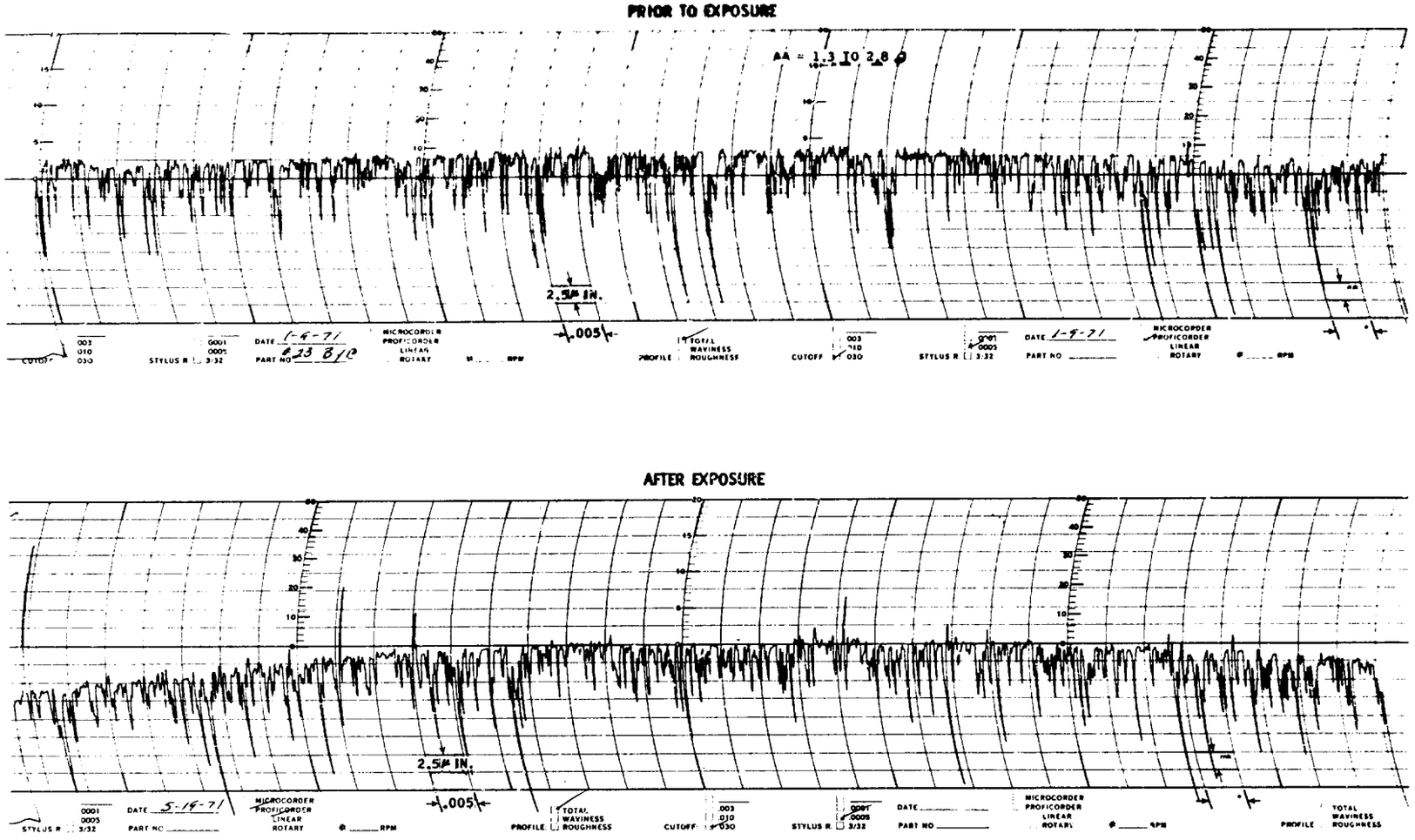

ALUMINUM OXIDE-Al_2O_3 - SAMPLE NO. 10

S.E.M. PHOTOS AFTER STATIC GF_2 EXPOSURE

5000X

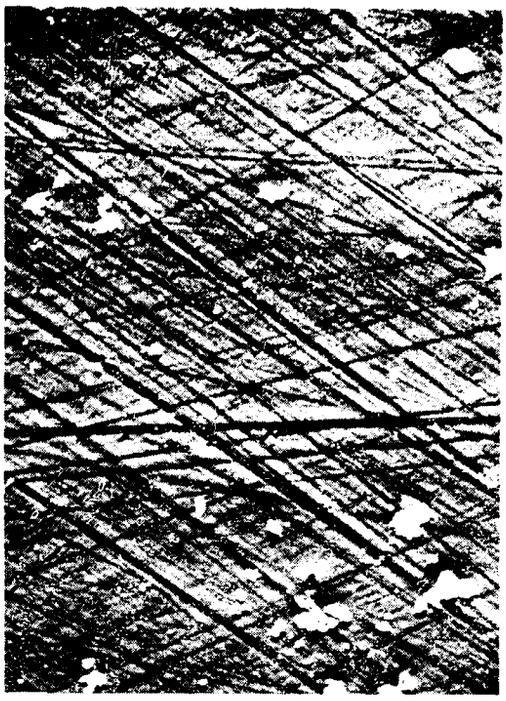

1000X

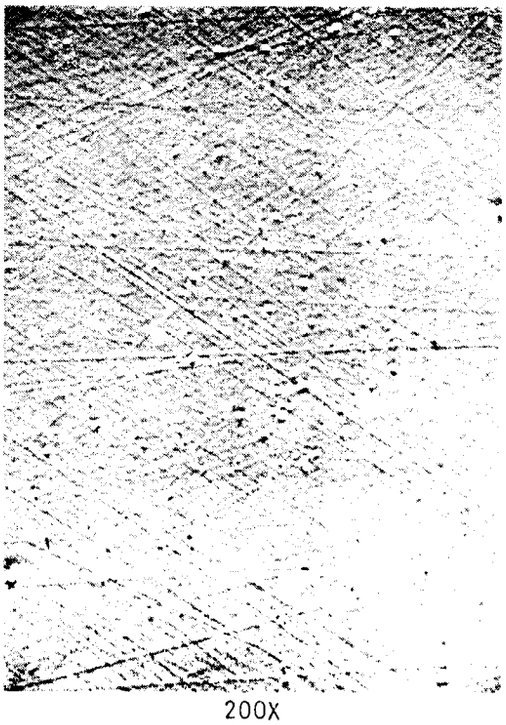

200X

Figure 16

ALUMINUM OXIDE-Al_2O_3 - SAMPLE NO. 11

S.E.M. PHOTOS AFTER STATIC ClF_5 EXPOSURE

5000X

1000X

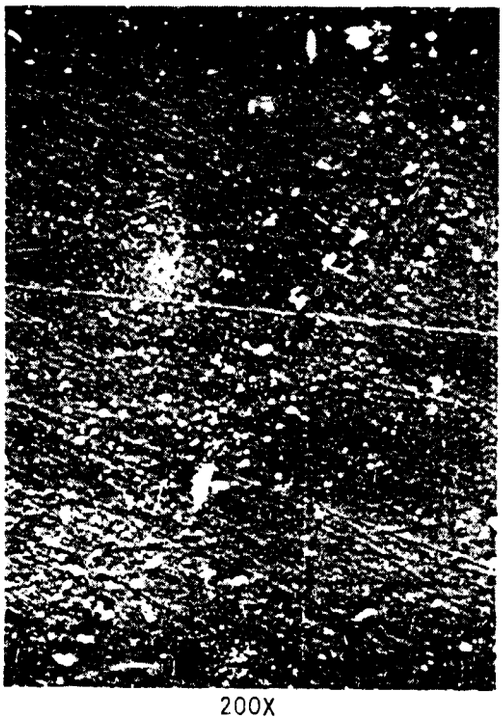

200X

Figure 47

4.1 Valve Configurations

A total of eight valve configurations was tested during the program. The two basic valves used as test beds were the same valve hardware as used during the impact testing. The only difference between the two basic valves was the spring rate of the flexures used to guide the main armature and provide closing forces. The first valve (normal impact) was the same as configuration number 2 described in the impact test section. This design provided a main armature flexure design spring rate of 280 lb/in with poppet self alignment design spring rate of 1300 lb/in. Stroke of the valve as assembled was 0.012 inch norminally. The second valve (low impact) provided a self alignment flexure spring rate identical to the normal impact valve (1300 lb/in) and a nominal main armature design spring rate of approximately 60 lb/in.

Variability in impact rates between the two valves was primarily provided as a result of the difference in main armature return spring rates. The design difference in return spring rates allowed the "low impact" valve armature to travel more slowly in closing. Since the impact force for any given material is primarily a function of the speed at which the poppet is traveling at the time of impact, the low rate return springs of the low impact valve provided relatively lower impact forces.

Impact force levels expected from poppet to seat contact in closing of the valves were calculated for each of the valve configurations tested. The calculated values of impact forces are shown in function of the valve configuration material and propellant fluid in Table VI. The forces calculated are based on the results of the impact tests in water and gaseous nitrogen. Some error is probably present in the calculations for the impact levels predicted in chlorine pentafluoride since fluid viscosity and density can significantly affect closing time of the valve. Since chlorine pentafluoride is considerably more dense and less viscous than water, the two effects may nearly cancel yielding approximate results close enough for this study. Results of the impact levels measured in GN_2 and calculated for GF_2 should be fairly close to reality since gases do not have as significant an effect on valve operating parameters.

4.2 Valve Preparation and Poppet to Seat Alignment

Preparation of the valves for testing was similar to that involved in preparation of the static exposure poppets as far as cleaning precautions were concerned. However, several additional steps were required in preparing each set of valves for testing. After completion of basic cleaning of the parts, the poppets were assembled into the armatures and the valves assembled with the exception of installation of seats and end caps. The valve assembly was then ready for poppet alignment.

TABLE VI

CALCULATED IMPACT FORCES FOR MATERIALS TESTED

MATERIAL	IMPACT LEVEL	TEST MEDIA	CALCULATED IMPACT FORCE (16)
K-96	Normal	ClF_5	48
Ni-301	Low	ClF_5	16
B_4C	Normal	ClF_5	38
B_4C	Low	ClF_5	15
Al_2O_3	Low	ClF_5	15
Al_2O_3	Low	GF_2	37
Al_2O_3	Normal	GF_2	83.3
WC	Normal	ClF_5	48

Mating of the seat and poppet flat surfaces is a primary factor in terms of valve wear and sealing capability. Some self alignment capability is provided in the basic valve design by virtue of the flexure assembly which holds the poppet. When operating the valve in a propellant other than fluorine or chlorine pentafluoride, some misalignment may be permissible. The seat and poppet materials are extremely hard materials and the resulting wear from physical abrasion or impact is very low because the materials are operated significantly below yield stress levels. However, because of the complication of low reaction initiation energy levels with fluorinated oxidizers and the relatively delicate protective passive films which are formed on the materials, malalignment which could result in high local stresses and/or local heating to reaction initiation levels as a result of seat edge to poppet surface contact assumes much greater importance.

Since breakdown of the passive film has been hypothesized as a prime factor in deterioration of the fine finish of the seating surfaces during operation of the valve in fluorinated oxidizers, every effort was made to preclude malalignment as far as possible. A special test fixture was designed and fabricated during the program to provide capability for precise alignment of the poppet and seating surfaces. The alignment fixture, shown in Figure 48, was designed and fabricated by Micro Surface Engineering Co., specifically for this application. It consists of an autocollimator, reference mirror and tool for bending the poppet self alignment flexure while the valve is installed in the fixture.

Operation of the fixture is straightforward. The autocollimator is a device which utilizes two reference mirrors, one internal and one provided by the surface of the poppet. Each has a superimposed scale, one crosshair and the other a graduated scale and center dot. When the two reference mirrors are in perfect alignment, the two scales superimpose. In operation of the fixture, a reference mirror is first used to align the beam and superimpose the scales. The valve assembly is then inserted into the fixture with the valve poppet becoming the second reference mirror. When the poppet self alignment flexures are bent so that the poppet surface is perpendicular to the beam and properly aligned, the scales again superimpose. Using this instrument it was possible to repeatedly align the poppets to less than 1/2 minute of angle misalignment.

Each poppet was aligned to less than 1/2 minute of angle misalignment using the poppet alignment fixture. The poppet and armature were then given a final ultrasonic cleaning and freon flush with gaseous nitrogen drying before completing valve assembly by installing the seat and end plate.

After completion of basic assembly, each valve was pressure checked to determine seat seal leakage and external leakage. No external leakage was allowed. When all static seals were properly functioning, typical leakage from the seat was on the order of 1 to 5 Standard Cubic Centimeters Per Hour (SCCH). Specific data on each valve assembled is provided in the section describing results of each valve test.

POPPET ALIGNMENT FIXTURE

NOT REPRODUCIBLE

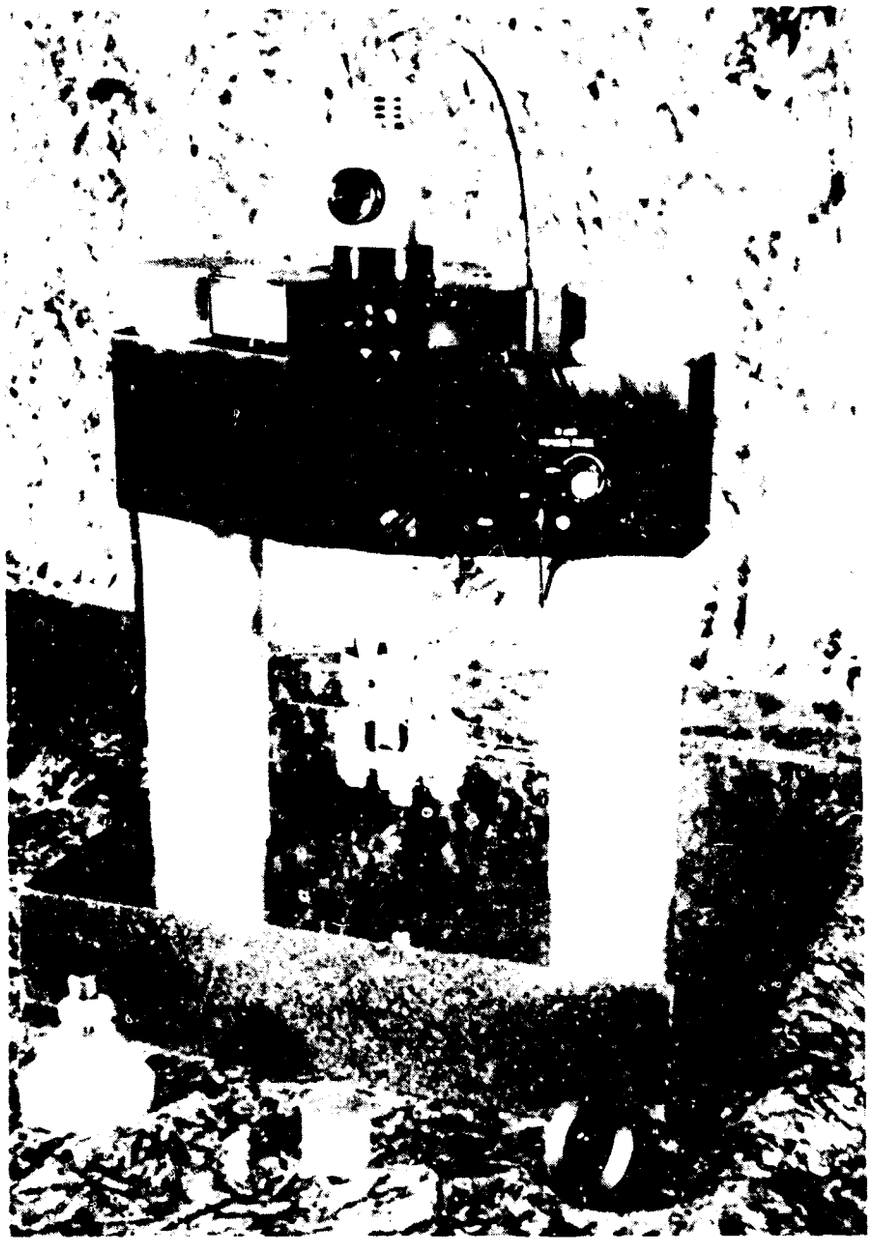

Figure 48

4.3 Final Preparations and Assembly into the Test Facility

After each set of test valves was assembled into the valve test breadboard, the assembly was pressure checked and given a vacuum bake cycle similar to that given the static exposure samples to preclude entrance of atmospheric moisture into the test samples. The breadboard was pressurized with dry nitrogen to 300 psig for transportation to the test facility. As with the static exposure specimens, precautions were taken to purge air from the facility and avoid entrance of moisture into the test breadboard and facility.

4.4 Test Procedure

The facility system used for conducting the tests was built specifically for performing the tests. A photo of the system is shown in Figure 49. The system, as designed, is primarily a nonflowing system. Purging capability is provided for emptying the system during installation of valves or for conducting in-test pressure checks. The test consisted of cycling the valves in the nonflowing environment with periodic purges to flush any particles generated during cycling from the seat area. Complete purging was performed at specific valve cumulative cycle intervals to conduct helium pressure leakage checks. In general, flushing was carried out at 10,000 cycle intervals with leakage tests conducted at 1, 100, 1000, 5000, 20,000 and 100,000 accumulated valve cycles.

4.5 Post Test Handling and Examination

After completion of each valve test, the valve breadboard, pressurized to about 300 psig with helium, was transported to a laboratory dry box for disassembly of the valves and visual inspection of the poppets and seats. Both the poppets and seats were maintained in the dry box environment until further inspection was conducted. Poppets were installed into sample holders identical to those used to hold the static exposure poppets for scanning electron microscope studies. The seats were individually placed in sealed glass jars until removed for vacuum baking to remove residual propellant and gaseous fluoride traces before final proficording and interference microscope inspections.

DYNAMIC IMPACT EXPOSURE TEST

MJL - CELL 4

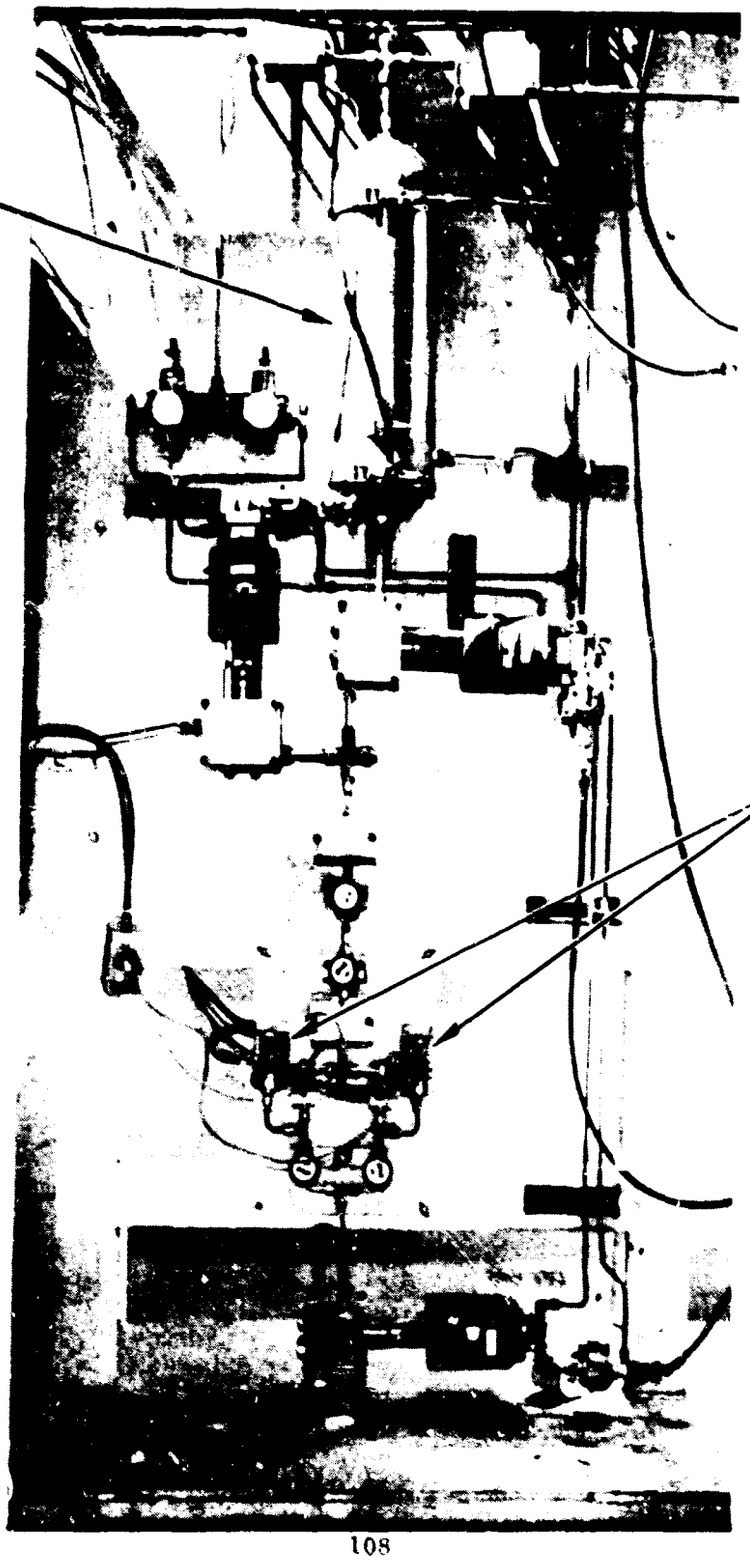

Figure 49

4.6 Leakage Test Results

Each valve configuration tested was subjected to periodic leakage tests throughout the period of accumulation of the required 100,000 valve cycles. In general, leakage tests were conducted at the time of installation into the test facility (prior to fluorine passivation) after passivation and at 100, 1000, 5000, 20,000 and 100,000 accumulated valve cycles. Since all valves were subjected to a common test procedure, leakage results are directly comparable. The results will be presented in this section, however, no attempt will be made to explain the differences in leakage rates recorded until discussion of results of examination of the seats and poppets.

Figures 50 through 57 show the leakage rates measured on each of the valve configurations as a function of valve cycles. The figures are presented in the order in which the valves were tested. Some of the valve leakage tests demonstrated considerable variability between successive tests. This variability is believed to be more a function of total valve and seat to poppet to seat seal performance than test setup problems. Several checks were made between initial buildup leakage rates measured by positive displacement of water in burette and the initial leakage test made prior to fluorine passivation of the valves in the propellant test facility. These tests indicated excellent correlation (within one or two SCCH measured difference) of the two leak rate measurement techniques. Several sources of problems in determining actual leakage in the test facility are apparent. Three of the valves (Ni-301, K-96 and WC) showed a significant change in leak rate immediately after GF_2 passivation. The immediate rise in excessive leak rates for these valves suggests that a static seal in the valve assembly which has a leak path parallel to the seat seal failed at passivation causing a significant percentage of the apparent leakage.

Another factor which could occur but which is not easily evaluated is the possibility that a wear or other foreign particles became trapped between the seat and poppet providing a large leak path. The boron carbide tested at normal impact indicates that type of problem since low leakage rates were measured up to and including 20,000 cycles with a sudden increase in leak rate at 50,000 cycles. That type of leakage rate change is not typical of valve seat seal wear. The valves were periodically flushed to attempt to avoid this problem; however, the nonflowing nature of the test system makes it more sensitive to accumulation of wear particles and/or entrapment of the particles as was apparent on the Al_2O_3 valves tested.

Only one valve nearly met the leakage goal of less than 30 SCCH of helium leakage at 450 psig inlet pressure throughout the test. This was the boron carbide tested at low impact force levels. At completion of the test leakage from this valve was only 1.4 SCCH. However, during the test period, one leakage point at 100 accumulated cycles was 47 SCCH. The K-96 valve marginally met the leakage goal periodically through the test cycle with some points above and some below the leakage goal. The

A71-9-036 90

VALVE LEAKAGE vs. CUM CYCLES

K-96 POPPET AND SEAT

VALVE TEST IN ClF_5

NORMAL IMPACT

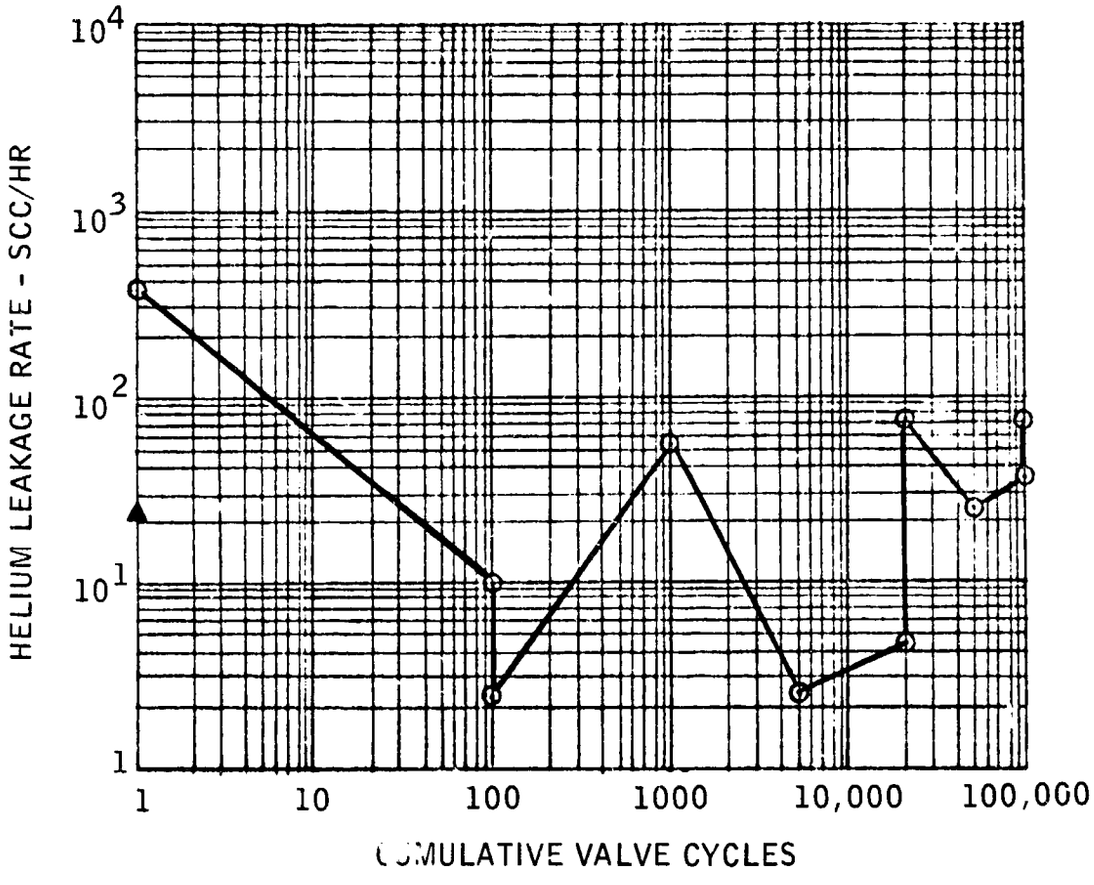

Figure 50

A71-9-036-89

VALVE LEAKAGE vs. CUM CYCLES

Ni-301 POPPET AND SEAT

VALVE TEST IN ClF_5

LOW IMPACT

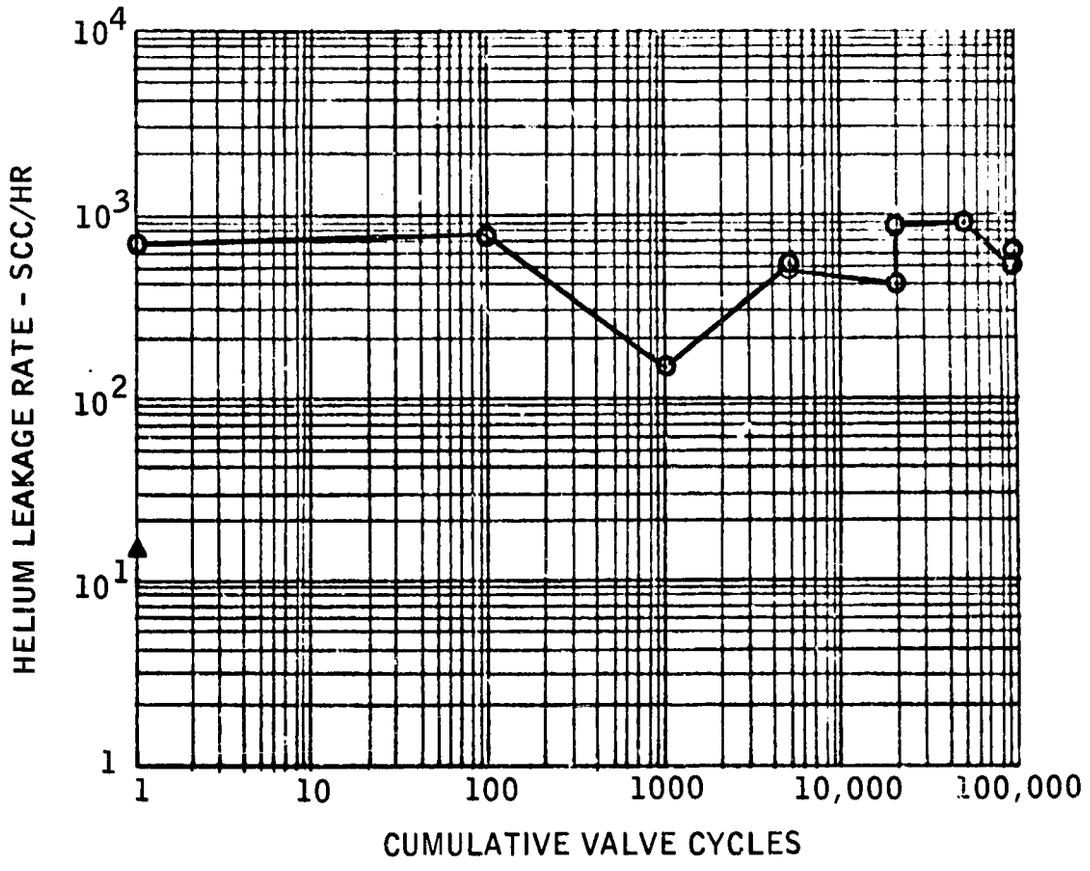

▲ INITIAL ASSEMBLY LEAK CHECK

⊙ IN-TEST LEAK CHECK

Figure 51

VALVE LEAKAGE vs. CUM CYCLES

B_4C POPPET AND SEAT

VALVE TEST IN ClF_5

NORMAL IMPACT

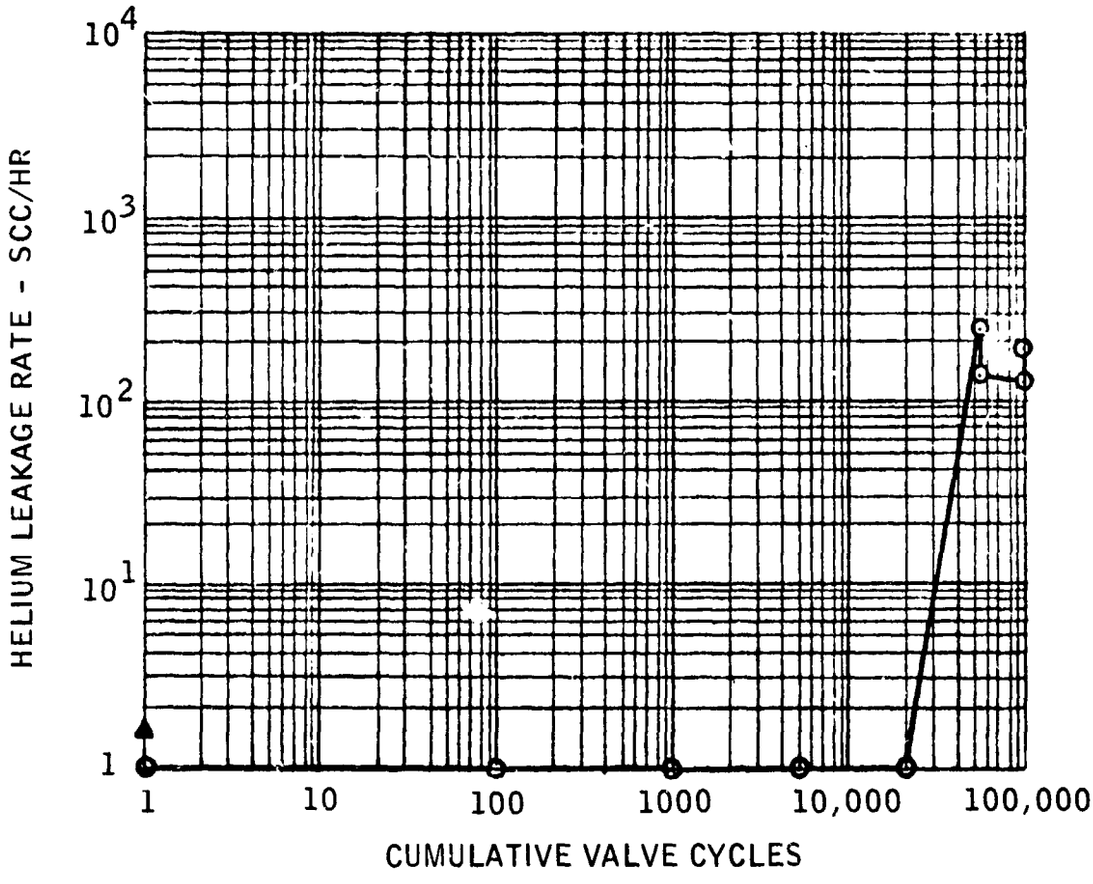

▲ INITIAL ASSEMBLY LEAK CHECK

o IN-TEST LEAK CHECK

Figure 52

VALVE LEAKAGE vs. CUM CYCLES

B_4C POPPET AND SEAT

VALVE TEST IN ClF_5

LOW IMPACT

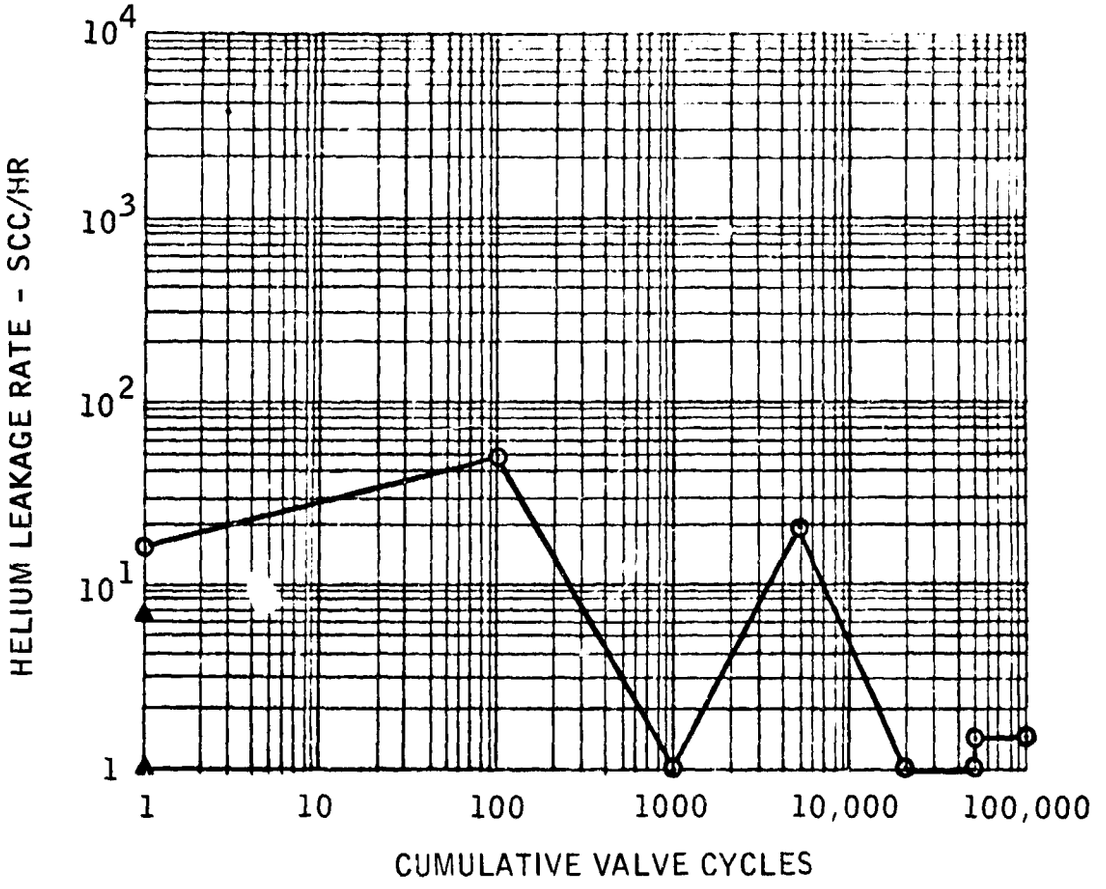

▲ INITIAL ASSEMBLY LEAK CHECK

○ IN-TEST LEAK CHECK

Figure 53

VALVE LEAKAGE vs. CUM CYCLES

WC POPPET AND SEAT

VALVE TEST IN ClF_5

NORMAL IMPACT

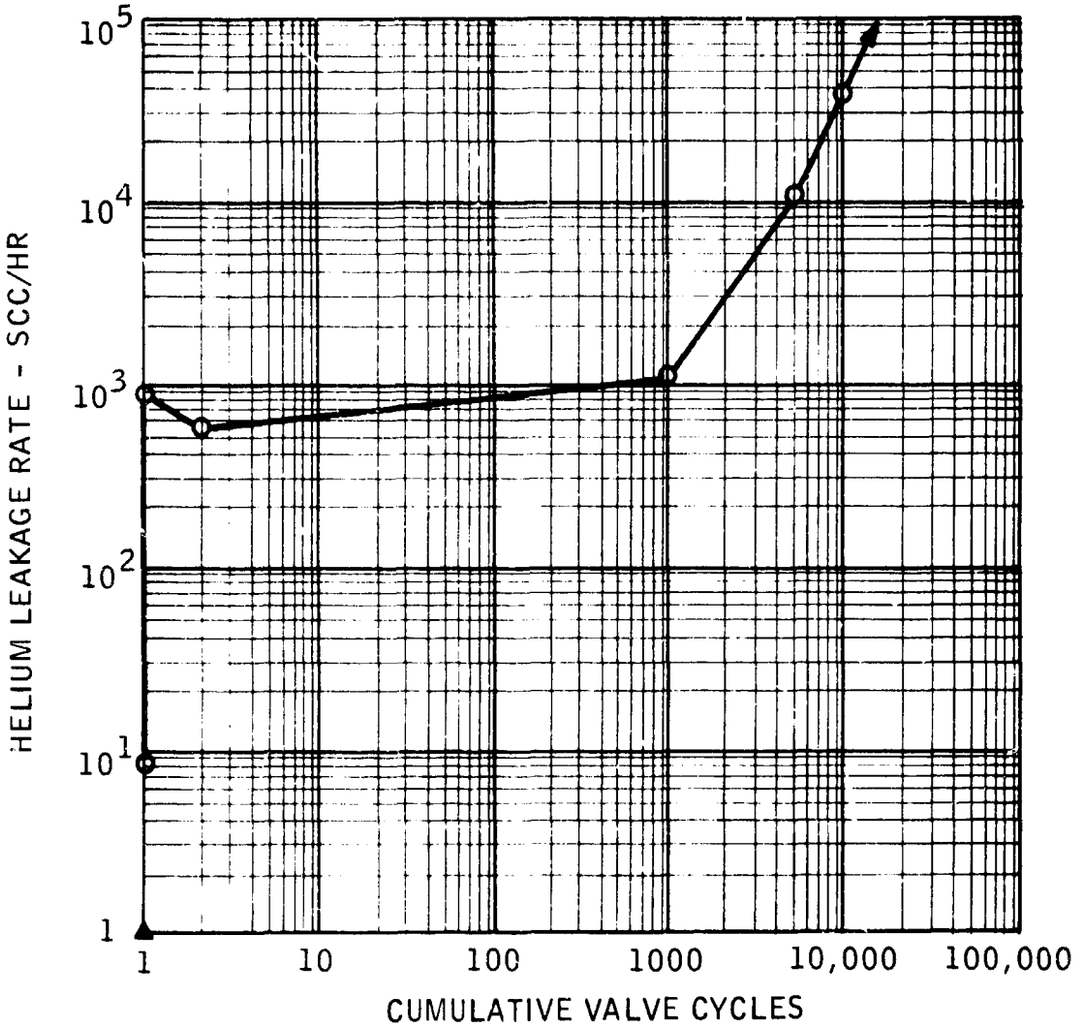

▲ INITIAL ASSEMBLY LEAK CHECK

O IN-TEST LEAK CHECK

VALVE LEAKAGE vs. CUM CYCLES

Al_2O_3 POPPET AND SEAT

VALVE TEST IN ClF_5

LOW IMPACT

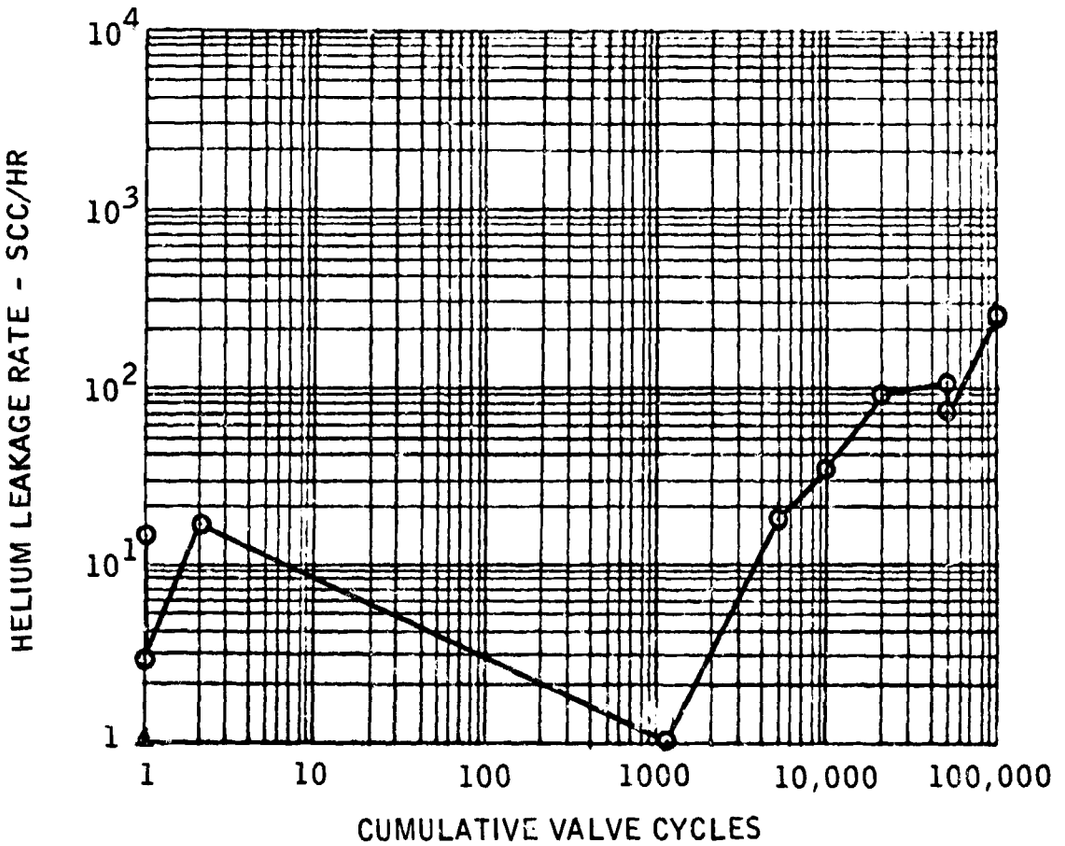

▲ INITIAL ASSEMBLY LEAK CHECK

○ IN-TEST LEAK CHECK

Figure 55

VALVE LEAKAGE vs. CUM CYCLES

Al_2O_3 POPPET AND SEAT

VALVE TEST IN GF_2

NORMAL IMPACT

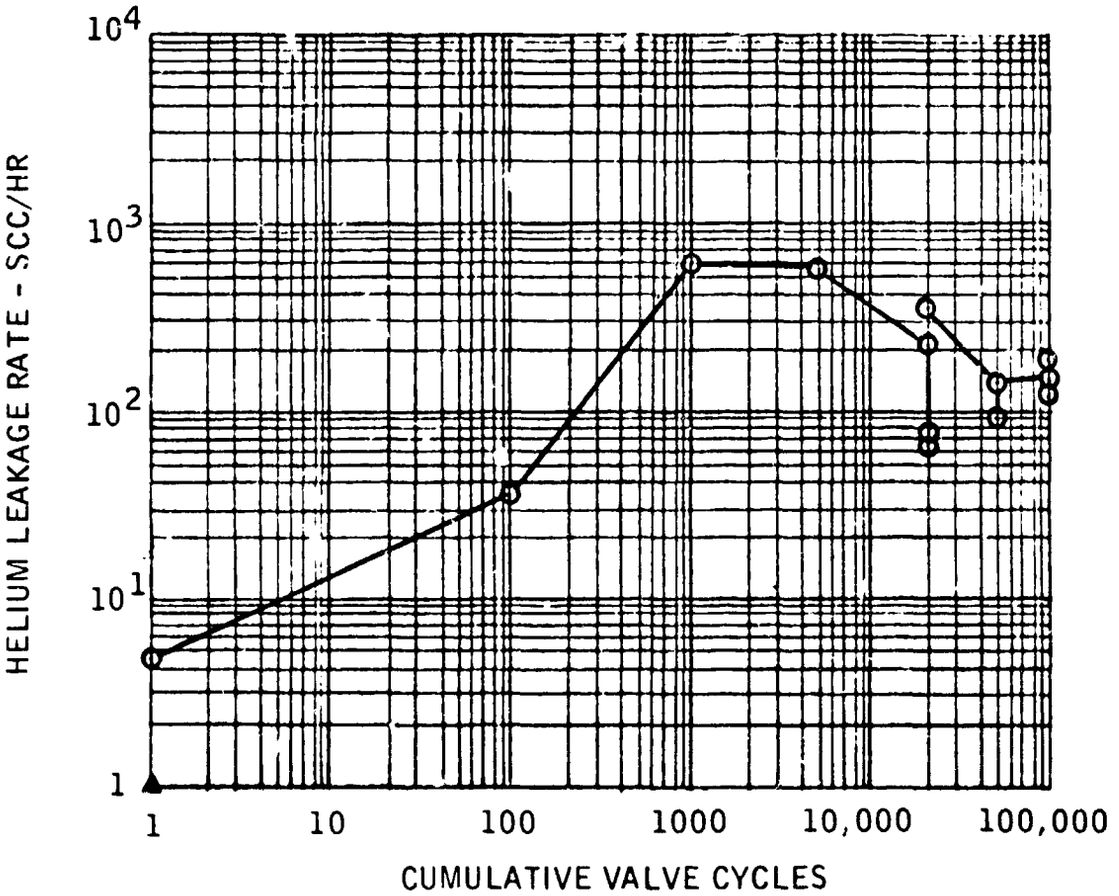

▲ INITIAL ASSEMBLY LEAK CHECK

○ IN-TEST LEAK CHECK

Figure 56

VALVE LEAKAGE vs. CUM CYCLES

Al_2O_3 POPPET AND SEAT

VALVE TEST IN GF_2

LOW IMPACT

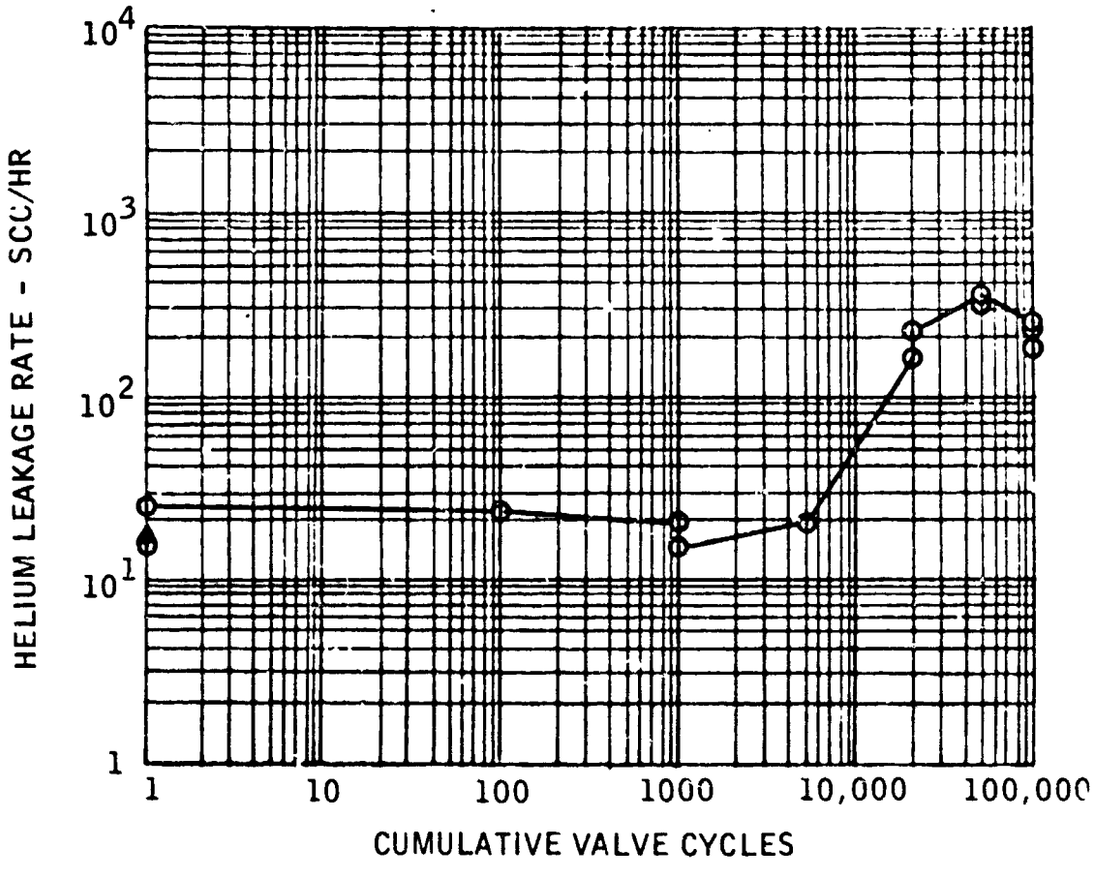

▲ INITIAL ASSEMBLY LEAK CHECK

○ IN-TEST LEAK CHECK

Figure 57

carbide poppet and seat tested at high impact met the leakage goal up to and including 20,000 cycles and then leakage increased at a rapid rate at 50,000 and 100,000 cycles. The remainder of the valves tested demonstrated acceptable leakage rates up to the 1000 to 5000 cycle range with the exception of the pure tungsten carbide poppet and seat which leaked almost 1000 SCCH immediately after passivation and progressively leaked worse as a function of added valve cycles and the Ni-301 valve which leaked at a consistently high rate after GF_2 passivation.

4.7 Poppet and Seat Inspections and Data Evaluation

Each of the poppets used in the valve tests was evaluated following the tests with the scanning electron microscope. Three areas were documented to show the nature of the surface of the poppet in the zone of impact of the poppet with the seat, the upstream exposed zone (outer edge of the poppet) and the downstream zone (center of poppet). Three examination points were required to determine the nature of the material surface which had been subjected to closing impact and the areas which had been only statically exposed to propellant upstream and downstream of the valve. The check exposed to propellant upstream and downstream of the valve. The check in the center of the poppet was primarily intended to determine if the downstream system had been completely protected from contamination with atmospheric moisture during the purge and helium leakage test cycles. All of the poppets appeared to be the same both inside and outside of the seat ring indicating that water contamination had not been a complicating factor in the test results. The results of the Scanning Electron Microscope (S.E.M.) studies are reported on all poppet areas studied even though some of the data may be repetitive.

In addition to S.E.M. studies of all of the test poppets, the seats were studied using the interference microscope and proficorder to provide additional data on the effects of poppet to seat impact.

The data thus far collected do not allow unambiguous conclusions in all cases. This is mainly due to the small number of individual tests performed. (Not one test condition was duplicated in the program). However, there appears to be a definite trend in the results obtained. For example, the degree of surface finish deterioration seems to be clearly a function of impact load, whereas no obvious difference in material compatibility exists between exposure to GF_2 as compared to CPF. The failure mechanism seems to be a different one for each material tested; however, it has to be kept in mind that factors not including the seat to poppet seal play a role in leakage yet cannot be readily separated, especially in a quantitative manner.

4.7.1 Ni-301 Material Evaluation

Duranickel 301 (Ni-301) was one of the original materials selected as a candidate seat and poppet material during design phases of the valve and had been previously tested at normal impact levels with poor results. It is a nickel base, age-hardenable alloy containing 93% nickel and 4.5% aluminum. Previous material compatibility studies had indicated that the passive film formed on this material with exposure to chlorine pentafluoride or fluorine was a tenacious film. Previous failures of the material to satisfactorily perform as a fluorine poppet and seat material had been attributed to breakdown of the film under the impact loading of valve closing. Ni-301 was selected for testing during this program for two reasons:

1. As a reference material from past tests.

2. To determine if testing at lower impact levels might result in less destruction of the passive surface film with attendant loss in surface finish and high leakage.

Results of the tests performed during this program were somewhat inconclusive as far as documentation of leakage under the lower impact levels is concerned. However, considerable insight was gained into the nature of the surface degradation which contributes to valve leakage when Ni-301 is used as the seat and poppet material.

The Ni-301 parts tested were about the best of all the test parts in terms of surface finish of the poppet and seat at the time of valve buildup. During the test period, however, the seating surfaces were degraded significantly. Figure 58 shows surface photographs and interferograms of the seat land surface prior to and after subjecting the seat to 100,000 cycles at low impact in chlorine pentafluoride. The original seat surface was considerably less than one microinch in surface finish after lapping. After testing, the seat surface subjected to valve closing impact was significantly degraded with the presence of a large concentration of lumps on the impact surfaces. The proficorder trace comparisons of the seat surface before and after testing (Figure 59) show that the mean level of the seating surface is the same as prior to testing with the surface lumps rising above the surface to a height of 30 to 35 microinches.

These results are similar to previous test results which indicated positive growth of deposits in the seating surface. Examination of some further photographs of the seat surface (Figure 60) shows that the nonimpacted zones are very similar to the surfaces of the statically exposed poppets. The general seat land surface was domed after the valve test exposure indicating some loss of material from the edges of the seat.

Figure 58

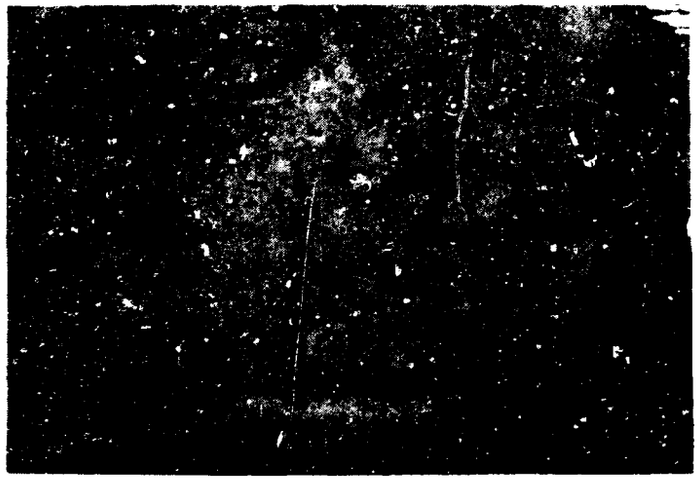

Ni-301 SEAT NO. 8 BEFORE LOW IMPACT
VALVE TEST IN ClF_5 - 210X SURFACE PHOTO

Ni-301 SEAT NO. 8 BEFORE LOW IMPACT
VALVE TEST IN ClF_5 - 210X INTERFERENCE PHOTO

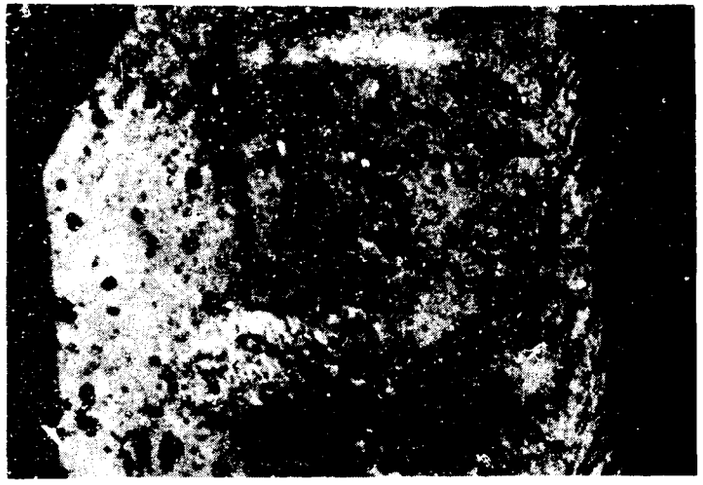

Ni-301 SEAT NO. 8 AFTER LOW IMPACT
VALVE TEST IN ClF_5 - 210X SURFACE PHOTO

Ni-301 SEAT NO. 8 AFTER LOW IMPACT
VALVE TEST IN ClF_5 - 210X INTERFERENCE PHOTO

A71-6-036-58

NI-301 SEAT

SURFACE PROFILE BEFORE AND AFTER 100,000 CYCLE VALVE TEST - LOW IMPACT - CIF_5

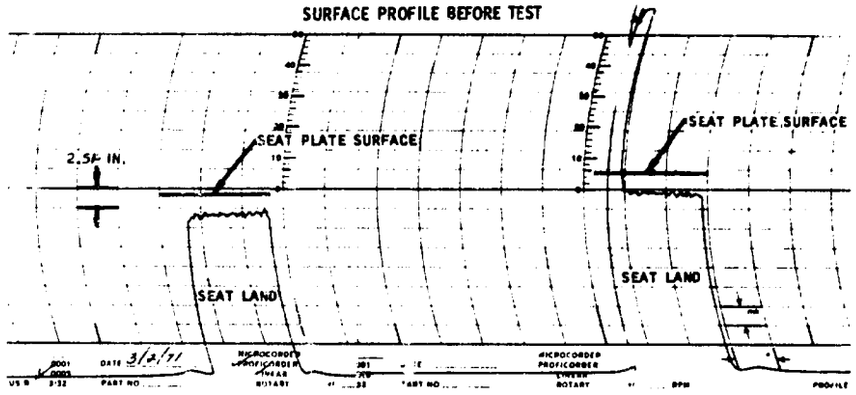

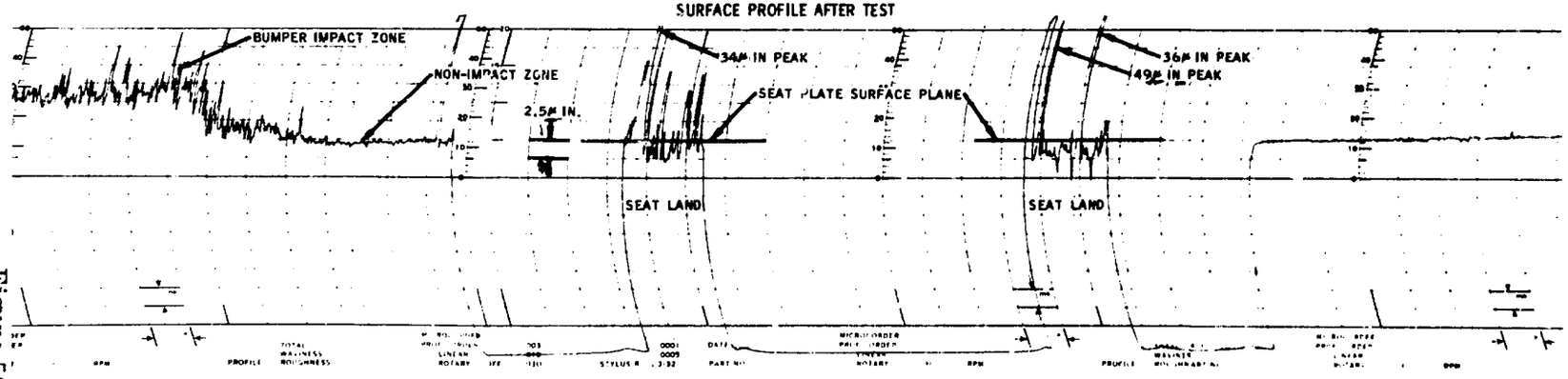

Figure 59

A71-6-036-47

Ni-301 SEAT NO. 8 AFTER LOW IMPACT VALVE TEST IN ClF_5 - IMPACT ZONE - 210X INTERF.

Ni-301 SEAT NO. 8 AFTER LOW IMPACT VALVE TEST IN ClF_5 - NONIMPACT ZONE - 210X INTERF.

Ni-301 SEAT NO. 8 AFTER LOW IMPACT VALVE TEST IN ClF_5 - IMPACT ZONE - 210X INTERF.

Ni-301 SEAT NO. 8 AFTER VALVE TEST IN ClF_5 SEAT LAND DOME - 210X INTERFERENCE

Figure 60

The poppet used in the Ni 301 valve test was examined following the test with the S.E.M. to provide further insight into the nature of the surface degradation. Three sets of photos were taken showing the seating area (impact zone), the upstream area and the downstream area just inside the seat land toward the center of the poppet. An attempt was made during the poppet examination to take a photo set which at the low magnifications would provide a reference as to the seat surface finish relative to the nonimpact upstream and downstream areas. Figure 61 shows a set of photos taken at 200X. In this set of photos, the buildup of solid deposits in the center of the seat land is vividly contracted to the appearance of the nonimpact, only statically exposed areas. The nonimpact areas are similar in appearance to the static exposure test specimens with no apparent surface degradation, while the center section of the seating area shows the random areas of growth of solid deposits. The nature of the seating surface is more clearly shown in Figure 62, the same area at 1000X magnification. In these photos, the light lapping marks are readily apparent on the nonimpacted surface, while the deposits in the seat area can be clearly identified as softly rounded hills. The center of the areas examined is shown at 5000X magnification in Figure 63. In these photos, the center of the seal area deposits is shown to have the appearance of a buildup of loose flakes, several of which can be seen adhering to the surface.

It is interesting to note that all of the nickel base alloys which have been tested in fluorine or chlorine pentafluoride have shown positive buildups in the impact zone. Since this effect is seen on both the poppets and seats, the "added material" must come from somewhere. Several explanations are possible, but most are not too probable. First, the raised surface in the impact area could represent the original surface level which had pieces of the original fluoride film flaked away as a result of the seating impact with the lower surrounding seat level resulting from continued chemical erosion of the continuously exposed surfaces. This explanation would, however, require that the surrounding areas be chemically eroded by at least 30 microinches, since that is the height of the lumps on the surface. That is not too likely, since the lap marks which are less than 1 microinch deep are still evident on the surface, both on the static and dynamic exposure parts and the passive surface film is less than 0.4 microinches. In addition, the mean level of the seat land after testing is the same as before the test. A more likely explanation is provided by reviewing the proficorder traces (Figure 59) and the interference photographs of the seat surface after dynamic exposure. The proficorder trace comparison shows that the edges of the seat surface land have been rounded off with the seat land domed after the 100,000 cycle test, with the center of the seat land being covered with lumps up to 35 microinches in height. A probable explanation for the occurrence of the lumps is that the fluoride material from the edges of the seat migrated through the mechanism of minute adhesive wear. Very slight lateral movement of the poppet relative to the seat is possible at the time the valve closes. This results from the situation that, after the poppet strikes the seat (flat), the poppet self alignment flexure compresses up to the point that the bumper strikes the outer seat flat

A71-6-036-45

NICKEL-301 - POPPET NO. 8

S.E.M. PHOTOS AFTER 100,000 CYCLE - ClF_5 VALVE TEST (LOW IMPACT)

PHOTOS ARE AT 200X

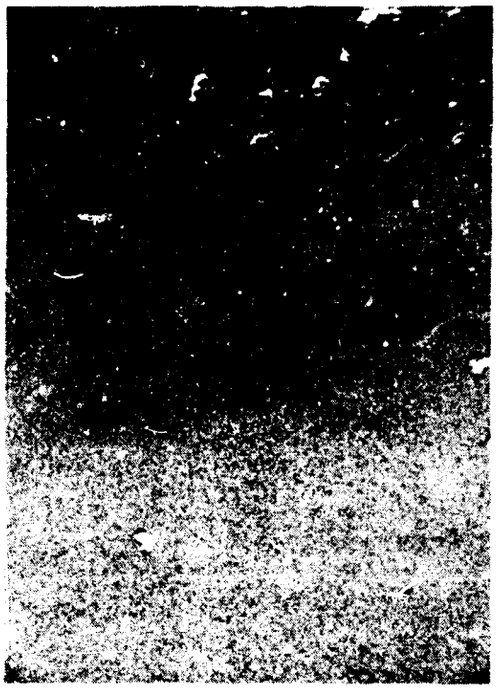

UPSTREAM OF SEAL

SEAL AREA

DOWNSTREAM OF SEAL

Figure 61

A71-6-036-46

NICKEL-301 - POPPET NO. 8

S.E.M. PHOTOS AFTER 100,000 CYCLE - ClF_5 VALVE TEST (LOW IMPACT)

PHOTOS AT 1000X

UPSTREAM OF SEAL

SEAL AREA

DOWNSTREAM OF SEAL

Figure 62

A71-6-036-23

NICKEL-301 - POPPET NO. 8

S.E.M. PHOTOS AFTER 100,000 CYCLE - ClF_5 VALVE TEST (LOW IMPACT)

PHOTOS AT 5000X

UPSTREAM OF SEAL

SEAL AREA

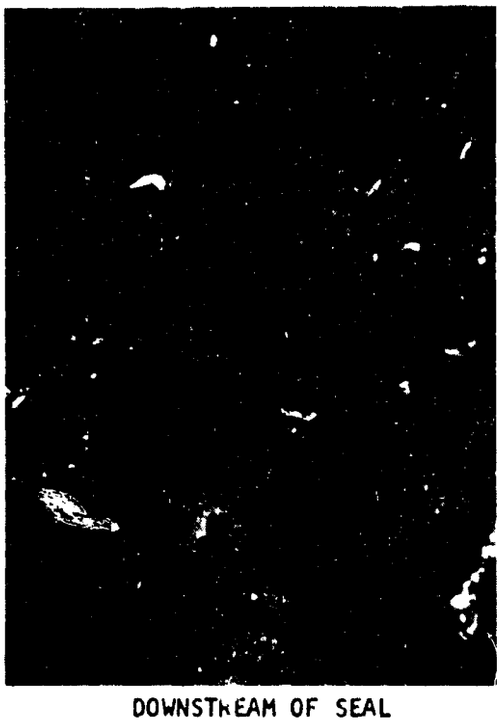

DOWNSTREAM OF SEAL

Figure 63

area. The bumper was designed to absorb the energy of the main portion of the valve armature during valve closing. Although the valve is designed to have both sides of the bumper strike simultaneously, in practice, examination of all the seats tested during this program as well as seats tested at Rocket Propulsion Laboratory, show that the impact energy of the armature is absorbed by only one side of the bumper. The main armature flexures are somewhat like an oilcan lid and would allow the bumper (and thus the poppet) to slide relative to the seat a minute amount. Thus, the nickel fluoride on the seat edges could be induced to migrate toward the center of the seat area through small lateral motions through adhesive wear and material displacement.

This effect was considerably less pronounced in the parts tested with the low impact armature than in those tested with the normal impact armature. Although both bumper impact areas could be seen on the Ni-301 seat, there was evidence that the bumper did not always strike in exactly the same spot and that minute lateral movement took place as evidenced by scratches pointing toward the center of the seat across the bumper land.

An alternate, more probable explanation might be that the buildup of material in the sealing area is caused by the preferential (as compared to nonimpact areas) reaction of nickel due to elevated temperature (created through impact and friction). Thus, the nickel/oxidizer reaction is significantly greater in the impact area as compared to the nonimpact area. Since nickel fluoride is a solid, the seat surface is raised because each nickel fluoride molecule occupies three times as much volume as the nickel from which the fluoride was formed.

One other factor to be considered in assigning a cause to the degradation and/or valve leakage resulting from the Ni-301 test valve tested in this program is the fact that immediately after passivation the valve leaked over 600 SCCH. Leakage did not appreciably increase with accumulated valve cycles as might be expected if the valve was really undergoing significant wear. In fact, several leakage points exhibited lower leakage rates than experienced immediately after passivation. These results indicate that in addition to the minor surface degradation which did occur with increased valve cycles, there was another complicating problem. The most probable cause of the high initial leakage measured after GF_2 passivation and throughout the test is failure of the downstream center seal. A review of Figure 64 will reveal that leakage of the center downstream seal cannot be distinguished from seat sealing closure leakage under test conditions, since both potential leak paths go to the same place. Even though the center seal checked out satisfactorily prior to passivation (low initial measured rate of leakage), the seal could have failed during passivation, resulting in the majority of leakage recorded throughout the test of this valve.

COMPONENT VALVE SEAT SEALS

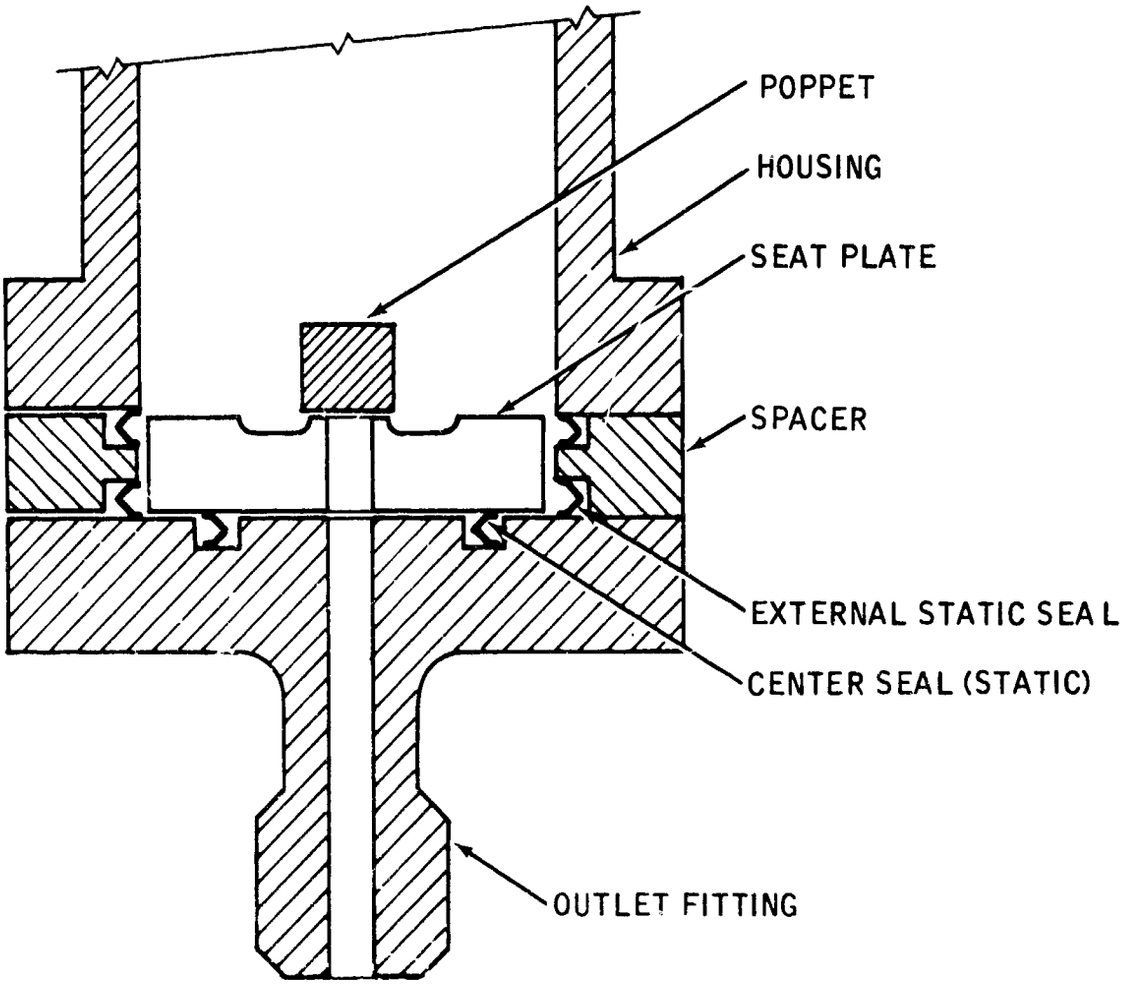

Figure 64

In the case of the nickel 301 valve tested at low impact, it is concluded that the failure of the test valve to adequately seal resulted from two sources:

1. Primary cause of measured leakage was probably failure of the valve downstream center seal during the passivation procedure.

2. A contributing source of probable additional (not verified) leakage was degradation of the poppet and seat seating surfaces through adhesive wear, resulting from extremely minor lateral motion of the poppet, relative to the seat after valve closure. This action resulted in a positive buildup of material in the poppet center section with resultant rounding of the sealing surface.

Although satisfactory leakage characteristics were not demonstrated using Ni-301, it still may be possible that properly used, the material may be satisfactory. From appearance of the statically exposed parts, it is apparent that the material retains a smooth surface without the influence of impact loads. Secondly, the seat and poppet tested at low impact loads performed better than previous tests at higher closing impact loads. Thus, the material may be made to perform satisfactorily if a design is conceived which could lower the impact loads further still. An alternate technique, probably not too promising, would be to increase impact loads above seat loads tested to date. Since the film is "tenacious", it might be possible to batter the thick films formed under impact flat enough to retain a passable sealing surface. The nickel surfaces may stand significant additional loading before erosion starts to occur. In conjunction with either approach, possibility of lateral motion of the poppet relative to the seat after initial contact should be eliminated as far as possible. Potential sliding, even at the low loads, is undesirable. A design change to reduce the possibility of sliding would help in obtaining reasonably satisfactory performance using Ni-301.

4.7.2 Tungsten Carbide (K-96) Material Evaluation

Tungsten Carbide K-96 was selected for testing during this program for several reasons. First, tests completed at Rocket Propulsion Laboratory, Edwards Air Force base, showed that the material had satisfactorily met the leakage goal throughout a 100,000 cycle test. Secondly, a reference data point was desirable in evaluating the performance of the additional new materials to be tested in this program. Thirdly, an additional data point proving K-96 to be suitable valve seat and poppet material for use with chlorine and pentafluoride and gaseous fluorine, was desirable. Tungsten Carbide K-96 is pure tungsten Carbide with 6% cobalt binder. It laps to a very fine surface finish and has excellent wear and impact resistance characteristics. Results of the tests performed during this program using K-96 were somewhat surprising insofar as the reactivity of the base material with chlorine pentafluoride and

gaseous fluorine was concerned. The leakages measured through the valve test confirmed previous test results and affirmed that the material is probably one of the better candidate seat and poppet materials.

The K-96 poppet and seat used for the normal impact valve test in this program was excellent with regard to apparent surface density and surface finish prior to starting the test. Finish degradation of the nonimpacted surface as well as significant deterioration of the seating surface was apparent after completion of the 100,000 cycle valve test at normal poppet to seat closure impact. Figure 65 shows surface photos and interferograms of the seat surface prior to and after the valve test. The photos of the seat land after the test show that the surface is considerably degraded from the initial surface finish. Not only was the surface finish degraded by the opening up of a significant number of holes on the surface, but the seat shows the effects of what appears to be considerable abrasive type wear. The interferogram of the seat after the test, shown in Figure 65, shows that the surface is grooved.

Depth of the grooves from the mean surface level averaged from 30 to 40 microinches. In addition to the grooving, a comparison of proficorder traces recorded before and after completion of the 100,000 cycle valve test (see Figure 66), the mean surface level of the seat to have been eroded 60 to 70 microinches as a result of the valve test. Interestingly enough, the grooves line up with the area of the seat plate where the bumper contacted the seat. General surface finish is rougher than the as-lapped surface, with occasional raised lumps. Examination of the K-96 seat as well as other seats tested in the normal impact valve configuration showed that only one side of the bumper contacted the seat plate during valve closing. The condition of nonuniform seat contact by the bumper was much more pronounced with the normal impact valve than with the low impact valve armature. Examination of the Ni-301 seat indicated that the bumper was hitting on both sides of the seat; however, the bumper didn't always strike in quite the same place, indicating some tiny lateral movement. The high spring rate (normal impact) always struck on only one side of the bumper. This condition can result in a turning moment being applied to the main armature as shown in Figure 67, with the result that although the poppet may initially strike the seat flat, it can be dragged across the seat by the action of the bumper applying a moment to the main armature, with the main armature flexures warping like an oilcan lid with eccentrically applied load.

Further examination of the poppet tested in the valve was conducted using the S.E.M. Three sets of photos were taken using the S.E.M. to document the nature of the surface both upstream and downstream of the seat land as well as in the sealing area. As with the Ni-301 parts, photos were taken so that the 200X photos showed both edges of the seating surface. Figure 68 shows the set of photos taken at 200X magnification. It is apparent that the surface in the sealing area is of different character than the

A71-6-036-48

K-96 SEAT NO. 4 BEFORE NORMAL IMPACT
VALVE TEST IN ClF_5 - 210X INTERFERENCE PHOTO

K-96 SEAT NO. 4 AFTER NORMAL IMPACT
VALVE TEST IN ClF_5 - 210X INTERFERENCE PHOTO

K-96 SEAT NO. 4 BEFORE NORMAL IMPACT
VALVE TEST IN ClF_5 - 210X SURFACE PHOTO

K-96 SEAT NO. 4 AFTER NORMAL IMPACT
VALVE TEST IN ClF_5 - 210X SURFACE PHOTO

Figure 65

K-96 SEAT

SURFACE PROFILE BEFORE AND AFTER 100,000 CYCLE VALVE TEST - NORMAL IMPACT - CIF_5

SURFACE PROFILE BEFORE TEST

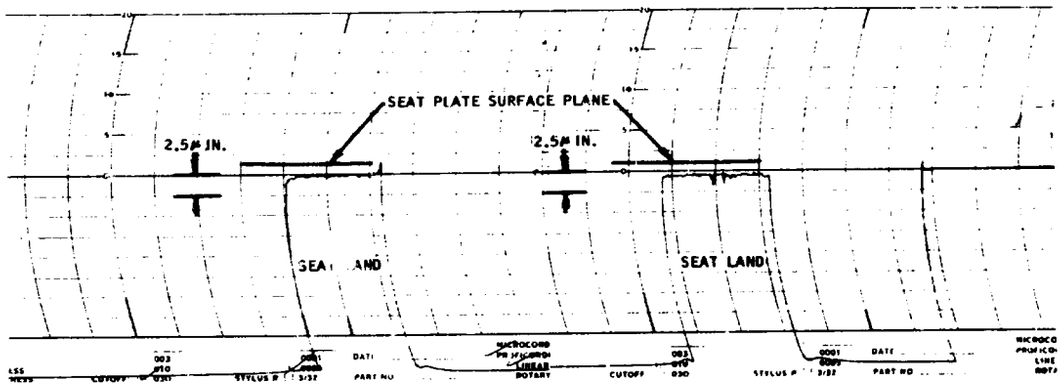

SURFACE PROFILE AFTER TEST

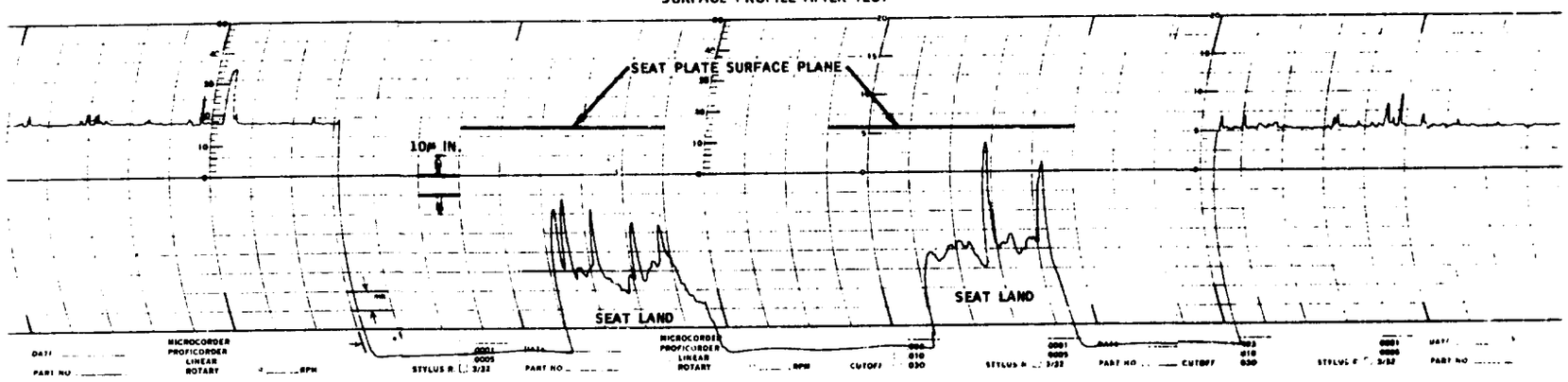

Figure 66

A71-6-036-34

NONUNIFORM BUMPER IMPACT

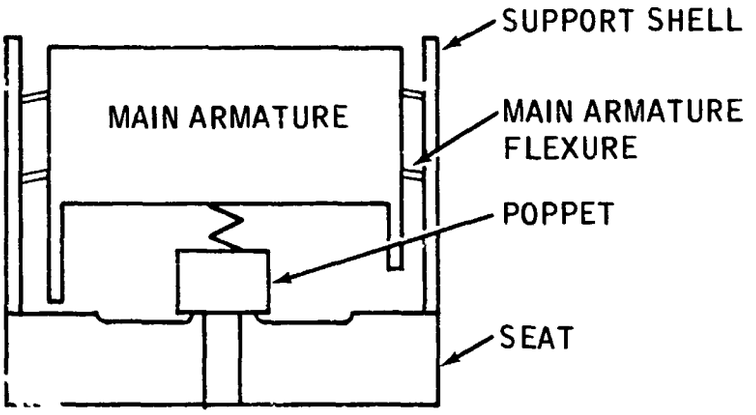

POPPET STRIKES FIRST

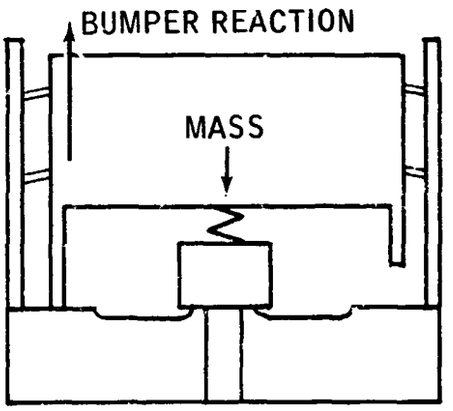

NONUNIFORM BUMPER IMPACT CAUSES COUPLE

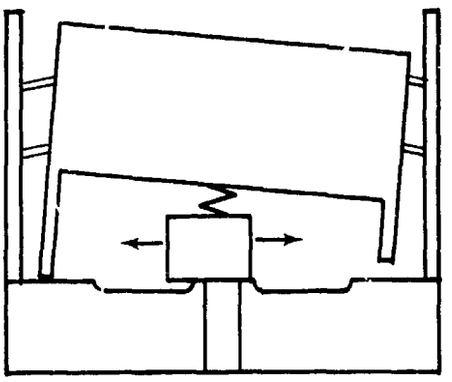

RESULT - LATERAL MOTION

Figure 67

TUNGSTEN CARBIDE K-96 - POPPET NO. 4

S.E.M. PHOTOS AFTER 100,000 CYCLE - ClF_5 VALVE TEST (NORMAL IMPACT)

PHOTOS AT 200X

UPSTREAM OF SEAL

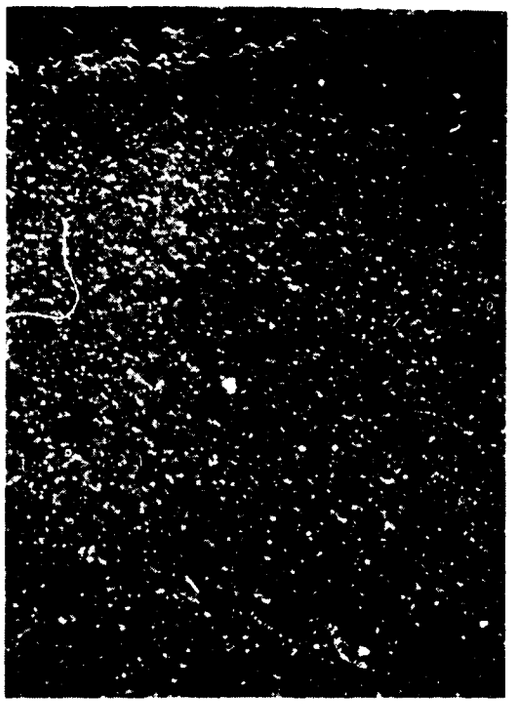

SEAL AREA

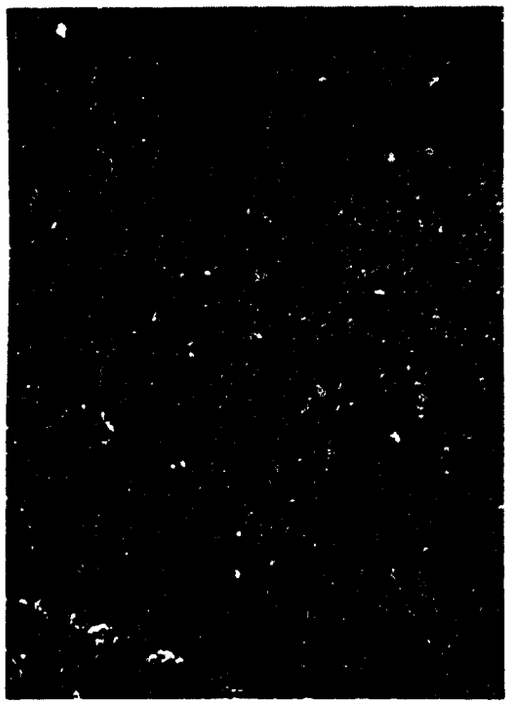

DOWNSTREAM OF SEAL

Figure 68

adjacent nonimpacted areas even at this low magnification. At 1000X magnification (see Figure 69), the difference becomes even more apparent. There is a coloration difference between the impact and nonimpact areas, with the seal area appearing to be more dense. The final set of photographs shows the difference quite clearly at 5000X, Figure 70.

The upstream and downstream areas shown in Figure 70 are quite similar in nature to the static exposure samples previously discussed. The smooth finely finished surface evident in the "as lapped" surface (Figure 40) have been etched to clearly show the individual hot pressed grainy structure of the K-96. In the sealing area, there is quite a difference in coloration as well as the optical effect of a considerably more dense surface. The difference in surface appears to be a real difference. It was through that the more dense surface evident on the seal area might be a function of the focus of the camera at the time the first set of photos was taken. To confirm the difference, a second set of photos was taken approximately a month after the initial set of photographs. They presented an almost identical view of the surface indicating there was really a difference in the two adjacent surfaces. Although the surface films formed on the test parts were really too thin to do good quantitative material analysis, several checks were made using the microprobe to attempt to define the difference between the impact and nonimpact surface areas. A check of cobalt concentration in the three areas revealed almost three times as much cobalt in the seal groove area as in the nonimpact areas. A check of fluorine concentration showed slightly more fluorine in the nonimpact area upstream of the seat than in the seating area. This could indicate that the difference in appearance between the impact and nonimpact surfaces was primarily a matter of cobalt concentration, since the fluorine concentration did not indicate that the material was cobalt fluoride by showing a high fluorine concentration, as well as high cobalt. This effect could result if the cobalt fluoride formed is relatively protective of the cobalt binder with the tungsten carbide being reacted away from the cobalt binder structure, leaving a high cobalt concentration. It may be possible that the primary factor contributing to the relative success of the valve in sealing throughout the test was the presence of excess cobalt remaining in the surface and being pounded down between and covering the grains of tungsten carbide.

Another factor to be considered in deciding the adequacy of the K-96 as a dynamic seal material is the fact that as with the Ni-301, a high leakage rate was measured immediately after passivation. Leak rate prior to passivation was 21 SCCH at 450 psig inlet pressure. Immediately after passivation, leakage rate measured at 450 psig was 377 SCCH. This data would indicate that either the valve trapped some contamination between the poppet and seat or, more likely, a leak was started in the center downstream seal. It is impossible to distinguish between static seal leakage and seat seal leakage with the valve configuration tested. By the time 100 valve cycles had accumulated, the measured leakage rate was down to 9.4 SCCH; however, leakage rates

TUNGSTEN CARBIDE K-96 - POPPET NO. 4

S.E.M. PHOTOS AFTER 100,000 CYCLE - ClF_5 VALVE TEST (NORMAL IMPACT)

PHOTOS ARE AT 1000X

UPSTREAM OF SEAL

SEAL AREA

DOWNSTREAM OF SEAL

Figure 69

TUNGSTEN CARBIDE K-96 - POPPET NO. 4

S.E.M. PHOTOS AFTER 100,000 CYCLE - ClF_5 VALVE TEST (NORMAL IMPACT)

PHOTOS ARE AT 5000X

UPSTREAM OF SEAL

SEAL AREA

DOWNSTREAM OF SEAL

Figure 70

measured throughout the remainder of test were not very repeatable. This would indicate that there may be some dynamic effects of pressure variation across the static downstream seal as well as intermittent performance of the seat because of the physical test setup. The test setup, as built for this test, is a nonflowing configuration. Although the system was periodically flushed to remove contaminating particles generated by seat wear, the setup did not materially contribute to flushing all wear particles away. Thus, a part of the nonrepeatable results could possibly be attributed to trapping eroded wear particles between the seat and poppet.

Even though the K-96 did not demonstrate complete conformance with the leakage goals established for the valve, it did marginally demonstrate good leakage test results throughout the test period. Failure of the valve to meet the leakage goals for the whole test period is attributed to the following:

1. Seat material erosion resulting from dragging of the poppet across the seat as a result of nonuniform bumper impact with the stop surface. This resulted in grooving of the surface through abrasive chemical wear with variability in leakage rates measured resulting from nonrepeatable location of the poppet relative to the seat.

2. Intermittent contribution to leakage by the center downstream seal. Total contribution of this cause to total leakage measured is an undefinable quantity.

Satisfactory leakage measurements have been recorded using K-96 as the poppet and seat material. It is felt that even though leakage goals were not met throughout this test program, the material has demonstrated capability to adequately perform provided there are no outside contributing factors causing unnecessary problems. The results indicate that the material might perform quite satisfactorily if the possibility of abrasive contribution to chemical wear were removed by a minor redesign of the valve to remove the bumper as an outside influence or make provisions for the bumper contact surfaces to be parallel to the seat, thus avoiding lateral movement and abrasion.

A second possibility exists for using a tungsten carbide material which uses a cobalt binder. Since the microprobe results indicate a high concentration of cobalt in the impact area and the valve performed marginally well, a change to increase the cobalt concentration of the binder might provide additional sealing margin for the base material.

7.3 Boron Carbide Material Evaluation

Pure boron carbide, hot pressed to provide better than 99% theoretical density was primarily selected for testing because of the low boiling points of the

fluorides which can be formed on the surface during exposure to chlorine pentafluoride and gaseous fluorine. As a result of the low boiling points, all fluorides formed are gaseous at room temperature. Two valve configurations were tested using boron carbide as the seat and poppet material. The only difference between the two valve configurations tested was the level of impact during poppet to seat closure, so both sets of data will be discussed in this section. Both valves tested demonstrated acceptable leakage rates for a significant number of cycles. The valve poppet and seat tested at normal impact showed no leakage up to and including 20,000 valve cycles. Leakage then increased to a rapid rate to about 200 SCCH at 50,000 cycles and 100,000 cycles. The poppet and seat tested at low impact demonstrated leakage rates consistent with the design goals of less than 30 SCCH leakage throughout the test with the exception of one test point at 100 accumulated cycles where the leakage rate measured was 48 SCCH at 450 psig inlet pressure. Leakage rate as a function of valve cycles is shown in Figure 52 for the normal rate armature tests and in Figure 53 for the low rate armature tests. Results of these tests indicate that boron carbide has considerable promise as a seat and poppet material for use in chlorine pentafluoride and gaseous fluorine.

There was some doubt as to the adequacy of boron carbide as a seat and poppet material when the parts were first received from the vendor. The parts, as received, were not only quite scratched from the lapping process, but appeared to have a considerable number of holes on the surface indicating probable poor density. Because of the poor original lapping, the valve test parts were relapped to attempt to obtain the desired finish. The relapped surfaces were far superior to the original surfaces; however, the presence of a significant number of holes was still apparent in the relapped part.

Figures 71 and 72 show surface photos and interferograms of the tested boron carbide seats before and after the valve test in chlorine pentafluoride. The valve seat tested at low impact, Figure 71, shows almost no effects of propellant cycling. The valve seat tested at normal impact, Figure 72, shows a significantly degraded surface from the original "as lapped" surface. After completion of the 100,000 cycle test in chlorine pentafluoride, each poppet was examined using the S.E.M. to document character of the after test poppet surfaces. As with the other test poppets, three sets of photographs were taken to document the surface of the poppet in the seating area and just inside and outside of the seat land area. The surfaces of the low impact valve poppet were not significantly affected; this applies to nonimpact as well as impact areas. Figure 73 shows the three areas of the low impact valve seat examined at 200X with the S.E.M. Appearance of the seating surface as well as the surfaces only statically exposed to the propellant are very similar in appearance to the surfaces of the poppet which was only statically exposed. A large number of randomly distributed pits are apparent on the surface, with concentration no higher in the impact or seating area than inside or outside. The 1000X photos, Figure 74, show essentially the same view except that

A71-6-036-44

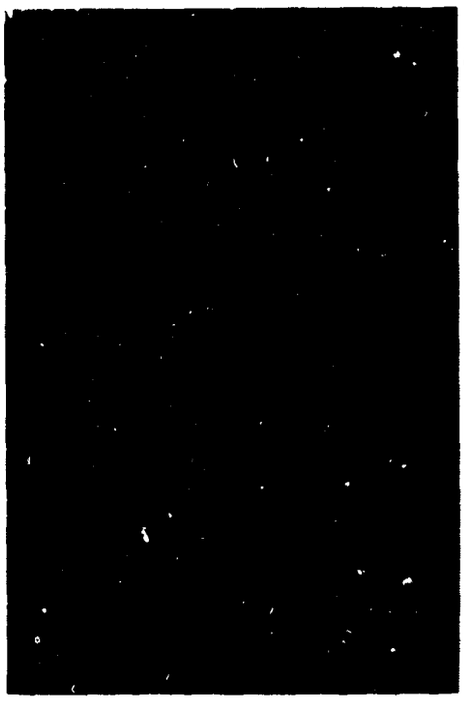

B_4C SEAT NO. 24 BEFORE LOW IMPACT VALVE TEST
IN ClF_5 - 210X INTERFERENCE PHOTO

B_4C SEAT NO. 24 AFTER LOW IMPACT VALVE TEST
IN ClF_5 - 210X INTERFERENCE PHOTO

B_4C SEAT NO. 24 BEFORE LOW IMPACT VALVE TEST
IN ClF_5 - 210X SURFACE PHOTO

B_4C SEAT NO. 24 AFTER LOW IMPACT VALVE TEST
IN ClF_5 - 210X SURFACE PHOTO

Figure 71

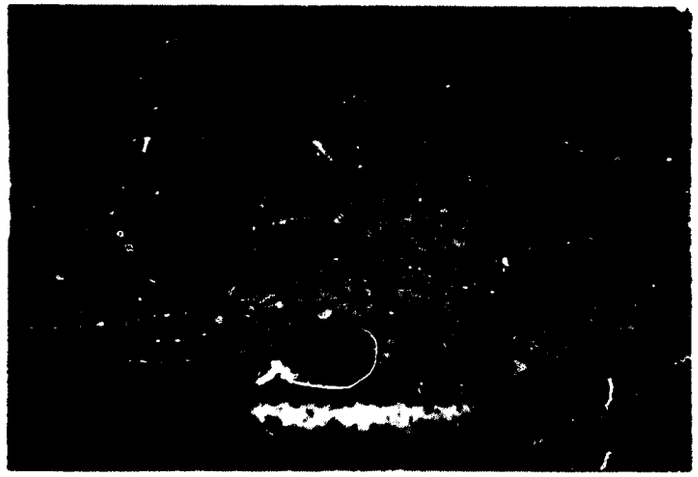

B_4C SEAT NO. 25 BEFORE NORMAL IMPACT VALVE TEST IN ClF_5 - 210X SURFACE PHOTO

B_4C SEAT NO. 25 BEFORE NORMAL IMPACT VALVE TEST IN ClF_5 - 210X INTERFERENCE PHOTO

B_4C SEAT NO. 25 AFTER NORMAL IMPACT VALVE TEST IN ClF_5 - 210X SURFACE PHOTO

B_4C SEAT NO. 25 AFTER NORMAL IMPACT VALVE TEST IN ClF_5 - 210X INTERFERENCE PHOTO

Figure 72

A71-9-036-61

BORON CARBIDE-B_4C - POPPET NO. 24

S.E.M. PHOTOS AFTER 100,000 CYCLE - ClF_5 VALVE TEST (LOW IMPACT)

PHOTOS AT 200X

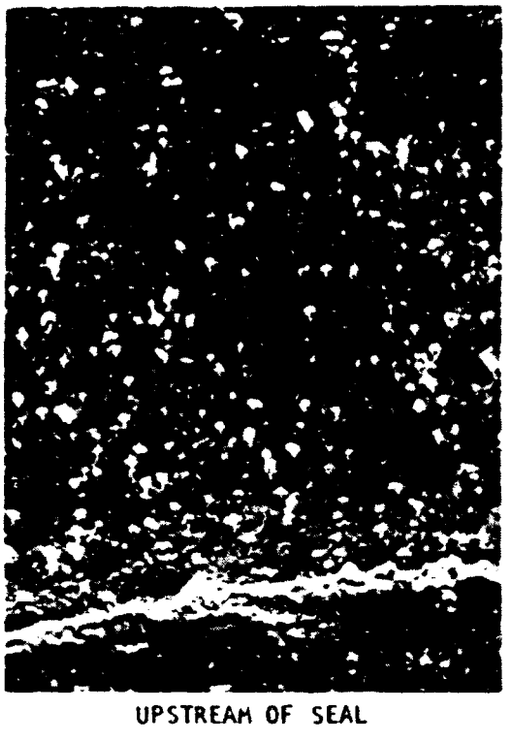

UPSTREAM OF SEAL

SEAL AREA

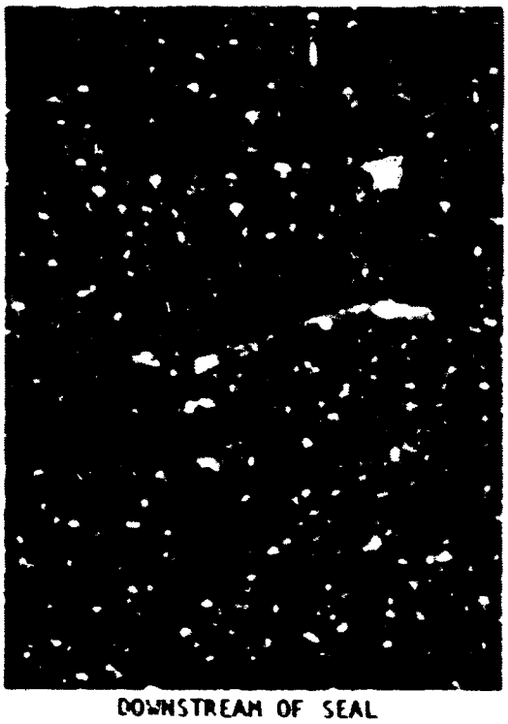

DOWNSTREAM OF SEAL

Figure 73

BORON CARBIDE-B_4C - POPPET NO. 24

S.E.M. PHOTOS AFTER 100,000 CYCLE - ClF_5 VALVE TEST (LOW IMPACT)

PHOTOS AT 1000X

UPSTREAM OF SEAL

SEAL AREA

DOWNSTREAM OF SEAL

Figure 74

the surface where seating of the poppet took place appears to be somewhat smoother. In the 5000X photos, Figure 75, the surface is again shown to be quite smooth with a few of the approximately 1/2 micron pits exposed. In general, the seating surface as well as the upstream and downstream surfaces, was in excellent condition after completion of the 100,000 cycle test Total wear of the seat was minimal with no significant erosion of the seating surface level as a result of the test. Comparison of pre and post test proficorder traces, Figure 76, shows the seat surface after the test to be at nearly the same level as before the test, with surface finish only slightly degraded as a result of the exposure and testing. Results of the test in general indicate that pure boron carbide in the low impact version of the valve is capable of functioning quite adequately as a seat and poppet material.

The seat and poppet tested in the normal impact version of the valve also provided within design goal leakage rates for a significant number of cycles. As shown in Figure 52, less than one SCCH leakage at 450 psig inlet pressure was measured up to and including 20,000 accumulated valve cycles. At conclusion of the test, leakage rates had increased rapidly to the order of 150 to 200 SCCH. Examination of the parts with the interference microscope and S. E. M. reveal the probable cause for the leakage rate recorded at the end of the test. Figure 72 shows surface photos and interferograms of the seat surface prior to and after completion of the 100,000 cycle test in chlorine pentafluoride. As with the K-96 tested in the normal impact valve, the post test seat surface was considerably degraded from the initial surface finish. Again, like the K-96 and WC poppets, the seat surface is grooved with average groove peak to Valley heights of up to 150 microinches, with the mean seat surface level eroded by 80 to 100 microinches from the original surface level as shown in Figure 77.

Further insight into the degradation of the seat which occurred during the test was gained during examination of the poppet used in the test with the Scanning Electron Microscope. Figure 78, a set of three 200X photos taken of the seat area, the upstream and the downstream areas shows the eroded seat surface quite clearly. As with the low impact valve parts, the surface is covered with random small pits, with distribution of pits approximately the same in the seal area as inside or outside. Figures 79 and 80 show the center of the test areas at 1000X and 5000X. Here the surface looks very much like the sample surface which was statically exposed to chlorine pentafluoride. The surfaces are covered with holes and small flakes which appear to be small platelets which have come loose or are about to come free from the surface. The seal area photos clearly show the grooving which resulted from apparently abrasive type wear. As with the K-96 poppet, the grooves in the seating area line up with the mark on the outer seat plate where the bumper contacted the seat plate stop.

A71-6-036-29

BORON CARBIDE-B_4C - POPPET NO. 24

S.E.M. PHOTOS AFTER 100,000 CYCLE - ClF_5 VALVE TEST (LOW IMPACT)

PHOTOS AT 5000X

UPSTREAM OF SEAL

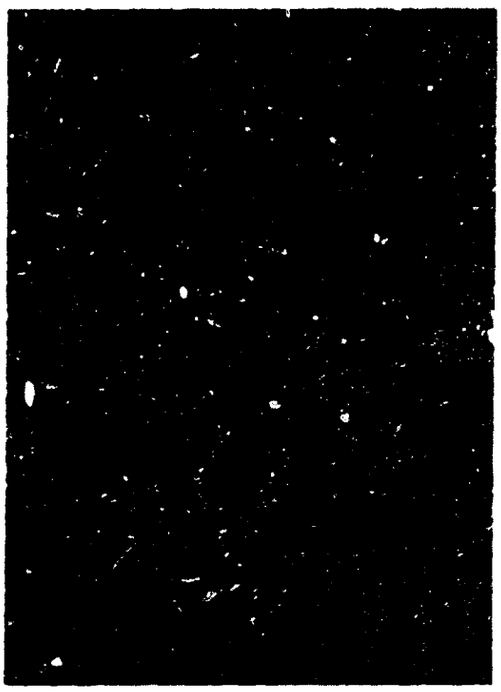

SEAL AREA

DOWNSTREAM OF SEAL

Figure 75

B_4C SEAT

SURFACE PROFILE BEFORE AND AFTER 100,000 CYCLE VALVE TEST - LOW IMPACT - ClF_5

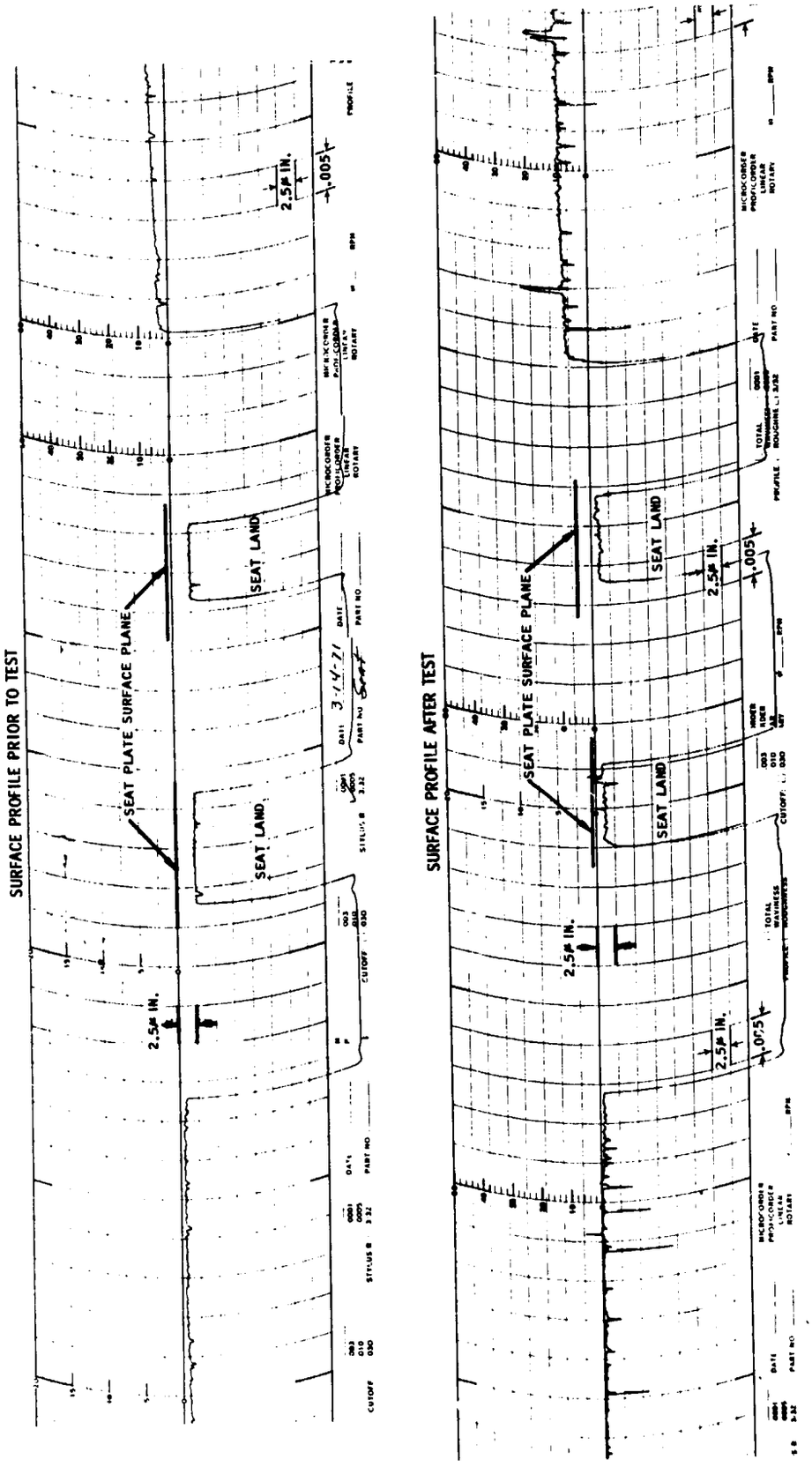

Figure 76

BORON CARBIDE SEAT

SURFACE PROFILE BEFORE AND AFTER 100,000 CYCLE VALVE TEST - NORMAL IMPACT - CIF_5

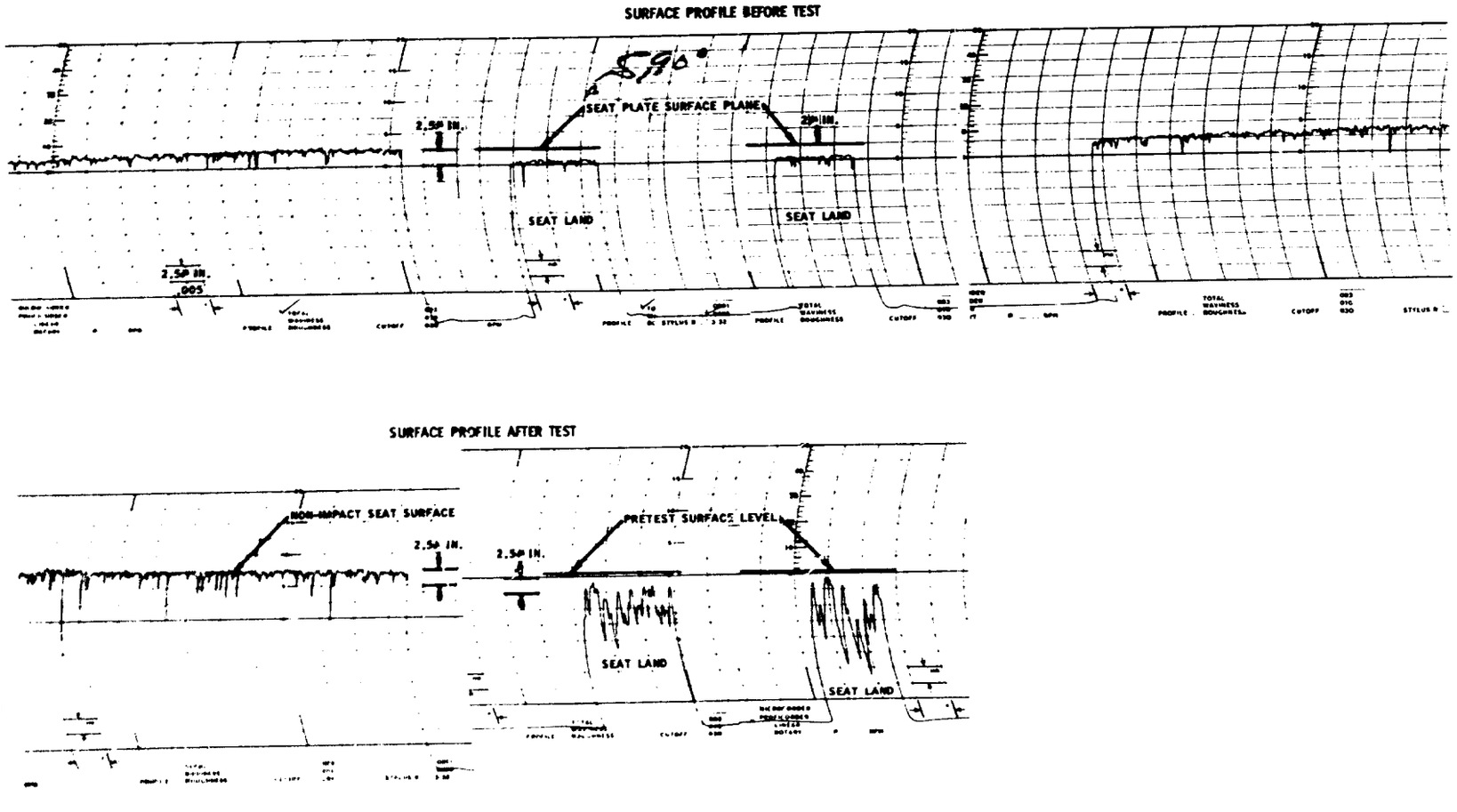

Figure 77

BORON CARBIDE - B_4C

S.E.M. PHOTOS AFTER 100,000 CYCLE - ClF_5 VALVE TEST (NORMAL IMPACT)

PHOTOS AT 200X

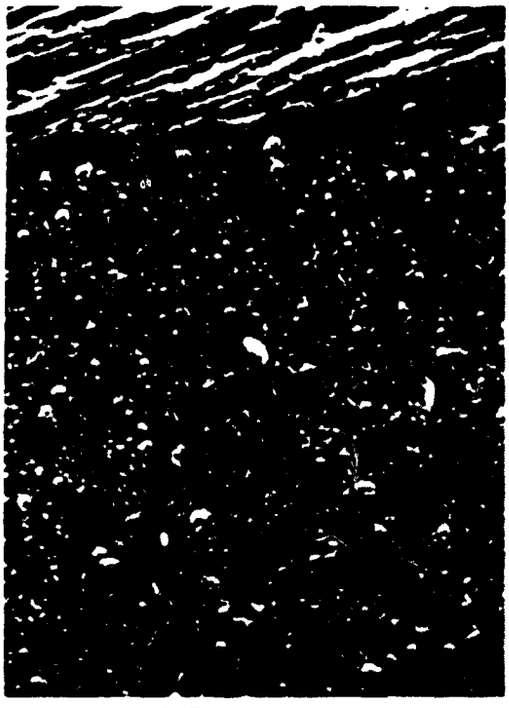

UPSTREAM OF SEAL

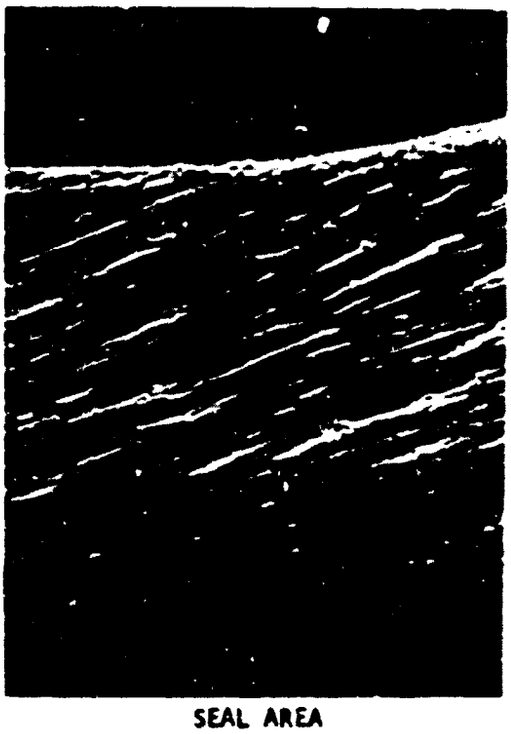

SEAL AREA

DOWNSTREAM OF SEAL

Figure 75

A71-5-036-31

BORON CARBIDE-B_4C - POPPET NO. 25

S.E.M. PHOTOS AFTER 100,000 CYCLE - ClF_5 VALVE TEST (NORMAL IMPACT)

PHOTOS ARE AT 1000X

UPSTREAM OF SEAL

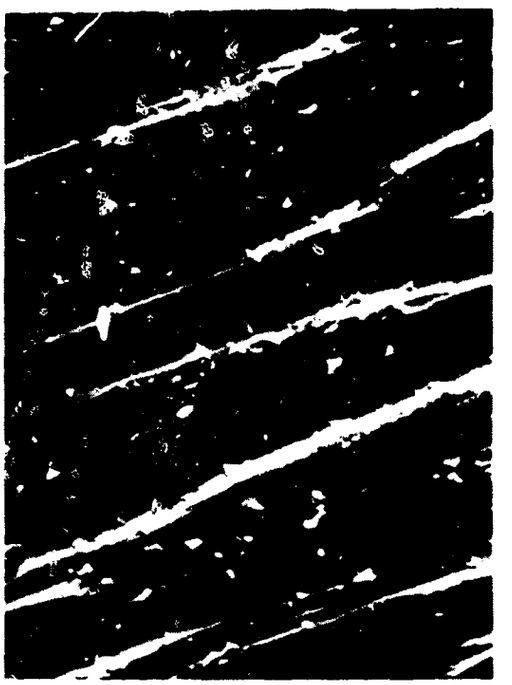

SEAL AREA

DOWNSTREAM OF SEAL

Figure 70

A71-6-036-33

BORON CARBIDE-B_4C - POPPET NO. 25

S.E.M. PHOTOS AFTER 100,000 CYCLE - ClF_5 VALVE TEST (NORMAL IMPACT)

PHOTOS AT 5000X

UPSTREAM OF SEAL

SEAL AREA

DOWNSTREAM OF SEAL

Figure 80

The hypothesis that the bumper striking with only one side causes the main armature to oilcan and eccentrically flex with resultant dragging of the poppet across the seat is again a significant probability contributing to the valve seat wear and resultant leakage. Why the seat and poppet functioned as well as they did up to 20,000 cycles, whereafter both failed, as evidenced by leakage rate rate measurements and surface finish degradation is difficult to explain. However, the seating location is highly repeatable and it is well within possibility that the seat and poppet grooves continued to mesh smoothly until late in the test cycle. It may also be possible that erosion of the seat resulted in loose granules which were not completely removed from the seating area during the flush or purge cycles.

Another possible cause of the significant erosion of the poppet and seat as seen in the normal impact test valve might be that the energy of impact is sufficient to start local surface reactions of the chlorine pentafluoride with the boron carbide resulting in high wear rates. This factor in combination with heat from the apparent abrasion on the normal impact poppet probably resulted in the significant recession seen in the normal impact boron carbide poppet and seat after completion of the tests.

All of the data accumulated on the low impact version of the valve indicated that pure boron carbide would adequately function as a seat and poppet material. Failure of the normal impact version of the valve to completely meet the leakage goals for the entire period of the test is attributed to the following cause:

1. Abrasive heat input to the poppet and seat resulting from non-uniform impact of the bumper with the stop. This results in eventual unacceptable leakage.

2. In view of the sudden increase in leakage rate, there is a strong possibility that the leakage rate was caused by a trapped particle or another component of the valve, i.e., the parallel static seal. That the sudden increase is a direct function of "wear" of the seat and poppet is hard to accept because nothing was changed in either the valve or operating procedure between the 20,000 and 50,000 cycle leakage test points.

The data indicates that the material might perform quite satisfactorily as a seat and poppet material for use in chlorine pentafluoride if the valve were slightly redesigned to provide uniform bumper impact with the seat stop or if the bumper were removed altogether as an outside influence on the closing mechanism.

4.7.4 Pure Tungsten Carbide Material Evaluation

Pure tungsten carbide was selected for testing in this program as a candidate poppet and seat material for two primary reasons. First, in the past, tungsten carbide with a 6% cobalt binder had given encouraging results (K-96). It was hypothesized that the K-96 had not performed as well as expected because the cobalt fluoride had formed a solid product resulting in excess surface roughness and contributing to valve leakage. Secondly, tungsten carbide forms only gaseous fluorides at room temperatures. Thus it was expected that the material might perform considerably better than the K-96 with cobalt binder as a result of good wear characteristics and the lack of solid fluoride formation in the presence of fluorine or chlorine pentafluoride. The tungsten carbide seat and poppet tested during this program failed to perform satisfactorily as a valve seat seal. Leakage was initially high after passivation with gaseous fluorine and consistently increased with cumulative valve cycling.

The tungsten carbide poppets and seats were quite rough with a significant number of holes present on the surface as they were initially received from the vendor. The parts used for static exposure tests were used "as is". However, it was felt that not relapping the parts would result in an unfair valve test so all of the parts intended for valve testing were relapped prior to assembly into valves. Only one tungsten carbide poppet and seat were tested to 100,000 cycles in the normal impact valve assembly. Initial leakage rates measured after passivation (see Figure 54) were over 800 SCCH. That leakage could result from either:

1. Contaminant caught in the seat land area
2. Severe surface degradation in the presence of chlorine pentafluoride
3. Partial failure of the downstream center end plate static seal

The surface of the tungsten carbide parts was quite satisfactory prior to the test, however, after the test, examination of the parts revealed significant deterioration of not only the sealing surface but also the adjacent statically exposed surfaces. Surface photos and interferograms of the seat surface prior to and after the test are shown in Figure 81. Prior to the test, the surface was smooth with randomly distributed surface holes. After the test in chlorine pentafluoride, the seating surface was degraded in finish with some grooving apparent on the surface of the seat land. As shown in Figure 82, the non-impact areas were quite pitted with considerably loss of material surface. Comparison of proficorder traces made of the seat prior to and after the test on the statically exposed poppet showed that the surface was still quite flat, however, a significant number of holes had been opened up. The seat land surface was too rough to proficord at 2.5 microinches per proficorder

WC SEAT NO. 18 BEFORE NORMAL IMPACT VALVE TEST IN ClF_5 - 210X SURFACE PHOTO

WC SEAT NO. 18 BEFORE NORMAL IMPACT VALVE TEST IN ClF_5 - 210X INTERFERENCE PHOTO

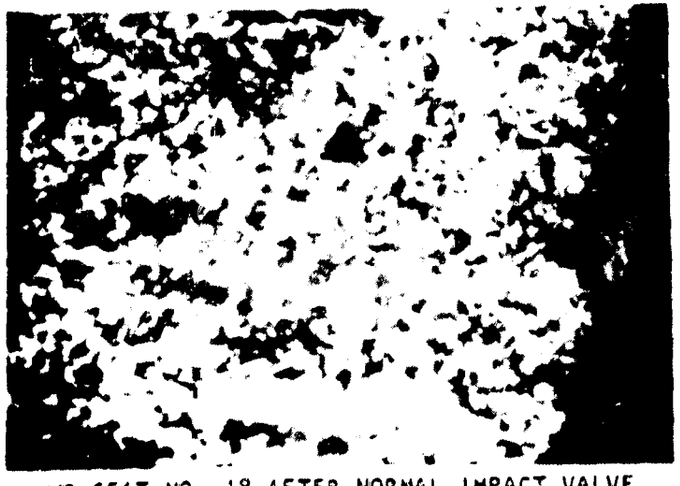

WC SEAT NO. 18 AFTER NORMAL IMPACT VALVE TEST IN ClF_5 - 210X SURFACE PHOTO

WC SEAT NO. 18 AFTER NORMAL IMPACT VALVE TEST IN ClF_5 - 210X INTERFERENCE PHOTO

Figure 91

Figure 52

WC SEAT NO. 18

NONIMPACT ZONE AND BUMPER IMPACT ZONES - 210X PHOTOS

NONIMPACT ZONE SURFACE PHOTO

NONIMPACT ZONE INTERFERENCE PHOTO

BUMPER ZONE IMPACT AREA INTERFERENCE PHOTO

paper division so the part was run at lower magnification as shown in Figure 83. The tungsten carbide part was the most severly degraded seat tested. Surface level of the seat was eroded approximately 250 microinches with grooves of 50 to 100 microinches peak to valley height on the seat surface.

Scanning electron microscope studies were performed using the poppet tests to further define the effects of exposure and dynamic impact on the seat surface. Figure 84 shows a set of 200X photos taken of the seat land, and just inside and outside the seat land. The seat land is clearly defined with about the same distribution of holes on the surface in and out of the seat area. At 1000X, Figure 85, the structure of the tungsten carbide crystals is more clearly defined and the surface grooves are more apparent. At 5000X, Figure 86, the large grain crystal structure is clearly defined. Lap marks are still evident on the nonimpact areas indicating relatively even corrosion rates. The crystal structure in the seal area appears to be the same as in the adjacent areas except that all evidence of lap marks is gone and the surface of the seat area is worn smooth, between grooves.

Abrasive wear alone would not be sufficient to account for all of the material that is missing from the seating surface of the tungsten carbide poppet and seat. Failure of the seat and poppet to perform in this application could probably be attributed to the energy absorbed by the poppet and seat under valve closing impact. Sufficient energy must be available to initiate local propellant/material reaction leading to chemical erosion of the seat with the abrasion which is apparent on the surface being a complicating factor. It is possible that the material might be able to provice the sealing function required even with the chemical erosion of the seat apparent if lateral movement of the poppet relative to the seat were not possible after the poppet first contacted the seat resulting in the apparent grooving of the seat.

The erosion of the tungsten carbide in the pure form was significantly higher than erosion of the K-96 tungsten carbide with the cobalt binder. It is probable that the cobalt fluoride formed on the surface may inhibit reaction of the tungsten carbide with the propellant resulting in lower apparent wear characteristics with the K-96.

4.7.5 Aluminum Oxide Material Evaluation

Three valves were tested using pure hot pressed aluminum oxide as the seat and poppet material. One test was performed using the low rate valve armature and chlorine pentafluoride as the test fluid. The other two valves were tested using GF_2 as the test fluid with one valve tested at normal impact level and one valve tested at low impact level. None of the aluminum oxide valves met the program objective of obtaining leakage rates less than 30 SCCH at 450 psig inlet pressure after 100,000 cycles. Study of the parts tested have however, provided some insight into why the parts failed to perform as expected. Aluminum

WC SEAT

SURFACE PROFILE BEFORE AND AFTER 100,000 CYCLE VALVE TEST - NORMAL IMPACT - CIF5

SURFACE PROFILE BEFORE TEST

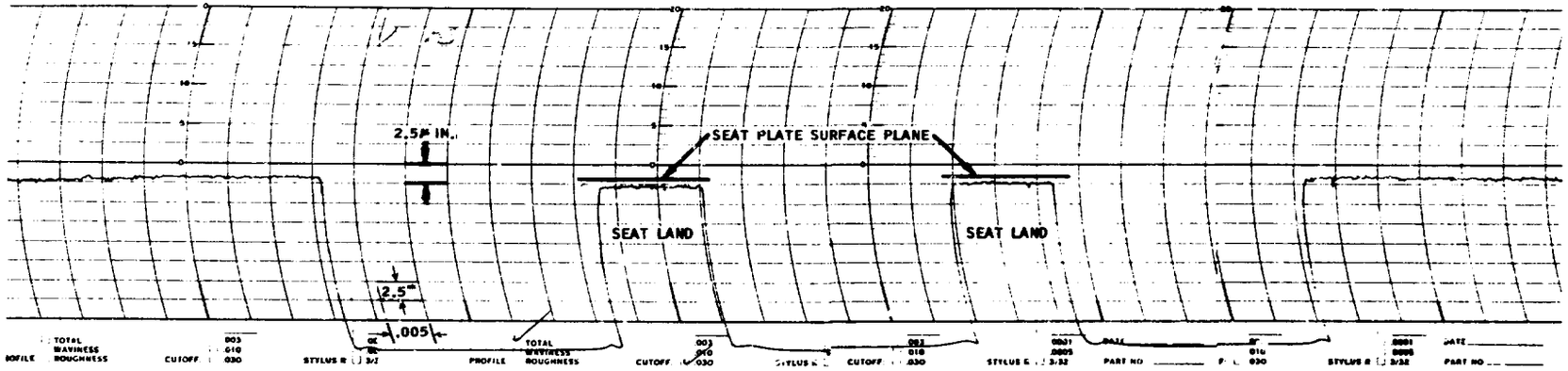

SURFACE PROFILE AFTER TEST

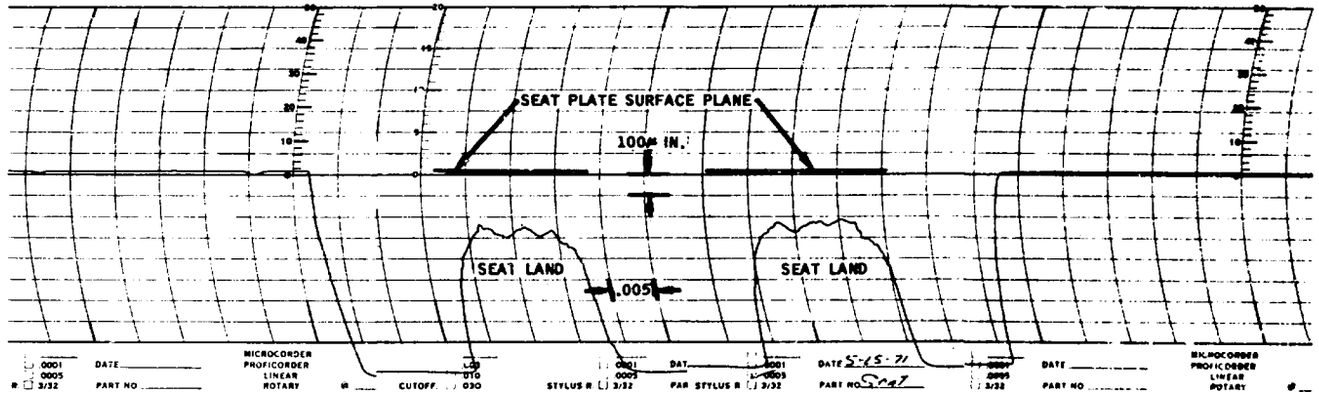

Figure 83

A11-6-036-36

A71-6-036-32

TUNGSTEN CARBIDE-WC - POPPET NO. 18

S.E.M. PHOTOS AFTER 100,000 CYCLE - CIF_5 VALVE TEST (NORMAL IMPACT)

PHOTOS ARE AT 200X

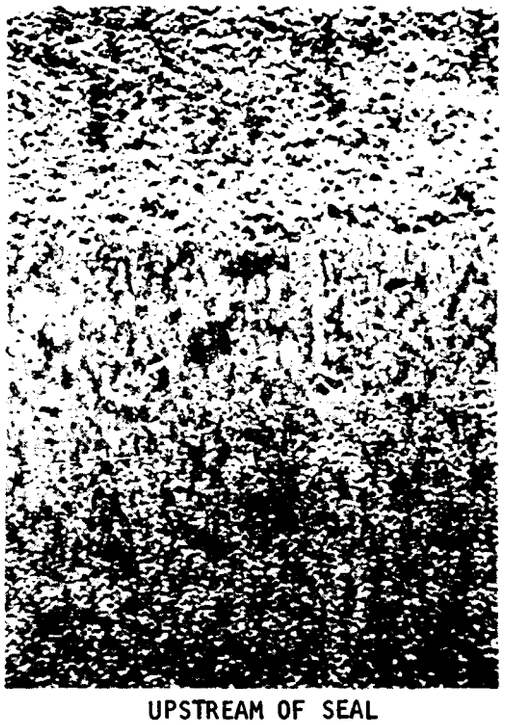

UPSTREAM OF SEAL

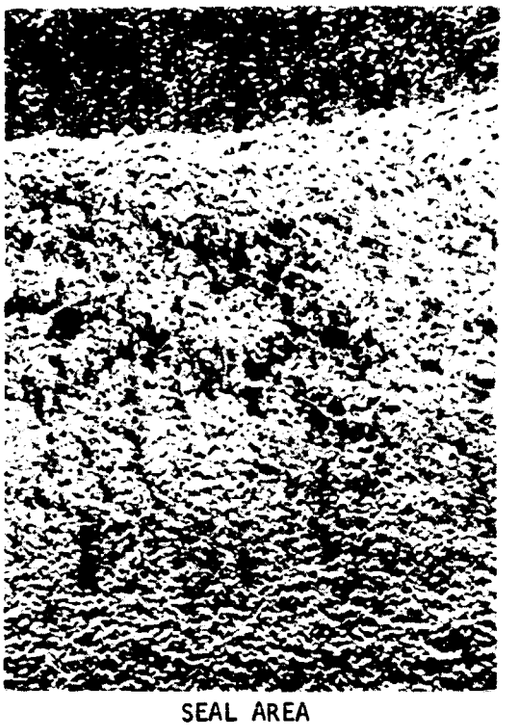

SEAL AREA

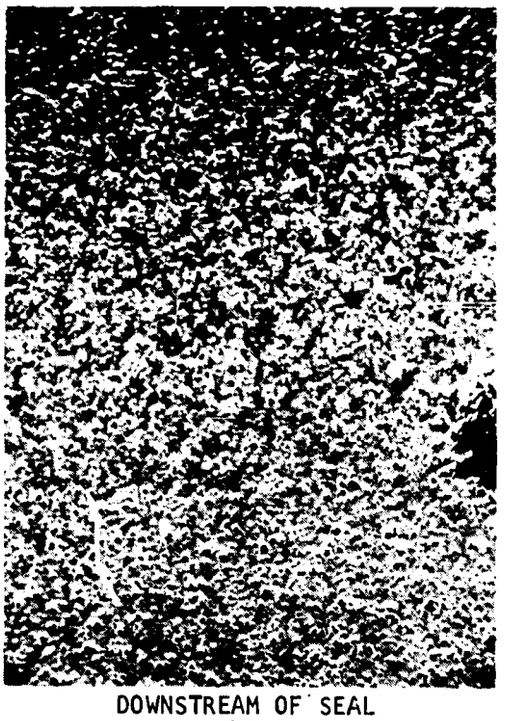

DOWNSTREAM OF SEAL

Figure 84

TUNGSTEN CARBIDE-WC - POPPET NO. 18

S.E.M. PHOTOS AFTER 100,000 CYCLE - ClF_5 VALVE TEST (NORMAL IMPACT)

PHOTOS ARE AT 1000X

UPSTREAM OF SEAL

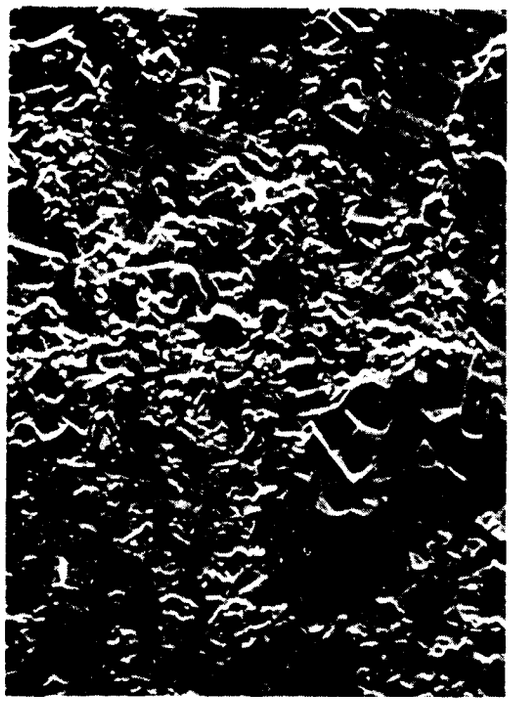

SEAL AREA

DOWNSTREAM OF SEAL

Figure 85

TUNGSTEN CARBIDE-WC - POPPET NO. 18

S.E.M. PHOTOS AFTER 100,000 CYCLE - ClF_5 VALVE TEST (NORMAL IMPACT)

PHOTOS ARE AT 5000X

UPSTREAM OF SEAL

SEAL AREA

DOWNSTREAM OF SEAL

Figure 86

oxide was selected as a seat and poppet candidate material because of the low volume of fluorides formed as a result of exposure to chlorine pentafluoride and fluorine. In that respect, the material proved out to be as good as any other tested and superior to several of the materials as rated by static exposure test results. Shortcomings of the material were apparent after completion of the valve test.

The aluminum oxide parts, as received from the vendor, were badly scratched from the lapping process and were not adequate as seat and poppet parts. All of the parts used in valves were relapped prior to use to provide a fair comparative test of all of the new materials. In the final lapped condition, the aluminum oxide parts presented an extremely smooth, dense surface. Pre-propellant exposure tests showed that an excellent seal was obtained on the two valves which had less than 1 microinch finish on the seat and poppet surfaces indicating that the new poppet and seat surface characteristics were adequate for sealing.

Figure 87 shows surface photographs and interferograms of the seat tested in chlorine pentafluoride before and after the test. Both sets of photographs indicate the surface before and after the test. Both sets of photographs indicate the surface before and after testing is smooth with no significant pits or other surface blemishes resulting from the test. Comparative proficorder trades made before and after the test (see Figure 88) show the surface finish degraded a minor amount as a result of the test; however, even the finish of the seat area was better than a 1 microinch finish after completion of 100,000 cycles which should be adequate to provide a seal. Total erosion of the seat surface from the original surface level was only on the order of 3 microinches indicating that the surface was not significantly affected by either the propellant exposure or the dynamic exposure of the poppet contacting the seat during valve closing. The poppet used in the test was examined using the scanning electron microscope to evaluate the changes in the seating surface. Figure 89 shows three 200X photographs of the seal area and immediately adjacent areas upstream and downstream of the seat seal. Figures 90 and 91 show the centers of the same areas at higher magnification. The only apparent difference between the impact and the non-impact areas is that in the seat area, there is an agglomeration of solid material buildup on the surface.

Loose debris was seen on several other samples during electron microscope examination, but only on the aluminum oxide parts was it apparently associated with the reaction of the propellants with the material. The buildup appears to be concentrated in the seal area and immediately downstream of the seal. The particles were too small to evaluate using the microprobe to determine composition. However, because of the location and distribution of the particles, they are assumed to be associated with the reaction of the aluminum oxide with the chlorine pentafluoride in the dynamic impact environment. Buildup of this debris, whether associated with the propellant/material reaction is the most probably cause of the progressively

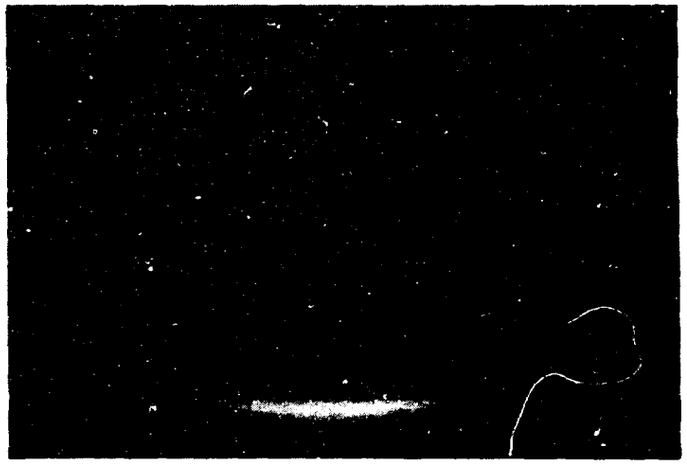

Al_2O_3 SEAT NO. 13 BEFORE LOW IMPACT VALVE TEST IN ClF_5 - 210X SURFACE PHOTO

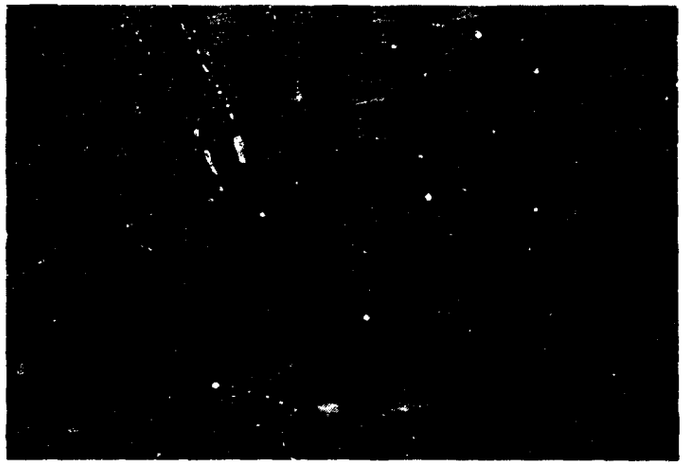

Al_2O_3 SEAT NO. 13 BEFORE LOW IMPACT VALVE TEST IN ClF_5 - 210X INTERFERENCE PHOTO

Al_2O_3 SEAT NO. 13 AFTER LOW IMPACT VALVE TEST IN ClF_5 - 210X SURFACE PHOTO

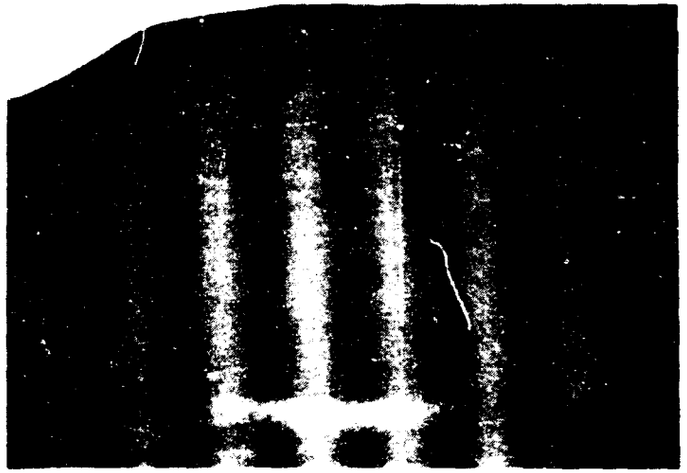

Al_2O_3 SEAT NO. 13 AFTER LOW IMPACT VALVE TEST IN ClF_5 - 210X INTERFERENCE PHOTO

Al_2O_3 SEAT

SURFACE PROFILE BEFORE AND AFTER 100,000 CYCLE VALVE TEST - LOW IMPACT - ClF_5

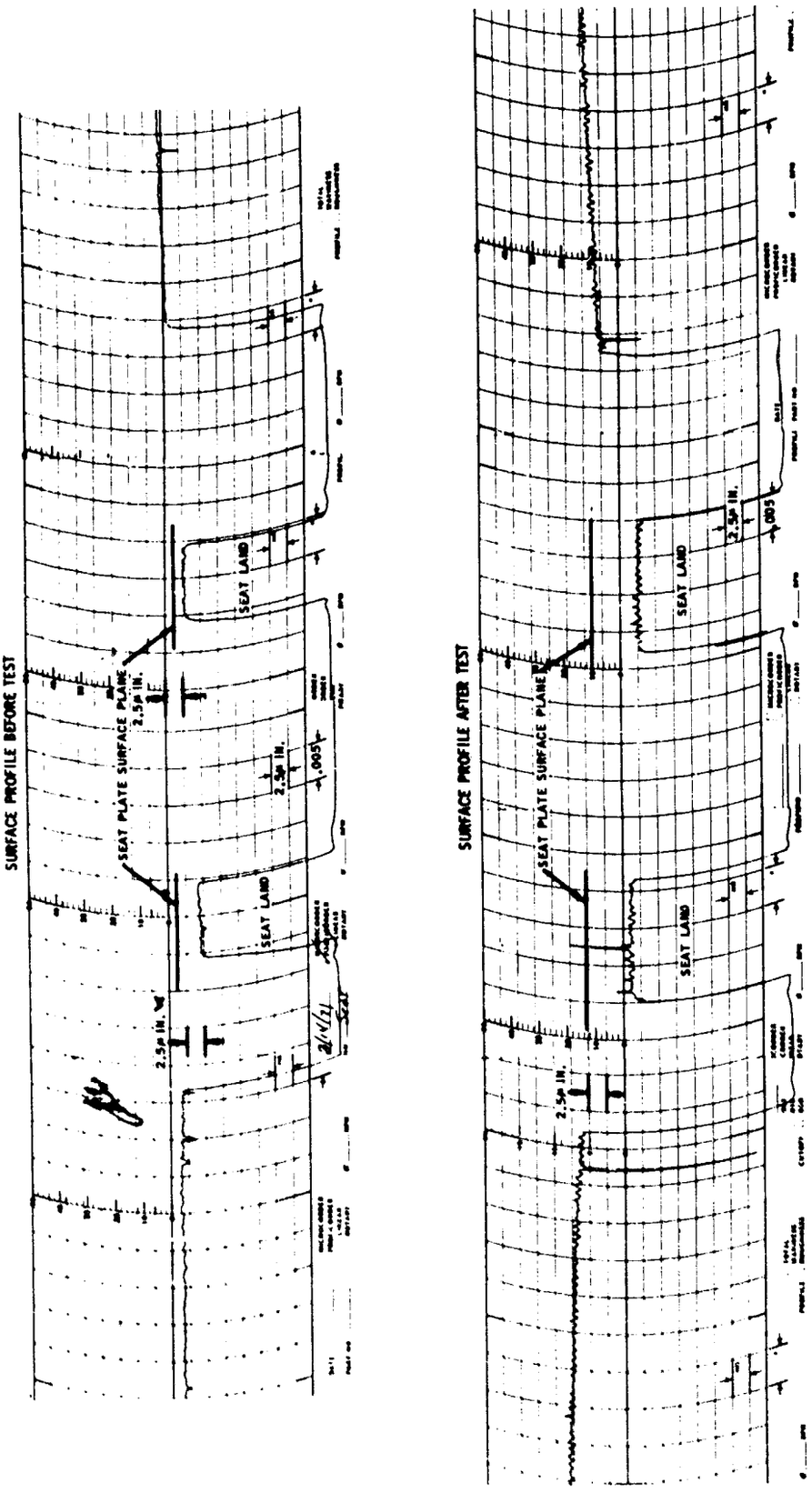

Figure 88

A71-6 038 42

ALUMINUM OXIDE-Al_2O_3 - POPPET NO. 13

S.E.M. PHOTOS AFTER 100,000 CYCLE - ClF_5 VALVE TEST (LOW IMPACT)

PHOTOS ARE AT 200X

UPSTREAM SEAL

SEAL AREA

DOWNSTREAM OF SEAL

Figure 89

ALUMINUM OXIDE-Al_2O_3 - POPPET NO. 13

S.E.M. PHOTOS AFTER 100,000 CYCLE - ClF_5 VALVE TEST (LOW IMPACT)

PHOTOS ARE AT 1000X

UPSTREAM OF SEAL

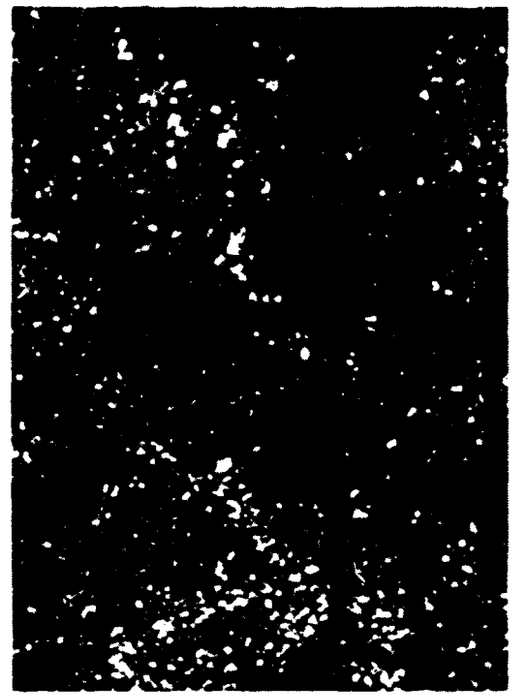

SEAL AREA

DOWNSTREAM OF SEAL

Figure 90

ALUMINUM OXIDE-Al_2O_3 - POPPET NO. 13

S.E.M. PHOTOS AFTER 100,000 CYCLE - ClF_5 VALVE TEST (LOW IMPACT)

PHOTOS ARE AT 5000X

UPSTREAM OF SEAL

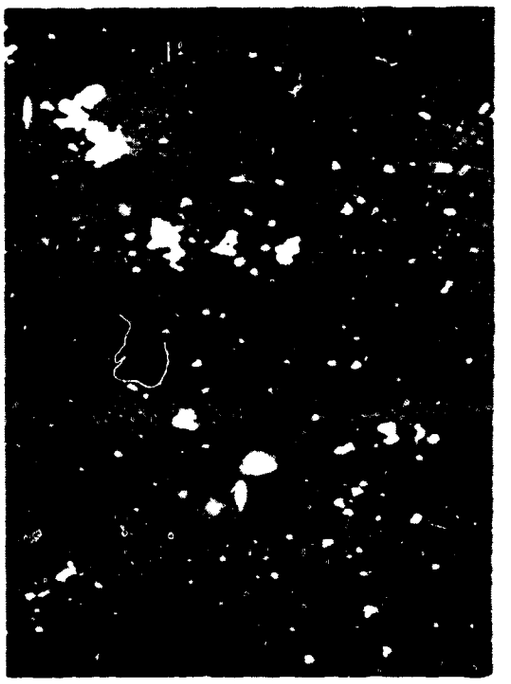

SEAL AREA

DOWNSTREAM OF SEAL

Figure 91

increasing valve leakage during the test. The only other change noted in the seat is that several chips appear to be missing from the periphery of the seat land indicating that the seat was approaching being fractured.

Appearance of the seat which was tested at low impact levels in gaseous fluorine was almost identical to that of the low impact seat tested in chlorine pentafluoride. Figure 92 shows surface photos and interferograms of the seat tested in gaseous fluorine at low impact prior to and after the test. As with the chlorine pentafluoride seat, the only change in the seat surface noticeable is the occurrence of random occasional lumps or surface contamination. No evaluation was made of the poppet from the valve tested at low impact in gaseous fluorine. It was necessary to coat the aluminum oxide parts with a thin carbon film to make them conductive for examination with the scanning electron microscope. Since there was some possibility of requiring parts for further examination which had been maintained in an inert atmosphere to prevent contamination and which had not been coated with carbon, it was decided to skip the electron microscope examination because two other parts were available which had been tested in both propellants. As it turned out, there was insufficient time available in the S. E. M. to examine all parts so the poppet would have been skipped in any case. Comparison of proficorder traces made of the seat land showed similar results to that obtained on the low impact seat tested in chlorine pentafluoride (Figure 93) with no significant differences apparent.

The third aluminum oxide seat and poppet was tested in the normal impact valve using GF_2. Leakage rates during the test progressively increased up to 1000 cycles and then decreased to the end of the test. Primary cause for the excessive leakage measured with the valve was discovered upon examination of the poppet and seat after the test. The seat land was found to have shattered in several areas. None of the cracks propagated completely across the seat explaining why the valve sealed to a degree. Figure 94 shows surface photographs and interferograms of the seat prior to and after the test. As with the other materials tested in the normal impact valve, there was evidence of some grooving of the seat surface. The average groove depth, however, was considerably less than the groove depth measured on the other test seats, only being 2 to 5 microinches deep. This was considerably less "wear" than seen on the other materials tested in the normal impact valve. Total erosion of the integral portion of the seat remaining was also less than that of any of the other seats tested. Figure 95 shows comparative proficorder traces made of the seat land prior to and after the test. These data indicate that the surface finish of the seat in general is still quite good even in the impact area, probably better than the surface of any of the other valve seats after testing. The poppet used for the normal impact test in gaseous fluorine was examined using the S. E. M. to evaluate the seating surface and to attempt to further define the cause of the leakage experienced. In addition to the cracks in the seat, there was considerable amount of debris found in the seat land area similar to that found on the other

Al_2O_3 SEAT NO. 12 BEFORE LOW IMPACT VALVE TEST IN GF_2 - 210X SURFACE PHOTO

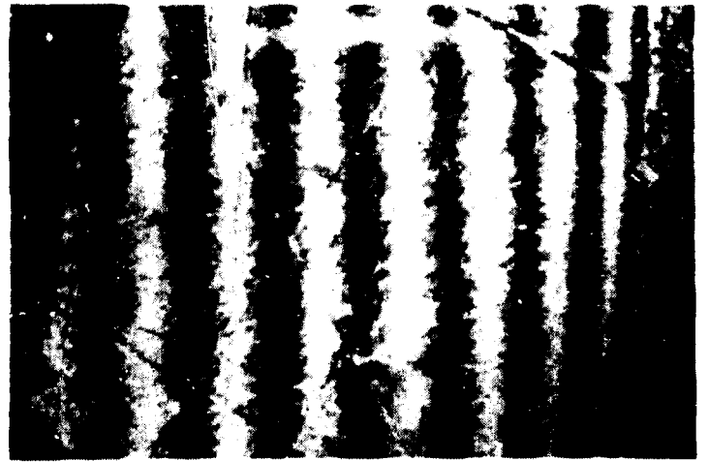

Al_2O_3 SEAT NO. 12 BEFORE LOW IMPACT VALVE TEST IN GF_2 - 210X INTERFERENCE PHOTO

Al_2O_3 SEAT NO. 12 AFTER LOW IMPACT VALVE TEST IN GF_2 - 210X SURFACE PHOTO

Al_2O_3 SEAT NO. 12 AFTER LOW IMPACT VALVE TEST IN GF_2 - 210X INTERFERENCE PHOTO

Figure 82

A-11-6-036-43

Figure 93

AL_2O_3 SEAT

SURFACE PROFILE AFTER 100,000 CYCLE VALVE TEST - LOW IMPACT - GF_2

NOTE:
NO PRETEST PROFICORDING
COMPARE SURFACE WITH
STATIC TEST EXPOSURE
POPPET, Fig. VI - 26

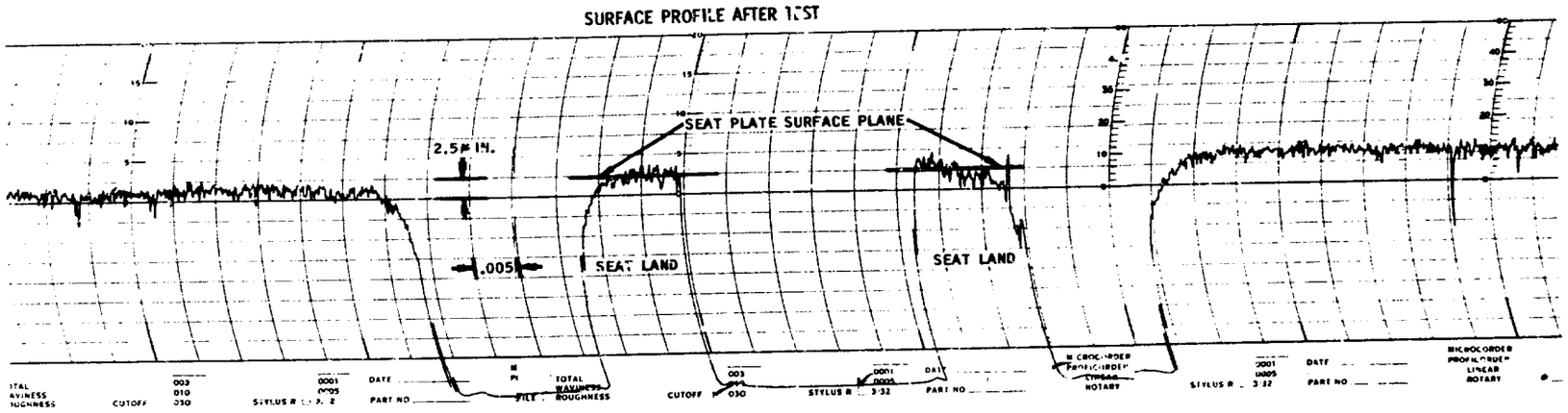

A 71-6-036-10

Al_2O_3 SEAT NO. 14 BEFORE NORMAL IMPACT VALVE TEST IN GF_2 - 210X SURFACE PHOTO

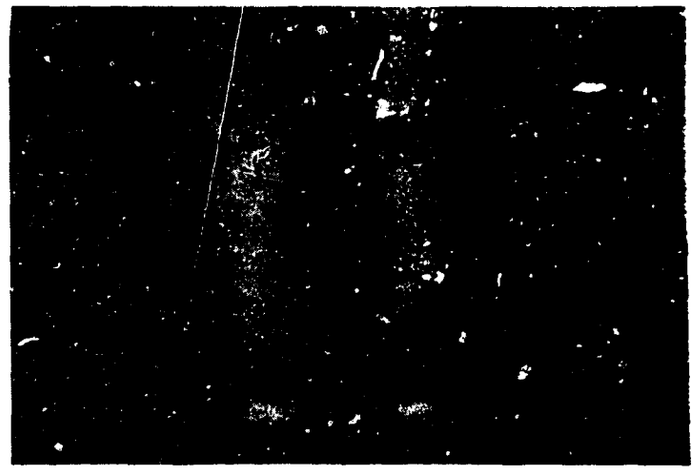

Al_2O_3 SEAT NO. 14 BEFORE NORMAL IMPACT VALVE TEST IN GF_2 - 210X INTERFERENCE PHOTO

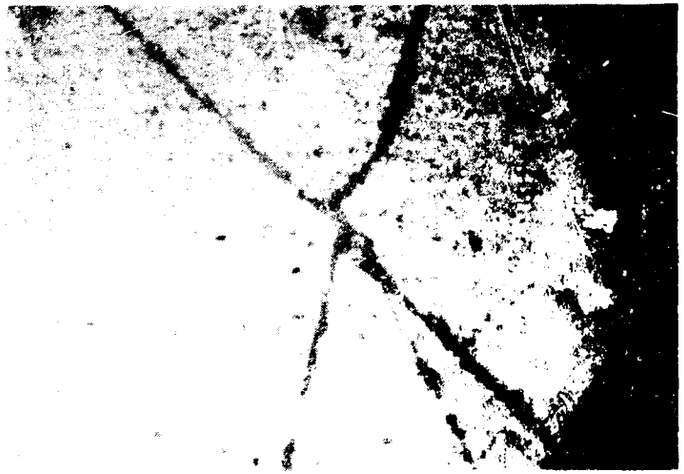

Al_2O_3 SEAT NO. 14 AFTER NORMAL IMPACT VALVE TEST IN GF_2 - 210X SURFACE PHOTO

Al_2O_3 SEAT NO. 14 AFTER NORMAL IMPACT VALVE TEST IN GF_2 - 210X INTERFERENCE PHOTO

Al_2O_3 SEAT

SURFACE PROFILE BEFORE AND AFTER 100,000 CYCLE VALVE TEST - NORMAL IMPACT - GF_2

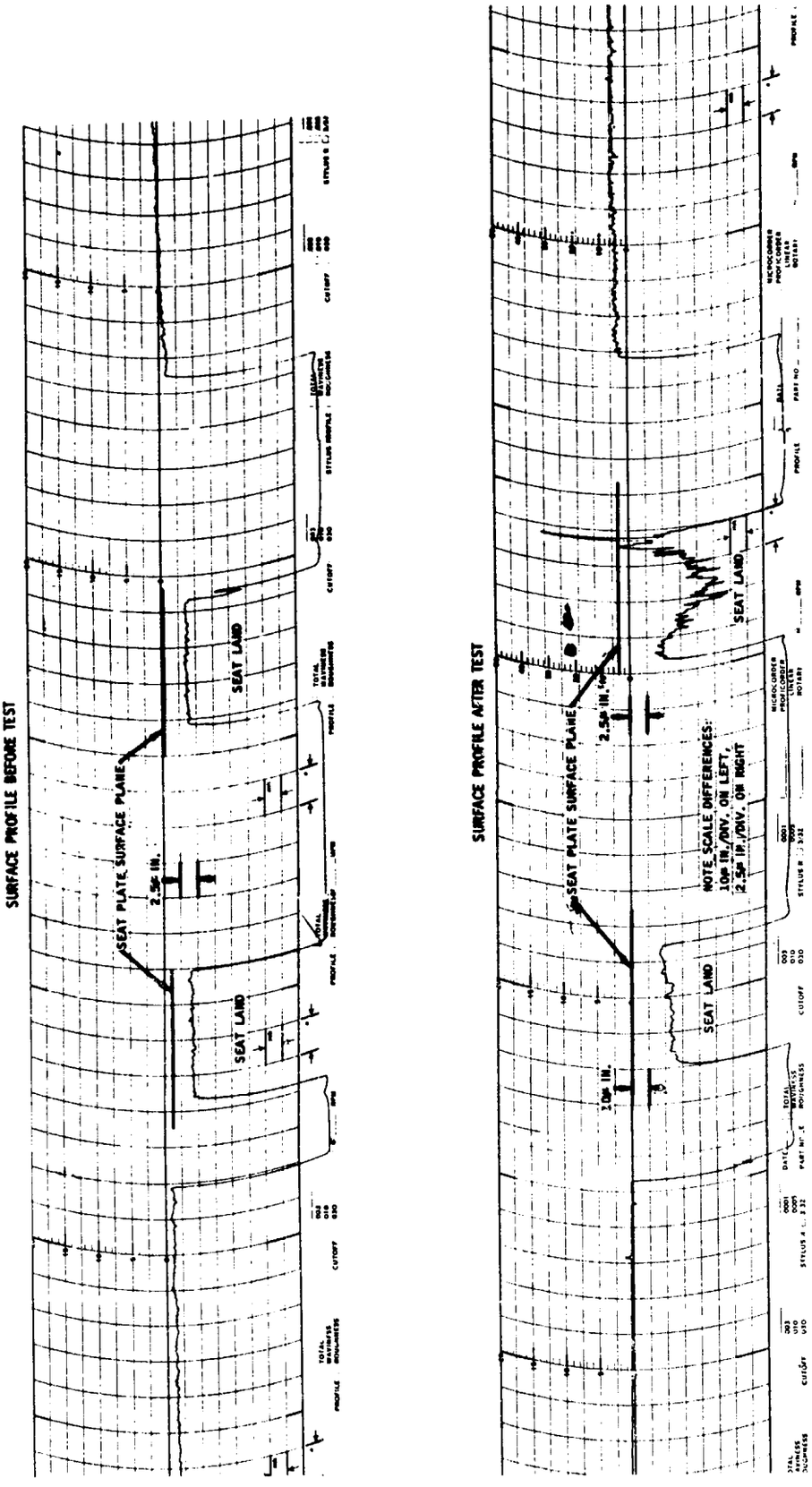

Figure 95

aluminum oxide poppet examined. It is evident that the surface buildup is test associated and not handling contamination, since the buildup is primarily associated with the seat land area. Figure 96 shows an S. E. M. photograph at 200X of the seal area and a portion of the downstream area. This photo clearly shows the edge of the seat land defined by the edge of the contamination.

The level of buildup of contamination on the surface is not too different than that of the valve tested in chlorine pentafluoride at low impact. At 1000X, Figure 97, an additional difference starts to become apparent between the normal impact gaseous fluorine poppet and the chlorine pentafluoride poppet seating surface. The surface under the contamination appears to be somewhat flaky. At 5000X, the base surface is clearly defined as shown in Figure 98. It appears that there are relatively large (1 micron) thin flakes on the surface. These flakes could be contamination, thin flakes of aluminum fluoride or aluminum oxide which have been loosened from the surface.

In general, the aluminum oxide poppets and seats tested demonstrated the best remaining surface finish after completion of testing in either the normal impact or low impact valve. Erosion of the low impact seat was comparable to that of the pure boron carbide seat tested under the same conditions. Erosion of the high impact seat area was less than that of any other valve tested. Primary causes of leakage in the low impact valves tested in gaseous fluorine and chlorine pentafluoride appear to be the buildup of a contaminant in the seat land areas resulting in loss of sealing capability. That factor is also apparent in results of the tests on the high impact valve tested in GF_2 with the added complication that a major portion of the normal impact tested seat shattered under the impact loads applied. Whether the foreign particles visible in the sealing surfaces of the poppets are products of reaction between the Al_2O_3 substrate and the oxidizer in this particular location (topographic reaction) or whether these particles were formed elsewhere and carried to and collected on the sealing surfaces cannot be distinguished. It is possible that the buildup might be eliminated by operating the valve in a flowing system rather than in the nonflowing environment provided for these tests. Flow over the seat on each cycle of the valve might provide the conditions necessary to maintain the seat surface in a "clean" condition. As far as the normal impact seat shattering is concerned, further investigation is required to determine whether the material might be used under identical impact conditions without shattering by slightly redesigning the seat profile to remove high stress points. Different fabrication techniques may be available to lower the shock sensitivity. Based on test results obtained in this program, it would appear that since some chipping was apparent on even one of the low impact valve seats, the material could not be safely used as is.

ALUMINUM OXIDE - Al_2O_3

S.E.M. PHOTO AFTER 100,000 CYCLE - GF_2 VALVE TEST (NORMAL IMPACT)

PHOTO IS AT 200X

NOT REPRODUCIBLE

DOWNSTREAM OF SEAL

SEAL AREA

Figure 96

ALUMINUM OXIDE - Al_2O_3

S.E.M. PHOTOS AFTER 100,000 CYCLE - GF_2 VALVE TEST (NORMAL IMPACT)

PHOTOS ARE AT 1000X

NOT REPRODUCIBLE

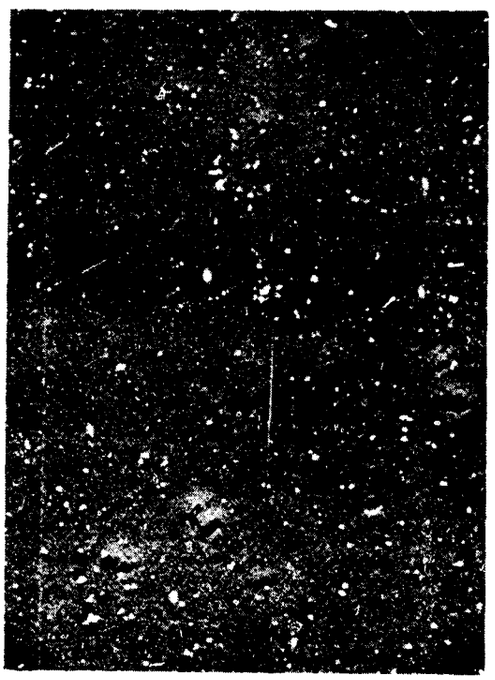

DOWNSTREAM OF SEAL

SEAL

Figure 9

ALUMINUM OXIDE - Al_2O_3

S.E.M. PHOTOS AFTER 100,000 CYCLE - GF_2 VALVE TEST (NORMAL IMPACT)

PHOTOS ARE AT 5000X

DOWNSTREAM OF SEAL

SEAL AREA

Figure 98

5. Data Evaluation Summary

General program results indicate that the materials selected after completion of the literature search and chemical analysis are potentially "good" materials for use as halogenated propellant valve seat and poppet materials although the program did not lead to exposure and testing of a "cure all" material. Results of the program have lead to more definitive design and material usage criteria for halogenated propellant valve materials.

Data accumulated during the program indicates that each of the materials tested is sensitive to a different mode of deterioration of the seat and poppet interface surfaces. In the hopeful category, one valve did almost meet the valve design leakage goal of less than 30 SCCH helium leakage at 450 psig inlet pressure after 100,000 accumulated valve cycles. In this section, the "failure modes" of each of the materials tested will be summarized with actions recommended which could lead to more successful usage of the material.

Two primary factors combined to insert some uncertainty into the program conclusions. These were the unknown contribution to total measured valve leakage of possible leakage of the valve downstream center static seal and the effects of lateral stability of the poppet relative to the seat after the poppet had contacted the seat. There is significant indication that in at least three of the valve tests, the low impact Ni-301, the K-96 normal impact, that the static downstream seal may have played a significant role in terms of total leakage contribution. In the valve tests in which the seal is suspected as being a major contributor, high leakage rates were experienced immediately after passivation. The Ni-301 and K-96 valves tested did not significantly change leakage level after a few cycles indicating that the primary contribution to leakage may have been from the seal. The pure tungsten carbide progressively increased leakage rate as a function of cycles accumulated indicating a more direct correlation of progressive seat deterioration with accumulated valve cycles. These data indicate that the Ni-301 may have and the K-96 probably did not leak significantly through the seat seal. From the deterioration of the pure tungsten carbide seat surface, the primary cause of leakage was probably chemical wear through accumulated valve cycles which was accelerated by lateral instability of the poppet relative to the seat.

Lateral stability of the poppet relative to the seat probably played a significant role in deterioration of the sealing surfaces of the valve materials tested using the normal impact armature. All of the valves tested using the normal impact armature demonstrated a grooved seat land surface after the tests were completed. While the extreme wear noted on some of the seats, i.e., 0.00025 inches wear on the tungsten

carbide, indicated significant chemical wear, the added factor of wear and grooving of the surface resulting from the poppet moving laterally relative to the seat was probably as significant. Even though a high degree of wear is evident, the wear should not result in leakage of the valve if there were no additional factors contributing to nonuniform wear as was evidenced in the grooved poppet and seat surfaces. Even the poppets tested using the low rate armature exhibited some evidence of seat to poppet relative movement indicating a design deficiency of the valve which could be corrected to improve the leakage performance and life of the valve seat interface.

Table VII shows a summary of the wear experienced on each of the test valves after completion of the 100,000 cycle tests. As far as "wear" is concerned, all of the test valves demonstrated acceptable wear characteristics except perhaps the pure tungsten carbide which eroded 250 microinches. For a 100,000 cycle life valve, that wear rate might be acceptable; however, when looking at a million cycle life valve, the wear rate is probably excessive. The low rates of chemical wear demonstrated feasibility of the sacrificial surface to seat and poppet material selection for valves to be operated in fluorinated oxidizers.

The "failure mode" hypothesized for the Ni-301 poppet and seat tested in this program test is as follows: The nickel fluoride formed on the surface of the poppet and seat is a cohesive, relatively tenancious film which has a high adhesion affinity for itself with a propensity toward "cold welding", i.e., a sticky film. All of the nickel base poppets and seats tested have shown a positive buildup from the mean original seat or poppet surface level. The buildup, as demonstrated in this program, is apparently formed of islands of fluorides protruding above the original mean surface level of the part. It is hypothesized that the positive buildup results from migration of the nickel fluoride from the edges of the seat toward the center through adhesion of one nickel fluoride surface to another, with free fluoride particles collecting to form mounds on the part surface. It will be remembered that the surface of the valve poppet tested in chlorine pentafluoride showed the presence of fine flakes on the surface between the mounds of the surface buildup. Possible solutions to this problem might be to further decrease the impact level to avoid fluoride buildup or more remotely, perhaps to increase impact levels to pound the fluoride islands flat.

The K-96, tungsten carbide with 6% cobalt binder, probably did not fail to perform as an effective seal during the program tests. The valve leaked a significant amount immediately after gaseous fluorine passivation indicating the downstream center seal to have possibly contributed to the leakage. Leakage throughout the remainder of test approached the design goal. With the uncertainty of performance of the static seal in the valve, it is probable that the seat performed adequately

TABLE VII

SEAT SURFACE EROSION DATA

MATERIAL	IMPACT FORCE LEVEL	TEST PROPELLANT	SEAT SURFACE LEVEL RELATIVE TO SEAT PLATE PLANE		PEAK TO VALLEY GROOVE HEIGHT POST TEST MICROINCHES
			AS LAPPED MICROINCHES	AFTER TESTING MICROINCHES	
B_4C	Normal	ClF_5	-2	-75 to -100	75 to 125
Ni-301	Low	ClF_5	-2	+5 to +10	10 avg
K-96	Normal	ClF_5	+1	-60 to -70	30 avg
Al_2O_3	Normal	GF_2	-3	-10 to -20	5 avg
Al_2O_3	Low	ClF_5	-2	-6 to -7	1.5 avg
B_4C	Low	ClF_5	-3	-3	1 avg
Al_2O_3	Low	GF_2	0	0	2 to 2.4
WC	Normal	ClF_5	-1	-250	50 avg

throughout the test. Examination of the poppet after test conclusion as well as examination of the static sample showed that the fine surface finish of the part was significantly degraded as a result of exposure to the propellant. The etching in propellant resulted in removal of the smooth surface finish and exposure of the grainy structure of the hot pressed tungsten carbide. As long as the tops of the exposed tungsten carbide particles furnished a flat surface, the seat should still function adequately as an effective microscopic labyrinth seal. The relatively low rate of the K-96 part as compared to the high wear rate of pure tungsten carbide part, coupled with the finding that the seal area of the K-96 part was quite high in cobalt concentration leads to the conclusion that the cobalt binder in the K-96 seat and poppet was less reactive than tungsten carbide, provided a protective film against further attack of the fluorinated oxidizer on the bare material, and thus contributed to effective sealing of the valve closure. This is possible since the cobalt probably only surrounds the grains of tungsten carbide, as hot pressed. Thus, the cobalt surfaces can be protectively coated with cobalt fluoride while the tungsten carbide particles are open to preferential attack by the chlorine pentafluoride. The pure tungsten carbide parts demonstrated significant enough wear to indicate the impact of the valve closing was probably sufficient to start minor reaction initiations leading to significant material loss not possible in a nonreactive fluid. In the K-96 part, the wear was significantly less indicating that the cobalt (cobalt fluoride coated) remaining after the surrounding tungsten carbide was etched or chemically worn away was pounded into the remaining open area providing the effective valve seal and also serving to prevent further direct attack by the propellant on the base tungsten carbide. A further improvement in valve leakage characteristics might be obtained by increasing the cobalt binder percentage thus further slowing the rate of attack of the base tungsten carbide.

Pure tungsten carbide as tested during this program, failed to provide an effective valve seal. Several factors probably combined to effect the net result of failure to seal. First, as previously discussed, the valve leaked an excessive amount after initial gaseous fluorine passivation. The leakage never decreased after that check point. That indicated the downstream center seal probably contributed to the overall leakage by a significant amount. Leakage progressively increased as a function of added valve cycles at a significant rate. By itself, the data would say that pure tungsten carbide was not adequate as a seat and poppet material. Two factors, however, could have materially affected the leakage cycle relationship. First, the particle size of the tungsten carbide was considerably higher than that of the K-96. This resulted in the effective closure portion of the resulting labyrinth seal being considerably shorter than in the case of the K-96 which was tested. It is possible that finer particle sizes could be obtained in the pure tungsten carbide to improve the seal surface area remaining after initial etching removed the fine surface finish obtained by lapping. A possible reason for the apparent presence of larger

crystallites in pure WC as compared to K-96 is believed to be the 6% cobalt content in the latter, which during sintering and hot pressing prevented formation of larger single crystals. Secondly, the poppet and seat, as did the others tested at normal impact, showed considerable evidence of grooving. The total wear of the part was considerably (approximately 0.00025 inches of material loss from both the poppet and seat surfaces). This indicates that the impact levels experienced in the "normal impact" valve are high enough to initiate or accelerate chemical wear of the base material surface. Even with that wear, however, the material might have served as an adequate seal if the relative surfaces had remained flat and not shown the tendency to groove. The grooving has to be associated with the potential for sliding of the poppet relative to the seat after initial impact provided by nonuniform bumper contact. Redesign of the valve to eliminate the sliding effect could aid in production of an effective valve seal.

Boron carbide demonstrated considerable promise as a seat and poppet material for use with chlorine pentafluoride during this program. The boron carbide poppet tested at low impact levels showed negligible wear as a result of the 100,000 cycle valve test. With the exception of one data point which might be attributed to debris accumulation in the seat area because of the nonflowing character of the test setup, the valve met all leakage requirements throughout the test. The high impact boron carbide poppet and seat tested met leakage requirements for at least 20,000 cycles. Total "wear" of the part after the test did indicate that the threshold of minor reaction initiation had been reached in the normal impact valve since considerable loss of seat and poppet surface material was noted on the post-test part examination. The contribution to the leakage rates measured on the normal impact valve of the scrubbing of the poppet relative to the seat after initial contact cannot be quantatively established; however, it is believed that if the tendency to groove and develop a no longer flat surface could be avoided through minor valve redesign, the material would furnish a more than adequate seat and poppet material for use with chlorine pentafluoride, even though some loss of seat/poppet material was experienced. Since the only criteria in sealing is the maintenance of flat relative surfaces, loss of seat or poppet material would only result in negligible increase in valve stroke with accumulated cycles over the valve operational life.

Aluminum oxide poppets and seats tested during the program demonstrated the highest resistance to chemical wear and static propellant exposure of any of the materials tested. The valves tested, however, failed to meet the leakage goal of the test program. "Wear" of the seats tested was extremely low with only on the order of 25 to 30 microinches measured on the poppet and seat tested at normal impact. The seating surface was still quite rough after the test however. In addition, and as with the other poppets tested in the normal impact valve configuration, it showed some grooving of the seating surface. A significant amount of apparent

debris was collected in the seat land area of all of the aluminum oxide parts tested in either gaseous fluorine or chlorine pentafluoride. The combination of debris and surface roughness in the seat area contributed to failure of the valves to successfully provide the required seal function throughout the period of the valve test. Two of the seats showed some tendency toward loss of edge of seat material through chipping and the seat tested at normal impact actually shattered in several places. Pure aluminum oxide is not considered satisfactory for direct incorporation into the present valve design, however the problems encountered with this material can be overcome.

The tendency toward shattering might be eliminated by redesign of the seat to avoid high stress concentration points, thus providing a structurally sound seat. Another approach believed worth investigation is annealing of the part after lapping. However, the tendency of the material to agglomerate particles of sluffed off material, whether base material or aluminum fluoride is a tendency which is not desirable in a valve seat/poppet material combination. This tendency may not be a real problem in a flowing system since the particles could possibly be washed away in a flowing stream. As with the other materials which exhibited a tendency toward grooving, that tendency might be eliminated by redesign of the valve structure to avoid the minute sliding actions causing it.

SECTION VII

CONCLUSIONS

Data accumulated during this program have led to the following conclusions with regard to the original objective of the program which was to determine the mechanism of failure of the Marquardt Advanced ACS valve in fluorine or chlorine pentafluoride service.

The original premise of failure of the valve to seal through degradation of the passive fluoride film on the surface of the seat and poppet under the impact load of the poppet contacting the seat during closing of the valve was positively confirmed.

"Wear" rate of materials having both gaseous and solid fluorides was shown to be a function of the level of impact force generated during valve closing. Wear rate, as a crude function of the impact force level was bracketed for two materials, Al_2O_3 and B_4C by testing the material in both the "normal" and "low" impact valve configurations. The low impact armature configuration demonstrated a significantly lower wear rate over the test period. Lowering of armature spring rate to provide slow closing of the valve and thus low impact forces resulted in marginally acceptable valve closing response. Other techniques of providing the desired low poppet to seat closing impact forces should be investigated and employed in a subsequent valve design iteration.

No apparent difference was found in exposed material surface degradation between exposure to chlorine pentafluoride or gaseous fluorine during this program.

It is possible to construct a valve which will meet the design specification goal of 100,000 cycles in chlorine pentafluoride gaseous fluorine with a maximum measured leakage rate of less than 30 SCCH helium at 450 psig inlet pressure.

Test techniques investigated and used to evaluate the test parts during the program were demonstrated to be of considerable aid in understanding causes of seal surface deterioration. The scanning electron microscope-microprobe analyzer in particular provided valuable data as to surface topographical features, however, a more sensitive instrument is required to document surface chemistry of the very thin film formed during exposure of parts to fluorine or chlorine pentafluoride.

At least three of the five materials recommended and tested during this program showed considerable promise of being satisfactory for poppets and seats in this valve application. Pure boron carbide appears to be the best material tested considering possibility for cryogenic applications.

Design criteria was developed for each of the specific materials tested which can lead to valve designs successfully meeting all specification requirements. "Failure" mechanism of each of the materials tested during the program appeared to be unique to the specific material under test. Design to accommodate the idiosyncrasies of the individual materials can result in successful operation of the valve using the selected materials.

Failure of some of the valves tested to meet the desired leakage goals throughout the full period of the test was probably due in part to outside factors which were not directly connected with the function of the seat and poppet seal interface. First, static seal failure probably contributed an unknown fraction of the measured leakage. Secondly, propellant/material reaction initiations as a result of impact of the poppet with the seat in closing were at least compounded by sliding the poppet relative to the seat after initial poppet contact due to nonuniform minute bumper contact with the seat stop. Third, the nonflowing nature of the test setup may have contributed to accumulation of wear particles which would have been removed from the sealing areas by the flowing gas or fluids. The valves were periodically flushed during the tests to preclude this problem but are not believed to have been completely successful.

SECTION VIII

RECOMMENDATIONS

The following recommendations are made based on the findings of the present program:

Three of the materials tested during this program are recommended for further study and testing to document operational characteristics of the chlorine pentafluoride and gaseous fluorine. These materials are:

Pure Boron Carbide - This material represents the primary recommended material because of demonstrated good performance during this program. In addition, it is the only material tested which should provide adequate high temperature service as well as excellent cryogenic service with liquid fluorine. It is the only one of the materials tested which has a gaseous fluoride at extremely low temperatures. Above -202F, boiling point of the fluoride, no problems with solid fluorides should be encountered. Below that temperature, the reaction rate should be sufficiently slow that no serious surface degradation should occur.

Aluminum Oxide - Although none of the aluminum oxide seat and poppet closures tested during the program met the leakage goal, there were apparent reasons why they failed. One shattered and the other two valves tested failed through agglomeration of debris in the seat area. These problems might well be eliminated by redesign of the valve to accommodate the brittle nature of Al_2O_3 and testing in a flowing system to avoid debris collection.

K-96 Tungsten Carbide - Marginally adequate performance was demonstrated using K-96 during this program. In addition, satisfactory results have been obtained using the material at Rocket Propulsion Laboratory, Edwards Air Force Base. These results indicate that the use of K-96 as a valve seat and poppet material warrants further study.

New Tungsten Carbide with higher percentage cobalt binder - K-96 demonstrated significantly lower wear rates during these tests as compared to pure tungsten carbide. It is possible that the addition of slightly more cobalt might further impede attack of the tungsten carbide by the fluorinated oxidizers, resulting in a better wear rate than measured with the K-96 during this program.

A program should be initiated to provide conclusive substantiation of some of the hypotheses proposed as individual failure mechanisms in this report. Conclusions were made on the basis of all available data, however, film thicknesses of fluorides formed on parts susceptible to the formation of solid fluorides remains an unknown factor.

The program should provide for further design refinement of the valve operating structure to eliminate minor design deficiencies discovered during the course of the present program. The design portion of the program should include re-examination of the relationship of the bumper and seat-poppet interactions to determine if a better way of controlling the factors leading to grooving of the sealing interfaces is available. Redesign of the valve would include elimination of the parallel leak path present in the single component valve used as a test bed device. A part of elimination of the potential parallel leakage path should include studies of brazing of the ceramic types of materials used for valve seats to a steel outlet fitting. Redesign of the valve seat configurations (particularly the Al_2O_3) should be conducted to eliminate sharp corners susceptible to chemical attach and causing residual stresses which can result in shattering of seat surfaces.

Impact force-wear relationships documented during the present program should be extended to the design of a new armature configuration specifically tailored to provide more optimum impact force levels for the materials recommended for further testing.

A test series should be conducted using the materials recommended for further study with the redesigned valve structure. This test program should be conducted in a test facility which provided for typical flow rates during each valve test cycle. The program should include sufficient tests to provide a statistically meaningful sample size.

REFERENCES

1. G. T. Pond and H. Wickmann, "Advanced ACS Valve Development Program," AFRPL-TR-69-250, AD864123, The Marquardt Co. December 1969.

2. V. Gutmann, ed, Halogen Chemistry, Academic Press, London & New York.

3. M. Stacey, J. C. Tatlow, A. G. Sharpe, eds., Advances in Fluorine Chemistry, Butterworths, Washington.

4. Thin Solid Films, (Journal) Elsevier Publishing Co.

5. Gmelins Handbuch der Anorganischen Chemie, Verlag Chemie, Weinheim.

6. G. F. Tellier, J. W. Lewellen, and H. Standke, "Survey of Contamination in Rocket Propulsion Fluid Systems," Rocketdyne, AFRPL-TR-67-290, AD829701, Nov. 1967.

7. J. H. Cabaniss, "Bibliography on Fluorine and Fluorine Oxygen Oxidizers for Space Application," NASA TM-X-53149, N 65-14430, Propulsion and Vehicle Engineering Lab., October 1964.

8. J. H. Cabaniss and J. G. Williamson, "A Literature Survey of the Corrosion of Metal Alloys in Liquid and Gaseous Fluorine," NASA MTP-P&VE-M-63-21, N 64 17691, December 1963.

9. R. F. Muraca, J. S. Whittick, and J. A. Neff, "Treatment of Metal Surfaces for Use with Space Storable Propellants: A Critical Survey," JPL, SRI-No. 951581-8, August 1968.

10. N. A. Tiner and W. D. English, "Compatibility of Structural Materials with High Performance O-F Liquid Oxidizers," Astropower Inc., No. 112-Q1 AD 287 762, Sept. 1962.

11. John C. Grigger and Henry C. Miller, "The Compatibility of Structural Materials with Hybaline A-5 and Compound A," AFML-TR-64-391, AD 458-159, December 1964.

12. R. J. Salvinski, G. W. Howell, and D. H. Lee, "Advanced Valve Technology, Vol. II, Materials Compatibility and Liquid Propellant Study," TRW Rept. 06641-6014-R000, Contract NAS7-436, Nov. 1967.

13. Sidney Kleinberg and James F. Tompkins, "The Compatibility of Various Metals with Liquid Fluorine," ASD-TDR-62-250, Air Products and Chemical, Inc., AD 423 551, March 1962.

14. C. J. Sterner, Alan H. Singleton, "The Compatability of Various Metals with Liquid Fluorine," WADD Tech, Rept. 60-819, Air Products Inc., AD 260 087, March 1961.

15. [redacted]

16. Roy M. Adams, ed. Boron, Metallo-Boron Compounds and Boranes Inter-Science Publishers, New York, 1964.

17. S. S. Wise, J. L. Margrave, H. M. Feder, and W. N. Hubbard, "Fluorine Bomb Calorimetry, III. The Heat of Formation of Boron Trifluoride," J. Phys. Chem 62, 2157 (1961).

18. E. Lingnau, "Das Verhalten der Werkstoffe Gegenüber Fluor," Werkstoffe and Korrosion 7, 634 (1956).

19. F. W. Fink and Earl L. White, "Corrosion Effects of Liquid Fluorine and Liquid Oxygen on Materials of Construction," Corrosion 17, (2) 58t (1961).

20. [redacted]

21. C. A. Crommelin, Chem. Weekbl. 18, 483 (1921).

22. N. A. Tiner, W. D. English, and S. M. Toy, "Compatibility of Structural Materials with High Performance O-F Liquid Oxidizers, Tech. Doc. AFML-TR-65-414, Astropower Lab. AD 477 002, Nov. 1965.

23. Harold W. Schemidt, "Handling and Use of Fluorine and Fluorine-Oxygen Mixtures in Rocket Systems," NASA SP-3037, 1967.

24. J. D. Jackson, "Compatibility of Materials with Fluorine and Fluorine-Base Oxidizers," Battelle Memorial Institute, DMIC Tech. Note, AD 463 017, April 1965.

25. E. Skinner, "Materials of Construction, High-Temperature Metals," Chem. Engr. 65, 127 (1958).

26. John Turner Pinkston, Jr., "The Halogen Fluorides." Chem. Rev. 41, 421 (1947).

27. W. F. Hady, et al, "Friction, Wear, and Dynamic Seal Studies in Liquid Fluorine and Liquid Oxygen," NASA/Lewis, TND-2453, August 1964.

28. A. K. Kuriakose and J. L. Margrave, "Kinetics of Reactions of Elemental Fluorine with Zirconium Carbide and Zirconium Diboride at High Temperatures," J. Phys, Chem. 68, 290 (1964).

29. A. K. Kuriakose and J. L. Margrave, "Kinetics of Reaction of Elemental Fluorine. II. The Fluorination of Hafnium Carbide and Hafnium Boride," J. Phys Chem. 68, 2343 (1964).

30. R. C. Purdy, J. Am. Ceramic Soc. 17, 39 (1934).

31. A. K. Kuriakose and J. L. Margrave, "Kinetics of Reaction of Elemental Fluorine. III. Fluorination of Silicon and Boron," J. Phys. Chem. 68, 2671 (1964).

32. John L. Margrave, "Thermodynamic and Kinetic Studies of Borides and Other Refractory Materials at High Temperatures," AFML-TR-65-123, AD 472 145, August 1965.

33. S. M. Toy, et al, "Tankage Materials in Liquid Propellants," Astropower Lab., AFML-TR-68-204, July 1968.

34. S. K. Asunmaa, et al, "Halogen Passivation Procedural Guide," AFRPL-TR-67-309, Astropower Lab., AD 826 478, Dec. 1967.

35. W. R. Myers and W. B. DeLong, "Fluorine Corrosion," Chem. Eng. Progress 44, 359 (1948).

36. Patricia M. OlDonnell and A. E. Spakowski, "The Fluorination of Copper," J. Electrochem. Soc. 111, 633 (1964).

37. J. M. Crabtree, C. S. Lees, and K. Little, "The Copper Fluorides, Part I - X-Ray and Electron Microscope Examination," J. Inorg. Nucl. Chem. 1, 213, 1955.

38. P. E. Brown, J. M. Crabtree and J. F. Duncan, "The Kinetics of the Reaction of Elementary Fluorine with Copper Metal," J. Inorg. Nucl, Chem. 1, 202, 1955.

39. J. C. Grigger, H. C. Miller, "Research on the Compatibility of Materials with Chlorine Trifluoride, Perchloryl Fluoride and Mixtures of These," WPAFB, Pennsalt Chemicals Corp., AD 244 009, August 1960.

40. R. Lynn Farrar, Jr., and Hilton A. Smith, "The Kinetics of Fluorination of Nickel Oxide by Chlorine Trifluoride," J. Phys. Chem. 59, 763, (1955).

41. R. L. Jarry, J. Fisher, and W. H. Gunther, "The Mechanism of the Nickel-Fluorine Reaction," J. Electrochem. Soc. 110, 346 (1963).

42. Patricia M. O Donnell, "Kinetics of the Fluorination of Iron," NASA/Lewis, TN D-3575, August 1966.

43. O. Ruff and M. Giese, Zt. anorg. Chem. 219, 143 (1934).

44. H. von Wartenberg, Zt. anorg. Chem. 241, 381 (1939).

45. H. M. Haendler, et al, "The Reaction of Fluorine with Copper and Some of its Compounds. Some Properties of Copper (II) Fluoride," J ACS 76 2178 (1954).

46. M. C. Sneed, et al., Comprehensive Inorganic Chemistry, Vol. III, D. Van Nostrand Co. (1954).

47. H. M. Haendler, et al, "The Reaction of Fluorine with Titanium, Zirconium and the Oxides of Titanium (IV), Zirconium (IV) and Vanadium (V)," JACS 76 , 2177 (1954).

48. Ralph Landau, "Corrosion by Fluorine and Fluorine Compounds," Corrosion 8, 283 (1952).

49. H. F. Priest and A. von Grosse, US 2, 419, 915.

50. Ulick R. Evans, The Corrosion and Oxidation of Metals: Scientific Principles and Practical Application, St. Martin's Press Inc., New York.

51. J. D. Jackson, "Corrosion in Cryogenic Liquids," Chem. Eng. Progress 57 (4) 61, (1961).

52. W. A. Cannon, W. D. English, and N. A. Tiner, "Halogen Passivation Studies," AFRPL-TR-67-232, AD 818 667, August 1967.

53. W. D. English, S. W. Pohl, and N. A. Tiner, "Compatibility of Structural Materials with High Performance O-F Liquid Oxidizers," Astropower, Inc., AD 403 062, March 1963.

54. R. J. Salvinski, TRW, Private Communication.

55. T. A. O'Donnell and D. F. Stewart, "Reactivity of Transition Metal Fluorides, I. Higher Fluorides of Chromium, Molybdenum, and Tungsten," Inorg. Chem. 5, 1434 (1966).

56. R. L. DeWitt and H. W. Schmidt, "Experimental Evaluation of Liquid-Fluorine System Components," NASA/Lewis, Tech. Note D-1727, N 63 16989, June 1963.

57. F. Q. Roberto and G. Mamantov, "Reaction of Platinum Hexafluoride with Chlorine Pentafluoride," Inorg. Chem., Acta. 2, 317 (1968).

58. R. Lynn Farrar, Jr., and Hilton A. Smith, "The Absorption of Chlorine Trifluoride on Porous Nickel Fluoride," JACS 77, 4502 (1955).

59. Handbook of Chemistry and Physics, The Chemical Rubber Company, 45th edition, (1964).

60. Helmut M. Haendler, et al, "The Reaction of Fluorine with Zinc, Nickel and Some of their Binary Compounds. Some Properties of Zinc and Nickel Fluorides," J ACS 74, 3167 (1952).

61. W. B. Pearson, Handbook of Lattice Spacings and Structures of Metals and Alloys, Pergamon Press, New York, (1958).

UNCLASSIFIED
Security Classification

DOCUMENT CONTROL DATA - R&D
(Security classification of title, body of abstract and indexing annotation must be entered when the overall report is classified)

1. ORIGINATING ACTIVITY (Corporate author)
The Marquardt Company, CCI Aerospace Corporation
16555 Saticoy Street, Van Nuys, California 91409

2a. REPORT SECURITY CLASSIFICATION
UNCLASSIFIED

2b. GROUP

3. REPORT TITLE
Advanced ACS Valve Sealing Surface Compatibility Investigation

4. DESCRIPTIVE NOTES (Type of report and inclusive dates)
Final Report Covering Period - May 1970 tc 1 July 1971

5. AUTHOR(S) (Last name, first name, initial)
Gerald R. Pfeifer, Horst Wichmann, Dr. Reinholdt Kratzer

6. REPORT DATE	7a. TOTAL NO. OF PAGES	7b. NO. OF REFS
September 1971	206	61

8a. CONTRACT OR GRANT NO.	9a. ORIGINATOR'S REPORT NUMBER(S)
FO4611-70-C-0052	
b. PROJECT NO. 3058	
c	9b. OTHER REPORT NO(S) (Any other numbers that may be assigned this report)
d.	AFRPL-TR-71-84

10. AVAILABILITY/LIMITATION NOTICES
Approved for public release; distribution unlimited.

11. SUPPLEMENTARY NOTES	12. SPONSORING MILITARY ACTIVITY
	Air Force Rocket Propulsion Laboratory Edwards AFB, California 93523

13. ABSTRACT

An integrated program of theoretical chemical analysis and testing was conducted to determine the cause of failure of the Marquardt Advanced ACS valve to meet defined leakage goals when operated in chlorine pentafluoride or gaseous fluorine. A total of 23 poppets and 8 valve seats were tested in either static or dynamic propellant exposure in test bed valves during the program. Prime objective, that of determining the mechanism of sealing surface deterioration, was accomplished during the program. In addition, design parameters were evolved which can lead to a successful design meeting all of the design objectives for valve operational performance in fluorinated oxidizers.

Failure mechanism of the valve was found to be a progressive degradation of the poppet and seat sealing surface through structural failure of the passive fluoride film formed on the parts under impact of the poppet with the seat during valve closing for those materials forming solid fluoride films. The use of materials forming gaseous fluorides which provided sacrificial seating surfaces was demonstrated to be a satisfactory way of maintaining an acceptable seat sealing surface through 100,000 valve cycles. Rate of sacrifice of seat material was demonstrated to be a function of the impact force and energy with which the seat was impacted by the valve poppet during valve closing. This chemical wear, caused by impact forces, was shown to be accelerated by minor lateral movements which caused grooving in some of the valve seats tested with leakage resulting.

DD FORM 1 JAN 64 1473

UNCLASSIFIED
Security Classification

14 KEY WORDS	LINK A		LINK B		LINK C	
	ROLE	WT	ROLE	WT	ROLE	WT
Bipropellant Valve						
Chlorine Pentafluoride						
Fluorine						
Metal-to-Metal Poppet and Seat						
Magnetically Linked						
Poppet Axial Guidance Flexure						
Poppet Self-Alignment Flexure						
Helium Leakage						

INSTRUCTIONS

1. ORIGINATING ACTIVITY: Enter the name and address of the contractor, subcontractor, grantee, Department of Defense activity or other organization *(corporate author)* issuing the report.

2*a*. REPORT SECURITY CLASSIFICATION: Enter the overall security classification of the report. Indicate whether "Restricted Data" is included. Marking is to be in accordance with appropriate security regulations.

2*b*. GROUP: Automatic downgrading is specified in DoD Directive 5200.10 and Armed Forces Industrial Manual. Enter the group number. Also, when applicable, show that optional markings have been used for Group 3 and Group 4 as authorized.

3. REPORT TITLE: Enter the complete report title in all capital letters. Titles in all cases should be unclassified. If a meaningful title cannot be selected without classification, show title classification in all capitals in parenthesis immediately following the title.

4. DESCRIPTIVE NOTES: If appropriate, enter the type of report, e.g., interim, progress, summary, annual, or final. Give the inclusive dates when a specific reporting period is covered.

5. AUTHOR(S): Enter the name(s) of author(s) as shown on or in the report. Enter last name, first name, middle initial. If military, show rank and branch of service. The name of the principal author is an absolute minimum requirement.

6. REPORT DATE: Enter the date of the report as day, month, year; or month, year. If more than one date appears on the report, use date of publication.

7*a*. TOTAL NUMBER OF PAGES: The total page count should follow normal pagination procedures, i.e., enter the number of pages containing information.

7*b*. NUMBER OF REFERENCES: Enter the total number of references cited in the report.

8*a*. CONTRACT OR GRANT NUMBER: If appropriate, enter the applicable number of the contract or grant under which the report was written.

8*b*, 8*c*, & 8*d*. PROJECT NUMBER: Enter the appropriate military department identification, such as project number, subproject number, system numbers, task number, etc.

9*a*. ORIGINATOR'S REPORT NUMBER(S): Enter the official report number by which the document will be identified and controlled by the originating activity. This number must be unique to this report.

9*b*. OTHER REPORT NUMBER(S): If the report has been assigned any other report numbers *(either by the originator or by the sponsor)*, also enter this number(s).

10. AVAILABILITY/LIMITATION NOTICES: Enter any limitations on further dissemination of the report, other than those imposed by security classification, using standard statements such as:

(1) "Qualified requesters may obtain copies of this report from DDC."

(2) "Foreign announcement and dissemination of this report by DDC is not authorized."

(3) "U. S. Government agencies may obtain copies of this report directly from DDC. Other qualified DDC users shall request through _____."

(4) "U. S. military agencies may obtain copies of this report directly from DDC. Other qualified users shall request through _____."

(5) "All distribution of this report is controlled. Qualified DDC users shall request through _____."

If the report has been furnished to the Office of Technical Services, Department of Commerce, for sale to the public, indicate this fact and enter the price, if known.

11. SUPPLEMENTARY NOTES: Use for additional explanatory notes.

12. SPONSORING MILITARY ACTIVITY: Enter the name of the departmental project office or laboratory sponsoring *(paying for)* the research and development. Include address.

13. ABSTRACT: Enter an abstract giving a brief and factual summary of the document indicative of the report, even though it may also appear elsewhere in the body of the technical report. If additional space is required, a continuation sheet shall be attached.

It is highly desirable that the abstract of classified reports be unclassified. Each paragraph of the abstract shall end with an indication of the military security classification of the information in the paragraph, represented as *(TS)*, *(S)*, *(C)*, or *(U)*.

There is no limitation on the length of the abstract. However, the suggested length is from 150 to 225 words.

14. KEY WORDS: Key words are technically meaningful terms or short phrases that characterize a report and may be used as index entries for cataloging the report. Key words must be selected so that no security classification is required. Identifiers, such as equipment model designation, trade name, militar project code name, geographic location, may be used as key words but will be followed by an indication of technical co text. The assignment of links, rules, and weights is optiona